Demand Response Management and Control Strategies for Integrated Smart Electricity Networks

Fayiz Faisal Alfaverh

Submitted to the University of Hertfordshire in partial fulfilment of the requirement of the degree of *Doctor of Philosophy*

May 2023

Abstract

Demand Response (DR) programs are being introduced by some electricity grid operators as resource options for curtailing and reducing the demand of electricity during certain time periods for balancing supply and demand. DR is considered as a class of demand-side management programs, where utilities offer incentives to end-users to reduce their power consumption during peak periods. DR is, indeed, a promising opportunity for consumers to control their energy usage in response to electricity tariffs or other incentives from their energy suppliers. Thus, successful execution of a DR program requires the design of efficient algorithms and strategies to be used in the utility grid to motivate end-users to actively engage in residential DR.

This thesis studies DR management using machine learning techniques such as Reinforcement Learning (RL), Fuzzy Logic (FL) and Neural Networks (NN) to develop a Home Energy Management System (HEMS) for customers, construct an energy customer behaviour framework, investigate the integration of Electrical Vehicles (EVs) into DR management at the home level and the provision of ancillary services to the utility grid such as Frequency Regulation (FR), and build effective pricing strategies for Peer-to-Peer (P2P) energy trading.

In this thesis, we firstly proposed a new and effective algorithm for residential energy management system using Q-learning method to minimise the electricity bills and maximise the user's satisfaction. The proposed DR algorithm aims to schedule household appliances considering dynamic electricity prices and different household power consumption patterns. Moreover, a human comfort-based control approach for HEMS has been developed to increase the user's satisfaction as much as possible while responding to DR schemes. The simulation results presented in this Chapter showed that the proposed algorithm leads to minimising energy consumption, reducing household electricity bills, and maximising the user's satisfaction.

Secondly, with the increasing electrification of vehicles, emerging technologies such as Vehicle-to-Grid (V2G) and Vehicle-to-Home (V2H) have the potential to offer a broad range of benefits and services to achieve more effective management of electricity demand. In this way, EVs become as distributed energy storage resources and can conceivably, in conjunction with other electricity storage solutions, contribute to DR and provide additional capacity to the grid when needed. Therefore, we proposed an effective DR approach for V2G and V2H energy management using Reinforcement Learning (RL) to make optimal decisions to charge

or delay the charging of the EV battery pack and/or dispatch the stored electricity back to the grid without compromising the driving needs. Simulations studies are presented to demonstrate how the proposed DR strategy can effectively manage the charging/discharging schedule of the EV battery and how V2H and V2G can contribute to smooth the household load profile, minimise electricity bills and maximise revenue. In addition, the potential benefits of EVs battery and V2G technology to provide grid frequency response services have also been investigated. We have designed an optimal real-time V2G control strategy for EVs to perform supplementary frequency regulation using Deep Deterministic Policy Gradient (DDPG). The main feature that distinguishes the proposed approach from previous related works is that the scheduled charging power of an individual EV is optimally tracked and adjusted in real-time to fulfil the charging demand of EV's battery at the plug-out time without using the forced charging technique to maximise the frequency regulation capacity.

Finally, a Peer-to-Peer (P2P) model for energy transaction in a community microgrid has been proposed. The concept of P2P energy trading can promote the implementation of DR by providing consumers with greater control over their energy usage, incentivising them to manage their energy consumption patterns in response to changes in energy supply and demand. It also stimulates the adoption of renewable energy sources. The proposed P2P energy-sharing mechanism for a residential microgrid with price-based DR is designed to engage individual customers to participate in energy trading and ensures that not a single household would be worse off. The proposed pricing mechanism is compared with three popular P2P energy sharing models in the literature namely the Supply and Demand Ratio (SDR), Mid-Market Rate (MMR) and Bill Sharing (BS) considering different types of peers equipped with solar Photovoltaic (PV) panels, EVs, and domestic energy storage systems. The proposed P2P framework has been applied to a community consisting of 100 households and the simulation results demonstrate fairness and substantial energy cost saving/revenue among peers. The P2P model has also been assessed under the physical constrains of the distribution network.

Acknowledgements

I would like to express my deepest appreciation and gratitude to my esteemed supervisors, Dr. Mouloud Denai and Prof. Yichuang Sun, for their unwavering support, expert guidance, and invaluable mentorship throughout my PhD journey. Their insightful comments, constructive feedback, and encouragement have been invaluable in shaping the direction of my research and in helping me achieve my academic goals.

I am also immensely grateful to the University of Hertfordshire for providing me with a conducive and stimulating environment for pursuing my doctoral studies. The resources, facilities, and opportunities offered by the university have been crucial in facilitating my research and enhancing my skills as a researcher.

My heartfelt thanks go to my family for their unending love, unwavering support, and constant motivation. Their sacrifices, understanding, and unwavering belief in my abilities have been the driving force behind my success, and I am forever grateful for their unwavering presence in my life.

I would also like to extend my sincere appreciation to my friend (Zaid) for his constant support, encouragement, and unwavering faith in my abilities. His unwavering support, listening ear, and valuable insights have been a source of inspiration and motivation throughout my PhD journey.

Finally, I would like to acknowledge the contributions of all those who have directly or indirectly supported me in completing this research. I am grateful for their support, encouragement, and guidance, and I am committed to making them proud.

Table of Contents

List of Figures

List of Tables

List of Abbreviations

ACE	Area Control Error
ADLC	Advanced Direct Load Control
AMI	Advanced Metering Infrastructure
AMM	Automatic Meter Management
AMR	Automated Meter Reading
ANNs	Artificial Neural Networks
ARR	Area Regulation Requirement
BESS	Battery Energy Storage Systems
BS	Bill Sharing
CPP	Critical Peak Pricing
DDPG	Deep Deterministic Policy Gradient
DLC	Direct Load Control
DR	Demand Response
DRL	Deep Reinforcement Learning
DSM	Demand Side Management
EDP	Extreme Day Pricing
EVs	Electric Vehicles
FiT	Feed-in Tariff
FR	Fuzzy Reasoning
HANs	Home Area Networks
HEMS	Home Energy Management System
HMI	Human-Machine Interface
I/C	Interruptible/Curtailable
IBR	Inclining Block Rate
ICT	Information and Communication Technologies
LFC	Load Frequency Control
MDMS	Meter Data Management System
MDP	Markov Decision Process
MGs	Microgrids
MMR	Mid-Market Rate
NANs	Neighbourhood Area Networks
P2P	Peer-to-Peer
PTR	Peak-Time Rebate
PV	Photovoltaic
RESs	Renewable Energy Sources
RL	Reinforcement Learning
RMS	Root Mean Square
RTP	Real-Time-Pricing
SDR	Supply and Demand Ratio
SFR	Supplementary Frequency Regulation
SG	Smart Grid
SOC	State-of-Charge
TOU	Time-of-Use
V2G	Vehicle-to-Grid
V2H	Vehicle-to-Home
WANs	Wide Area Networks

Chapter 1 Introduction

1.1 Background

Electricity demand is increasing rapidly due to the global population and economic growth. The current global energy demand mainly relies on fossil fuel resources such as oil, natural gas, and coal which are contributing to high carbon emissions and are subject to fluctuating prices. Further, due to the limited fossil fuels reserves, meeting the future energy demand has become a great challenge.

Renewable Energy Sources (RESs) are considered as clean energy and offer a promising solution to mitigate global warming and reduce the environmental impacts. However, the wide-scale integration of RESs may have negative impacts on the stability of the power grid. Increased penetration of intermittent RESs causes fluctuations in the generation side, and this leads to mismatching energy between the demand and supply, resulting in significant deviations in the system frequency.

Recent advances in Information and Communication Technologies (ICT) and the deployment of Advanced Metering Infrastructure (AMI), are paving the way to the emerging concept of a Smart Grid (SG) and demand side programs via enabling bidirectional communication between utility and consumer. In general, these programs encourage consumers to use less energy while receiving the same or improved quality of energy services.

Demand Side Management (DSM), when integrated into the smart grid concept, means that electricity demand is adjusted to electricity generation and the available electricity in the grid. With DSM electricity demand is reduced, especially during peak hours therefore leveraging congestion in the grid. Demand Response (DR) is one of these DSM techniques which focuses on providing price signals to end-users to incentivise them to manage their electricity usage. DR provides a great opportunity for residential consumers to play a significant role in the operation of the electric grid by reducing or shifting their electricity consumption during peak demand hours in response to price signals.

Key enabling technologies such as smart meters, smart sensors, bidirectional communication, smart home appliances, Home Area Network (HAN) and Home Energy Storage System (HESS), etc. have experienced a significant development in recent years. This has provided the foundation for the development of Home Energy Management Systems (HEMS). Smart HEMS are an essential technology for the successful implementation of DSM strategies

in SGs. HEMS allows end-users to monitor and control their home appliances in real-time, based on their preferences to achieve a cost-effective and efficient electricity usage. According to DR objectives, HEMS enables automated and/or manual shifting and curtailing electricity demand during peak hours in response to DR signals without affecting the customer's preferences.

More recently, there has been a gradual shift towards the adoption of Electric Vehicles (EVs) in the automotive industry. The main drivers are the economic and environmental benefits, the technological improvement in batteries' energy density, and government policies offering financial rewards such as tax breaks or rebates to EV owners. Therefore, emerging technologies such as Vehicle-to-Grid (V2G) and Vehicle-to-Home (V2H), or in short, Vehicle-to-Everything (V2X) have the great potential to offer a broad range of valuable services and benefits hence promoting DR implementation. EVs are seen as distributed energy storage resources and can conceivably, in conjunction with other electricity storage technologies, contribute to DR and provide additional capacity to the grid when needed. Indeed, the emerging V2G technology with a bi-directional flow of power provides the grid with access to mobile energy storage for DR, frequency regulation and demand-supply balancing in the local distribution system.

In recent years, smart consumers along with the expansion of distributed renewable energy resources such as roof-top solar panels and EVs at the residential demand side are considered as prosumers. Prosumers can trade their energy excess with the main grid for further minimising their electricity cost under the Feed-in Tariff (FiT) scheme. However, the benefits to prosumers when participating in FiT are not significant. In addition, the amount of exported energy to the grid may pose some issues in the system, such as reverse power flow and over-voltage issues. Peer-to-Peer (P2P) energy sharing, where prosumers directly trade their excess of electricity generated from solar with consumers, has recently emerged as a potential solution to overcome the limitations of the FiT scheme. Furthermore, it contributes towards the wide-scale adoption of renewable energy sources. In addition, P2P energy sharing not only offer economic benefits to prosumers but also contributes to the enhancement of the stability of the utility grid.

1.2 Research Aim and Objectives

As energy demand continues to increase, DR programs are gaining momentum and their adoption is set to grow gradually over the years ahead. DR schemes seek to support grid

balancing of supply-demand, facilitate large adoption of green energy resources and improve the stability and reliability of the power grid.

The residential sector is more attractive for the implementation of DR programs than the industrial and commercial sectors, due to several reasons. Firstly, electricity consumption in the residential sector has increased rapidly because of the global trend towards a modern lifestyle. Currently, the residential sector consumes 30-40% of the energy supplied from fossil fuels across the world, which is responsible for the larger seasonal and daily peak demand followed by industrial and then commercial sectors [1]. In the UK, households are the largest consumers of electricity. In fact, domestic electricity consumption has registered a year-over-year growth in 2020, reaching roughly 108 terawatt-hours [2].

Unlike industrial and commercial loads, residential loads are more elastic, interruptible, and shiftable. However, some challenges regarding the implementation of DR in residential areas must be addressed. One of these challenges is how to ensure the balance between cost saving and convenience. As DR programs seek to change energy consumption patterns by shifting the household loads from peak hours when the electricity prices are high to off-peak, this may compromise the consumers' preferences leading to the unwillingness of consumers to participate in the DR scheme. Thus, optimal DR strategies must be proposed to ensure a balance between cost-saving and user's comfort while implementing DR programs. Furthermore, most household consumers do not want to spend time calculating and analysing their energy consumption and scheduling their household appliances to reduce their electricity bills. Therefore, the monitoring, controlling, and scheduling of household loads must be completely automated to stimulate consumers to participate in DR programs.

Another issue related to residential DR is the diversity of household appliances which can be divided into schedulable and non-schedulable loads, where the schedulable loads can further be classified into interruptible or non-interruptible loads. Flexibility is crucial in DR strategies, to manage and control these types of appliances and deal with different types of household sources such as renewable energy sources and home energy storage systems. The key motivating factor for consumers to participate in DR programs is the monetary benefits. Thus, fairness in users' electricity payments must be considered in pricing mechanisms to encourage them to actively participate in DR. The pricing mechanism is fair only if those users who actively contribute to the program pay less than the others.

With the increase in the electrification of transportation, EVs have become an essential source of schedulable loads in residential areas. What distinguishes EVs from other loads is that they can also be used as an energy storage system. EVs can supply power to the electricity grid at peak demand periods and store the excess of generation at low consumption periods. Therefore, the integration of EVs into DR strategies necessitates a comprehensive investigation of owner driving patterns, diverse EV types, varying battery capacities, and distinct arrival and departure schedules. This holistic analysis ensures the effective management of EV batteries, facilitating optimised participation of EVs in DR initiatives. On the other hand, EVs can provide frequency regulation services in the power grid due to their fast response characteristics. Therefore, to benefit from EVs when they are charged and not being used, a V2G control strategy should be developed to contribute to frequency regulation services while satisfying the driving needs of EV owners.

This, therefore, inspires the main aim of the research which can be stated as:

To develop and design efficient algorithms and strategies for successful demand side management to be utilised in smart grid in order to motivate end-users to actively and widely participate in residential demand response, aiming to an increase in energy usage efficiency, reduction in electricity bills, larger adoption of intermittent renewable energy sources, better supply-demand balance, and more stable and reliable power grid.

To achieve the main aim of this thesis, the following objectives have been set:

- Study of the residential energy usage patterns, modelling of the HEMS including solar panels, power electronic devices, and household appliances, developing a DR strategy for HEMS and improving the satisfaction of residents while participating in DR programs. ***(This objective has been addressed in Chapter 4).***
- Analysis the availability of EVs to be integrated into DR programs, which depends on several factors, such as the EV owners' travelling patterns and usage, EVs' type, the capacities of their batteries, and the arrival and departure times, investigating the impact of V2G and V2H technologies on the increase of energy efficiency at both home and distribution network levels. ***(This objective has been addressed in Chapter 5).***
- Investigation of the potential benefits of EVs battery storage and V2G technology to provide grid frequency response services and proposing an optimal strategy for EV charging management aiming to stabilise the power grid and fulfil the driving demand of EV's owners. ***(This objective has been addressed in Chapter 6).***

- Modelling and investigation of Peer-to-Peer energy sharing with stochastic models of different types of households equipped with PV distributed generation and EVs. Evaluation of the impact of the P2P market on smoothing of the electricity demand in community microgrids through the participation of residents in such markets. ***(This objective has been addressed in Chapter 7).***

1.3 Key Contributions

This section outlines the main contributions of this thesis, which are discussed from both the home-level and the power grid perspectives.

At the home level, firstly in Chapter 4, we have proposed a new and flexible DR strategy to make optimal decisions to schedule the operation of smart home appliances by shifting controllable appliances from peak periods to off-peak hours. RL, a goal-oriented decision method, is used to deal with dynamic electricity prices and different power consumption patterns. We have also designed a human comfort-based control approach for HEMS to increase the user's satisfaction as much as possible while participating in DR schemes. Four comfort-factor have been used namely, the priority of the appliance to be shifted, the appliances power rating, the operating time interval, and the waiting time. In Chapter 5, we have designed an effective DR strategy for V2G and V2H energy management to make optimal decisions to charge or delay the charging of the EV battery pack and/or dispatch the stored electricity back to the grid without compromising the driving needs. In this chapter, simulations are presented to demonstrate how the proposed DR strategy can effectively manage the charging/discharging schedule of the EV battery and how V2H and V2G can contribute to smooth the household load profile, minimise electricity bills and maximise revenue.

On the power grid side, we have developed an optimal real-time V2G control strategy for EVs to perform frequency regulation in Chapter 6. In the proposed V2G control strategy, a Deep Deterministic Policy Gradient (DDPG) agent is used to dynamically adjust the V2G power scheduling to satisfy the driving demand of EV users and simultaneously perform frequency regulation services. The proposed strategy is validated on a two-area interconnected power system with 100 EV charging stations each accommodating 500 EVs. The EV parameters such as arriving time, departure time, and the initial and the expected State-of-Charge (SOC) of EV batteries are generated randomly using Monte Carlo simulations. Along with the higher local consumption of renewable energy, P2P electricity trading can help reduce investments related to the generation capacity and transmission infrastructure needed to meet the peak demand. To

this end, we have addressed the energy cost minimisation problem associated with P2P energy sharing among smart homes in Chapter 7. A P2P pricing mechanism is proposed to motivate individual customers to participate in energy trading and ensure that not a single household would be worse off. The P2P energy trading market is modelled considering the uncertainties in household demands, PV generation and EVs flexibility. The performance of the proposed pricing mechanism is compared with three popular P2P sharing models in the literature namely the Supply and Demand Ratio (SDR), Mid-Market Rate (MMR) and bill sharing (BS) considering different types of peers equipped with solar panels, electric vehicle, and domestic energy storage system.

1.4 Thesis Organisation

The rest of this thesis is organized as follows:

Chapter 2 firstly provides a comprehensive background on smart grids and related technologies and discusses the current developments of smart grids across the globe. Secondly, we present a state-of-the-art of DR management and its enabling technologies. Finally, DR programs, benefits and applications are highlighted in this chapter.

Chapter 3 discusses the application of Machine Learning tools to DR in more detail, with a focus on fuzzy logic, neural networks, and deep reinforcement learning. This Chapter provides an overview of Machine Learning methods utilised for DR applications.

Chapter 4 focuses on energy management at the home level. In this chapter, we propose an effective energy management system for residential DR using Reinforcement Learning (RL) and Fuzzy Reasoning (FR). The proposed strategy aims to make optimal decisions to schedule the operation of smart home appliances by shifting controllable appliances from peak periods, when electricity prices are high, to off-peak hours, when electricity prices are lower without affecting the customer's preferences.

Chapter 5 investigates the integration of EVs into DR programs, and how consumers can benefit from their EVs while parked at home in smoothing their household load profile, minimising electricity bills and maximising revenue.

Chapter 6 focuses on the potential benefits of EVs battery storage and V2G technology to provide grid frequency response services and improve the stability of the power grid. Thus, an optimal real-time V2G control for EVs is proposed to perform supplementary frequency

regulation and simultaneously maximise the benefits of EV owners while fulfilling the driving needs of EV owners.

Chapter 7 focuses on the energy sharing problem within a residential community. A P2P pricing mechanism is proposed and tested on a community consisting of 100 households to incentivise individual customers to participate in energy trading and to ensure that not a single household would be worse off with considering the physical network constraints.

Chapter 8 concludes the work presented in the thesis. The main findings of the research are summarised, and some future research directions are given.

1.5 List of Publications

- Alfaverh, F., Denaï, M. and Sun, Y., 2020. Demand response strategy based on reinforcement learning and fuzzy reasoning for home energy management. *IEEE access*, 8, pp.39310-39321.
- Alfaverh, F., Denaï, M. and Sun, Y., 2021. Electrical vehicle grid integration for demand response in distribution networks using reinforcement learning. *IET Electrical Systems in Transportation*, 11(4), pp.348-361.
- Alfaverh, F., Denaï, M. and Sun, Y., 2023. Optimal vehicle-to-grid control for supplementary frequency regulation using deep reinforcement learning. *Electric Power Systems Research*, 214, p.108949.
- F. Alfaverh, M. Denai and Y. Sun, 2023. "A Dynamic Peer-to-Peer Electricity Market Model for a Community Microgrid with Price-Based Demand Response," *IEEE Transactions on Smart Grid*, vol. 14, no. 5, pp. 3976-3991.
- F. Alfaverh, M. Denaï and Y. Sun, 2023. "User Comfort-Oriented Home Energy Management System Under Demand Response," *2023 IEEE IAS Global Conference on Emerging Technologies (GlobConET)*, London, United Kingdom, 2023, pp. 1-7

Chapter 2 Background and Literature Review

2.1 Introduction

Electricity demand has dramatically increased over the past few years along with the rapid growth in the world's population, the industrial and technological developments, reaching approximately 25,300 terawatt-hours in 2021 as shown in Figure 2-1. Between 1980 and 2021, electricity consumption has more than tripled, while the global population increased by roughly 75 %. Industrialisation and economic growth across the globe have further boosted electricity demand [3].

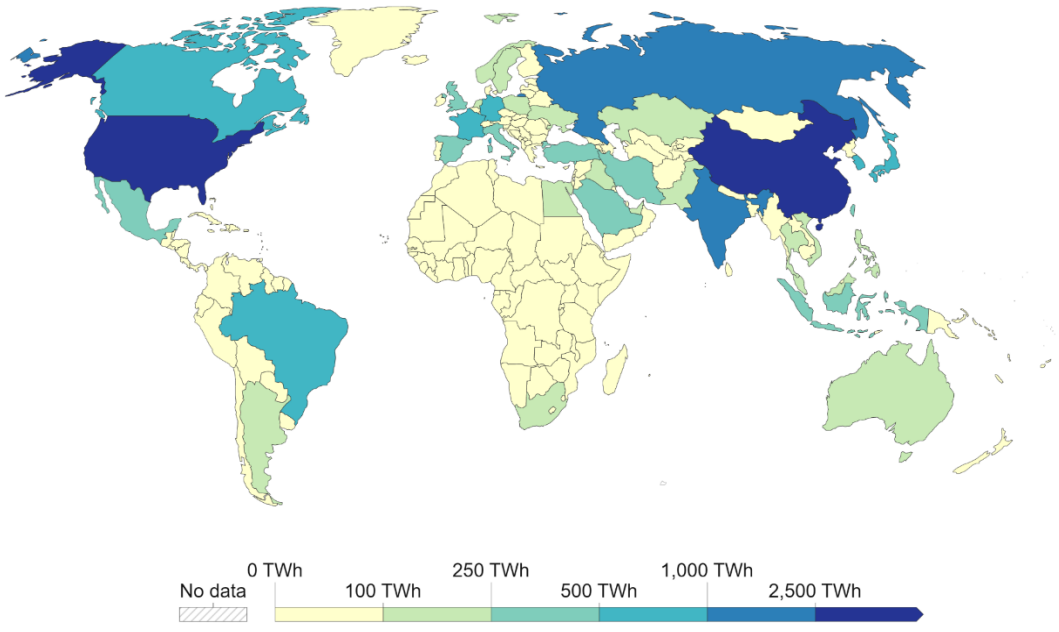

Figure 2-1 Global electricity demand in 2021 [4].

This energy production largely relies on fossil fuel resources such as oil, natural gas, and coal, as 80 % of the current global primary energy demand covered by fossil fuel sources. Figure 2-2 presents the electricity generation from fossil fuels in different countries [5]. For example, the United States produced 2500 terawatt-hour of electricity from fossil fuels in 2021. However, when fossil fuels are burned to generate electricity, they release large amounts of greenhouse gases, such as carbon dioxide and methane, into the atmosphere, which trap heat and contribute to global warming. Figure 2-3 shows the trend in global emissions of carbon dioxide (CO_2) over time. It can be noted that the increase in CO_2 emissions was relatively slow

until the mid-20th century. In 1950, a total of 6 billion tonnes of CO_2 has been recorded. By 1990, the global emissions have reached more than 22 billion tonnes. Indeed, these emissions have continued to grow rapidly and reached over 35 billion tonnes in 2021 [6].

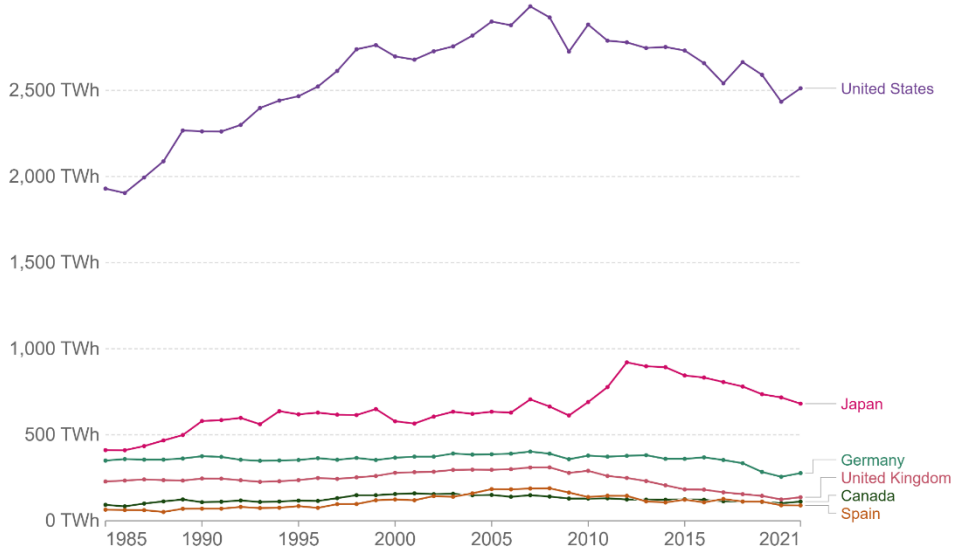

Figure 2-2 Electricity generation from fossil fuels. [5]

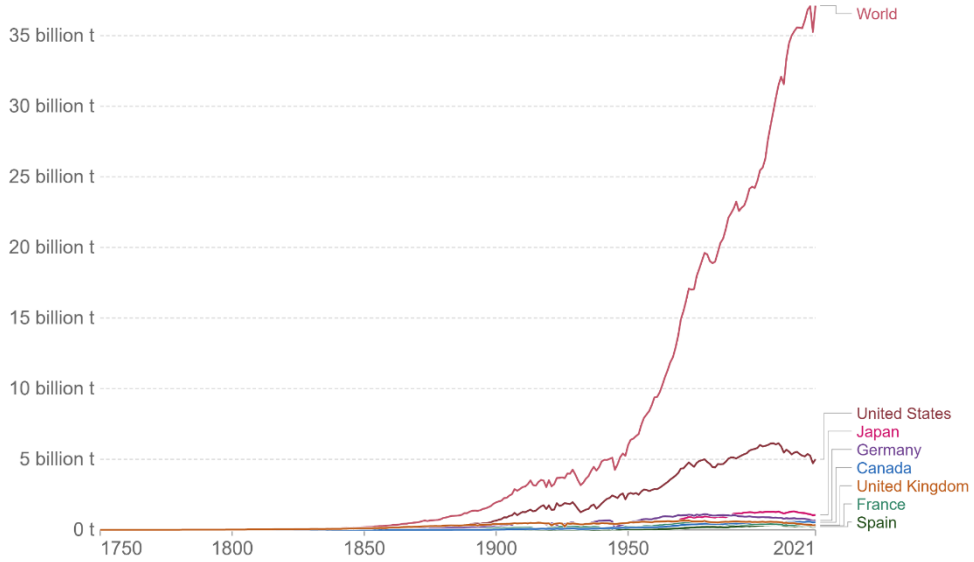

Figure 2-3 Annual CO_2 emissions. [6]

Furthermore, the rapid increase in energy demand had a negative impact on the flexibility and reliability of the electricity network. In addition, this unprecedented demand for energy imposed new investments for the reinforcement and expansion of power grid infrastructures to ensure the balance between supply and demand which has led to higher electricity prices. According to the International Energy Agency (IEA) reports published in January 2022 [7], the price index for major wholesale electricity markets, across the globe, has almost doubled. In

Europe**,** the average wholesale electricity prices in the fourth quarter of 2021 were more than four times those experienced during 2015-2020. Besides Europe, there were also sharp price increases in Japan and India.

Consequently, the supplier-consumer unidirectional model has been transformed into a bidirectional model that allows two-way flows of both electricity and information. This transformation has introduced the Smart Grid (SG) concept which is considered as an intelligent electric network that ensures efficient energy flow control from generation to consumption. SG seeks to improve the power systems in terms of reliability, security, economics and efficiency. The reliability of the power system is improved by reducing the frequency and duration of outages, providing adequate power quality, and improving consumer services. The security of the power system is enhanced by increasing its resilience to cyber-attacks and natural disasters and hazards. In terms of economics, SG helps with reducing future electricity prices and offering consumers options to manage and control their energy consumption leading to reduced electricity bills. SG improves the efficiency of the power system by reducing transmission and distribution losses, maintenance and expenditures. In addition, SG brings great environmental benefits by enabling the large-scale deployment of renewable energy resources leading to reduced emissions of greenhouse gases.

Advanced Information and Communication Technologies (ICT) enable consumers to become key players in the future SG since they can adjust their electricity usage patterns and preferences in response to signals received from the utility (incentives and disincentives). This leads to another term in SG called Demand Side Management (DSM), which can be defined as "*the technologies, actions and programmes on the demand-side of energy metres that seek to manage or decrease energy consumption, in order to reduce total energy system expenditures or contribute* to achieve *policy objectives such as emissions reduction or balancing supply and demand.*" [8].

Therefore, Demand Response (DR) is considered one of the DSM's techniques, where power utilities provide incentives to consumers to reduce their energy usage during peak hour periods. DR is, indeed, a promising solution for end-users to manage their power consumption based on different techniques such as peak clipping, valley filling, or load shifting in response to electricity tariffs or other incentives from their energy suppliers.

This chapter presents a comprehensive literature review on SGs, DR management in SGs and different approaches to promote DR implementation in the residential sector, such as Home

Energy Management System (HEMS), Vehicle-to-Grid (V2G) and Peer-to-Peer (P2P) energy sharing to maximise the benefits for both power utilities and consumers.

2.2 Smart Grid

Future electricity grids are expected to make extensive use of modern ICT to enhance the resilience and performance of the network and provide secure, flexible, and cost-effective services. Various definitions of the SG have been used by different countries across the globe and no single universal definition has been agreed on. According to the European Technology Platform, "*A Smart Grid is an electricity network that can intelligently integrate the actions of all users connected to it—generators, consumers and those that do both—in order to efficiently deliver sustainable, economic and secure electricity supplies."* [9].

Another definition for SG by the US Department of Energy stating that: *"An automated, widely distributed energy delivery network, Smart Grid will be characterized by a two-way flow of electricity and information and will be capable of monitoring everything from power plants to customer preferences to individual appliances. It incorporates into the grid the benefits of distributed computing and communications to deliver real-time information and enable the near-instantaneous balance of supply and demand at the device level"* [10].

In 2014, the UK Government set out its vision for SG and defined it as: *"A modernised electricity grid that uses information and communications technology to monitor and actively control generation and demand in near real-time, which provides a more reliable and cost-effective system for transporting electricity from generators to homes, business and industry."*[11]

Figure 2-4 depicts the worldwide market development of modern networks from 2017 to 2023 by region [12]. It is noted that SG technologies are growing gradually around the world and the global market is expected to triple in size reaching a total of $61 billion. The leading countries which are currently upgrading and modernising their electricity networks with SG technologies include Europe, North America, and Asia Pacific with investments' values $15.4, $16.8, and $17.9 billion, respectively. It can be noted that Asia Pacific has the highest investment in SG technology development and is predicted to be the largest market for SG technologies.

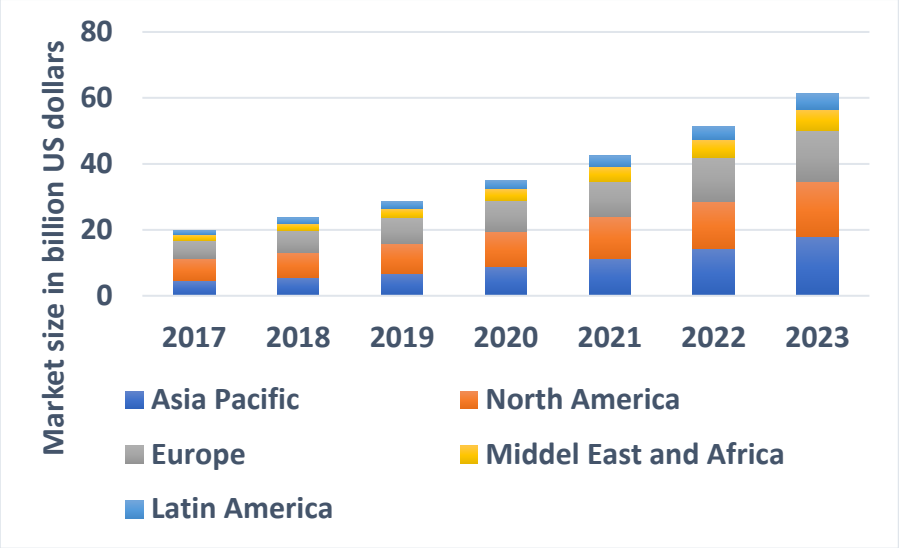

Figure 2-4 Market value of SGs worldwide from 2017 to 2023, by region.

Many countries have focused on developing their power grids and adopting different approaches and roadmaps according to their needs. The United States has started working on this by establishing policies for SG, which was echoed in two Acts, the first one is the Energy Independence and Security Act of 2007 [13] that aimed to specify and establish a coordinated fund program to invest in SG. The second policy was the American Recovery and Reinvestment Act of 2009, that aimed to modernise the country's infrastructure to achieve energy independence by 2020 [14].

In the UK, a significant progress has been made in the deployment of SG technologies, including research, development, and demonstration projects. These projects have been delivered through a range of initiatives, including the Office of Gas and Electricity Markets (Ofgem) price control model, which aimed to place great emphasis on supporting grid innovation; and the creation the Low Carbon Networks Fund (LCNF) that devoted £500 million to network companies to undertake innovation projects and implement new SG technologies and solutions. The UK has already started deploying mart meters in all residential areas and small businesses. A total of £8.6 billion have been spent on the replacement of gas and electricity meters. The total suppliers' benefits reached £6.33 billion, including £2.69 billion saved from manual meter reading, and £1.13 billion from reducing inquiries and customer overheads. On the other hand, the total consumer's benefits were £6.43 billion, including energy savings (£4.23 billion) and load shifting (£1.06 billion).

In Europe, the deployment of SGs is one of the three priority thematic areas under the Trans-European Networks for Energy (TEN-E), aiming to integrate renewable energy sources and

allow consumers to better regulate their energy consumption. By 2024, it is expected that 225 million smart meters will be deployed in the European Union (EU) [15].

According to the European Environment Agency (EEA) report "Trends and Projections in Europe 2021", European Union (EU) has achieved its three 2020 climate and energy targets of reducing greenhouse gas emissions by 20%, increasing renewable energy to 20% and making 20% energy efficiency improvement [16].

Essentially, SG seeks to improve energy generation, transmission, and distribution by integrating smart metering/monitoring and bi-directional communication. Figure 2-5 illustrates a general architecture of a SG infrastructure which integrates energy and information flow, with a communication infrastructure to support: 1) advanced electricity generation, delivery, and consumption; 2) advanced information metering, monitoring, and management; and 3) advanced communication technologies.

This smart infrastructure offers a reliable energy delivery from generation sources including local, renewable, and distributed generation to end users including industrial, commercial, and residential consumers. Using remote control and condition monitoring, power disturbances and outages caused by equipment failures, capacity constraints, and natural accidents and disasters, can be largely avoided. Integrating large-scale energy storage technologies into the SG will enhance the stability and flexibility of the power grid. Energy storage contributes to different services to the power system such as energy management, load shifting, frequency regulation and peak shaving. End-users can also benefit from residential energy storage systems which allow a more efficient exploitation of their local renewable energy sources, less dependent on the grid and lower electric bills. Smart meters, which enable two-way communication, ensure more accurate bills for consumers, and enable them to better control their energy usage. The distribution automation is associated with smart meters, by collecting information faster and providing a wide-area monitoring and linking devices across the grid.

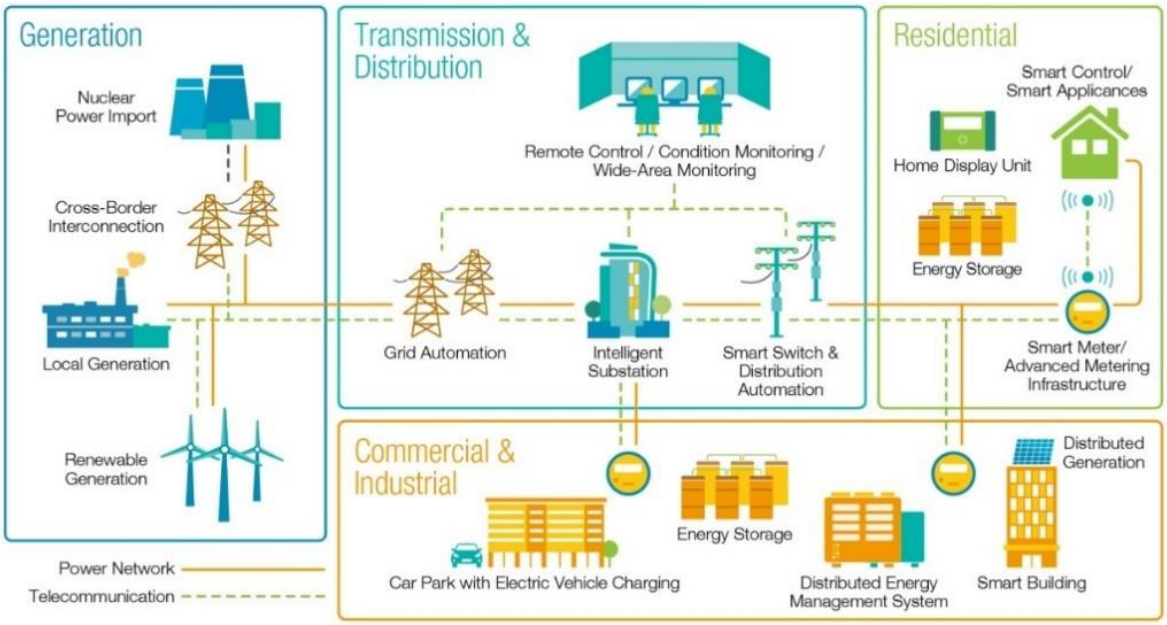

Figure 2-5 General architecture of a smart grid infrastructure [17].

With the development of SGs, the influence of various energy management programs has been enlarged and promoted. In general, these programs aim to reduce consumption in peak demand periods or shift consumption from peak demand periods to off-peak demand periods. Among these programs, DR has received increasing interest due to its ability to engage customers and increase their flexibility during their energy consumption.

2.3 Demand Response in Smart Grid

2.3.1 Concept

DR programs are being introduced by some electricity grid operators as resource options for curtailing and reducing the electricity demand during certain time periods for balancing supply and demand. DR is considered as a class of DSM programs, where utilities offer incentives to end-users to reduce their power consumption during peak periods [18]. DR is, indeed, a promising opportunity for consumers to control their energy usage in response to electricity tariffs or other incentives from their energy suppliers [19], [20]. Therefore, DR refers to "*changes in electric usage by end-use customers from their normal consumption patterns in response to changes in the price of electricity over time, or to incentive payments designed to induce lower electricity use at times of high wholesale market prices or when system reliability is jeopardized*" [21]. DR aims to promote the interaction and responsiveness of the customers to achieve short-term impacts on the electricity markets, leading to economic benefits for both the customers and the utility. Moreover, by improving the reliability of the power system and,

in the long term, lowering peak demand, it reduces the overall plant and capital cost investments and postpones the need for network upgrades.

2.3.2 Classification of DR programs

Generally, DR schemes are commonly classified into two categories namely incentives-based programs and price-based programs as shown in Figure 2-6. According to some studies, these schemes have other names, such as “system-led” and “market-led,” “emergency-based” and “economic-based” or “direct” and “indirect” DR.

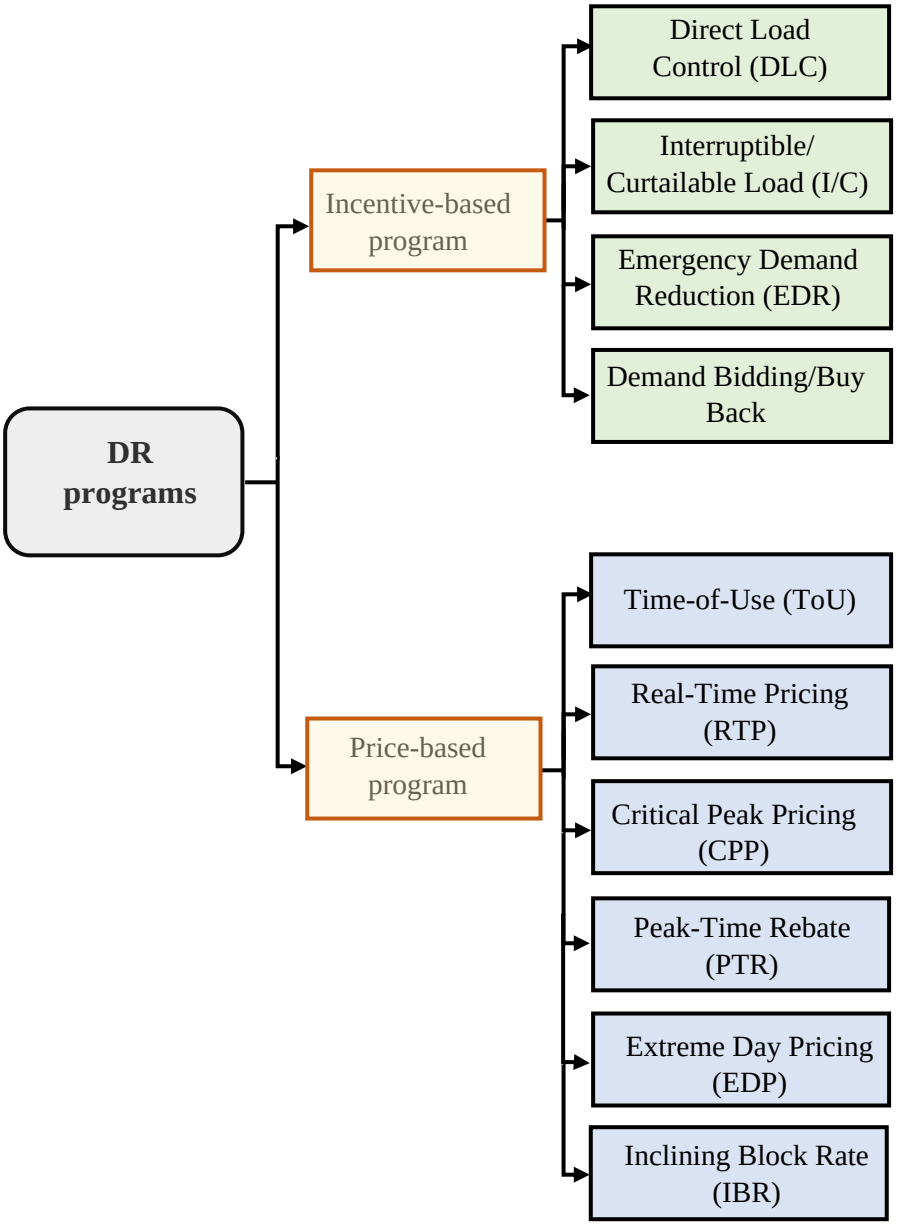

Figure 2-6 Demand Response programs.

A. Incentive-based DR

In incentives-based programs, participants receive fixed or time-varying payments for their consent to reduce power consumption during peak demand or system contingencies. They can be classified into two categories: classical programs and market-based programs. Participating in classical programs offers participation payments such as bill credits or discount rates. In market-based programs, customers receive monetary rewards depending on their performance after they consent to reduce their power consumption during peak periods [22].

Incentive-based programs include Direct Load Control (DLC), Interruptible/Curtailable (I/C) and Emergency DR programs. DLC programs are considered as classical incentive-based programs. They enable utility companies to remotely turn off consumers' electrical loads. Participants in this program receive payments in return of reducing their energy usage below a pre-defined threshold.

Many studies have been undertaken on load management using DLC to design optimisation methods aiming to achieve different objectives such as peak load reduction, cost saving and power shortage minimisation. Using DLC, it is essential to encourage end-users to actively participate in the program to maintain their comfort level and gain financial benefits. In [23], the authors proposed an Advanced Direct Load Control (ADLC) model to temporarily shut down the electric connection between the power grid and smart houses. The simulation results show that smart houses equipped with ADLC can reduce operating costs and lower their CO_2 emissions. In [24], a thermodynamic model has been designed for a water heater and controlled using the DLC program. The results show that electricity usage has been significantly reduced for consumers without affecting their lifestyle. DLC program is also used in [25] to control air conditioners considering the users' comfort.

In I/C DR programs, the power utility can curtail a specific part of the total users' consumption to a certain level during emergency situations and, in return, participants are offered economic incentives. Consumers who do not reduce their energy consumption receive penalties as per the program's pre-defined terms and conditions. Emergency DR programs are a combination of both DLC and I/C programs and are considered as market-based programs. The authors in [26] studied the impacts of changes in incentives and penalties on the microgrid using I/C program considering the operation cost, customer profit and load reduction. In [27], the authors investigated the effect of emergency DR in improving the reliability of the power system in case of failure of generation units.

B. Price-based DR

Price-based programs, on the other hand, can be considered as an indirect means of controlling customers' loads. Using these programs, time-varying prices are offered to customers based on electricity costs at different time periods. Customers willing to reduce their energy usage during peak hours, when electricity prices are high, can participate in these programs. They are expected to adjust their demand in response to electricity price signals [28]. Price-based programs are of: Time-of-Use (TOU) pricing, Real-Time-Pricing (RTP), Critical Peak Pricing (CPP), Peak-Time Rebate (PTR), Extreme Day Pricing (EDP), and Inclining Block Rate (IBR).

In the TOU tariff plan, electricity pricing varies depending on the time of the day, day of the week and season. It includes three time periods namely, off-peak, mid-peak and on-peak. TOU pricing is easy to follow and gives participants the opportunity to take control of their energy usage by shifting their electricity consumption to lower-price hours. The study presented in [29] investigated the impacts of TOU implementation on consumption patterns in residential customers. The results show that an effective TOU is urgently required with a high penetration level of renewable energy. The authors in [30], studied the implementation of the TOU program for industrial consumers. However, while TOU pricing reduces electricity demand during peak hours, the risk is this may create a similar or larger peak demand during off-peak periods [31]. Under RTP, electricity prices change over short time periods typically hourly or less and are announced in advance by energy suppliers. RTP is considered as one of the most efficient DR programs. With RTP, smart homes receive the electricity price signals in real-time and users can instantly and adequately control and manage their energy consumption in response to the energy prices. CPP programs are used when the reliability of the system is compromised, or the generated energy cost is higher. Thus, electricity prices under these conditions will be higher than standard rates (based on the TOU program). The period of this critical peak occurs usually only a few days or hours per year. Therefore, the CPP tariffs are like the TOU rates, which provide higher prices during peak hours. Under PTR, which is also called Critical Peak Rebate (CPR), small residential and commercial users will be offered flat prices. Consumers are be rewarded if they reduce their energy usage during peak hours, otherwise they are required to pay the electricity price at the standard rate. The EDP scheme uses a similar technique to TOU program, but it applies a higher electricity price for a limited number of days. The EDP has only one difference from the CPP, which is that the standard electricity price is provided only one day before the actual implementation. Therefore, the Extreme Day CPP (ED-CPP) program can also be used as a DR program which has the specifications of both

CPP and EDP schemes. The IBR program has a two-level rate structure with lower and higher electricity prices. It aims to incentivise users to avoid high prices by distributing their consumption across different periods of the day.

2.4 Enabling DR Technologies

DR management requires collecting and storing massive data on the power consumption of each consumer, generation from renewable energy resources, and energy storage state of charge. It also seeks to exchange this amount of data in real-time with power utilities to provide services such as time-based pricing signals, load management, and electricity bills. Thus, an AMI must be in place. AMI is an integrated system containing smart meters with communication networks, such as home area networks (HANs), wide area networks (WANs), and neighbourhood area networks (NANs), which provides several improvements over the previous Automated Meter Reading (AMR) and Automatic Meter Management (AMM) technologies. Figure 2-7 illustrates the information and data flow in an AMI.

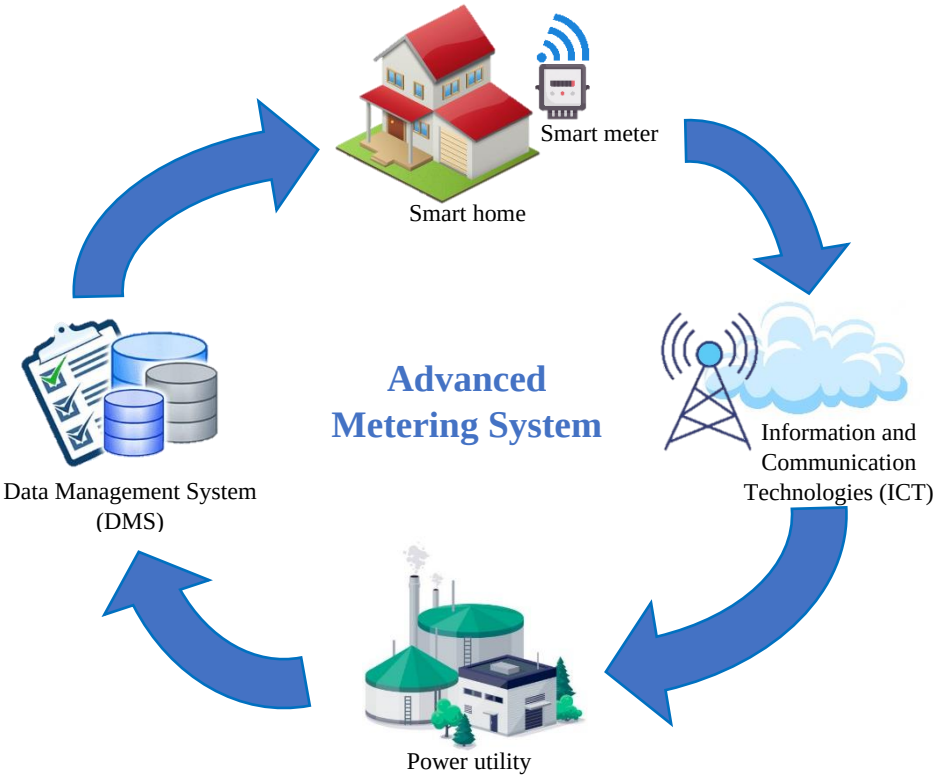

Figure 2-7 Architecture of the Advanced Metering Infrastructure (AMI) system.

AMI aims to efficiently facilitate DR implementation by improving the measurement and transmission of energy consumption data via a bidirectional information flow between power utilities and consumers. For power utilities, AMI can provide many benefits, such as the ability

to automatically and remotely record energy usage, control/manage loads, detect tampering, identify and isolate outages, and monitor voltage. Combined with customer technologies, such as a Human-Machine Interface (HMI), programmable communicating thermostats and HEMS, AMI also enables end-users to be better aware of their power usage and make sensible decisions to control and manage their energy consumption and storage, hence reducing their electricity bills and contributing to peak demand minimisation.

2.4.1 Smart meters

A smart meter is an advanced electricity measurement device that collects consumers' total energy consumption data and sends it to the power utility to be utilised for different purposes such as monitoring and billing. In addition, the smart meter is an enabling technology for the deployment of DR programs in the residential sector due to its ability to, remotely, disconnect/reconnect some specific loads. The smart meter also plays an important role in the implementation of HEMS in smart homes by monitoring and controlling the user's appliances based on the preference settings of the user.

From the end user's perspective, smart meters inform customers how much energy they are using through an In-Home Display (IHD). This information helps customers manage their energy use and save on their energy bills hence contributing to GHG emissions reduction. Furthermore, smart meters communicate automatically with energy suppliers, which avoids manual meter readings and provides customers with more accurate bills. From the power grid's perspective, real-time electricity pricing can be issued based on the data collected from smart meters, and then sent to consumers in order to incentivise them to reduce their electricity usage during peak demand periods. This can help in improving the reliability and stability of the power system.

Nowadays, several millions of smart meters have been deployed all over the world. In the UK, smart meters were introduced in 2011. According to the report published by the UK government in Smart Meter Statistics in Great Britain, 28.8 million smart and advanced meters were installed in homes and small businesses across the UK at the end of March 2022. In the UK, 51% of all energy meters are now smart or advanced meters, with 25.2 million operating in smart mode [32].

2.4.2 Information and Communication Technologies (ICT)

The collected information using smart meters needs to be transferred to Meter Data Management System (MDMS) for analysis to enable power utilities make decisions regarding

pricing, billing, energy management and other operational commands. This issued data is then sent back to end-users to inform them about new electricity prices and their energy costs. This makes users more aware of their bills hence motivating them to better manage their energy consumption. Considering the high number of end-users and installed smart meters at their premises, an effective and reliable communication network is needed for transferring that high volume of data. Thus, two-way communication plays a crucial role in AMI.

To design an appropriate communication network, some factors must be carefully considered, such as the transmission of a massive amount of data, restrictions on data accessibility, confidentiality of sensitive data and others. Generally, communication networks can be divided into three main categories based on the geographical area namely Home Area Network (HAN), Neighbourhood Area Network (NAN) and Wide Area Network (WAN) as presented in Figure 2-8. HAN represents the interface between the smart meter and various household appliances such as solar PV panels, EV and HEMS (managing energy consumptions, storage and generation devices for the home). Therefore, the logged data in this network area does not require a high transmission rate. For HAN, Zigbee communication technology is used and developed according to the IEEE 802.15.4 standard to transmit data at a rate of 250 kbps at 2.4 GHz frequency. Although this technology can cover only a small area, it shows good performance in HAN due to its lower power consumption characteristic, lower installation costs and higher reliability. Bluetooth technology is another communication technology used for HAN that is developed based on IEEE 802.15.1 standard to transmit data at a rate of 721 kbps and a frequency of 2.4 GHz. Since Bluetooth has a lower power consumption, its capability of massive data transmission is limited.

NAN provides an information flow between consumers and the power utility via smart meters. This network enables various services such as monitoring, controlling and pricing energy delivery to each end-user, demand response, distribution automation and outage management. Due to the huge amount of data collected, this requires a high data rate and large coverage distance. Different communication technologies such as Wi-Fi and Power Line Communication (PLC) are widely used for NAN. The third network is WAN which is considered as the backbone of the communication network in the power grid. This network connects smaller distributed networks such as transmission substations, and control centres for different applications including real-time monitoring, control and protection. Therefore, these applications require a higher number of data points at high data rates (10 Mbps - 1 Gbps), and

long-distance coverage (10 - 100 km). The communication technologies used for WAN are GSM, 3G, and WiMAX.

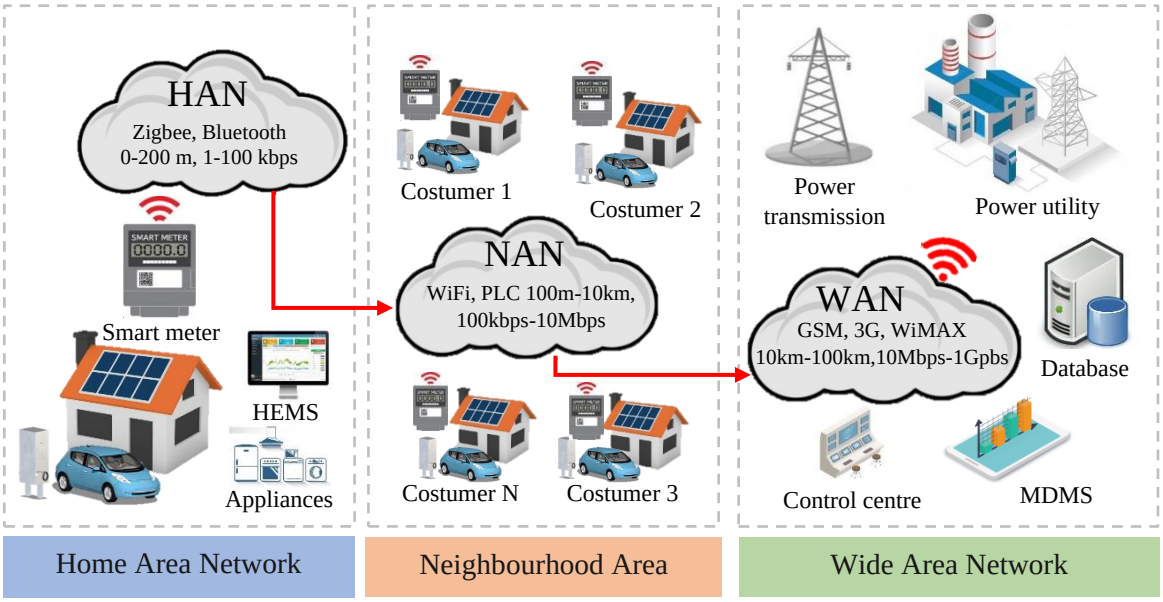

Figure 2-8 Communication networks of smart grid.

2.4.3 *Meter Data Management Systems*

MDMS is considered as the key element in AIM. This system aims to collect the data from different smart meters, then process and store them properly to be used for various functions such as DR implementation, load forecasting and load management as shown in Figure 2-9. According to [33], MDMS can be defined as *"a meter data management system (MDMS) collects and stores meter data from a head-end system and processes that meter data into information that can be used by other utility applications including billing, customer information systems and outage management systems"*.

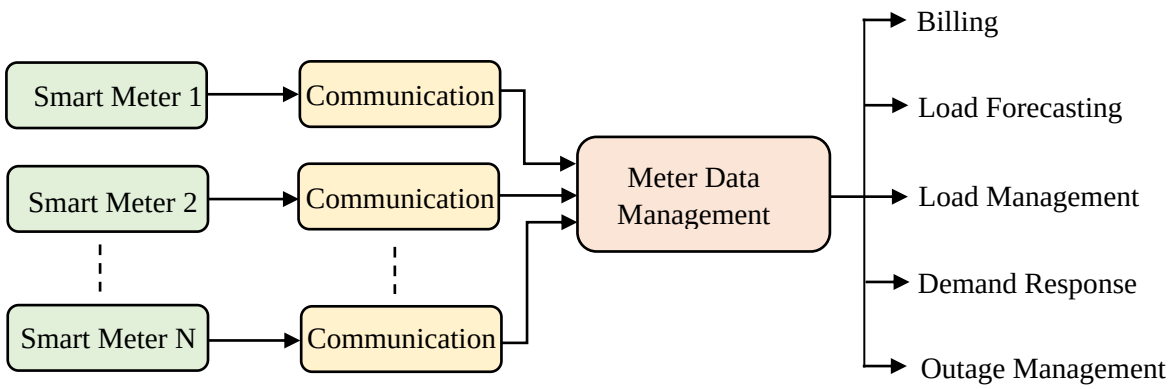

Figure 2-9 Meter Data Management functions.

2.5 Benefits of DR programs

In a power system, there are many independent players who can benefit from DR programs, these include transmission and distribution system operators, end-users and the environment. Figure 2-10 summarises the benefits that can be obtained from DR for end-users, the grid, and the environment.

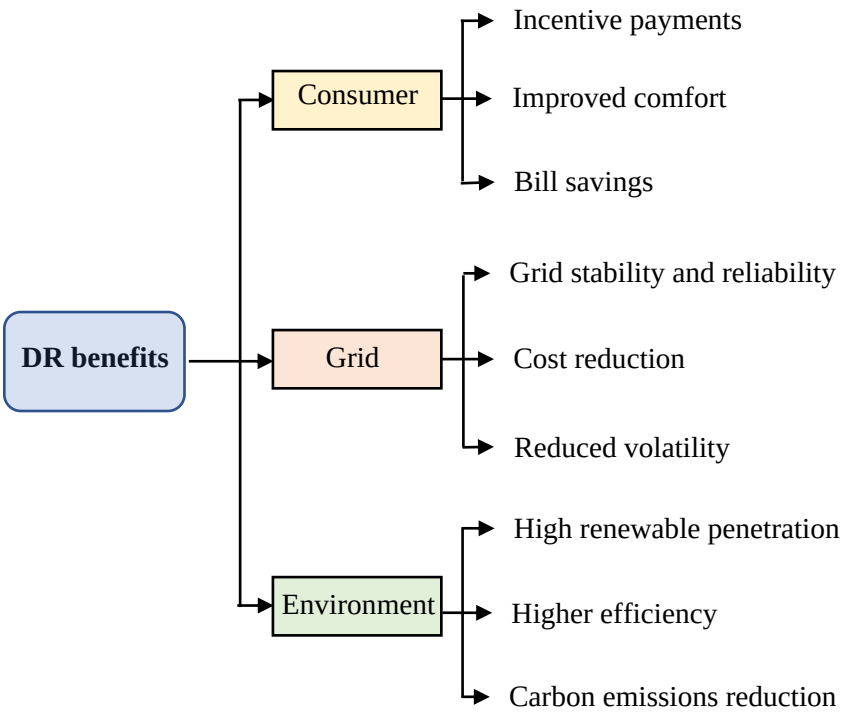

Figure 2-10 Benefits of DR programs.

- *Grid perspective*: DR programs can provide a more efficient and cost-effective way of reducing the energy demand during peak periods and limiting the activation of expensive peak generators. This results in an overall reduction of carbon emissions and electricity prices. In addition, DR schemes can improve the reliability of the power grid due to the dynamic curtailment in loads leading to reduction of outages risks and power losses in transmission lines. Furthermore, DR programs can contribute to higher penetration of renewable energy resources at a large scale due to their ability to mitigate the fluctuation caused by such resources. The peak demand reductions achieved by smart management reflect a reduced need for infrastructure upgrades, decreased overall investment and operating costs, and thus increased overall market efficiency.
- *End-user perspective*: with the deployment of DR schemes, consumers can have an opportunity to considerably reduce their electricity bills due to the efficient usage of energy. Shifting loads to low peak periods enables consumers to capitalise on reduced

electricity prices to minimise their energy costs. End-users can also obtain financial rewards upon agreeing to control their loads during peak demand hours or higher generation from RES. In addition, DR programs increase the awareness of consumers regarding their electricity consumption, thus contributing to promote the increased adoption of renewable energy [34].

- *Environment perspective*: the electric power system relies largely on fossil fuel resources such as oil, natural gas, and coal to generate electricity. The utilisation of DR programs can reduce the high carbon emissions of peak generators shifting the electricity demand to off-peak hours. DR brings great environmental benefits by enabling the large-scale deployment of RES leading to a further reduction of greenhouse gases.

2.6 DR Applications

Technologies regarding energy control/management systems, metering infrastructures including smart meters and ICT, and other technologies associated with EVs such as V2G all have, in fact, significantly promoted the adoption of DR programs at the residential level. These technologies have increased the opportunity for residential consumers to monitor and adjust their electricity usage. Therefore, these enabling technologies are crucial to successfully achieve the DR objectives.

DR schemes can be applied for residential, commercial or industrial consumers. To implement DR programs, AMI including smart meters, communication devices and energy controllers need to be installed at the consumers' premises to monitor and record the energy consumption in real-time and communicate the data to the power utility.

Domestic appliances are more curtailable, shiftable, interruptible, and flexible than other types of loads. In addition, the deployment of a two-way communication network between the power utility and homes makes residential loads suitable for DR programs among all types of consumers.

2.6.1 Home energy management system

HEMS is considered as a key technology in implementing DR programs. HEMS enables residential customers to actively participate in DR programs by controlling their energy usage and reducing or shifting their consumption outside periods of grid stress in response to financial rewards such as tax breaks or rebates. However, DR trials across the world have shown that most of the customers remain reluctant to enrol into these programs due to unwanted

interruptions and strict guidance from the utilities which cause inconvenience to the consumers. In addition, most of household consumers do not want to spend time on calculating and analysing their energy usage and scheduling their household appliances to reduce electricity consumption. Therefore, to promote DR implementation at residential customers' premises, HEMS should be more flexible and able to manage different types of household resources, such as RERs and Home Energy Storage System (HESS), and household appliances. Power consumption and electricity pricing should be offered to users in real-time to enable them to choose their preferences to schedule the operation time of various appliances via a Human-Machine Interface (HMI) which in turn improves their energy usage efficiency.

2.6.2 Electric vehicles

The widespread adoption of Electric Vehicles (EV) has led to the introduction of larger electricity consumers due to their larger energy consumption compared to all other appliances in a household, leading to severe grid problems such as network congestion and peak power demand. However, with the concept of V2G and V2H technologies, a broad range of benefits and services may be offered to achieve more effective management of electricity demand hence enabling EV owners to save on energy costs and generate revenue through price arbitrage. Therefore, EVs are considered as an important resource for managing DR, provided that an effective and flexible energy management strategy is designed for EV charging and discharging operations without compromising the owner's driving needs and convenience to maximise the profits for both the utilities and EV owners.

2.6.3 Peer-to-peer energy trading

Consumers owning local energy resources such as solar PV panels, small-scale wind turbines, and EV battery storage are referred to as Prosumers. Prosumers can directly trade their excess of local energy resources with each other without the need to go through an intermediate retailer. As some appliances in the smart home can be scheduled by using DR implementation based on RTP, the implementation of Peer-to-Peer (P2P) energy sharing in the smart home can also provide a further reduction in the electricity cost of the consumer due to energy sharing with other prosumers instead of the grid.

Chapter 3 Overview of Machine Learning Approaches for Demand Response

3.1 Introduction

Artificial Intelligence (AI) is a broader concept that encompasses the simulation of human intelligence in machines, aiming to perform tasks that typically require human intelligence, such as problem-solving, understanding natural language, and making decisions. AI can encompass various techniques, including Machine Learning (ML). On the other hand, ML is a subset of AI that focuses on the development of algorithms and statistical models that enable computers to learn from and make predictions or decisions based on data without explicit programming. Essentially, while AI represents the broader goal of creating intelligent machines, ML serves as one of the key methodologies within AI to achieve that goal, primarily by training models to improve their performance over time through data-driven learning processes. The widespread adoption of ML is revolutionising industries such as healthcare, finance, transportation, manufacturing, and more. It enables organisations to use the power of data and advanced analytics to gain valuable insights, automate processes, and optimise performance, leading to improved outcomes and competitive advantages.

For example, in healthcare, ML is being used for disease prediction, diagnosis, personalised treatment plans, and drug discovery, leading to improved patient care and outcomes [35]. In finance, ML is being applied for fraud detection, risk assessment, portfolio optimisation, and trading strategies, contributing to more accurate financial decision-making [36]. In transportation, ML is being employed for autonomous vehicles, traffic prediction, route optimisation, and smart logistics, leading to enhanced transportation efficiency and safety [37]. In manufacturing, ML is being used for predictive maintenance, quality control, supply chain optimization, and smart manufacturing, resulting in improved production processes and cost savings [38].

These are just a few examples of the wide-ranging applications of ML in various fields. The adoption of ML is rapidly increasing due to their ability to analyse vast amounts of data, detect patterns, and make intelligent decisions. Furthermore, with advancements in technologies such

as deep learning, natural language processing, and reinforcement learning, ML is continuously evolving and enabling even more sophisticated applications.

In recent years, there has been a heightened interest in utilising DR as a means of enhancing flexibility and improving the cost-effectiveness and reliability of energy systems. However, the high complexity of the tasks associated with DR, the utilisation of extensive data, and the need for rapid and optimal decision-making have highlighted the significance of ML as key technologies for enabling demand-side response. ML techniques can address a broad spectrum of challenges, including acquiring knowledge of customers attributes and preferences, implementing dynamic pricing, scheduling and controlling devices, incentivising participants in DR schemes, and ensuring they are compensated fairly and efficiently.

Fuzzy logic (FL) is regarded as an AI-based method which emulates human reasoning and decision-making. FL allows for imprecise data analysis and can handle multiple variables. It has been used to develop control strategies for DR by adjusting heating and cooling systems based on occupancy levels and outside temperature. Neural Networks (NN), on the other hand, are a type of ML that can learn and model complex and nonlinear relationships between inputs and outputs. They have been used in DR for predicting energy consumption patterns based on historical data. Finally, Deep Reinforcement Learning (DRL) is a more advanced form of ML that uses trial-and-error to optimize energy consumption. It has been used to develop DR strategies for large industrial consumers.

In this chapter, we will discuss the application of these ML tools to DR in more detail, with a focus on fuzzy logic, neural networks, and deep reinforcement learning. This Chapter provides an overview of ML methods utilised for DR applications.

3.2 Fuzzy Logic (FL)

FL, by Lotfi Zadeh in the 1960s, is based on the idea that numerous concepts and variables in the real world cannot be precisely defined using crisp numerical values. This is due to the fact that certain terms, such as "hot," can hold different meanings for different people and may not be associated to an exact temperature value that corresponds to the concept of "hot." As a result, FL provides a more adaptable and refined method of representing these concepts by assigning degrees of membership to values that capture them.

FL has been used in a variety of applications, such as control systems, decision-making, pattern recognition, and data modelling. In control systems, it can be used to adjust the output of a

system based on multiple input variables, such as temperature and humidity, and their degrees of membership in the fuzzy sets. In decision-making, FL can be used to evaluate the uncertainty and imprecision of data and make decisions based on fuzzy rules.

As FL deals with approximate values rather than exact values. A Fuzzy Inference System (FIS) provides the mapping from the inputs to the outputs, based on a set of fuzzy rules and associated fuzzy Membership Functions (MFs). There are two types of FIS, Mamdani-type FIS and Sugeno-type FIS. Figure 3-1 shows the block diagram of Fuzzy Logic Controller (FLC).

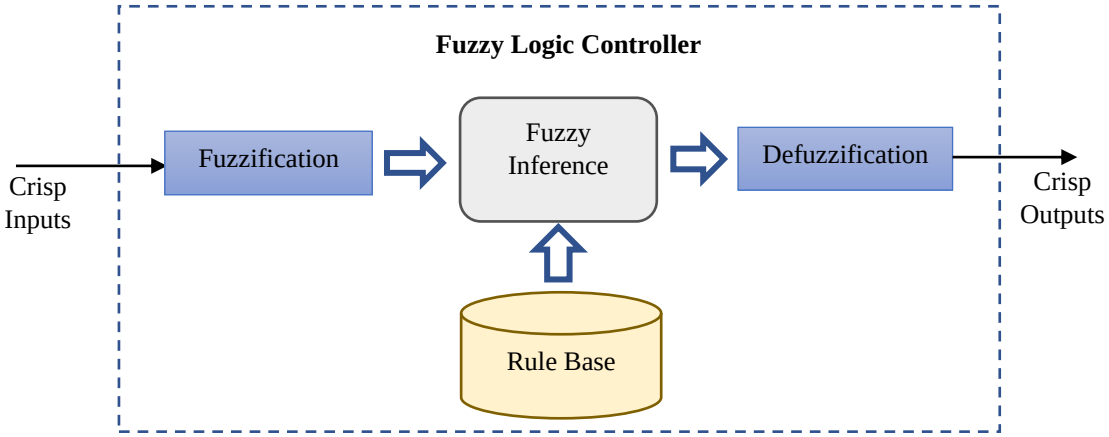

Figure 3-1 Block diagram of a FLC.

FL can be applied to a problem by taking following steps:

- Define the problem and identify the variables involved to determine the inputs and outputs of the fuzzy logic system.
- Determine the fuzzy sets and their membership functions: The next step is to determine the fuzzy sets for each input and output variable. This involves defining the range of values for each variable and assigning membership functions that describe the degree of membership of a particular value to a particular fuzzy set.
- Define the rules: The rules define how the inputs are combined to produce the output. These rules are usually expressed in the form of "if-then" statements, where the "if" part corresponds to the inputs and the "then" part corresponds to the output.
- Fuzzification: The next step is to fuzzify the input variables. This involves determining the degree of membership of each input value to each fuzzy set.
- Apply the rules: The fuzzy logic system applies the rules to the fuzzified input variables to determine the degree of membership of each output value to each fuzzy set.

- Defuzzification: The final step is to defuzzify the output variables to obtain crisp values. This involves determining the degree of membership of each output value to each fuzzy set and combining them to obtain a single crisp value for each output variable.
- Evaluate the performance of the system: The performance of the fuzzy logic system can be evaluated using metrics such as accuracy, precision, and speed. The system can be refined by adjusting the membership functions and rules to improve its performance.

FL has been integrated into many software packages, including MATLAB and Python, which provide libraries for FL programming. In addition, FL has been combined with other AI techniques, such as neural networks and genetic algorithms, to create hybrid intelligent systems that can handle complex problems.

3.3 Artificial Neural Networks (NN)

Artificial Neural Networks (ANNs) are ML models inspired by biological neurons of the brain. They are used in various fields due to their ability to learn complex patterns and relationships in data. ANNs consist of interconnected layers of nodes (neurons), which process input signals and produce output signals that are passed to other neurons as shown in Figure 3-2. ANNs are trained using backpropagation, which adjusts the weights between neurons to minimise error. ANNs are successful in applications such as image recognition and natural language processing and continue to be an active area of research in AI.

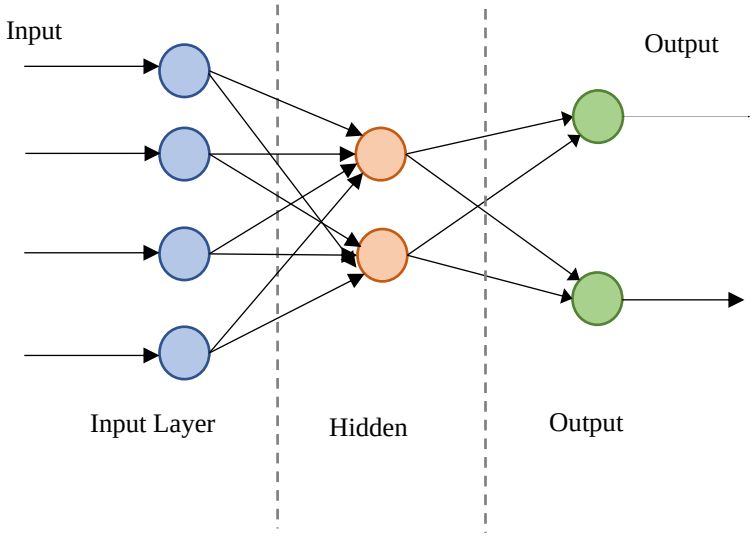

Figure 3-2 Architecture of a typical artificial neural network

ANNs have been widely used in smart grids due to their adaptability and efficiency as predicting energy demand and supply, optimising energy consumption, managing distributed energy resources, load balancing, and DR. For instance, ANNs can be employed to forecast future energy demand based on historical records and weather predictions, allowing for optimised energy production and distribution, thus improving the system's efficiency.

3.4 Reinforcement Learning (RL)

Reinforcement Learning (RL) has emerged as a promising approach to address the challenges of optimising energy management in smart grids. RL algorithms allow for the optimisation of complex decision-making processes in dynamic and uncertain environments. RL does not require a mathematical model and is suitable for complex and real-time applications.

In the context of smart grids, RL has been used to develop control policies for DR, energy storage management, and renewable energy integration. RL's ability to learn from experience makes it particularly suitable for addressing the challenges of optimising energy consumption and minimising costs, which involve large amounts of data and require near real-time decision making.

RL algorithm has six parameters namely, the agent, environment, state space S, action space A, rewards R, and action-value $Q(s, a)$. Generally, the RL-agent interacts with an environment as illustrated by Figure 3.4.

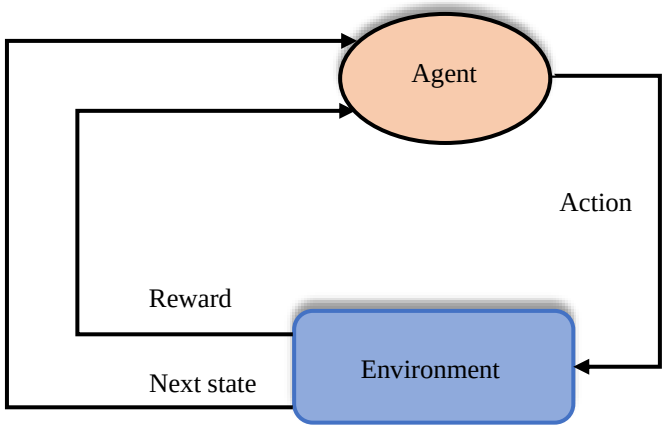

Figure 3-3 Reinforcement learning process.

Firstly, at each time step $t = \{0, 1, 2, \dots\}$, the agent executes an action according to a certain policy π at a current state $s_t \in S$. The environment then computes the new state $s_{t+1} \in S$ and a numerical reward $r(s_t, a_t)$ and feed it back to the agent in order to evaluate the action taken

as shown in Figure 3-3. Based on the reward received, the agent is able to optimise its policy π and hence maximise the total rewards it will receive in the future.

The action-value function which indicates how good is the action taken in each state is denoted by $Q_\pi(s_t, a_t)$. According to a certain policy π, $Q_\pi(s_t, a_t)$ expresses the value of action taken a_t and is selected from a valid set of actions space A in the current state s_t:

$$Q_\pi(s, a) = E_\pi[\sum_{k=0}^{\infty} \gamma^k r_{k+1} \mid s_t = s_0, a_t = a_0] \tag{3.1}$$

E_π denotes the expectation of total rewards defined by policy π. s_0 and a_0 are the initial state and initial action, respectively. γ is called the discount rate and indicates the relationship between the future and current rewards. It takes a fraction between [0, 1]. When $\gamma = 0$, the agent considers only the current reward, while $\gamma = 1$ means that the agent will strive for the future rewards. For each state, there is at least one optimal action which receives the highest reward. Therefore, the policy works by selecting the action with the highest Q-value as follows:

$$\pi(a_t|s_t) = argmax\ \{Q(s_t, a_t)\} \tag{3.2}$$

Q-Learning algorithms are RL techniques that are adopted to acquire the optimal policy π. The main procedure of Q-Learning is to assign a Q-value $Q(s_t, a_t)$ to each state-action pair at time step t, and then update this value at each iteration in order to optimise the agent's performance. The optimal $Q_\pi^*(s_t, a_t)$ expresses the maximum discounted achieved with the future reward $r(s_t, a_t)$ for action a_t taken at state s_t, which is expressed as follows:

$$Q_\pi^*(s_t, a_t) = r(s_t, a_t) + \gamma . \max Q(s_{t+1}, a_{t+1}) \tag{3.3}$$

Once the action a_t is taken based on a certain policy π, the defined reward $r(s_t, a_t)$ (or calculated using reward function) will be received, and then the agent assumes a new state s_{t+1}. Simultaneously, the action-value $Q(s_t, a_t)$ is updated using the following equation:

$$Q(s_t, a_t) \leftarrow (1 - \alpha)Q(s_t . a_t) + \alpha[r(s_t, a_t) + \gamma . \max \mathrm{Q}(s_{t+1}, a_{t+1})] \tag{3.4}$$

Where α denotes the learning rate which determines how much the new reward affects the old value of the $Q(s_t, a_t)$. For example, $\alpha = 0$ means that the new information acquired is not used in the leaning process and hence the reward received does not affect the Q-value. When $\alpha = 1$, only the latest information is considered.

3.5 Deep Reinforcement Learning (DRL)

Deep Reinforcement Learning (DRL) is an advanced subfield of RL that has recently gained significant attention and is being applied in various domains, including smart grids. DRL models use ANNs to learn complex representations of states and actions, enabling them to make informed decisions on how to act in a given environment as shown in Figure 3-4.

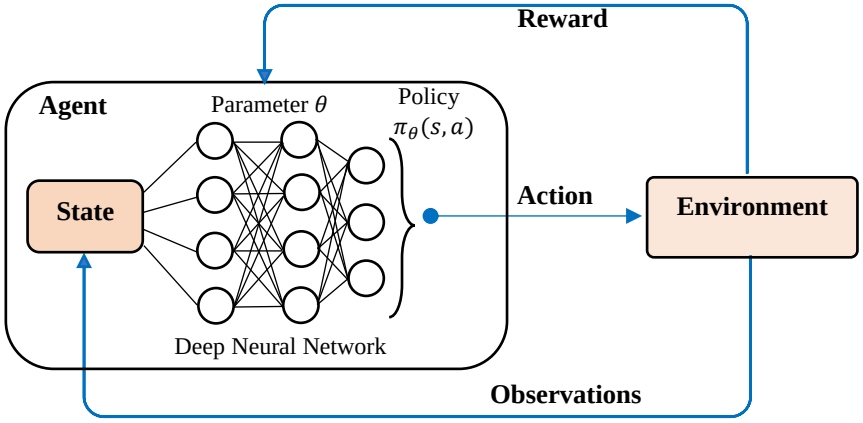

Figure 3-4 Deep reinforcement learning process [39].

In contrast to traditional RL methods, DRL is capable of handling high-dimensional and continuous state and action spaces, making it very suited for complex tasks such as DR management in smart grids.

One of the most common deep RL algorithms is Deep Deterministic Policy Gradient (DDPG) due to its ability of solving continuous state and action optimisation problems. Using the DDPG agent, two neural networks are employed to approximate the Q-function given by Equation (3.1) and the policy function π. These neural networks are known as critic network $Q(s_k, a_k|\theta^Q)$ and actor network $\mu(s_k|\theta^\mu)$, with θ^Q and θ^μ being parameters of these networks, respectively. For a certain state, the actor network will take an action as an output. Then the state-action pair will be transmitted to the critic network as an input returning the Q-value based on the state-action pair. In addition, two other networks, namely, the target actor network $Q'(s, a|\theta^{Q'})$ and the target critic network $\mu'(s|\theta^{\mu'})$ are used to continuously update the parameters of the actor and critic networks, which significantly improve the stability of the optimization. Under these conditions, the target networks' parameters ($\theta^{Q'}$ and $\theta^{\mu'}$) are used to update the traditional networks' parameters (θ^Q and θ^μ) at every time step using the smoothing factor τ as follows:

$$\begin{cases} \theta^{Q'} \leftarrow \tau\theta^{Q} + (1-\tau)\theta^{Q'} \\ \theta^{\mu'} \leftarrow \tau\theta^{\mu} + (1-\tau)\theta^{\mu'} \end{cases} \tag{3.5}$$

To allow the agent to explore the environment and interact with it during the training process, the number of episodes must be defined where each episode consists of a series of steps. After each iteration, a sampled noise $N(\sigma)$ generated from the Ornstein-Uhlenbeck (OU) process is added to the output of the actor network: $a_k = \mu(s_k|\theta^{\mu}) + \mathcal{N}(\sigma)$, while the hyperparameter σ is utilised to evaluate the exploring process of the environment. Then the experience replay memory $\mathcal{D}$ (experience buffer) is used to store the tuple (s_k, a_k, r_k, s_{k+1}), and take the minibatches (independent and identically distributed sets of samples) for training. The critic network will be updated by minimising the loss function across all selected experiences (N):

$$L(\theta^{Q}) = \frac{1}{N}\sum_{i=1}^{N}\left(y_i - Q(s_i, a_i|\theta^{Q})\right)^2 \tag{3.6}$$

Where the sample y_i is determined from the sum of the present reward and the expected Q-value at the next state s_{i+1} considering the outputs of target actor and critic networks:

$$y_i = r_i + \gamma Q'\left(s_{i+1}, \mu'\left(s_{i+1}|\theta^{\mu'}\right)\middle|\theta^{Q'}\right) \tag{3.7}$$

To improve the policy, the score function is minimized by using the gradient ascent to the actor network. The gradient is approximated by averaging the gradients of the policy score function across the minibatch:

$$\nabla_{\theta\mu} J \approx \frac{1}{N}\sum_{i=1}^{N}\left(\nabla_a Q(s_i, a|\theta^{Q})|_{a=\mu(s_i)} \nabla_{\theta\mu}\mu(s_i|\theta^{\mu})\right) \tag{3.8}$$

Chapter 4 Demand Response Strategy for Home Energy Management

4.1 Introduction

HEMS provides the interface for consumers to monitor and control their various household electrical devices in real time. HEMS can be considered as the enabling technology for realizing the potential of DR strategies and enabling consumers to improve energy usage and minimise electricity bills by shifting and curtailing their loads in response to electricity tariffs during peak periods without compromising their lifestyle and preferences [18], [19], [40], [41].

User comfort has mainly been considered in HEMS. In [42], the authors proposed a scheduling model for HEMS considering energy payment and user preferences level as a comprehensive objective in the optimization process. A HEMS is proposed in [43] with the objective to reduce electricity costs and avoid compromising consumers' lifestyles and preferences. The authors in [44] focused on the HEMS algorithm considering customer preferences setting, the priority of appliances and comfortable lifestyle.

Although HEMS technology is still in its early stages, in the past few years, the market for HEMS has been on the rise and is quickly expanding. Many researchers have worked on developing HEMS using rule-based control strategies. In [45], the author proposed a Hybrid Genetic Particle Swarm Optimisation (HGPO) to schedule the appliances of a house with local generation from RES. However, this algorithm attempts to minimise electricity bills without considering consumer's preferences. Optimisation techniques based on Integer Linear Programming (ILP) and Dynamic Programming (DP) have been used to manage energy usage and reduce the electricity cost in smart homes.

In [46], household appliances are divided into two types; appliances with a flexible starting time and a fixed power, and other appliances with a flexible power and a predefined working time. This approach aimed to achieve the desired trade-off between electricity bill reduction and discomfort where the users can modify the starting time of the first type of appliances or reduce the energy consumption of the second appliances to reduce the bills. However, this algorithm does not consider consumer's comfort. The authors in [47] focused on load scheduling problems and power trading using DP algorithm. This enables users to sell their surplus of generated power to the power grid or other local users. However, due to its

computational complexity, the model is difficult to implement in real-time. Recently, much attention has been devoted to the development of controllers based on computational intelligence and machine learning techniques for HEMS [48], [49]. According to RTP program, end-users receive energy prices from power utility an hour-ahead in order to make a decision to shift or reduce their energy consumption. Therefore, in [49], Artificial Neural Networks (ANN) have been used to design energy price forecasting models and overcome the uncertainty in future prices. The ANN approach is used due to its ease of implementation, good performance and it is less time-consuming.

Recently, Reinforcement Learning (RL) has emerged as a potential machine learning algorithm for energy management, decision and control. RL models have excellent decision-making ability due to their potential to solve problems without a priori knowledge of the environment. Multi-agent reinforcement learning has been proposed for the optimal scheduling of household appliances to optimise the energy utilisation [48], [50]. However, multi-agents RL requires setting several agents, where each household appliances represents an environment that has its own agent with different actions and rewards. Therefore, the learning process becomes more complex [51]. Other studies have focused on using Q-learning and SARSA (State-Action Reward-State-Action) algorithms in HEMS to schedule controllable appliances and shift the operation time of shiftable devices [52], [53]. However, these algorithms require many state-action pairs and consequently the convergence speed of the Q-values is reduced.

In this chapter, we proposed a new and flexible strategy for HEMS, to smooth the power consumption profile without compromising user comfort and preferences. The proposed approach works with a single agent and uses a reduced number of state-action pairs and fuzzy logic for rewards functions.

4.2 HEMS Components

Figure 4-1 presents the general architecture of a HEMS, which comprises the following components:

- *Sensing and measuring device.*

Sensors provide monitoring and tracking in real-time routine activities to help with a wide range of smart home functions. These sensors can record and detect physical quantities such as motion, temperature, sound and light, and then send data to HEMS via user-interface about user's activities and environment changes.

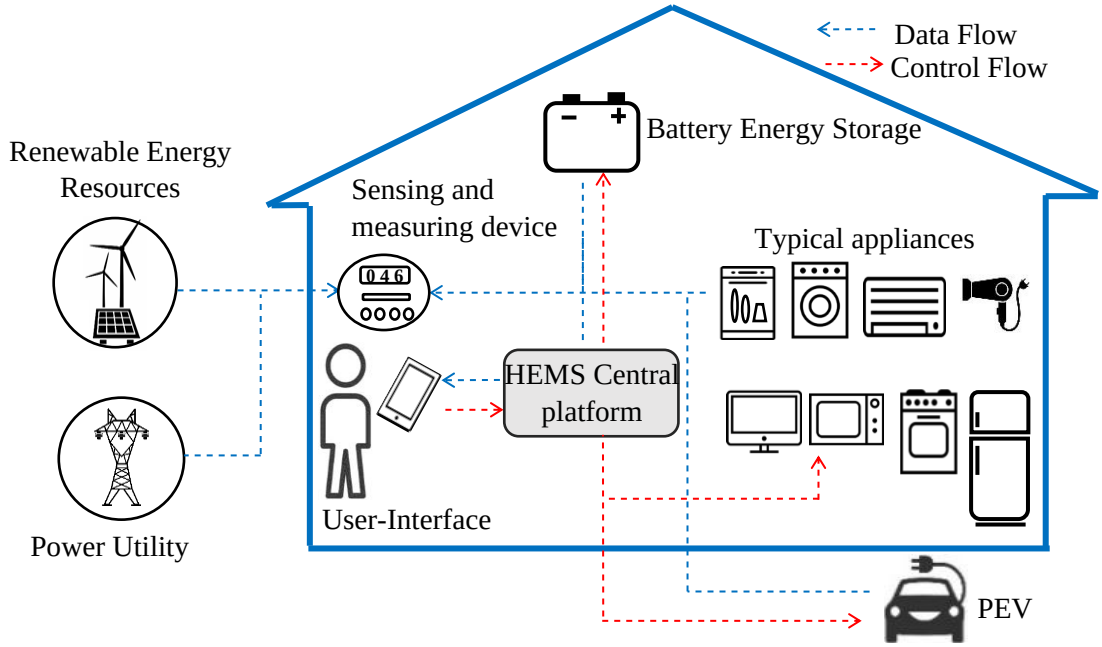

Figure 4-1 Smart HEMS components.

Smart meters are commonly used by HEMSs, which are responsible for collecting energy consumption data of individual appliances and other energy resources such as the renewable energy and the main grid. The main advantage of smart meters is that they provide a two-way communication between HEMS and the utility.

- *Smart appliances*

Smart household appliances contain typical devices such as dishwasher, refrigerators or air conditioning units, and energy generation devices such as solar PV panels and wind turbines, EV and energy storage. Smart appliances communicate with a central platform which handles all measured data and coordinates appliance uses.

- *User interface*

The information regarding energy consumption and energy cost can be displayed via user interface device. In other words, interfaces allow for the interaction between the user and HEMS. It also enables users to specify their preferences, including appliance priorities, comfort parameters or scheduling goals. User interface could be a touch screen or mobile application.

- *Central platform*

The central platform aims to manage and control energy consumption in smart home. It receives the collected data via smart meters and then implements a scheduling mechanism in order to optimise the energy usage and then minimise the energy cost.

In a HEMS, smart meters are continuously aggregating information regarding the energy usage of household appliances. Disaggregation techniques such as Non-Intrusive Load Monitoring (NILM) can be used to collect data for the individual appliance [54]. The collected data is then sent to the central platform for storing, processing and then making decisions regarding the power flow and appliances scheduling. To meet the user preferences, a scheduling strategy based on DR programs must be designed to analyse the operating times of the household appliances and then select which appliance needs to be shifted in order to minimise the electricity bills without affecting user comfort.

4.3 Home Energy Management Model

The proposed HEM system works based on RTP, which is considered as a dynamic pricing. Using this DR program, customers receive price signals on hour-ahead and day-ahead basis as the electricity price varies at different time intervals of a day. Therefore, smart meters are used to receive the RTP signal from a utility and record the current power consumption data of all household appliances in near real-time (every time-step) in order to re-schedule them, and then send the collected data to the HEM system. In addition, this proposed algorithm works based on load priority and customer comfort preference. A user-interface is used to enable customers to set the priority of shiftable appliances. Consequently, the HEM system can shift the operating time of appliance that has the lowest priority during peak demand when required, and then turn on the appliance that has the highest priority during off-peak hours.

The household appliances are divided mainly into two categories; shiftable appliances that have the ability to re-schedule their operating time based on load priority and preference setting such as washing machine, dish washer and electric vehicle. Non-shiftable appliances require a permanent power supply during operating time regardless of the electricity price.

The household appliances are divided into shiftable and non-shiftable appliances, and the total energy demand (in kWh) of shiftable $E_d^{shift}(t)$ and non-shiftable $E_d^{non}(t)$ appliances are calculated by:

$$E_d^{shift}(t) = \sum_{n=1}^{N} e_t^{n,shft} . J_t^n \tag{4.1}$$

$$E_d^{non}(t) = \sum_{m=1}^{M} e_t^{m,non}.J_t^m \tag{4.2}$$

$$E_d(t) = E_d^{shift}(t) + E_d^{non}(t) \tag{4.3}$$

Subject to:

$$E_d^{max} > E_d(t) > E_d^{min} \tag{4.4}$$

Where $e_t^{n,shft}$ and $e_t^{n,non}$ represent the rated power of each shiftable appliance and non-shiftable appliance, respectively. J_t^n denotes the status of the appliance and takes values 0 (off) or 1 (on). $t \in \{1, 2, 3, \dots, 24\}$ represents the hour of the day where the sample time is set to 5 minutes, $n \in \{1,2, \dots, N\}$ is the appliance number and N is the total number of the shiftable appliances. $m \in \{1,2, \dots M\}$ refers to the appliance number and M is the total number of the non-shiftable appliances. The cost of energy usage indicates as:

$$C_t = \min\left\{0, \sum_{t=1}^{24} E_d(t) \times P_h(t)\right\} \tag{4.5}$$

$P_h(t)$ is the electricity price (in £/kWh) received from the utility grid and C_t is the total cost of energy consumption (in £). The proposed HEMS works based on RTP, which is considered as a dynamic pricing.

A useful simulation platform for HEMS algorithms has been designed to enable researchers and developers to implement and test their proposed control algorithms. The proposed HEM model includes mainly solar PV panel, power electronic devices, household appliances, energy storage system and user-interface as shown in Figure 4-2 (see Appendix A for more details). The household appliances can be supplied by the PV generation, discharging the battery or importing energy from the main grid. The DC/DC converter controls the bidirectional power flow by using current control technique. The DC/DC converter can act as a buck or boost converter during charging or discharging mode, respectively. The AC/DC converter, on the other hand, converts the DC PV and battery power to AC to supply the household appliances. The user-interface is used to manage the power flow among the PV, battery and power grid.

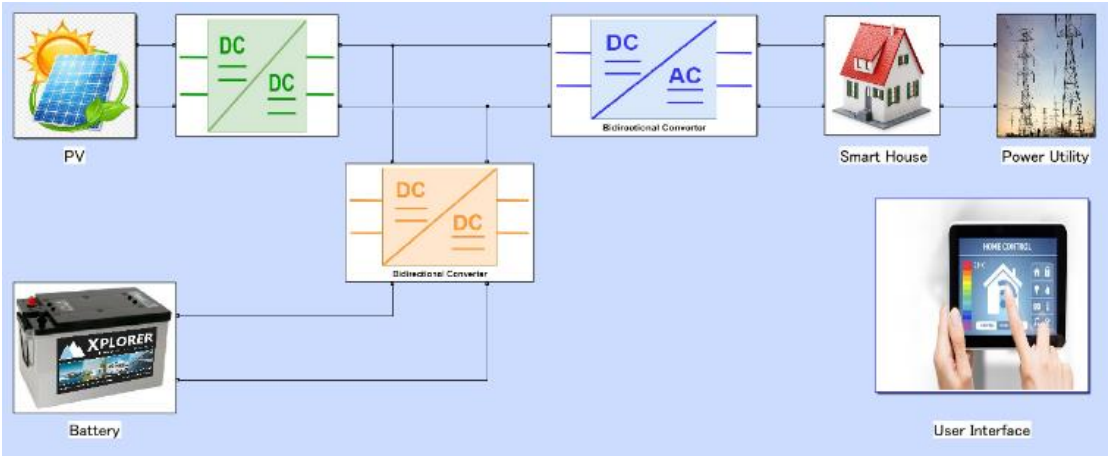

Figure 4-2 HEMS model developed in MATLAB.

4.4 Methodology

4.4.1 Background on Reinforcement Learning

Household Energy Management (HEM) is an optimisation problem, which aims to minimise the total power consumption of electrical appliances and reduce the electricity bills in a smart home. A typical HEMS can neither be adapted to a variety of appliances with varying scheduling complexity nor it is appropriate for real-time application. Reinforcement Learning (RL) algorithms have been recently proposed as potential candidates to address these issues due to their adaptability and ability to learn customer's preferences and optimise the management of energy systems which are often subject to various inputs such as dynamic electricity prices, forecast data and energy consumption patterns [55].

4.4.2 Q-Learning model

RL is adopted to make an optimal decision in a stochastic environment (dynamic electricity prices and different energy consumption patterns) using an intelligent agent. Practically, the agent can control a dynamic system by executing sequential actions. Where the dynamic system could be characterised by a state-space and a numerical reward that evaluates the new state when a given action is taken. In this work, the Q-learning model components are defined as follows:

- **State space**

The state-space here is represented by the energy demand and the electricity price signal. To reduce the computation time and make the model much simpler, the energy demand ($E_{t,index}^{total}$) is divided into three levels namely; low, average and high-power demand. Whereas the price signal (P_t^{index}) is categorised into cheap and expensive price as follows:

$$E_{t,index}^{total} = \begin{cases} E_{low}^{total} & \text{if } E_d(t) \leq E_d^{min} \\ E_{average}^{total} & \text{if } E_d^{min} < E_t^{total} < E_d^{max} \\ E_{high}^{total} & \text{if } E_d(t) \geq E_d^{max} \end{cases} \quad (4.6)$$

$$P_t^{index} = \begin{cases} P_t^{cheap} & \text{if } P_h(t) \leq \mathrm{P}_{average} \\ P_t^{expensive} & \text{if } P_h(t) > \mathrm{P}_{\mathrm{average}} \end{cases} \quad (4.7)$$

Where E_d^{min} and E_d^{max} represent the lower and upper limits of the average energy demand in kWh, respectively. $\mathrm{P}_{average}$ is the acceptable electricity price in (£/kWh). Where these values are set by the user according to their energy consumption profile. In this work, we set the acceptable price to 0.1 £/kWh. For each time step (5 minutes), the state is defined to contain both power demand and electricity price indexes:

$$s_t = \left[E_{t,index}^{total}, P_t^{index}\right] \quad (4.8)$$

Table 4-1 summarises all available states that can be created from power demand and real-time electricity price. It also shows the index of each state.

Table 4-1 Indexing of all states.

Power Demand (kWh)	Price (£/kWh)	State Index
$\mathrm{E}_{\mathrm{high}}^{\mathrm{total}}$	$\mathrm{P}_{\mathrm{t}}^{\mathrm{expensive}}$	6
$\mathrm{E}_{\mathrm{high}}^{\mathrm{total}}$	$\mathrm{P}_{\mathrm{t}}^{\mathrm{cheap}}$	5
$\mathrm{E}_{\mathrm{average}}^{\mathrm{total}}$	$\mathrm{P}_{\mathrm{t}}^{\mathrm{expensive}}$	4
$\mathrm{E}_{\mathrm{average}}^{\mathrm{total}}$	$\mathrm{P}_{\mathrm{t}}^{\mathrm{cheap}}$	3
$\mathrm{E}_{\mathrm{low}}^{\mathrm{total}}$	$\mathrm{P}_{\mathrm{t}}^{\mathrm{expensive}}$	2
$\mathrm{E}_{\mathrm{low}}^{\mathrm{total}}$	$\mathrm{P}_{\mathrm{t}}^{\mathrm{cheap}}$	1

- **Action space**

The aim is to shift the operating time of the specific appliance that has the lowest priority during peak demand when required, and then turn on the appliance that has the highest priority during off-peak hours.

Based on the relationship of the real-time price, the total power demand of all household appliances, taking into account load priority and customer preferences, the agent (HEMS) chooses one action from the action space A that given by:

$$A = ["do\ nothing" \quad "shifting" \quad "valley \quad filling"] \tag{4.9}$$

Where shifting action shifts the lowest priority device. This mode occurs always during peak demand when the price and the power consumed are high. Valley-filling action seeks to turn on the shifted appliance with the highest priority, usually during off-peak demand hours. When do-nothing is set, the system works in normal conditions and there is no need to shift any appliance.

- **Rewards function implementation using fuzzy logic**

Let $r(s_t, a_t)$ denote the numerical reward that the agent receives after executing a random action and observing a new state. The aim of this reward is to evaluate how much the action taken a_t is suitable for a certain state s_t. Fuzzy logic is used here to evaluate the action taken at a certain state. Fuzzy reasoning is a decision-making model that deals with approximate values rather than exact values. A Fuzzy Inference System (FIS) provides the mapping from the inputs to the outputs, based on a set of fuzzy rules and associated fuzzy Membership Functions (MFs). There are two types of FIS, Mamdani-type FIS and Sugeno-type FIS. Mamdani method is used in this study because it offers a smoother output. The inputs variables to the fuzzy reward model are the power demand E_t^{total} and the electricity price P_t (referred to as "states" in Q-learning) and the outputs variables are the evaluation of shifting, valley-filling and do-nothing (refer to as "actions" in Q-learning) as shown in Figure 4-3.

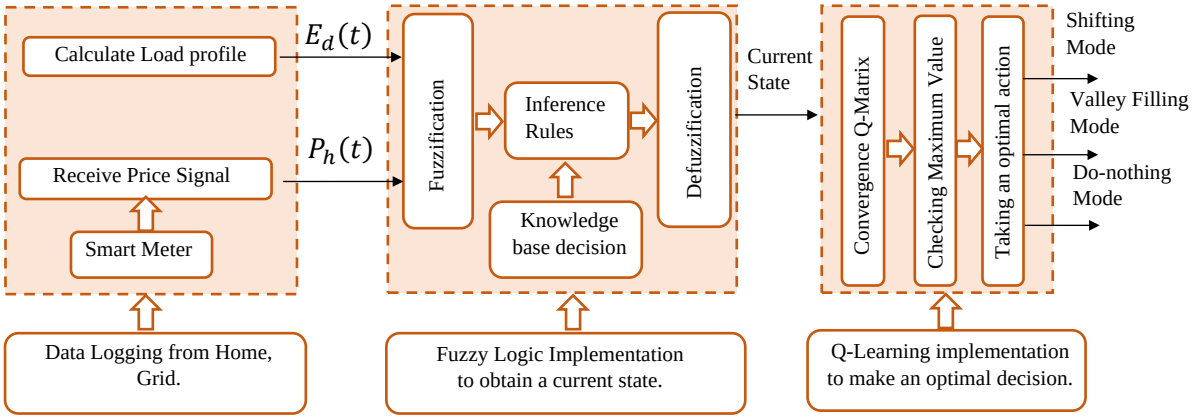

Figure 4-3 FIS system of the reward function.

Based on the relationship between the power demand and the electricity price, the FIS system will firstly determine a state, then take a random action from the action space (shifting, valley filling or do-nothing). The FIS reward system will evaluate the taken action by providing a numerical reward. The MFs for the input variable "power demand" are triangular and are labelled as: Low, Average and High. The universe of discourse of power demand is chosen as [0 6300] (Watt) as shown in Figure 4-4.

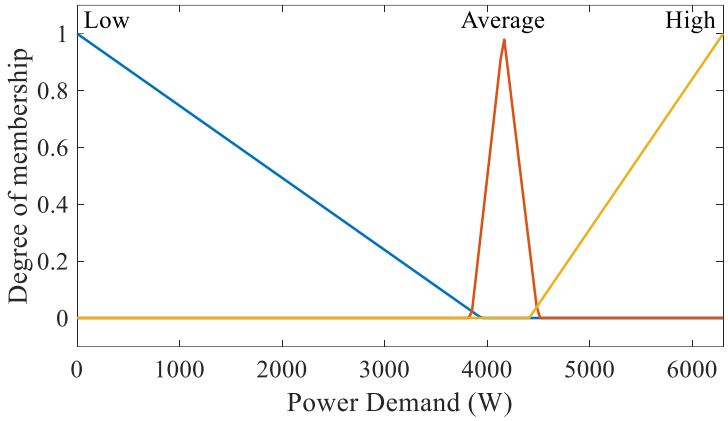

Figure 4-4 Fuzzy sets and MFs of power demand input.

The fuzzy sets of electricity price are defined as "cheap" and "expensive". The MFs are Gaussian and the universe discourse is [0 0.16] (£/kWh) as shown in Figure 4-5. The outputs of the system are the evaluation of the random action which was defined in Q-learning. For each action taken (output), the fuzzy sets are determined as Bad Action (BA), Good Action (GA) and Very Good Action (VGA). The universe of discourse of MFs is defined as [0 100] to evaluate all possible actions with values out of 100 as shown in Figure 4-6.

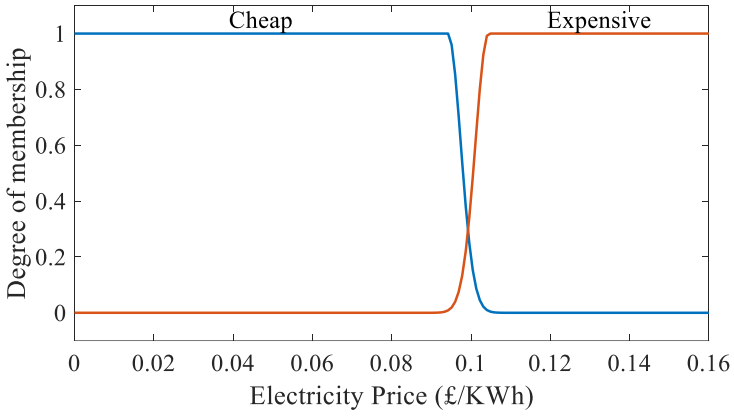

Figure 4-5 Fuzzy sets and MFs of electricity price input.

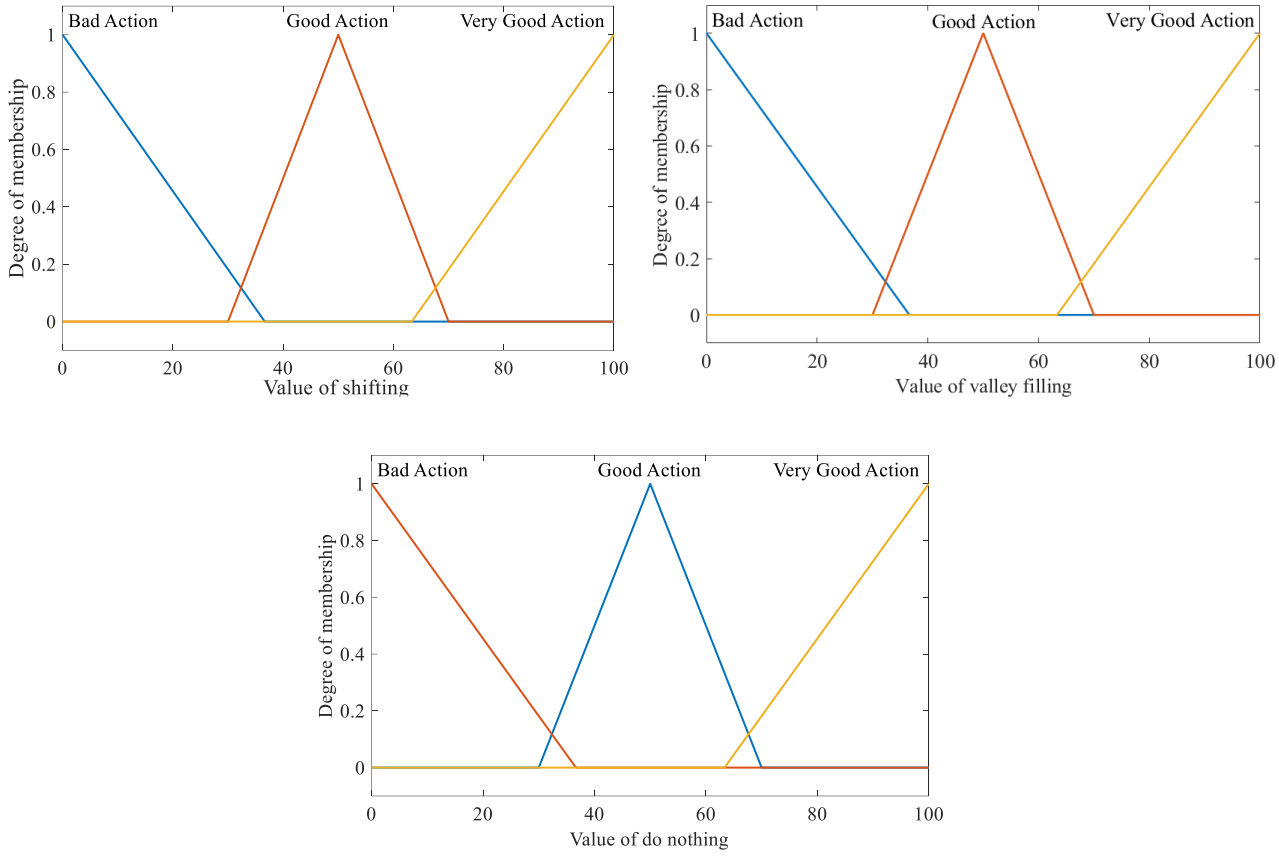

Figure 4-6 Fuzzy sets and MFs of output variables.

Table 4-2 shows the list of fuzzy rules. Figure 4-7 illustrates an example of how the FIS evaluates the possible actions for each state. The example shows that the power demand is 5500 Watts, and the electricity price is 0.14 £/kWh which refers to state index 6 according to Table 4-1. The values of the three actions are 86.5 for shifting action, 13.5 for valley-filling action and 13.5 for do-nothing action. Therefore, if the agent selects shifting and will receive a reward of 86.5. Conversely, it will receive a reward of only 13.5 if either valley-filling or do-nothing action is selected.

Table 4-2 Fuzzy rules of FIS system.

Power Demand	Electricity Price	Shifting	Valley filling	Do nothing
Low	Cheap	BA	VGA	GA
Low	Expensive	BA	GA	GA
Average	Cheap	BA	GA	VGA
Average	Expensive	BA	BA	VGA
High	Cheap	BA	BA	VGA
High	Expensive	VGA	BA	BA

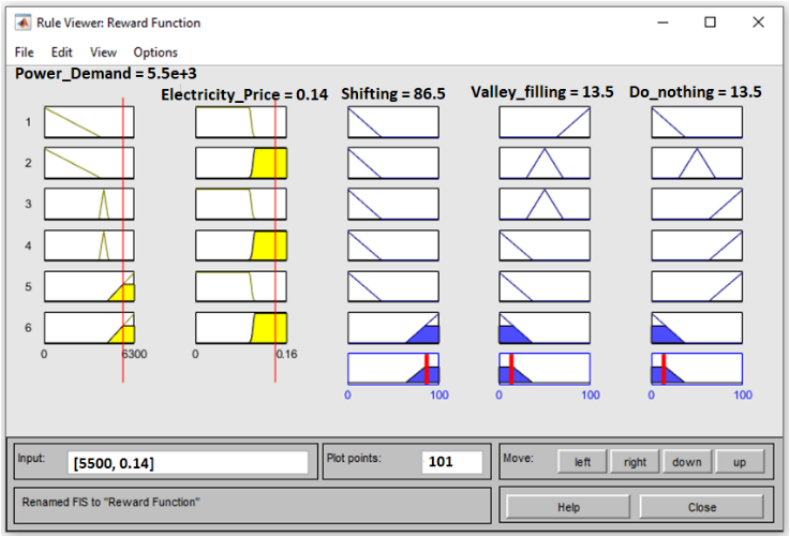

Figure 4-7 Example of FIS process.

4.4.3 Home energy management algorithm using Q-learning

Q-learning is considered as an off-policy RL algorithm that seeks to make the best decision at a given state. Off-policy means that the Q-learning function learns from taking random actions without following a current policy. Therefore, a policy is not needed during a training process. The Q-matrix, which has a dimension of $[states \times actions]$, should be initialised to zero (i.e. the Q-value of each state-action pair is assigned a value zero). Then, the agent will interact with the environment and update each pair in that matrix after each action taken at a certain state using Equation (3.4).

In this study, a random action called "exploring" is applied. In this case, a sufficient number of iterations will be required to explore and update the values of $Q(s_t, a_t)$ for all state-action pairs at least once. After convergence of the Q-matrix the optimal Q-values will be obtained.

The pseudo-code listed in Table 4-3 (Algorithm 1) illustrates the procedure of the main algorithm of the HEM using Q-learning. Firstly, the numerical rewards are defined using fuzzy logic. The parameters γ and α are set to 0.8 and 0.2 respectively and Q-value matrix entries are initialised to zeros. For each current state, all possible actions are specified, and then an action will be selected randomly. After the selected action is executed, the numerical reward (using fuzzy logic) for that action and the new state will be observed by the agent. The maximum Q-value for the next state should be also determined and then the Q-value of the state-action pair will be updated using Equation (3.4). Finally, the next state will be used as a current state.

Table 4-3 Home energy management using Q-learning algorithm.

ALGORITHM 1

1. Set $\boldsymbol{\gamma}$,$\boldsymbol{\alpha}$ parameters and environment rewards in matrix.
2. Initialise $\boldsymbol{Q(s_t, a_t)}$, $\forall \boldsymbol{s} \in \boldsymbol{S}, \forall \boldsymbol{a} \in \boldsymbol{A}$.
3. **For** each time step t do
4. Choose a random initial state from the electricity price and household power consumption.
5. **While** hour = 1:24
6. Determine all available actions as shown in equation (4.9).
7. Select random action from all possible actions for the current state.
8. Execute the selected action $\boldsymbol{a_t}$, and observe the new state $\boldsymbol{s_{t+1}}$ and numerical reward $\boldsymbol{r(s_t, a_t)}$.
9. Determine the maximum Q-value for next state in Q-matrix.
10. Update the $\boldsymbol{Q(s_t, a_t)}$ using Equation (3.4).
11. Set the next state as current state.
12. **End while**
13. **End for**

Figure 4-8 shows an example of Q-matrix updating. Each row indicates a state, and each column indicates an action. Assume that the current state index at time step t is 6 (which represents high power demand and expensive price [$E_{high}^{total}, P_t^{expensive}$]), the random selected action is '$shifting$'. Using the fuzzy model, the reward will be obtained as a value of shifting action. The next state is observed as 4 (i.e. state [$E_{average}^{total}, P_t^{expensive}$]). max $Q(s_{t+1}, a_{t+1})$ is 3.19 which is found in Q-matrix based on the next state. Using Equation (3.4), the new Q-value for [state: 6, action: 1] is 2.60.

State \ Action	Shifting	Valley filling	Do nothing
1	3.29	2.64	2.80
2	2.80	2.79	3.36
3	2.84	2.79	3.34
4	2.64	2.85	3.19
5	2.82	3.03	3.17
6	2.63	3.38	2.70

Max Q (st+1, at+1)

State \ Action	Shifting	Valley filling	Do nothing
1	3.29	2.64	2.80
2	2.80	2.79	3.36
3	2.84	2.79	3.34
4	2.64	2.85	3.19
5	2.82	3.03	3.17
6	2.60	3.38	2.70

Q* (st, at)

Figure 4-8 Simple example of Q-matrix updating.

To allow the agent to visit all state-state pairs and learn new knowledge, the training process is set to 1000 iterations, The average computational time required to determine the optimal policy

of the Q-learning is 2 hours with 10,000 iterations. The convergence of the Q-Matrix after execution of this number of iterations is shown in Table 4-4.

Table 4-4 Convergence Q-matrix after 10000 iterations.

State \ Action	Shifting	Valley filling	Do nothing
1	2.57	3.21	2.96
2	2.62	3.01	3.17
3	2.62	3.00	3.27
4	2.92	2.47	3.30
5	2.62	2.87	3.21
6	3.34	2.72	2.67

4.4.4 User's satisfactions

An effective energy management system for residential demand response using Reinforcement Learning (RL) and Fuzzy Reasoning (FR) is proposed to reduce energy usage and minimise electricity bills by scheduling household appliances, in response to electricity price signal. However, in this section, DR strategy is developed to improve the user's satisfaction. Using the proposed DR strategy presented in previous section, the customers receive price signals on hour-ahead or day-ahead basis as the electricity price varies at different time intervals of a day. Therefore, smart meters are used to receive the RTP signal from a utility and record the current power consumption data of all household appliances during their operation times, and then send them to the HEMS. The HEMS manages and schedule the shiftable appliances by taking an optimal action whether Shifting, Valley filling or Do-nothing:

a) Mode 1: Shifting

According to the proposed strategy described in Section 3.4.3, the Shifting Mode occurs when $P_h(t)$ is higher than P_{avg}, $E_d(t)$ is greater than E_d^{max} and $E_d^{shift}(t)$ is greater than zero. In this case, the power deficiency to meet the average power demand as shown in Figure 4-9 by shifting the shiftable appliances to off-peak period is calculated as:

$$E_{def}^{sh}(t) = |E_d(t) - E_d^{max}| \tag{4.10}$$

$E_{def}^{sh}(t)$ is the deficiency power of shifting mode. E_d^{max} and E_d^{min} denotes the upper and lower limit of the average power, respectively.

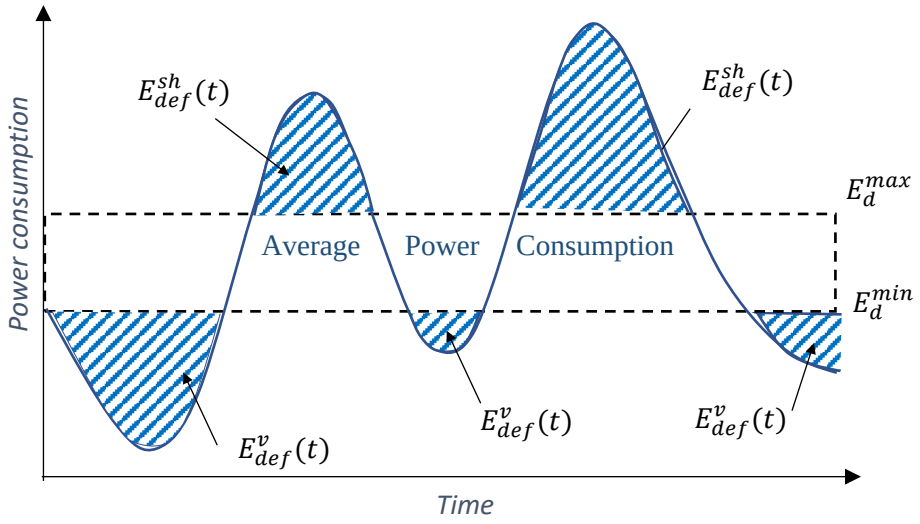

Figure 4-9 Household power consumption and average power region.

To shift the appliances, there are two possible scenarios, firstly, when the deficiency power is higher than the total power demand of the deferable appliances that are working at that time step:

$$E_{def}^{sh}(t) - E_d^{shift}(t) \geq 0 \tag{4.11}$$

In this case, all deferable appliances will be shifted. However, when the deficiency power is lower than the demand of the deferable appliances, there is no need to shift all appliances to meet the average power demand.:

$$E_{def}^{sh}(t) - E_d^{shift}(t) < 0 \tag{4.12}$$

In this case, the system selects the appliances based on user-comfort factors to achieve the user's satisfaction as much as possible namely, priority of the appliance to be shifted, the power rate of the appliances, the operating time interval and the waiting time which are defined below:

- priority of each appliance set by the user, and this means how much the user can manage without this appliance at this time step:

  $$\delta_s = [\delta_s^1, \delta_s^2, \dots, \delta_s^N] \tag{4.13}$$

  δ_n indicates the priority value of n appliances, hence each appliance takes a value between 0 and 1 to evaluate the priorities, where 1 means the appliance is not essential to be working.

- When $E_{def}^{sh}(t)$ is lower than $E_n^{shift}(t)$, the power rate e_t^n of each appliance is considered for selecting which appliance is to be shifted compared to $E_n^{shift}(t)$.

Consequently, the probability of each appliance to be shifted based on power rate (ω_s^n) of each appliance is calculated as:

$$\omega_s^n = 1 - \left| \frac{e_t^n - E_{def}^{sh}(t)}{e_t^n + E_{def}^{sh}(t)} \right| \tag{4.14}$$

Where the appliance that has the power rate (e_t^n) closer to the power deficiency $E_{def}^{sh}(t)$ will have the highest probability.

- The operating time interval (T_n) of each appliance is considered. The appliance that has shorter operating time interval to finish its task will have the higher probability to be shifted to off peak period. The shifting probability (β_s^n) based on the operating time interval $T_{n,o}$ of each appliance is calculated as:

$$\beta_s^n = \begin{cases} 0 & \text{when } T_{n,o} = t \\ \dfrac{t}{T_{n,o}} & \text{when } T_{n,o} \neq t \end{cases} \tag{4.15}$$

- The system considers the shifted appliances (appliances that have been shifted before). The shifting time T_n of each appliance is calculated and compared to the time step t. The shifting probability based on the shifting time (φ_s^n) of each appliance is calculated as:

$$\varphi_s^n = \begin{cases} 0 & \text{when } T_{n,s} = t \\ \dfrac{t}{T_{n,s}} & \text{when } T_{n,s} \neq t \end{cases} \tag{4.16}$$

The total shifting probability γ_n for each appliance will be calculated by adding up the four previous calculated probabilities, hence, the highest γ_s^n will shift first:

$$\gamma_s^n = \frac{\delta_s^n + \omega_s^n + \beta_s^n + \varphi_s^n}{4} \tag{4.17}$$

b) Mode 2: Valley Filling

This mode occurs when $P(t) < P_{avg}$ and $E_d(t) < E_d^{min}$. This mode aims to turn on the appliances that have been shifted during on peak period. Therefore, the total power demand of the shifted appliances ($E_n^{shifted}$) to be operating again is calculated as:

$$E_n^{shifted} = \sum_{n=1}^{N} \rho_n \times e_t^n \tag{4.18}$$

ρ_n indicates the shifting signal of each appliance and takes value 1 if the appliance has been shifted during shifting mode and 0 if not. The power deficiency ($E_{def}^{v}(t)$) required to meet the lower limit of average power (E_d^{min}) is:

$$E_{def}^{v}(t) = \left|E_d(t) - E_d^{min}\right| \tag{4.19}$$

To select which appliance needs to be turned on, $E_{def}(t)$ is compared to the $E_n^{shifted}$. Therefore, there are also two scenarios. First, when the power deficiency is higher than the total rated power of appliances ($E_d^{shifted}(t)$) which have shifted:

$$E_{def}^{v}(t) - E_d^{shifted}(t) \geq 0 \tag{4.20}$$

In this case, all shifted appliances will be switched on as the demand will not exceed the lower limit of the average power, However, when the power deficiency is lower than the rated power of the shifted appliances, it is not desirable to run all shifted appliances. Therefore, the selection of the appliance depends on user-comfort factors, the priority of the appliances to be filled (δ_v), the power rating of the appliances (ω_v^n), The operating time interval (φ_v^n) and the waiting-time of the appliance (ε_v^n):

$$E_{def}^{v}(t) - E_d^{shifted}(t) < 0 \tag{4.21}$$

- For how long the user needs to operate each specific shifted appliance. This value denoted by:

  $$\delta_v = [\delta_v^1, \delta_v^2, \dots, \delta_v^N] \tag{4.22}$$

  δ_v^n is the valley filling priority for appliance n. The appliance with the highest priority has more chance to switch on.

- When $E_{def}^{v}(t) < E_d^{shifted}(t)$, it is better to distribute the shifted appliances on the valley filling time period rather that switching on all shifted appliances at the same time to keep $E_d(t)$ in the average demand region. Therefore, the rated power of the shifted appliance is considered and the probability to be switch on (ω_v^n) is calculated as:

  $$\omega_v^n = 1 - \left|\frac{e_t^n - E_{def}^{v}(t)}{e_t^n + E_{def}^{v}(t)}\right| \tag{4.23}$$

  When ω_v^n is 1 (highest value), this means the appliance's power rating equals the power deficiency ($e_t^n = E_{def}(t)$) and has the highest probability to be turned and meet the average power demand.

- In Valley Filling mode, the waiting-time of an appliance that has been shifted is considered. The appliance that has the longest waiting time has highest priority to operate. The probability of switching on (ε_v^n) the appliance is defined as follows:

$$\varepsilon_v^n = \begin{cases} 0 & \text{when } T_{n,w} = t \\ 1 - \dfrac{t}{T_{n,w}} & \text{when } T_{n,w} \neq t \end{cases} \tag{4.24}$$

  $T_{n,w}$ is the waiting time of appliance n and ε_v^n is the probability of switching on of the appliance.

- The probability of the time interval (φ_v^n) required by the appliance to finish its task is given by:

$$\varphi_v^n = \begin{cases} 0 & \text{when } T_{n,s} = t \\ 1 - \dfrac{t}{T_{n,s}} & \text{when } T_{n,s} \neq t \end{cases} \tag{4.25}$$

At each time step t, the system reads the profile of each appliance (a_n) and determines the shifting and valley filling probabilities denoted by R_s and R_v respectively:

$$a_n = \left[J_t^n\ , e_t^n\ , T_{n,o}\ , T_{n,s}, T_{n,w}\right] \tag{4.26}$$

$$R_s = \left[\begin{array}{cccc|c} \delta_s^1 & \omega_s^1 & \beta_s^1 & \varphi_s^1 & \gamma_s^1 \\ \vdots & \vdots & \vdots & \vdots & \vdots \\ \delta_s^N & \omega_s^N & \beta_s^N & \varphi_s^N & \gamma_s^N \end{array}\right] \tag{4.27}$$

$$R_v = \left[\begin{array}{cccc|c} \delta_v^1 & \omega_v^1 & \varepsilon_v^1 & \varphi_v^1 & \gamma_v^1 \\ \vdots & \vdots & \vdots & \vdots & \vdots \\ \delta_v^N & \omega_v^N & \varepsilon_v^N & \varphi_v^N & \gamma_v^N \end{array}\right] \tag{4.28}$$

The pseudo-code listed in Table (4-5) (Algorithm 2) illustrates the procedure for selecting the appliances to be shifted or turned on based on the user comfort-factors. Firstly, the upper and lower of the average power are set, with the priority of each appliance. Then the R_s and R_v will be set to zeros. For each time step, the system will read the total power demand and the status of all shiftable appliances with their power rate. Based on the detected mode (Shifting, Valley filling, do-nothing) that received from the RL agent, the system makes a decision which appliances need to be shifted during the Shifting mode, or which appliances need to be switched on during Valley filling mode, based on the calculated probability of each appliance.

Table 4-5 Selection procedure of shiftable appliances.

Algorithm 2

- Set δ_s and δ_v for all shiftable appliances, E_d^{min} , E_d^{max}, and P_{avg}.
- Initialise R_s and R_v.
For each time step τ do
- Read $E_d(t)$ and $P_h(t)$.
- detects the active mode.
    While Shifting mode is active and $E_d^{shift}(t) > 0$
        - Determine $E_{\boldsymbol{def}}^{sh}(t)$ using Equation 6 and
          $a_n = [J_t^n , e_t^n , T_{n,o} , T_{n,s}, T_{n,w}]$.
        If $E_{def}^{sh}(t) - E_d^{shift}(t) \geq 0$
        - Shift all deferable appliances.
        Elseif $E_{def}^{sh}(t) - E_d^{shift}(t) < 0$
            - Calculate γ_s^n for each appliance using Equations (4.9-4.13).
            - Identify R_s, select and shift the appliance that has highest probability value γ_s^n.
            - Update a_n and R_s.
        End if
    End while
    While Valley filling mode is active and
          $E_d^{shifted}(t) > 0$
        - Determine $E_{\boldsymbol{def}}^{v}(t)$ using Equation 15 and
          $a_n = [J_t^n , e_t^n , T_{n,o} , T_{n,s}, T_{n,w}]$.
        If $E_{def}^{v}(t) - E_d^{shifted}(t) \geq 0$
            - Shift all operating appliances.
        Elseif $E_{def}^{v}(t) - E_d^{shifted}(t) < 0$
            - Detect the shiftable appliances that are working and read $a_n = [J_t^n , e_t^n , T_{n,o} , T_{n,s}, T_{n,w}]$.
            - Calculate γ_v^n for each appliance using Equations (4.18- 4.21).
            - Identify R_v, select and run the appliance that has highest probability value γ_v^n.
            - Update a_n and R_s.
        End if
    End while
End for

4.5 Results and Discussion

4.5.1 Implementation of the proposed strategy

Based on the convergence Q-Matrix that shown in Table 3.6, an optimal decision could be made by HEMS system to shift the operating time of the shiftable the appliance that has the lowest priority during peak demand by activating *Shifting Mode*. Then the system will turn on the appliance that has been shifted and has the highest priority during off-peak hours by activating *Valley Filling Mode.* This process works based on the relationship between the real-time price, the consumed power by all household appliances considering load priority and customer comfort preference. Figure 4-10 shows the electricity price in £/kWh received from the utility grid.

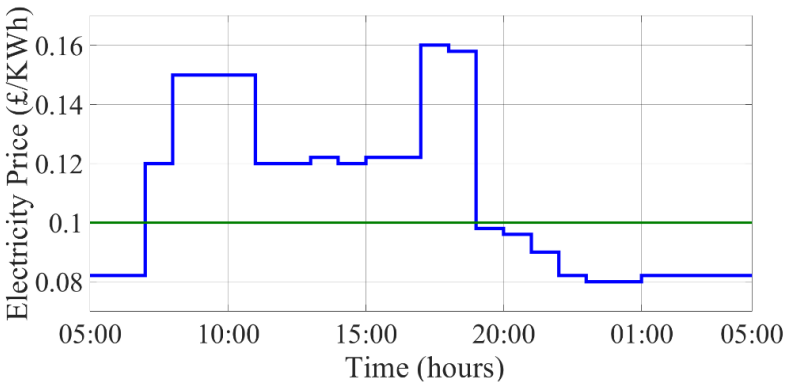

Figure 4-10 Real time price (blue) and average price (green) signals.

In Figure 4-11 is shown the total power demand in Watts of the smart home including all electrical appliances. These two values define the state and are passed to the agent at each time step. Based on the convergence Q-matrix, the action will be selected as the maximum Q-value for that current state.

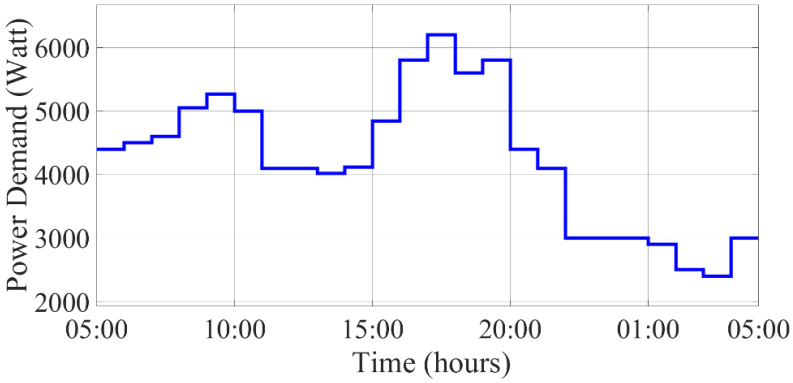

Figure 4-11 Total power demand of the smart home.

Table 4-6 and Table 4-7 show the rated power of non-shiftable and shiftable appliances, respectively. For the shiftable appliances, the priority of each appliance is set by users and can be different from user to another based on their own preferences.

Table 4-6 Rated power for non-shiftable appliances.

Appliance	Rated Power (W)
Iron	1000
Oven	2000
Laptop	20
Microwave	600
Television	200
Lighting	100
Refrigerator	200
Water heater	2000

Table 4-7 Rated power for shiftable appliances with priority.

Appliance	Rated Power (W)	Priority order
Washing machine	800	1
Dish washer	1100	2
Clothes dryer	400	3
Hair dryer	450	4
Hair straightener	20	5
PEV	1200	6

Figure 4-12 shows all the states that are detected based on the relation between the electricity price and power demand signal using Equations 4.6-4.8. For instance, at 6:00 am the electricity price is low (£0.082/kW) and the power demand is average (4500 W). Thus, the state index is 3 using Table 4-1. Using Table 4.4, the maximum value is 3.27 that refers to *do-nothing* action as shown in Figure 4-13.

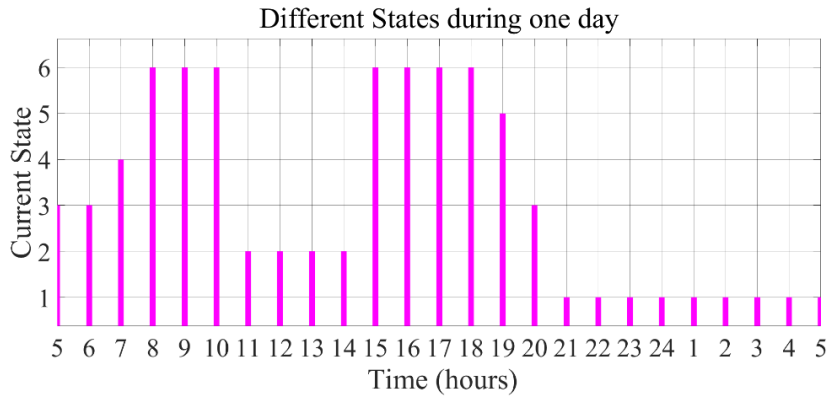

Figure 4-12 All different states based on the price signal and power demand.

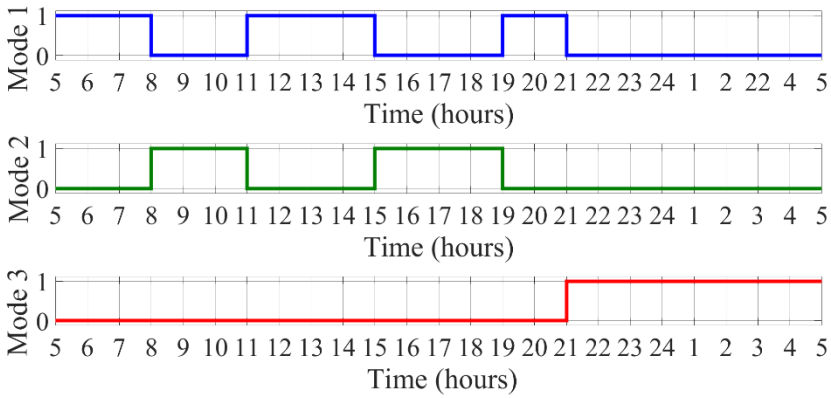

Figure 4-13 Action taken based on the current state and convergence of Q-matrix; Mode 1: Do nothing, Mode 2: Shifting and Mode 3: Valley filling.

At 8:00 am, the energy price is high (£0.15/kW) and the power demand is also high (5000 W). According to Table 4.4, the value is 3.34 which indicates that a *shifting* action should be applied. During night-time, for example at 23:00 pm, the action of valley-filling is desirable because the price of electricity is cheap (£0.08/kW) and the power consumption is low (3000 W).

Based on this technique, Figure 4-14 shows the final power consumption profile of the household appliances over 24 hours. The proposed RL shows that the power consumption has been reduced by 13.45% and 19.35% during morning and evening periods respectively. Three periods are identified namely, *shifting* which occurred during [7am-9am] and [15pm-18pm], *valley-filling* occurred during [21pm-5am] and *do-nothing* occurred during [5am-7am], [11am-14pm] and [19pm-20pm].

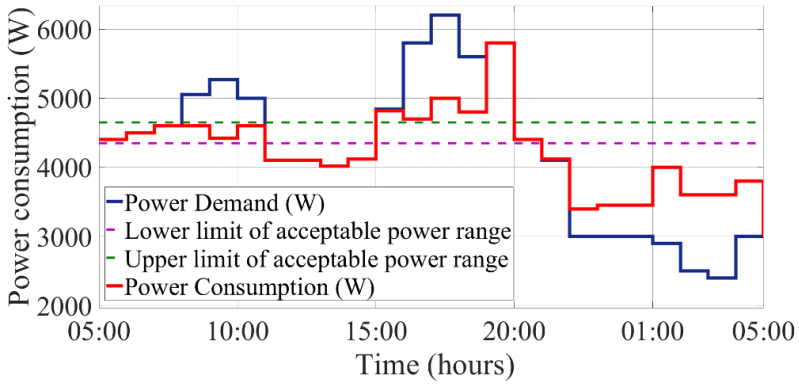

Figure 4-14 Power consumption profile after the implementation of RL algorithm.

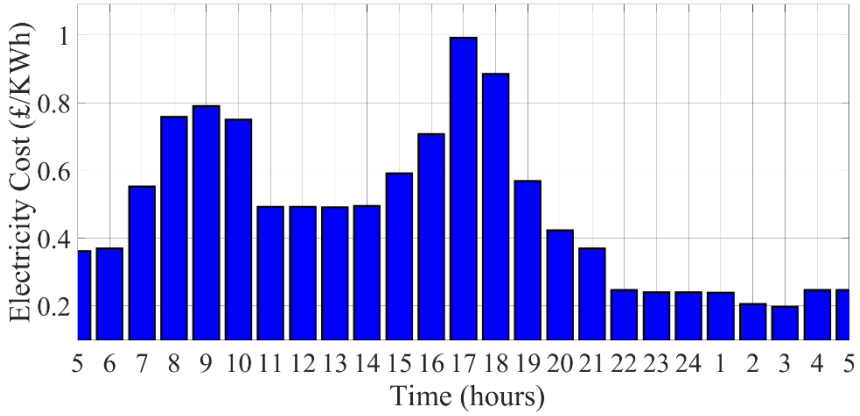

Figure 4-15 Electricity cost without Q-learning.

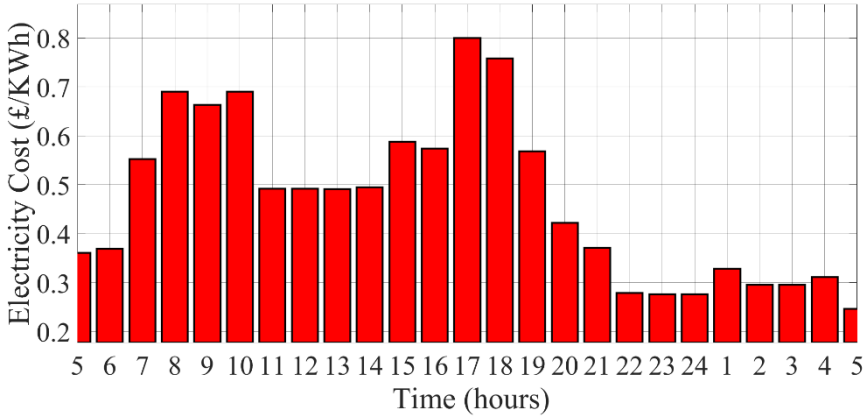

Figure 4-16 Electricity cost with Q-learning.

Figure 4-15 and Figure 4-16 show the total electricity cost of all appliances for each hour without and with the Q-value algorithm. The energy cost is reduced during peak demand (when the electricity price is higher). For example, during morning peak demand the energy cost is reduced from £0.8 to £0.7, and from £1.0 to £0.8 during evening peak period. Which demonstrates the effectiveness of the proposed Q-learning-based HEM scheme.

4.5.2 Implementation of comfort-based control strategy

In the previous Section, an effective energy management system for residential demand response using RL and FR is proposed to minimise energy utilisation and electricity bills by scheduling household appliances, in response to electricity price signal. However, in this Section, DR strategy is developed to improve the satisfaction based on user's comfort factors as discussed in Section 4.4.3. To demonstrate how this strategy can increase the user's satisfaction, the electricity price signal received from the utility grid is used as shown in Figure 4-17. The total household power demand that HEMS received from the smart meter is used as shown in Figure 4-18. Then, using Q-learning algorithm, HEMS detects the *Shifting*, *Valley filling* and *do-nothing* modes as shown in Figure 4-19. For example, at 8:00 am, the energy price (£0.14/kW) is higher than the average price and the power demand is higher than the upper limit of the average power demand, therefore the *shifting* mode is detected. At 3:00 pm the electricity price is low (£0.08/kW), and the power consumption is located between the upper and lower limits of the average demand. Thus, the *do-nothing* mode is active. During night-time, for example at 1:00 am, the *valley-filling* mode is detected because both the electricity price and power consumption are low.

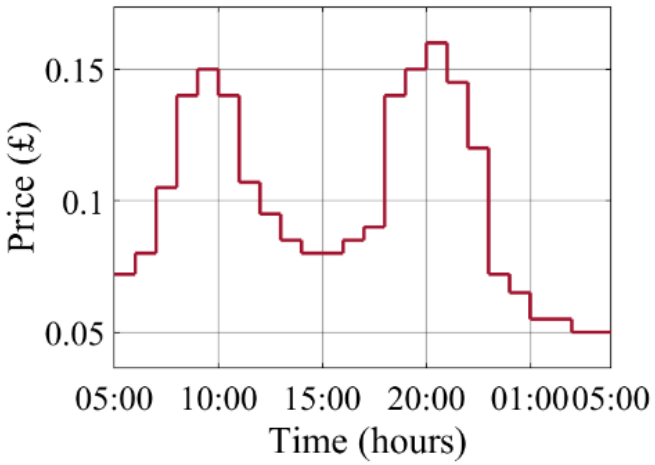

Figure 4-17 Real time energy price signal.

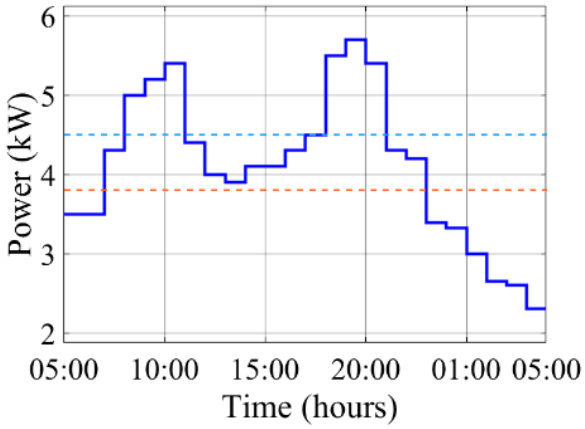

Figure 4-18 Power demand of household appliances.

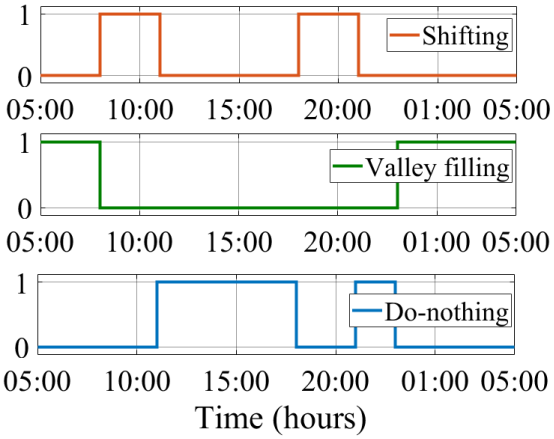

Figure 4-19 Output of DR strategy consisting of three modes.

During *shifting* and *valley filling* modes, Algorithm 2 is implemented to select which appliance needs to be shifted or turned on. The selecting process of sample hours is shown in

Table 4-8. For example, at 8:00 am, Hair Dryer (HD), Clothes Dryer (CD) and Washing Machine (WM) are supposed to be operating, because the shifting mode is active during this hour and the deficiency power to meet the average demand is less than the total power consumption of these three appliances, only the HD is shifted. In the next hour (9:00 am), Dish Washer (DW), CD and Hair Straightener (HS) need to be operating but the DW and HS are shifted because they have the highest shifting priority to meet the average demand. After shifting these two appliances, the power consumption becomes lower than the upper limit of the average demand. Therefore, HD can be turned on as it has been shifted during the previous hour. The final operation status of the shiftable appliances is presented in Figure 4-20. The total power consumption of the household appliances throughout a day is shown in Figure 4-21.

Table 4-8 Selection process of sample hours for the proposed strategy

Time	Mode	Appliance detail	R matrices	Actions
8:00		$a=\begin{bmatrix} Inx & J_t^n & e_t^n & T_{n,o} & T_{n,s} & T_{n,w} \\ 1 & 1 & 800 & 1 & 0 & 0 \\ 2 & 0 & 1100 & 0 & 0 & 0 \\ 3 & 1 & 450 & 2 & 0 & 0 \\ 4 & 1 & 400 & 3 & 0 & 0 \\ 5 & 0 & 20 & 0 & 0 & 0 \end{bmatrix}$	$R_s=\left[\begin{array}{ccccc\|c} Inx & \delta_s^n & \omega_s^n & \beta_s^n & \varphi_s^n & \gamma_s^n \\ 1 & 0.1 & 0.7692 & 0.25 & 1 & 0.5298 \\ 3 & 0.3 & 0.9474 & 0.25 & 1 & 0.6243 \\ 4 & 0.4 & 0.8888 & 0.1667 & 1 & 0.6139 \end{array}\right]$	Shift No.3
9:00	*Shifting*	$a=\begin{bmatrix} Inx & J_t^n & e_t^n & T_{n,o} & T_{n,s} & T_{n,w} \\ 1 & 0 & 800 & 0 & 0 & 0 \\ 2 & 1 & 1100 & 1 & 0 & 0 \\ 3 & 0 & 450 & 2 & 1 & 1 \\ 4 & 1 & 400 & 2 & 0 & 0 \\ 5 & 1 & 20 & 1 & 0 & 0 \end{bmatrix}$ $a=\begin{bmatrix} Inx & J_t^n & e_t^n & T_{n,o} & T_{n,s} & T_{n,w} \\ 1 & 0 & 800 & 0 & 0 & 0 \\ 2 & 0 & 1100 & 1 & 1 & 0 \\ 3 & 1 & 450 & 1 & 0 & 0 \\ 4 & 1 & 400 & 2 & 0 & 0 \\ 5 & 1 & 20 & 1 & 0 & 0 \end{bmatrix}$	$R_s=\left[\begin{array}{ccccc\|c} Inx & \delta_s^n & \omega_s^n & \beta_s^n & \varphi_s^n & \gamma_s^n \\ 2 & 0.2 & 0.7778 & 0.5 & 1 & 0.6195 \\ 4 & 0.4 & 0.7272 & 0.25 & 1 & 0.5940 \\ 5 & 0.5 & 0.0556 & 0.5 & 1 & 0.5139 \end{array}\right]$ $R_s=\left[\begin{array}{ccccc\|c} Inx & \delta_s^n & \omega_s^n & \beta_s^n & \varphi_s^n & \gamma_s^n \\ 4 & 0.4 & 0.2222 & 0.25 & 1 & 0.4675 \\ 5 & 0.5 & 0.5714 & 0.5 & 1 & 0.6435 \end{array}\right]$	Shift No.2 Turn on No.3 Shift No.5
10:00		$a=\begin{bmatrix} Inx & J_t^n & e_t^n & T_{n,o} & T_{n,s} & T_{n,w} \\ 1 & 0 & 800 & 0 & 0 & 0 \\ 2 & 0 & 1100 & 1 & 1 & 0 \\ 3 & 1 & 450 & 1 & 0 & 0 \\ 4 & 1 & 400 & 1 & 0 & 0 \\ 5 & 0 & 20 & 1 & 1 & 1 \end{bmatrix}$	$E_{def}^{sh}(t)-E_d^{shift}(t)\geq 0$	Shift all
23:00		$a=\begin{bmatrix} Inx & J_t^n & e_t^n & T_{n,o} & T_{n,s} & T_{n,w} \\ 1 & 0 & 800 & 0 & 2 & 4 \\ 2 & 0 & 1100 & 0 & 1 & 14 \\ 3 & 0 & 450 & 0 & 3 & 13 \\ 4 & 0 & 400 & 0 & 2 & 13 \\ 5 & 0 & 20 & 0 & 3 & 14 \end{bmatrix}$	$R_s=\left[\begin{array}{ccccc\|c} Inx & \delta_v^n & \omega_v^n & \varepsilon_v^n & \varphi_v^n & \gamma_v^n \\ 1 & 0.5 & 0.6777 & 0.875 & 0.75 & 0.7007 \\ 2 & 0.4 & 0.5430 & 0.9643 & 0.5 & 0.6018 \\ 3 & 0.3 & 0.9535 & 0.9615 & 0.8333 & 0.7621 \\ 4 & 0.2 & 0.9876 & 0.9615 & 0.75 & 0.7248 \\ 5 & 0.1 & 0.0930 & 0.9643 & 0.8333 & 0.4977 \end{array}\right]$	Turn on No.3
00:00	*Valley filling*	$a=\begin{bmatrix} Inx & J_t^n & e_t^n & T_{n,o} & T_{n,s} & T_{n,w} \\ 1 & 0 & 800 & 0 & 2 & 5 \\ 2 & 0 & 1100 & 0 & 1 & 15 \\ 3 & 0 & 450 & 0 & 2 & 6 \\ 4 & 0 & 400 & 0 & 2 & 14 \\ 5 & 0 & 20 & 0 & 3 & 15 \end{bmatrix}$ $a=\begin{bmatrix} Inx & J_t^n & e_t^n & T_{n,o} & T_{n,s} & T_{n,w} \\ 1 & 0 & 800 & 0 & 2 & 5 \\ 2 & 0 & 1100 & 0 & 1 & 15 \\ 3 & 0 & 450 & 0 & 2 & 6 \\ 4 & 0 & 400 & 0 & 2 & 14 \\ 5 & 0 & 20 & 0 & 3 & 15 \end{bmatrix}$	$R_v=\left[\begin{array}{ccccc\|c} Inx & \delta_v^n & \omega_v^n & \varepsilon_v^n & \varphi_v^n & \gamma_v^n \\ 1 & 0.5 & 0.75 & 0.9 & 0.75 & 0.725 \\ 2 & 0.4 & 0.6076 & 0.9667 & 0.5 & 0.6186 \\ 3 & 0.3 & 0.9677 & 0.9177 & 0.75 & 0.7339 \\ 4 & 0.2 & 0.9090 & 0.9643 & 0.75 & 0.7058 \\ 5 & 0.1 & 0.08 & 0.9667 & 0.8333 & 0.4950 \end{array}\right]$ $R_v=\left[\begin{array}{ccccc\|c} Inx & \delta_v^n & \omega_v^n & \varepsilon_v^n & \varphi_v^n & \gamma_v^n \\ 1 & 0.5 & 0.0722 & 0.9 & 0.75 & 0.5556 \\ 2 & 0.4 & 0.0531 & 0.9667 & 0.5 & 0.4799 \\ 4 & 0.2 & 0.1395 & 0.9643 & 0.75 & 0.5134 \\ 5 & 0.1 & 0.5 & 0.9667 & 0.8333 & 0.6000 \end{array}\right]$	Turn on No.3 Turn on No.5
04:00		$a=\begin{bmatrix} Inx & J_t^n & e_t^n & T_{n,o} & T_{n,s} & T_{n,w} \\ 1 & 0 & 800 & 0 & 0 & 0 \\ 2 & 0 & 1100 & 0 & 0 & 0 \\ 3 & 0 & 450 & 0 & 1 & 9 \\ 4 & 0 & 400 & 0 & 1 & 10 \\ 5 & 0 & 20 & 0 & 1 & 8 \end{bmatrix}$	$E_{def}^{sh}(t)-E_d^{shift}(t)\geq 0$	Switch on all

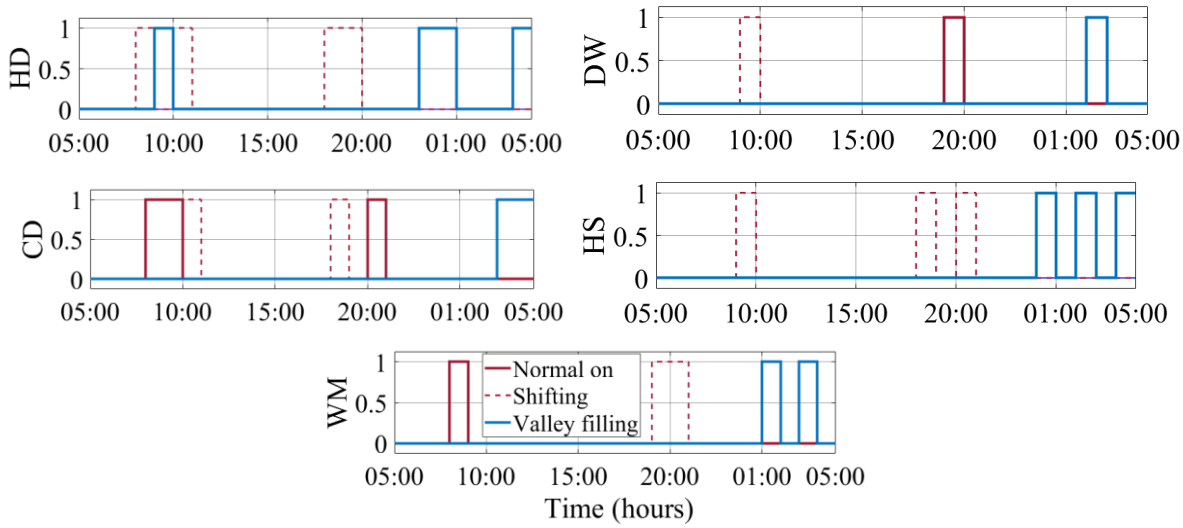

Figure 4-20 Status of the shiftable appliances after implementing the proposed strategy; WM: Washing Machine, DW: Dish Washer, CD: Clothes Dryer, HD: Hair Dryer and HS: Hair Straightener.

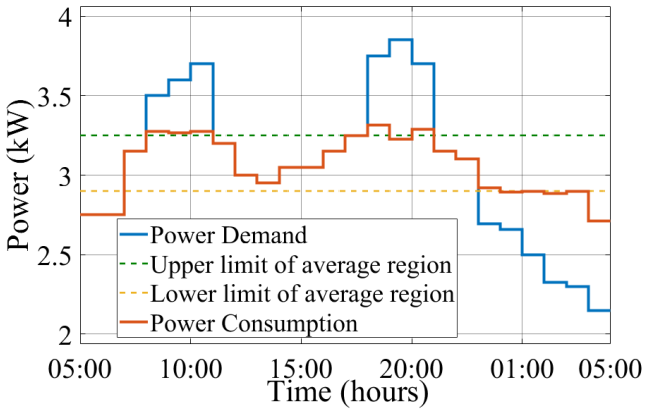

Figure 4-21 Power demand and power consumption after implementing both strategies.

The cost of energy usage is calculated as:

$$C_t = \min\left\{0, \sum_{t=1}^{24} E_d(t) \times P_h(t)\right\} \tag{4.5}$$

$P_h(t)$ is the electricity price received from the utility grid and C_t is the total cost of energy consumption. The proposed HEMS works based on RTP, which is considered as a dynamic pricing. Figure 4-22 shows the comparison of the cost reduction using both algorithms.

To evaluate how much the proposed strategy can increase the user's comfort, the dissatisfaction index is calculated as:

$$\pi_t = (1 - \frac{1}{S}\sum_{n=1}^{S} \gamma_s^n)^2 - \left(\frac{1}{V}\sum_{n=1}^{V} \gamma_v^n\right) \tag{4.30}$$

Where the first term indicates the user's dissatisfaction rate occurred by shifting *S* appliances during shifting mode, which depends on the user-comfort factors. While the dissatisfaction index can be reduced by switching on *V* appliances during *valley-filling* mode as described by the second term. Figure 4-23 shows the variations of the dissatisfaction index throughout the day.

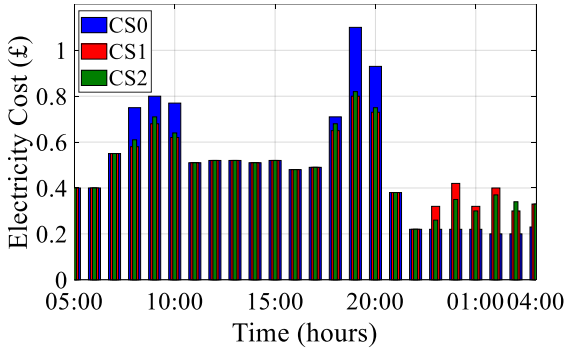

Figure 4-22 Electricity cost; CS0: cost without HEMS, CS1: cost using without considering user's comfort, CS2: cost under proposed strategy.

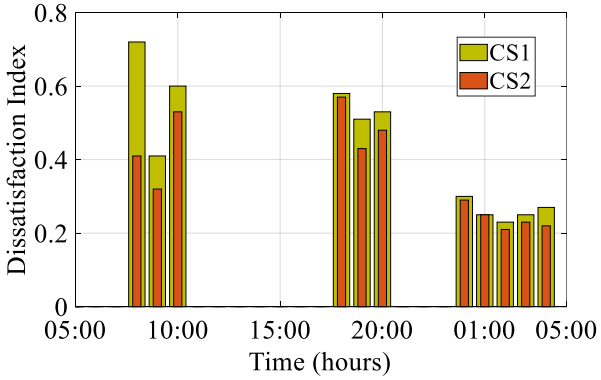

Figure 4-23 Dissatisfaction index during Shifting and valley filling modes.

4.6 Conclusion

This chapter proposed a demand response algorithm to minimise energy utilisation and electricity bills by shifting load demand, in response to electricity price signal and consumer preferences, from peak periods when the electricity price is high, to off-peak demand when the electricity price is low. In this study, an effective household energy management is developed

using Q-learning to deal with the dynamic electricity prices and different power consumption patterns without compromising the users' lifestyle and preferences. The proposed RL-based approach uses a single agent with a smaller number of states and actions to deal with 14 household appliances which in turn makes the implementation much easier with a better performance and lower time-consuming as compared to other techniques. Fuzzy reasoning is also used to mimic human decision-making in evaluating the random action that the agent could take as a reward function.

Simulation results have shown that the proposed DR approach results in a smooth energy usage profile and a reduction in the overall electricity costs by 16.4% and 17.5% during morning and evening peak periods respectively without using the user's comfort strategy comparing to 15% and 18.5% with the implementation of the user's comfort strategy, respectively. This is because without using the comfort-based strategy, all appliances are shifted during the Shifting mode, while the shifting process depends on the four factors by implementing the comfort-based strategy in order to increase the user's satisfaction. Therefore, the proposed approach has reduced the dissatisfaction index by 18.2% with implementing user's comfort strategy.

Chapter 5 Integration of Electric Vehicles into Demand Response

5.1 Introduction

More recently, there has been a gradual shift towards the adoption of Electric Vehicles (EVs) in the automotive industry. The main drivers are the economic and environmental benefits, the technological improvement in batteries' energy density, and government policies offering financial rewards such as tax breaks or rebates to EV owners [56]. In a report published by the UK National Grid in Future Energy Scenarios, the number of EVs is expected to grow significantly to 11 million by 2030 and to 36 million by 2040 [57]. EVs charging during peak hours leads to the electricity price increase, additional demand and imposes severe stress on the distribution grid. This may create problems such as feeder congestion, distribution transformer overloads and excessive voltage drops which may impact the overall electricity network [58]. In contrast, off-peak EV charging benefits EV owners from lower electricity prices and helps reduce stress on the power grid. On the other hand, EVs could also serve as a temporary energy storage and supply power to home appliances during short-term outages, provide emergency charging to other EVs or feed power to the utility grid when needed. However, draining the complete EV battery energy during the day could potentially disrupt EV availability for travel needs [59]. Therefore, a more sophisticated management of the EV battery is required. As such, a holistic approach must be adopted for EVs to serve as a DR resource and close the energy gap. For example, in [60], a fair demand response with electric vehicles (F-DREVs) is proposed for a cloud-based energy management service to maximise incentives by minimising global cost within the given time period, and smooth fluctuations of EVs loads. In [61], a new scheduling approach is proposed for isolated microgrids (MGs) with renewable generations by incorporating demand response of EVs.

V2G technology has attracted a great deal of research interest in recent years both within the academic community and industry. A review on the impact of V2G technology is presented in [62]. In [63], different control schemes to enable EV grid integration are reviewed and the advantages and disadvantages of V2G integration are discussed with respect to the transient stability of the power grid at the transmission and distribution levels. The authors in [64] proposed a combined control and communication approach to ensure efficient energy transfer and maintain a balance between energy suppliers and consumers. Energy management of EV

battery is proposed in [65] by taking into consideration the V2G connection, prices for selling and purchasing electricity, and the daily load profile of household appliances. In [66], an optimised smart charging and discharging coordination scheme using Linear Programming (LP) based on a heuristic algorithm is proposed for V2G technology. The aim of the proposed algorithm is to cope with a variety of loads and departure times of EVs. Bayesian Neural Networks (BNN) have been proposed in [67] for predicting electricity prices for charging/ discharging EV battery while minimising charging costs over a long-term time horizon. Classical optimisation methods such as linear programming, dynamic programming and their counterparts have been applied to the scheduling of EV charging/discharging. However, these methods suffer from the curse of dimensionality and cannot adapt to the environment's stochasticity including unpredictable load profile, price signals and changing driving patterns. Global search methods such as genetic algorithm, swarm intelligence and their hybrids with the linear optimisation methods are also used for solving power management problems. However, these methods are generally slow and computationally intensive; thus they are not suitable for real-time. In addition, when using such methods, which do not have a learning component, optimisation iterations are needed for every new load and generation profile, which is also computationally intensive.

Machine learning techniques such as reinforcement learning algorithms offer a better alternative as they can be trained offline for a general load and generation profile and then they can be applied online for any load profile, dynamic electricity price signal and various driving patterns. Multi-agent reinforcement learning has been proposed for the optimal scheduling of household appliances including V2G technology in smart home to optimise the energy utilisation [68]. However, multi-agents RL requires setting several agents, with each agent having different actions and rewards therefore making the learning process more complex. Other studies have focussed on using Markov Decision Process (MDP) algorithms in HEMS to determine the optimal strategy for the scheduling of EV charging and discharging [69]. However, these algorithms require historical data, such as electricity prices and battery SOC as inputs to compute the charging/discharging schedules in real-time.

5.2 Overview on V2G technology

V2G and V2H are two technologies in which EVs equipped with bidirectional power flow capability can connect to the charging station to draw power from the grid, deliver power to the grid or provide back-up electricity supply to a home. A typical bidirectional EV battery

charger consists of bidirectional AC/DC and DC/DC converters as shown in Figure 5-1 [70]. In charging mode, the bidirectional AC/DC converter is used to convert the AC grid power to DC for the battery and in discharging mode, the DC battery power is converted to AC power and injected back to the grid or used to supply the house. The DC/DC converter, on the other hand, controls the bidirectional power flow by using current control technique. The DC/DC converter can act as a buck or boost converter during charging or discharging mode, respectively.

With the advancement in battery technologies, the energy storage capacity of EVs has significantly improved. Currently, the capacity of EV batteries varies from 1 to 100 kWh. Battery capacity of a Nissan Leaf 2018 is 40 kWh, that of a Tesla Model 3 is 80 kWh and Tesla Model S is 100 kWh.

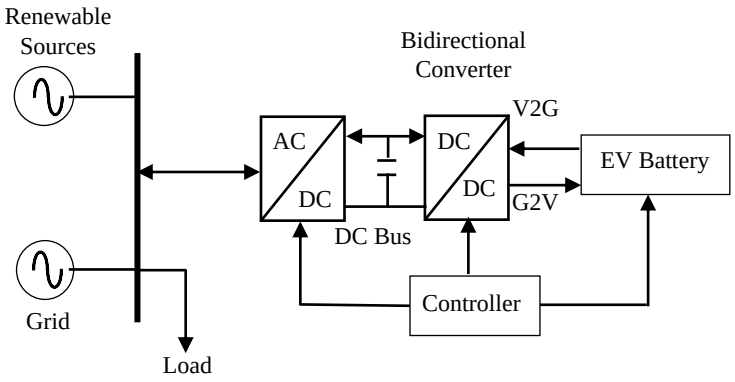

Figure 5-1 V2G using bidirectional converters. V2G, vehicle to grid.

5.2.1 V2G technology

Using V2G technology, EVs can be connected to the power grid to charge, as well as feed energy back to the grid when required. V2G technology is attractive due to its benefits to grid operators and EV owners. EVs with V2G capability are considered as an alternative energy source for the grid and can provide ancillary services to the grid such as frequency/voltage support, load balancing, support to intermittent power of renewable energy, reactive power support, valley filling and peak shaving. Therefore, an effective energy management is required to coordinate the charging/discharging modes of the EV battery. Smart chargers and their energy management system are key factors in the implementation of bidirectional V2G scheme. In [71], the authors proposed a controllable EV charger that enables an autonomous smart energy management system in a residential sector. The proposed power converter topology allows charging/discharging operations at different power levels. Several V2G demonstrator

projects have been conducted around the world over the recent years most of them in Europe. Some of these V2G models have been adopted by leading car manufacturers and are already in the marketplace. In the UK, the Sciurus project is among the world's largest V2G projects aimed to develop and deploy a large number of chargers for domestic use. This project aims to validate the technical and commercial benefits of V2G technology to the power grid and demonstrate its value to EV manufacturers [72]. In Germany, the world's leading car manufacturer Nissan, the transmission system operator TenneT and The Mobility House energy supplier have successfully completed a substantial V2G pilot project. The project aims to respond to the increasing concern of Germany about saving the surplus of energy generated from renewable, intermittent sources such as wind energy. In this project, Nissan Leaf batteries are used for energy storage. When fully charged, the batteries feed the stored energy back to the grid when needed [73]. The SEEV4-City project, funded by the EU Interreg North Sea Region, aims to deploy V2G technology to use EV batteries as short-term storage of renewable energy to support the grid or redirect the available energy form vehicles to homes, neighbourhoods, or cities [74].

5.2.2 V2H technology

V2H enables an EV to act as a backup power source and supply electricity to a home during short-term power outages or contribute to peak demand reduction, smooth home energy consumption, and minimise energy purchase from the grid. Some of the very significant and unique features of V2H technology is its simple implementation and some car manufacturers have already started deploying this technology. For example, Mitsubishi Motors Corporation (MMC) announced a new EV model called Dendo Drive House (DDH) at the 89th Geneva Motor Show [75]. This model is considered as a packaged system comprising an EV/PHEV, solar panel and a bidirectional V2H charger. DDH offers owners savings on charging costs and an emergency power source. Nissan Australia launched a new version of Nissan Leaf Plus that incorporates V2H capability [76] V2H-equipped Leaf can be used as energy storage with the capability to supply energy to household appliances.

5.3 Modelling of the Grid Integration Framework

5.3.1 Modelling of V2G and V2H systems

Figure 5-2 depicts the overall structure of the EV model interfaced with the grid and the home and illustrates the operations modes and services it can provide during these modes.

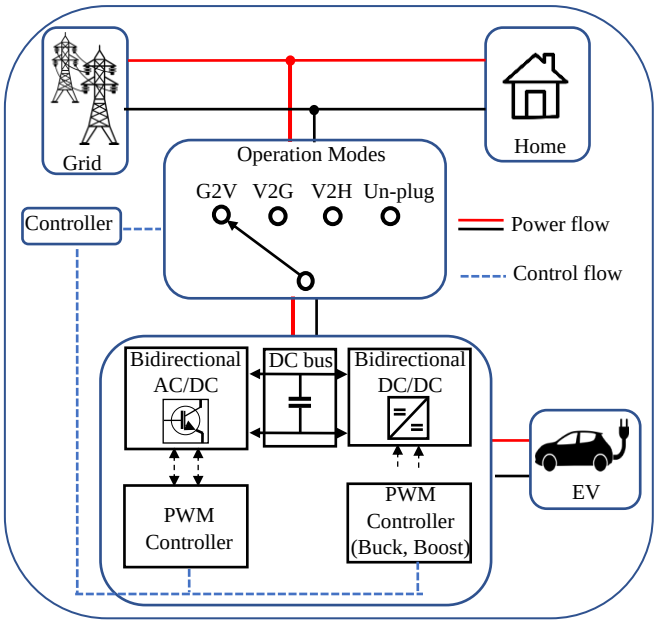

Figure 5-2 Selection of EV operation modes.

Table 5-1 shows different types of EVs with different battery capacity and brands. The Nissan LEAF 2018 model is used in the simulations. The battery has a maximum capacity of 40 kWh which gives a driving autonomy of 151 miles, a charging time empty to full of 8 hours (230 VAC 15 A).

Table 5-1 Different Type of EV.

Manufacturer	Model	kWh	Miles	Battery type
Ford	2018 Focus Electric	33.5	115	Liquid-cooled lithium-ion battery
Volkswagen	2018 Volkswagen e-Golf	35.8	120	Lithium-ion battery
Nissan	2018 Nissan LEAF	40	151	Lithium-ion battery
Chevrolet	2018 Chevy Bolt	60	238	nickel-rich lithium-ion
Tesla	2018 Tesla Model 3	75	285	Lithium-ion battery

The total energy stored in the EV battery is given by:

$$E_{EV}^{Total} = E_{int} + \Delta E_{ch} - \Delta E_{dis-A} - \Delta E_{dis-grid} - E_{trip} \quad (5.1)$$

Where E_{EV}^{Total} is the net energy stored in the battery, E_{int} is the initial energy stored in the battery, ΔE_{ch} is the energy drawn from the grid to charge the EV battery, ΔE_{dis-A} represents the energy delivered to the household appliances, $\Delta E_{dis-grid}$ is the energy fed to the grid and E_{trip} denotes the total energy consumed by the EV during the trip.

$$\Delta E_{ch} = m_{G2V} \int_{t_{in}}^{t_{out}} P_{ch}(t).dt \tag{5.2}$$

$$\Delta E_{dis-A} = m_{V2H} \int_{t_{in}}^{t_{out}} P_{dis}(t).dt \tag{5.3}$$

$$\Delta E_{dis-grid} = m_{V2G} \int_{t_{in}}^{t_{out}} P_{dis}(t).dt \tag{5.4}$$

Where $P_{ch}(t)$ and $P_{dis}(t)$ are the charging and discharging powers respectively. m_{V2H}, m_{V2G} and m_{G2V} represent the status of the EV connection mode and assume values 0 or 1.

The proposed management strategy depends also on the SOC of the battery which is the key parameter in the EV as it is a measure of the amount of the energy stored in it. The typical estimation of the SOC of the EV battery is based on the charging/discharging energy as follows:

$$SOC = SOC_{int} + \frac{\Delta \mathrm{E_{ch}} + \Delta E_{dis-A} + \Delta E_{dis-grid}}{E_{EV}^{rat}} \tag{5.5}$$

Where SOC_{int} is the initial SOC and E_{EV}^{rat} is the energy capacity of the battery.

Considering the battery lifecycle, some constraints have been imposed on the power delivered by the EV to the grid (V2G) or to the home (V2H) and on the battery State-of-Charge (SoC). Equation (5.6) shows that the EV power is constrained between the minimum operating power P_{min} to be supplied to the EV and the maximum power range P_{max} to be injected in the grid/home.

$$P_{max} \geq P_{dis}, P_{ch} \geq P_{min} \tag{5.6}$$

Similarly, Equation (5.7) prevents deep discharging and over-charging of the EV battery by imposing a minimum SoC (SOC_{min}) and a maximum SoC (SOC_{max}) respectively:

$$SOC_{min} < SOC < SOC_{max} \tag{5.7}$$

5.3.2 Modelling of EV driving patterns

The EV model is interfaced to *Google map* via the App Designer Tool of MATLAB and allows the calculation of the distance, power required, arrival and departure time for each trip. This

information will be employed for scheduling the battery charging and discharging times to make sure the vehicle is always sufficiently charged for the next trip.

The availability of EV refers to whether the vehicle is parked at home and accessible for either V2H or V2G connections and is defined as follows:

$$C_{ev} = \begin{cases} 1 & \text{EV available} \\ 0 & \text{EV not available} \end{cases} \tag{5.8}$$

Using the designed user-interface, the EV owner can schedule his/her trip by selecting the destination and departure times as shown in Figure 5-3.

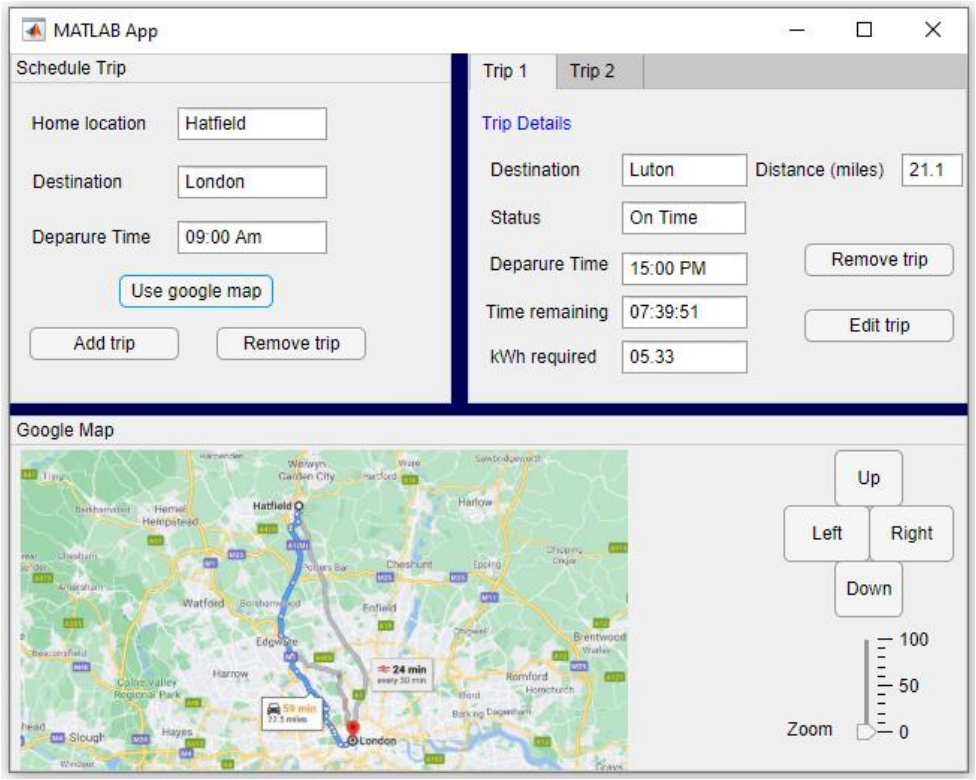

Figure 5-3 User-interface for scheduling trips.

Once the trip distance is determined, the energy required for the trip is calculated as follows:

$$E_{trip} = \frac{D_{trip}}{D_{max}} \times E_{EV}^{rat} \tag{5.9}$$

Where D_{trip} and D_{max} are the distance of the trip and the maximum distance the EV can travel with full SOC, respectively, E_{EV}^{rat} denotes the maximum energy capacity of the EV battery.

5.3.3 Modelling of the household load profile

Generally, the daily power consumption of a typical household contains two peaks occurring during the morning and evening times when energy prices are higher as shown in Figure 5-4.

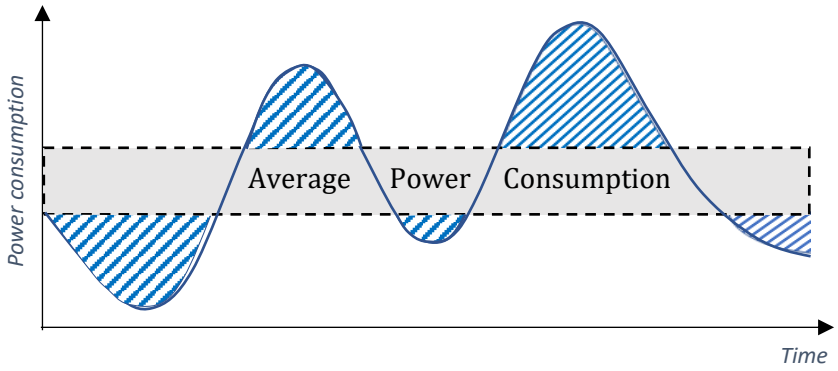

Figure 5-4 Typical household energy consumption.

The off-peak period corresponds to the period of the day when electricity prices are lower since household activities such as washing, cleaning, cooking, and watching TV are reduced. As mentioned before, the household appliances are divided into shiftable and non-shiftable appliances. Therefore, at each time step (considered as an hour in this work), the total power demand of all appliances during a certain hour is:

$$E_h^T = \sum_{n=1}^{N} e_n^{shft} . J_n^{shft} + \sum_{m=1}^{M} e_m^{non} . J_m^{non} \tag{5.10}$$

Where e_n^{shft} and e_m^{non} represent the rated power of each shiftable appliance and non-shiftable appliance, respectively. $J_{n/m}^{shft/non}$ denotes the status of the appliance and takes values 0 (off) or 1 (on) respectively, $t \in \{1, 2, 3, \dots, 24\}$ represents the hour of the day, $n \in \{1,2, \dots, N\}$ is the appliance number and N is the total number of the shiftable appliances. $m \in \{1,2, \dots M\}$ refers to the appliance number and M is the total number of the non-shiftable appliances.

5.4 V2G Demand Response Based on Q-Leaning

With V2G technology, EVs become a distributed energy storage and can offer a range of ancillary services by back-feeding power to the electricity grid such as DR, peak-load management, voltage support, frequency regulation. The provision of these grid services will enable EV owners to save on energy costs and generate revenue through price arbitrage. V2G technology is evolving at an accelerated pace and research is ongoing to enhance its functionality and implementation. In this chapter, an effective V2G-based DR approach for the energy management of residential loads using Q-learning and RTP is presented.

5.4.1 Q-learning model for the EV

RL is adopted here to make an optimal decision on charging or discharging of EV battery under dynamic electricity prices and different energy consumption patterns using an intelligent agent which controls the dynamic process by executing sequential actions. The dynamic process is characterised by a state-space and a numerical reward that evaluates the new state when a given action is taken. In this study, the Q-learning model components are defined as follows:

A. State-space implementation using fuzzy logic

To reduce the number of states, the Fuzzy Logic toolbox of MATLAB software is used. The state-space here is represented by the total household loads profile, SOC of the EV battery, availability of the EV and the electricity price signal. To simplify the model and reduce the computation time, the household power demand is divided into four levels Extremely Low, Low, High and Extremely High. The SOC of the EV battery is defined as Extremely Empty, Low, High and Extremely Full; the EV availability can be Available or Unavailable. Finally, the price signal is categorised into Cheap and Expensive price.

The state is formulated using Fuzzy Logic. Fuzzy reasoning is a decision-making model that deals with approximate values rather than exact values. The FIS based on Mamdani method is used because it offers a smoother output. The input variables of the fuzzy state model are the total home power demand (E_t^{total}) , the electricity price (P_t) , the SOC of the EV battery (SOC_t) and the availability of EV (C_v), and the output variable is the States.

The MFs for the input variable "Total household loads" are triangular and are labelled as: Extremely Low, Low, High and Extremely High. The universe of discourse of power demand is chosen as [0 6300] (Watt). The fuzzy sets of electricity price are defined as Cheap and Expensive. The MFs are Gaussian and the universe discourse is [0 0.16] (£/kWh). For the SOC, the universe discourse is defined [0 100] %, and the associated fuzzy sets are Extremely Empty, Low, High and Extremely Full as shown in Figure 5-5. The output of the system is the State, and there are 25 States in total as shown in Figure 5-6. The fuzzy rules are shown in Table 5-2.

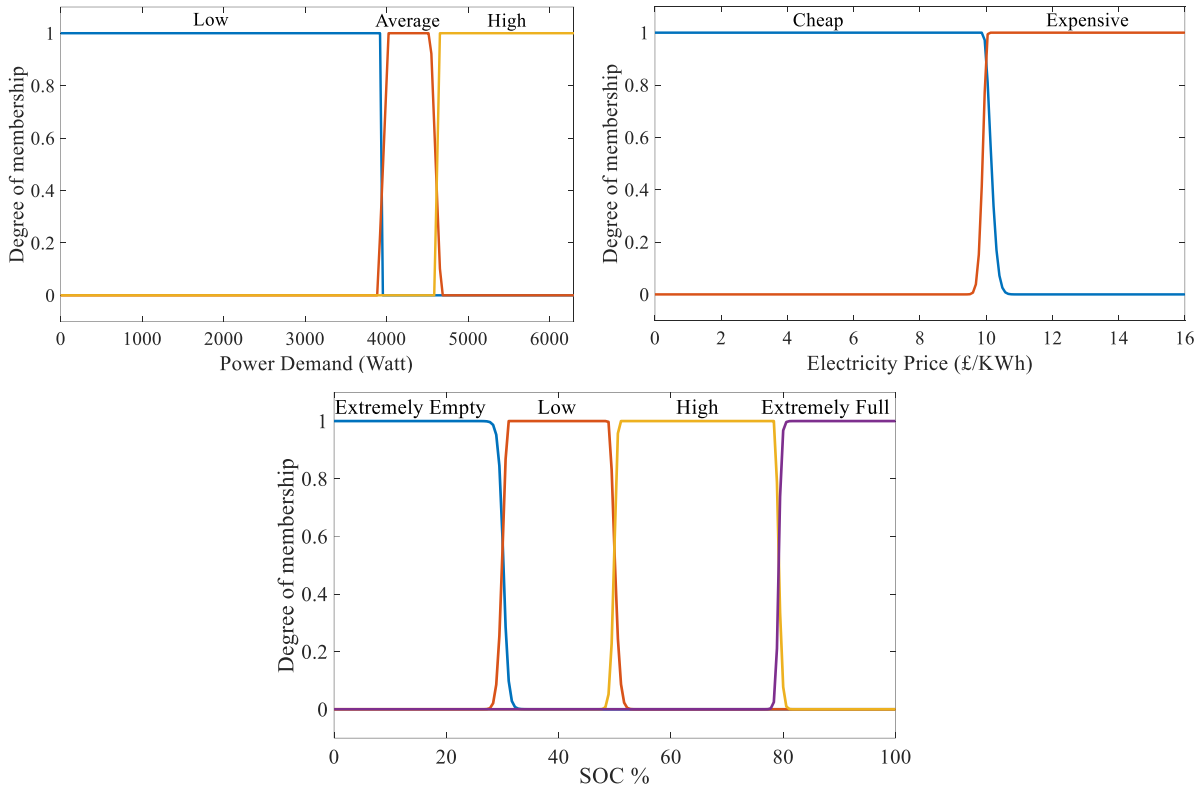

Figure 5-5 Fuzzy sets and MFs of input variables for States.

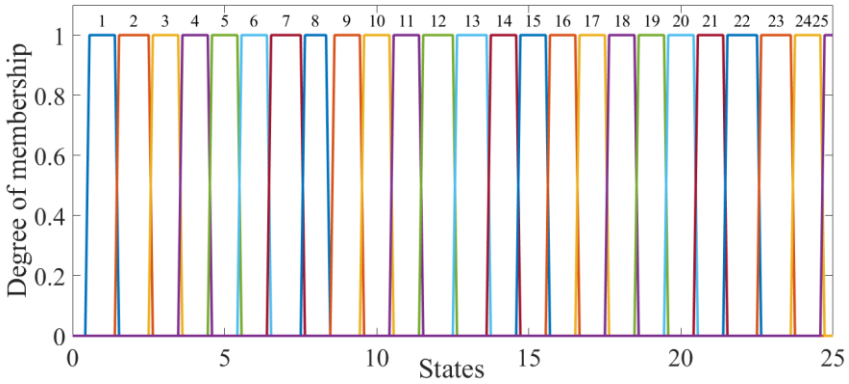

Figure 5-6 Fuzzy sets and MFs of output variable for States.

Table 5-2 Fuzzy rules of FIS system for the state space.

SOC	E_t^{TOTAL}	Price	Cv	State
-	-	-	Unavailable	1
Extremely Low	Low	Cheap	Available	2
Low	Low	Cheap	Available	3
High	Low	Cheap	Available	4
Extremely High	Low	Cheap	Available	5
Extremely Low	Average	Cheap	Available	6
Low	Average	Cheap	Available	7
High	Average	Cheap	Available	8
Extremely High	Average	Cheap	Available	9
Extremely Low	Average	Expensive	Available	10
Low	Average	Expensive	Available	11
High	Average	Expensive	Available	12
Extremely High	Average	Expensive	Available	13
Extremely Low	High	Cheap	Available	14
Low	High	Cheap	Available	15
High	High	Cheap	Available	16
Extremely High	High	Cheap	Available	17
Extremely Low	High	Expensive	Available	18
Low	High	Expensive	Available	19
High	High	Expensive	Available	20
Extremely High	High	Expensive	Available	21
Extremely Low	Low	Expensive	Available	22
Low	Low	Expensive	Available	23
High	Low	Expensive	Available	24
Extremely High	Low	Expensive	Available	25

B. Action space

The proposed strategy aims to schedule the charging time of the EV to be during off-peak hours when electricity prices are lower. It also aims to manage the energy stored in the EV battery whether to supply the household appliances during high energy prices or outage (V2H), or to deliver the energy back to grid using (V2G) depending on the SOC and availability of the EV.

Therefore, the actions set can be summarised as Charging, Discharging/Appliances, Discharging/Grid and Do nothing. Based on the current State, the agent chooses one action from the action space A that given by:

$$A = \left[Charging, Discharging_{appliances}, Discharging_{grid}, Donothing\right] \quad (5.14)$$

C. Reward function implementation using fuzzy logic

The agent receives a numerical reward $r(s_t, a_t)$ after executing a random action and observing the new state. This reward value aims to evaluate how good is the action taken by the agent for

a certain state. Fuzzy logic is also used here to evaluate the action that will be taken for a certain state.

The input variable of the reward function's FIS is the current state s_t which is the output of the FIS system of the state space as shown in Figure 5-6. The outputs of the system are the evaluation of the random action which was defined in Q-learning. For each action taken (output), the fuzzy sets are determined as Bad Action (BA), Good Action (GA) and Very Good Action (VGA). The universe of discourse of MFs is defined as [0 100] to evaluate all possible actions with values out of 100 as shown in Figure 5-7.

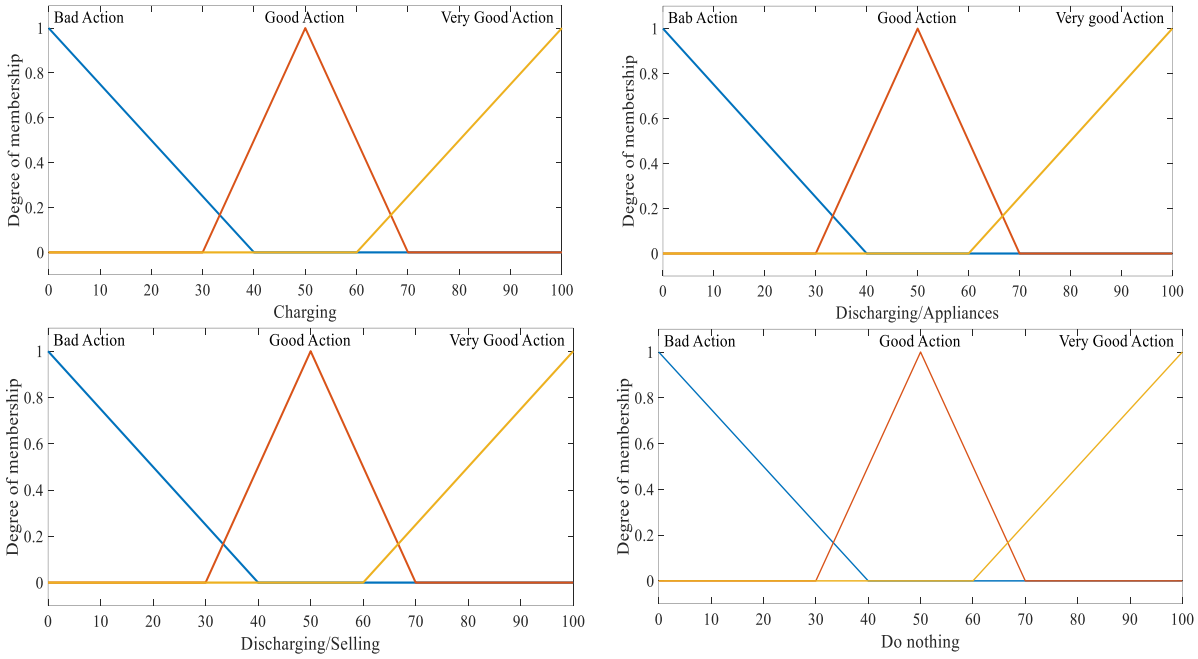

Figure 5-7 Fuzzy sets and MFs of output variable for States.

Table *5-3* shows the list of fuzzy rules. The evaluation actions process works as follows; firstly, the FIS system of the state-space will identify the current state, based on the current space, the agent will take a random action from the actions space. The FIS system of the reward function evaluates all the possible actions with value out of 100 and then the agent will receive a numerical value corresponding to the action taken.

Table 5-3 Fuzzy rules of FIS system for reward function.

State	Charging	Discharging/Appliances	Discharging Selling	Do nothing
1	BA	BA	BA	VGA
2	VGA	BA	BA	BA
3	VGA	BA	BA	BA
4	VGA	BA	GA	BA
5	BA	BA	GA	VGA
6	GA	BA	BA	VGA
7	GA	BA	BA	VGA
8	BA	GA	BA	VGA
9	BA	GA	BA	VGA
10	BA	BA	BA	VGA
11	BA	BA	VGA	GA
12	BA	GA	VGA	BA
13	BA	GA	VGA	BA
14	GA	BA	BA	VGA
15	BA	GA	BA	VGA
16	BA	GA	BA	VGA
17	BA	GA	BA	VGA
18	BA	BA	BA	VGA
19	BA	VGA	BA	GA
20	BA	VGA	BA	GA
21	BA	VGA	BA	BA
22	BA	BA	BA	VGA
23	BA	BA	VGA	GA
24	GA	BA	VGA	BA
25	BA	BA	VGA	BA

5.4.2 EV energy management strategy using Q-learning

Using the Q-learning off policy, the agent learns from taking a random action at a certain state without following a current policy. This means that a policy is not required during a training process. The Q-matrix with a dimension of $[states \times actions]$, should be initialised to zero (i.e. the Q-value of each state-action pair is assigned the value zero). Then, the agent will interact with the environment and update each pair in that matrix after each action taken using Equation (3.4). In the proposed model, a random action called "exploring" is applied in which case, an appropriate number of iterations will be required to explore and update the values of $Q(s_t, a_t)$ for all state-action pairs at least once. After convergence of the Q-matrix, the optimal Q-values will be obtained.

The pseudo-code listed in Table 5-4 (Algorithm 1) illustrates the procedure of the main algorithm for training Q-learning agent which has been implemented in MATLAB. Firstly, a certain state and a numerical reward are defined using fuzzy logic. The parameters γ and α are set to 0.8 and 0.2 respectively and the Q-value matrix entries are initialised to zeros. For each current state, all possible actions are specified, and then an action will be selected randomly. After the selected action is executed, the numerical reward (using fuzzy logic) for that action and the new state will be observed by the agent. The maximum Q-value for the next state should also be determined and then the Q-value of the state-action pair will be updated using Equation (3.4). Finally, the next state will be used as a current state. To allow the agent to visit all state-state pairs and learn new knowledge, the training process is set to 1000 iterations.

Table 5-4 EV energy management using Q-learning algorithm.

Algorithm 1

- Set $\boldsymbol{\gamma}$,$\boldsymbol{\alpha}$ parameters and environment rewards.
- Initialise $Q(s_t, a_t)$, $\forall s \in S, \forall a \in A$.
For each time step t do
- Choose a random initial state.
While hour = 1:24
- Determine all available actions.
- Select random action from all possible actions for the current state.
- Execute the selected action $\boldsymbol{a_t}$, and observe the new state s_{t+1} and numerical reward $r(s_t, a_t)$.
- Determine the maximum Q-value for next state in Q-matrix.
- Update the $Q(s_t, a_t)$ using Equation (3.4).
- Set the next state as current state.
End while
End for

5.5 Results and Discussion

5.5.1 Implementing the proposed strategy with a single EV in a household

The proposed EV management strategy works based on the relationships between the household power demand, electricity price, and SOC and availability of EV. Once the EV arrives at home, HEMS will receive a signal of EV availability with the percentage of SOC.

Consequently, HEMS can make an optimal decision whether the EV battery needs to be charged from the grid, there is a need to supply the appliances or sell energy to the grid using the convergence Q-matrix. The time simulation is set for one day (24 hours) with 5 minutes time-steps in order to address the uncertainties with the variation in electricity prices. We assumed that the price signal received from the utility grid as shown in Figure 5-8. It is assumed that the user leaves the house by 09:00 am and returns at 14:00 pm.

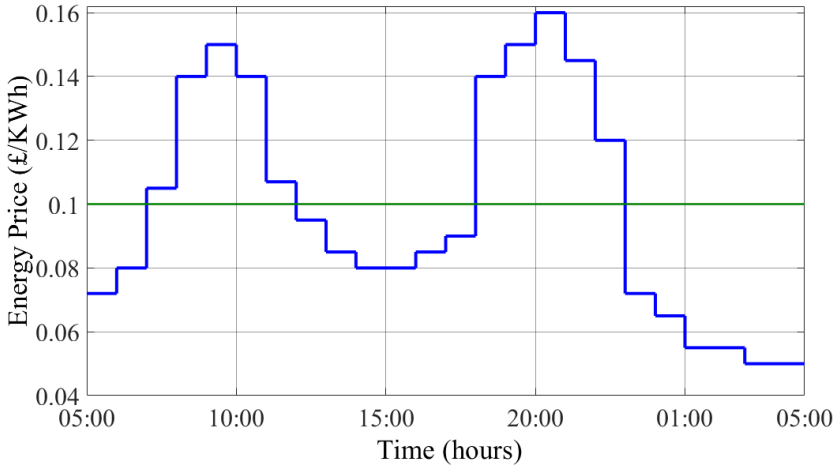

Figure 5-8 Real time price (blue) and average price (green) signals.

The total power demand of the household appliances is shown in Figure 5-9. There are two peak periods, morning peak hours [7:00 am-10:00 am] when the households wake up and evening peak period [18:00 pm -21:00 pm] when they start cooking, watching TV and doing other activities. The mid-peak period occurs after and before these two peak periods. Off-peak period occurs usually after mid-night till the morning.

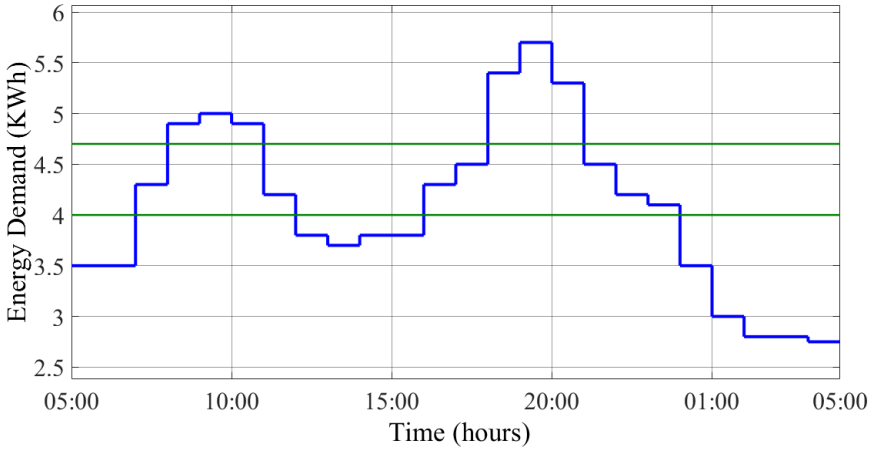

Figure 5-9 Total power demand of the smart home.

A. Case 1: Weekdays with 70% of SOC

In this case, the initial SOC of the EV battery is set to 70%. based on the relationship between the electricity price signal, the total power demand and the Q-values. Figure 5-10 (a) shows all the actions taken. For example, the total energy demand is low (3.5 kWh) during the period [5:00 am-7:00 am], the energy price is 0.07 £/kWh at 5:00 am and 0.08 £/kWh at 6:00 am, the SOC is high at 70 % and the EV is available $C_{EV} = 1$. Therefore, the current state is defined as $s_t = [Low, Cheap, High, 1]$. According to the Q-value, the maximum Q-value for this State refers to the Charging action. To protect the battery from the overcharging, the maximum SOC is set to 80%. Therefore, from Figure 5-10 (b), it can be observed that the charging mode is stopped during the last half an hour because the SOC reached 80%, and the *Do-Nothing* mode is active. At 7:00 am, the system moves to another State because the energy demand is average (4.3 kW), the price is high (0.11£/kWh) and the battery is fully charged with an SOC of 80 %. Therefore, it is better to sell energy to the grid using V2G connection during this hour. In the next hour (8:00 am), the demand jumps to 4.8 kW (High), the energy price is 0.14 £/kWh and the SOC remains high at 70%, then the best decision is to supply the household appliances using V2H connection during this hour.

The user leaves his house with the EV at 9:00 am and returns at 14:00 pm, during this period the EV is not available, hence *Do-Nothing* mode is issued. When the EV returns home at 14:00 pm, the SOC is low, and the energy demand and price are also low (3.8 kW and 0.08 £/kWh respectively). Therefore, the EV battery is charged for two hours from 14:00 pm -16:00 pm till the SOC reached 60 %. During the next two hours (16:00 pm -18:00 pm), the action taken is *Do-Nothing* because the SOC is high, the energy price is low, and the energy demand is average. Therefore, there is no need to charge or discharge the battery. During the evening peak period from 18:00 pm to 21:00 pm, the energy demand and price are quite high, the EV battery has 60 % of SOC.

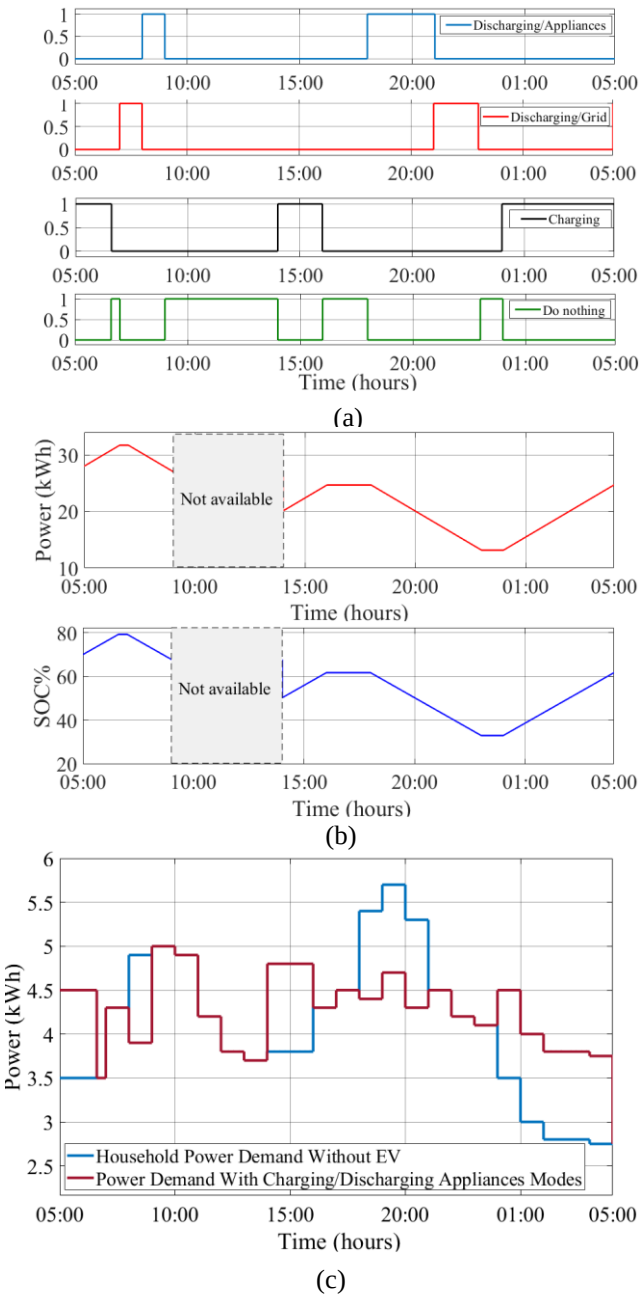

Figure 5-10 Initial SOC = 70 % (a) Actions, (b) SOC changes, (c) Power consumption.

Discharging/Appliances mode is triggered to supply energy to the appliances and reduce the electricity cost as shown in Figure 5-10 (c). Finally, during the period from 21:00 pm to 23:00 pm, *Discharging/Selling* mode is activated to export energy back to the grid since the SOC is at 50%. This period leads to a maximum user's revenue and reduces the stress on the power utility. The SOC drops to 30% at 24:00 pm, hence *Do-Nothing* mode is issued. The *Charging*

mode is activated at 24:00 pm till 5:00 am, and the SOC reaches 60 % to be ready for the next day.

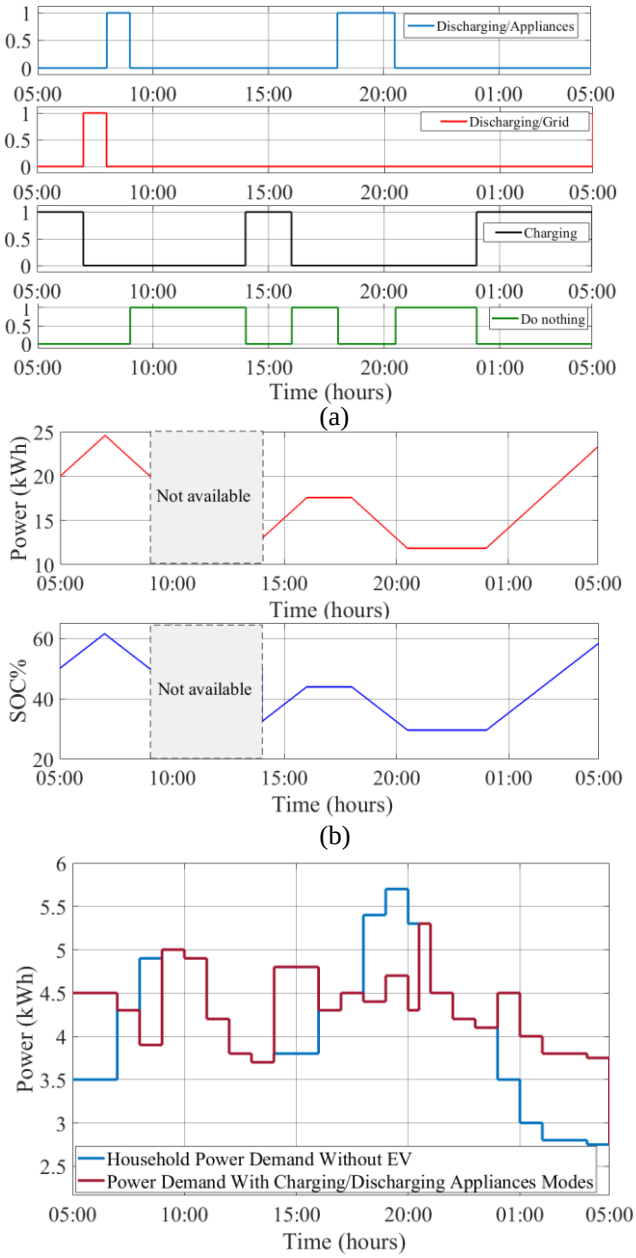

Figure 5-11 Initial SOC = 50 % (a) Actions, (b) SOC changes, (c) Power consumption.

B. *Case 2: Weekdays with 50% of SOC*

In this case, the initial SOC of the EV battery is set to 50 %. Because the SOC is reduced by 20 % from Case 1, the amount of energy sold to the grid is also reduced. Figure 5-11 (a) illustrates all the actions taken. The EV starts the day with a SOC of 50 % as shown in Figure

5-11 (b). The first two hours [5:00 am-7:00 am], the *Charging* mode is active till the SOC reaches 60%. During the morning peak hours [7:00 am-9:00 am], the EV battery is used to inject power to the grid at 7:00 am and supply the household appliances with different states and actions at 9:00 am as shown in Figure 5-11 (c). When the EV returns home at 14:00 pm, the mode *Charging* is activated for the hours [14:00 pm-16:00 pm] to charge the EV battery at a lower price and to have it available for the evening peak period. The V2H model is active during [18:00 pm - 21:00 pm] to supply the household appliances using *Discharging/Appliances* action. From 24:00 pm to 5:00 am (off-peak period), the EV starts charging to be ready for the next day's trips, the SOC reaches 60 %.

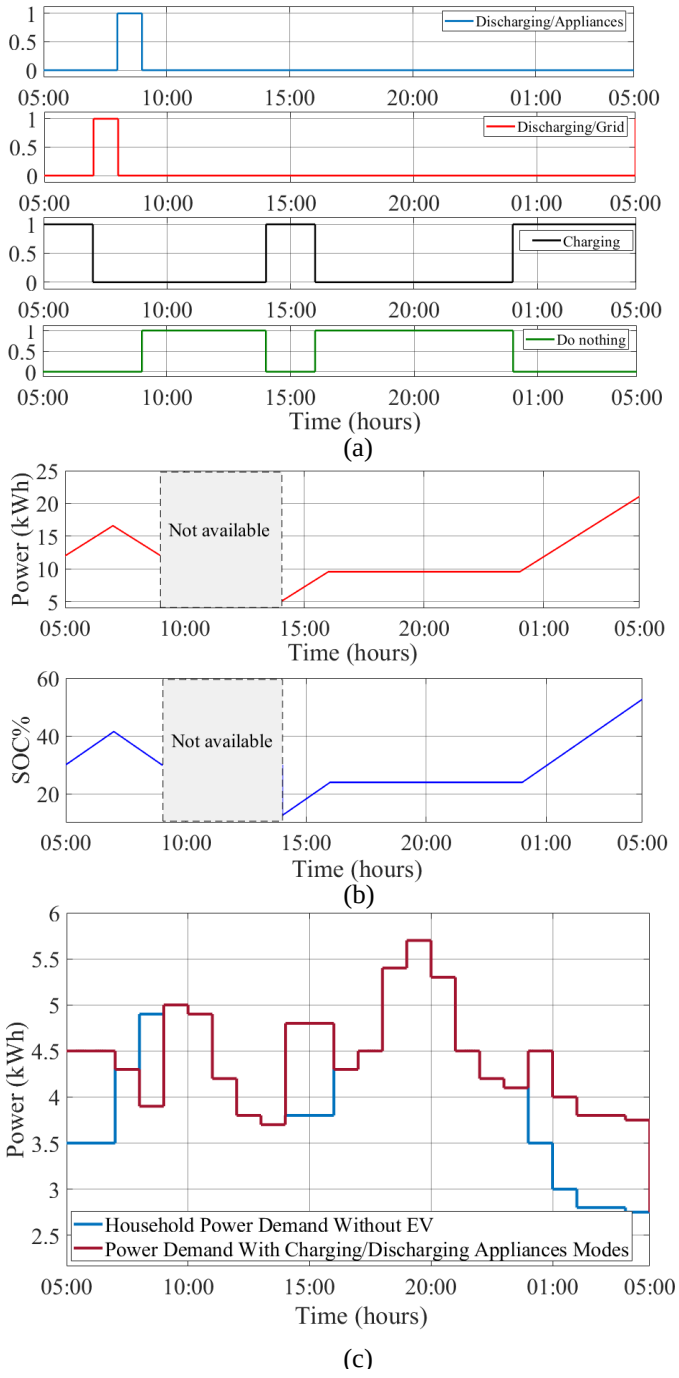

Figure 5-12 Initial SOC = 30 % (a) Actions, (b) SOC changes, (c) Power consumption.

C. Case 3: Weekdays with 30% of SOC

The initial SOC of the EV is 30 % in this case. All actions taken during this scenario are shown in Figure 5-12 (a). The charging action is active during [5:00 am-7:00 am] as shown in Figure 5-12 (b) till the SOC reaches 40%. Although the SOC is lower, the battery is used as much as possible to supply the home appliances and sell power to the grid. This minimises the electricity bills and reduces the burden on the grid. Therefore, the EV exports energy to the grid only for one hour [7:00 am-8:00 am] in this case, The EV also supplies energy to the appliances for one

hour during the morning peak period [8:00 am- 9:00 am] as shown in Figure 5-12 (c). After midnight, the EV starts charging and the SOC reaches 50 %.

D. Case 4: Weekend days

Figure 5-13 illustrates the hourly power demand during weekends and weekdays. Hourly power consumption patterns of weekdays and weekends are quite different. The weekend pattern has a clear morning peak start at 10:00 am and lags weekday pattern. The different features are quite understandable because people usually start later during weekend mornings and generally spend more hours at home during the time slot from 10:00 am to 14:00 pm while they spend more time at work or on outdoor activities at the same time slot during weekdays. In this scenario, it is assumed that the EV leaves the home twice [13:00 pm - 15:00 pm] and [20:00 pm - 22:00 pm], the EV starts the day with 50% of SOC.

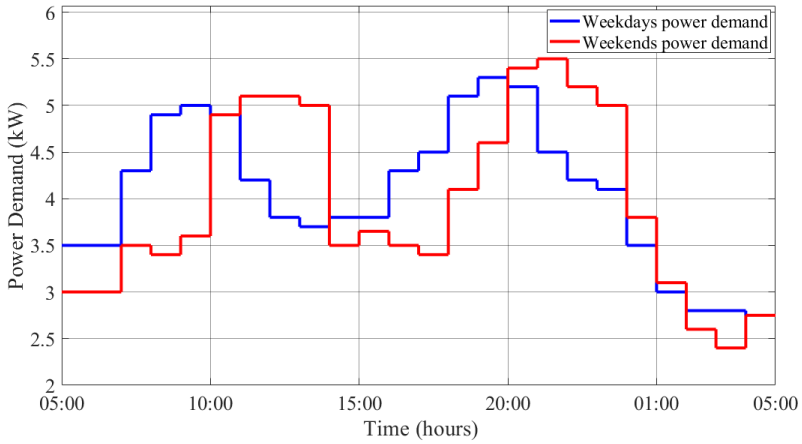

Figure 5-13 Hourly household electrical demand of weekend and weekday.

During the time interval [5:00 am - 7:00 am], *Charging* mode is detected as shown in Figure 5-14 (a) as the power demand (3 kWh) and electricity price are lower. The SOC increases from 50 % to 70 % as shown in Figure 5-14 (b). Because it is weekend day, EV owner is staying at home, the SOC is quite high and power demand is low, therefore it is better to sell energy to grid.

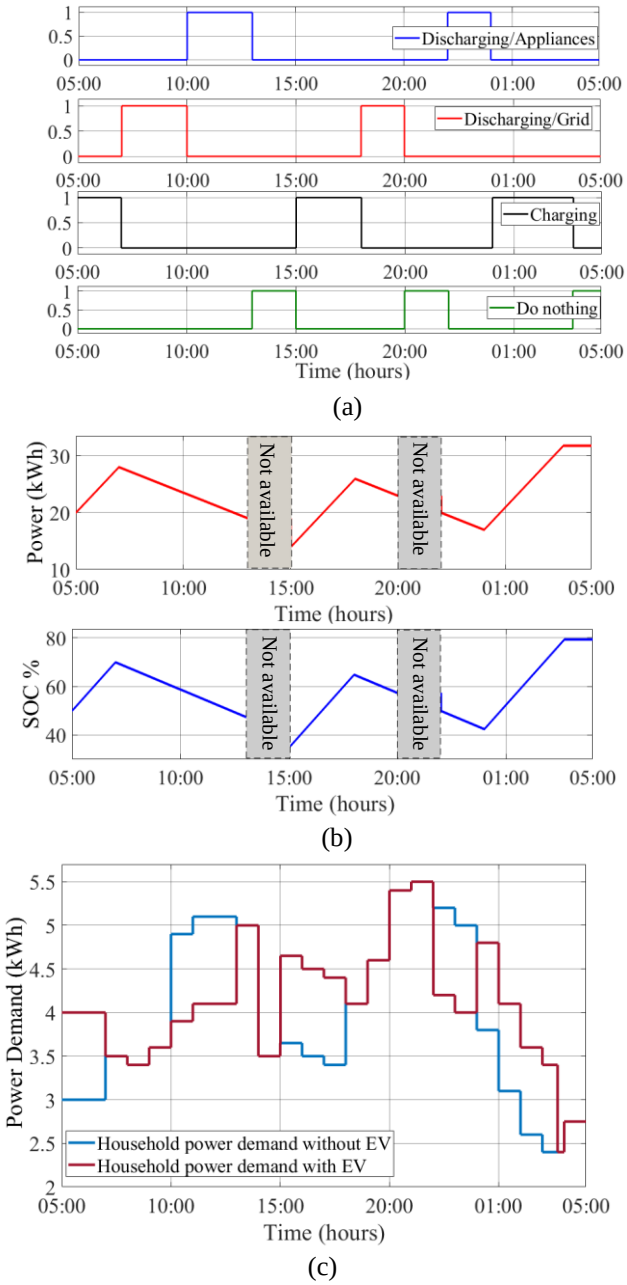

Figure 5-14 Weekend days with Initial SOC = 50 % (a) Actions, (b) SOC changes, (c) Power consumption.

Therefore, *Discharging/Selling* mode is active from 7:00 am-10:00 am and SOC decreases to 60%. The next three hours [10:00 am- 13:00 pm], the power demand is high as it is morning peak demand. *Discharging/Appliances* mode is issued to supply power to the home appliances. The EV leaves the home at 13:00 pm and comes back at 15:00 pm with a low SOC of 38%. Hence *Charging* mode is detected for three hours [15:00 am- 18:00 pm] and the SOC increases to 65%. During [18:00 pm- 20:00 pm], the SOC is quite high, and the electricity price is high, the demand is average, hence *Discharging/Selling* mode is active to feed energy back to the grid. The EV leaves the home at 20:00 pm and returns at 22:00 pm at which time, the evening peak demand begins. Therefore, the EV starts supplying the household appliances for two hours

till the SOC drops to 41%. At 24:00 pm, the off-peak demand is detected with low energy price. The EV starts charging till the SOC reaches 80% at 04:00 am and then *Do-Nothing* mode is active.

Figure 5-15 shows the cumulative daily household energy cost for the base case and different cases (SOC = 30 %, 50 % and 80 %). It can be observed that the proposed method reduces the cost by 12 % when the EV starts the day with a low SOC of 30% and by 21% of the cost reduction when the SOC is at 50%. When the SOC is higher at 80%, the energy cost is reduced by 27%.

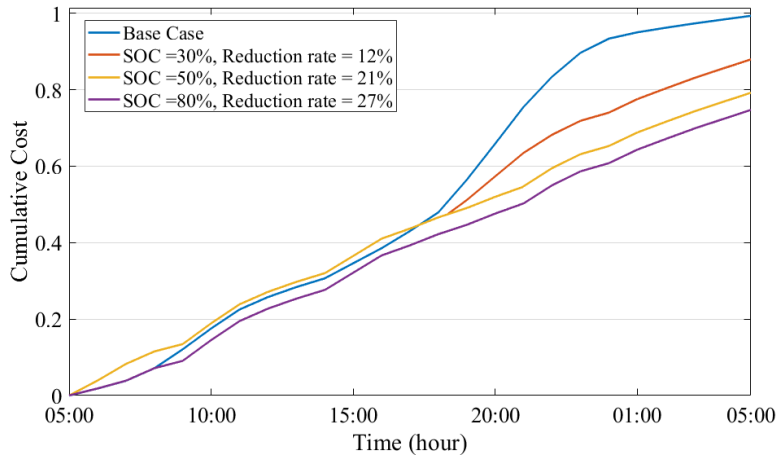

Figure 5-15 Cumulative electricity cost

5.5.2 Implementing the proposed strategy on a fleet of EVs connected to the distribution network

A fleet of EVs with bi-directional power capability represents a considerable energy storage resource and has the potential to provide ancillary services to the utility grid. To evaluate the effectiveness of the proposed scheduling scheme, a low-voltage (LV) distribution network connected to a residential area is used. The residential area consists of 100 houses with 50 households each owning an individual EV is used for the simulation using MATLAB software as shown in Figure 5-16. Since there are different EVs with different battery capacity in the market therefore, in the model, EVs battery capacities are selected randomly among [20, 30, 40 and 50 kWh] as presented in Figure 5-17 (a). The random initial SOC for each EV is chosen. Figure 5-17 (b) shows the number of EVs with different SOCs.

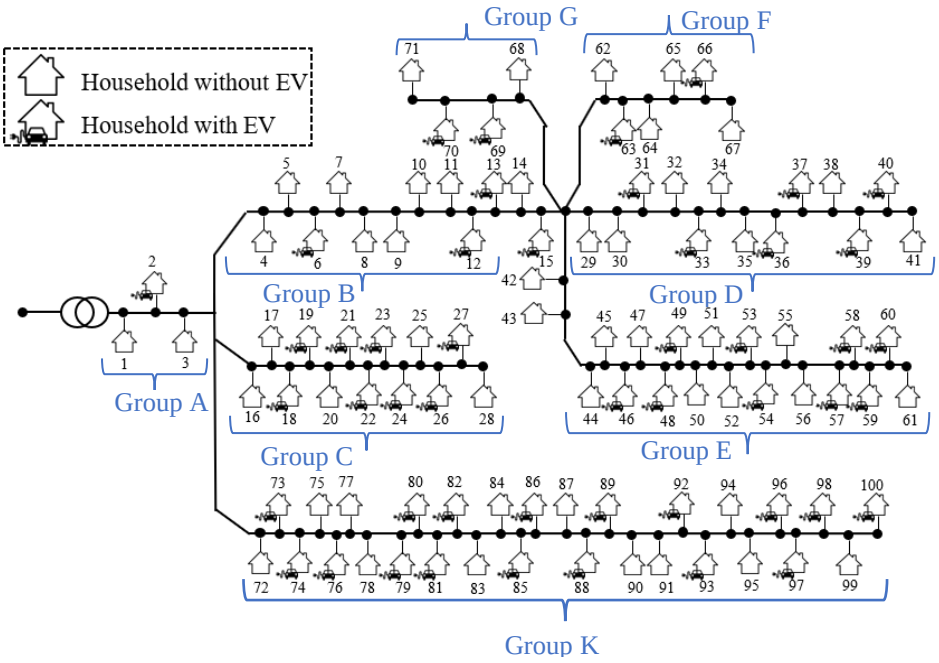

Figure 5-16 Test residential LV network.

In this model, three variables are defined for each EV which are the departure time, arrival time and energy consumption during a trip. Also, for simplicity, it is assumed that each EV performs only one trip during a day. However, the model can be easily extended to accommodate multiple trips for each EV. These three variables are modelled with a probability density function having a normal distribution. The intervals for departure and arrival times are [7 am - 10 am] and [16 pm - 22 pm] respectively as shown in Figure 5-17 (c). The energy consumed by each EV during a trip is in the range [0-10 kWh].

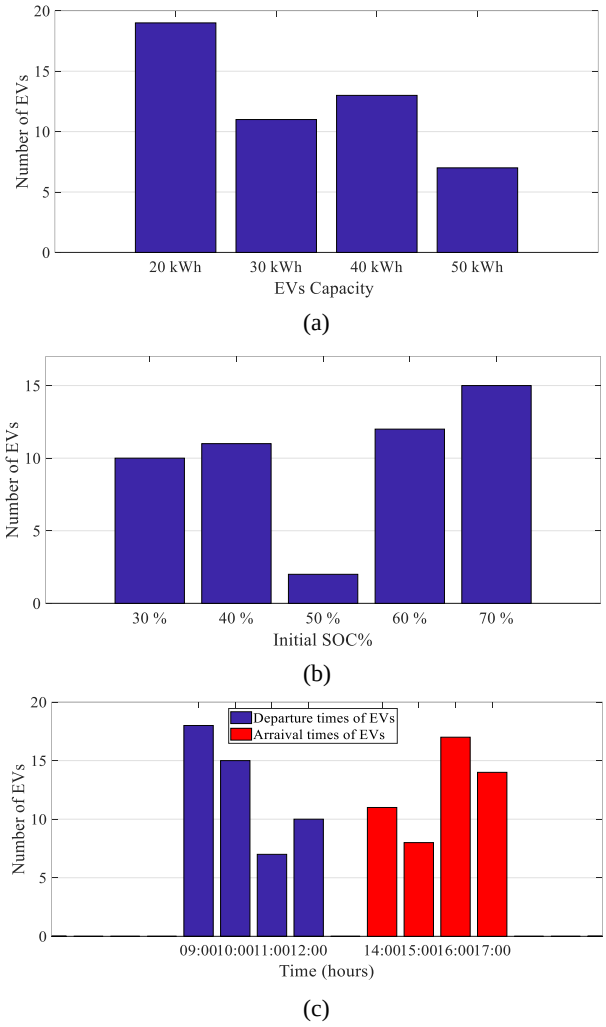

Figure 5-17 Number of EVs with different (a) capacity (b) initial SOC (c) departure and arrival times.

The energy consumption in the residential area in real time is presented as follows:

$$E_{MG}(t) = E_{hs}(t) + \Delta E_{ch}^{N_{ch}}(t) - \Delta E_{dis}^{N_{dis}}(t) \tag{5.15}$$

Where $E_{MG}(t)$ is the consumed energy in the residential area. $E_{hs}(t)$ refers to the energy consumption by households' appliances. $\Delta E_{ch}^{N_{ch}}(t)$ and $\Delta E_{dis}^{N_{dis}}(t)$ are the charging and discharging energy by EVs, respectively.

$$E_{hs}(t) = \sum_{n=1}^{N_h} E_h^T \tag{5.16}$$

$$\Delta E_{ch}^{N_{ch}}(t) = \sum_{n=1}^{N_{ch}} P_{ch}(t) \tag{5.17}$$

$$\Delta E_{dis}^{N_{dis}}(t) = \sum_{n=1}^{N_{dis}} P_{dis}(t) \tag{5.18}$$

Figure 5-18 shows the power consumption profile of the residential area in a typical weekday without EVs charging load. The peak hours occur during morning time [7:00 am - 11:00 am] and evening time [18:00 pm - 21:00 pm].

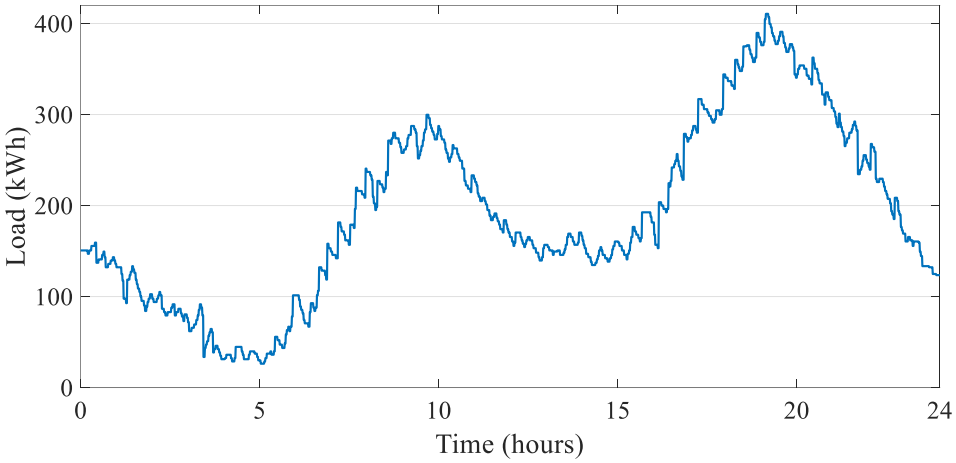

Figure 5-18 Load profile of the residential area.

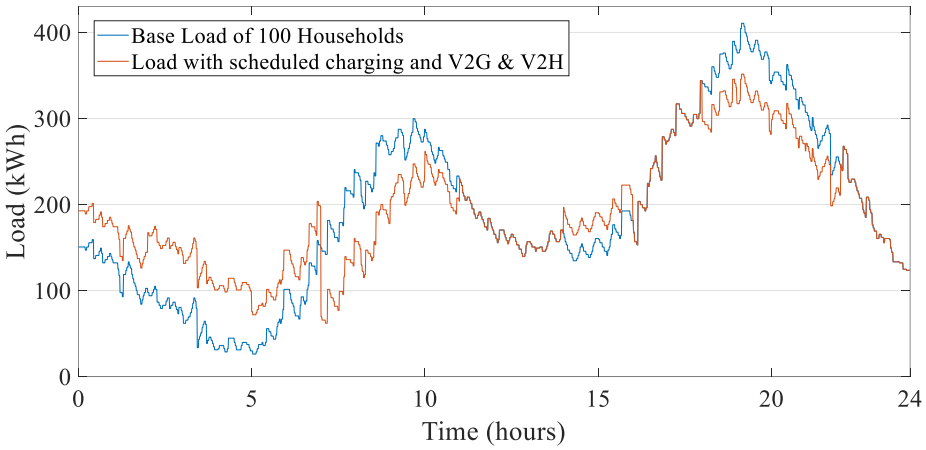

Figure 5-19 Network power profile after implementing the proposed strategy.

Figure 5-19 shows the power profile curve of the residential area after implementing the proposed strategy for each EV in the network. Some users start charging their EVs during off peak [12 am- 7 am] based on the SOC, departure time of each EV, this results in filling the valley. It can be observed that the morning and evening peak periods have been reduced by 23% and 15 % respectively. This is the result of EVs feeding power back to the grid via V2G

and supplying energy to the household to power the appliances via V2H which reduced the energy imported from the grid.

Table 5-5 summarises the results of this simulation. The total peak reduction during morning hours is 23% (15 % using V2H and 8 % using V2G) and a reduction of 15 % occurred at evening time (10.49 % using V2H and 4.51 % using V2G). It can be observed that EVs with higher initial SOC have the highest probability to feed energy back to the grid and supply the household appliances. Therefore, the number of EVs that start the day with 70 % is 15. These EVs have the highest contribution in reducing the morning peak by 7.20 % and 6.0 % during evening peak hours. However, the EVs with lowest initial SOC (30 %) could not deliver energy during both morning and evening peak periods, but they are still able to power the household appliances and contribute to load reduction (1.61 % at morning and 1.05 % at evening).

Table 5-5 Contribution of EVs to energy reduction during morning and evening peak periods.

SOC	No. of EVs	EVs Capacity (kWh)				Reduction of peak loads			
						Morning		Evening	
		20	30	40	50	By V2H	By V2G	By V2H	By V2G
70%	15	7	1	5	2	5.20%	4.00%	3.90%	2.10%
60%	12	2	6	1	3	4.5%	2.40%	2.35%	2.15%
50%	2	0	1	1	0	0.59%	0.10%	0.28%	0.17%
40%	11	6	1	2	2	3.10%	1.50%	2.91%	0.09%
30%	10	4	2	4	0	1.61%	0.00%	1.05%	0.00%
Total	**50**	**19**	**11**	**13**	**7**	**15.00%**	**8.00%**	**10.49%**	**4.51%**
						23%		**15%**	

5.6 Conclusion

This chapter proposed a DR strategy for charging/discharging energy management of EVs equipped with bidirectional V2G and V2H functionalities. The proposed strategy aims to minimise the household energy consumption and EV charging costs by charging the battery during off-peak hours when energy prices are lower or discharging to supply home appliances during peak periods or support the electricity grid during peak demands which also generates revenue to the EV owner. The EV energy management system is designed using Q-learning to coordinate the charging/discharging modes considering the travel needs of the EV owner. RL is employed as a decision model, where the EV is defined as an agent and utilises a signal agent to make an optimal decision. A signal agent approach is used to reduce the number of state-action pairs which simplifies the implementation, leads to a better performance, and reduces the computation time as compared to other techniques. Fuzzy reasoning is introduced to define

the current state based on the input variables and evaluate the random action that the agent could take as a reward function. Fuzzy logic-based implementation of the state and reward function overcomes the limitation of rules-based technique (crisp values) and leads to a better performance. The proposed strategy was also successfully applied to a fleet of EVs of a simulated residential area. The results show that the scheduled charging load can contribute to reducing peak loads by 23 % at morning and 15 % at evening hours.

Chapter 6 Optimal V2G Control for Supplementary Frequency Regulation

6.1 Introduction

The raising penetration of intermittent RESs in the power grid causes fluctuations in the generation side and this results in power mismatch between supply and demand leading to system frequency deviations. In addition, RESs such as wind power generators, are composed of power electronic converters, and when decoupled from the electricity grid they contribute to the reduction of the total power system inertia, thus affecting the overall dynamic stability of the system [77], [78].

Utility-scale Battery Energy Storage Systems (BESS) are a promising technology option to enhance the reliability and stability of the electricity grid and a key enabler for the transition towards a greener and reliable energy landscape. Owing to their rapid response time, BESSs are particularly well-suited for frequency regulation but can also provide other functions such as ramping, arbitrage and load following. Several recent studies have discussed the potential impact of BESS integration on the power grid's stability [79], [80].

The wide-scale adoption of EVs can pose great challenges to the power system operation, namely increasing peak demand, stress on the transmission lines, and impacting the power system security. V2G technology enables EVs to activity participate in the demand side management and contribute to frequency response services for grid stability enhancement. In this way, EVs to serve as mobile battery storage devices with a bidirectional power flow. EVs can contribute to suppressing the frequency deviation by compensating the supply-demand mismatch caused by intermittent energy sources such as wind and solar energy [82]. In addition, ~~to~~ the fast response of the EV battery, makes the EVs more attractive to provide various ancillary services [83].

Several V2G pilot projects have been carried out across the world over the past few years. These V2G technologies have also been adopted by the world's largest car manufacturers and are already in the marketplace. In the UK, Vehicle to Grid Britain (V2GB) project evaluates the long-term integration of V2G into the UK's utility network as well as the early opportunities for this technology in the UK power markets, offering services to the System Operator (SO),

mainly Firm Frequency Response (FFR) [84]. In Italy, Fiat Chrysler Automobiles (FCA), in partnership with ENGIE, has started the first phase of its V2G pilot project which will use EVs' batteries to provide grid services [85].

The participation of EVs in the grid frequency regulation has been the subject of intensive research in recent years. In [86], the authors focused mainly on the EV contributions for primary frequency control to enable a secure and large-scale integration of intermittent RESs. In [87], the authors proposed a Load Frequency Control (LFC) strategy based on V2G technology. The simulation results show how the V2G power control can be applied to compensate for the inadequate LFC capacity and thereby to improve the frequency stability of power grids. In [88], the stability of the LFC system in a microgrid with EVs and communication delay is investigated. In [89], the authors analysed the impact of the integration of EVs and RESs on the grid stability. A standard IEEE 13-bus test feeder is used in this study under a number of scenarios which are critical for the grid stability. In [81], a droop-based control scheme has been developed to adjust the V2G power of the EV battery according to the frequency signal. A V2G control was proposed in [90] to enable EVs to actively participate in frequency regulation considering high frequency regulating signals. The authors in [91] developed a power model of EVs for effective frequency regulation considering wide-scale wind energy integration.

However, the storage capacity of a single EV's battery cannot provide frequency regulation services. Thus, a V2G aggregator agent is designated as a mediator between the utility network's operator and the fleet of EVs providing grid ancillary services. The V2G aggregator plays an important role in managing the charging and discharging of each EV participated in frequency regulation to ensure the satisfaction of EVs' driving demand and optimise the tracking performance of frequency control signal [92]. Thus, the optimal dispatch strategy is crucial for the V2G aggregator to ensure that the EV driving needs are fulfilled while providing optimal frequency regulation to the power grid.

The dispatching strategy for V2G aggregator participating in frequency regulation is currently a research hotspot. Some researchers focused on proposing dispatch strategies based on economy problems to optimise the monetary benefits of EV owners or EV aggregators [93]–[96]. In [93], the authors assessed the economic profits of EVs participating in the frequency regulation markets from the perspective of the EV owner. The simulation results show that the EV owner can make an annual profit ranging between €100 and €1100 when participating in

frequency regulation. In [94], a Mixed Integer Linear Programming (MILP) is used to optimise the daily benefits gained by EV users from providing frequency regulation. In [95], the expected V2G incomes from participating in frequency regulation has been estimated considering the EV battery price. The results show that the estimated benefits exceed the EV battery prices in the current markets indicating that V2G regulation is an economically viable grid service. Nevertheless, these studies mainly focused on benefits and costs from the electricity market, where the regulation tasks and the charging demand of the battery were not considered.

Other studies have focused on the optimal dispatching strategies considering the capacity of EVs participating in frequency regulation. In [97], a queuing network model is used to predict the number of EVs to estimate the energy storage capacity required for frequency regulation based on a constant charging power for each EV. In [98], an optimal dispatch strategy for V2G aggregator is proposed to satisfy the driving demands of EVs and maximise the economic benefits of the aggregator while providing frequency regulation. However, the expected SOC of the EV battery was considered as an inequality constraint under which the scheduled charging of EVs could not be performed by the proposed optimal strategy. In [99], a V2G control strategy is proposed to achieve the frequency regulation considering the expected SOC levels of EV batteries while providing real-time adjustments of their scheduled V2G power. However, these adjustments on the V2G power reduce the EV battery capacity to perform frequency regulation.

Several studies have focussed on the design of optimal V2G control strategies for EVs to maximise the frequency regulation capacity and maintaining SOC levels within the desirable range [81] [100][101] [102]. An optimal dispatch strategy is proposed in [81] using the modern interior point optimisation method to enhance EVs contribution in SFR considering the driving needs of EV owners. The dispatch signal is fairly distributed from the control centre among EVs using the Area Control Error (ACE) and Area Regulation Requirement (ARR) criteria. In [100], a dynamic strategy for EV frequency regulation is proposed considering the driving patterns of EV owners and the EV charging/discharging power is regulated based on the frequency signal. The authors in [101] and [102] proposed a real-time V2G control using a state-space model which offers higher computational efficiency, higher accuracy, and a lower real-time communication requirement. Although all previously mentioned studies have considered the charging demands of EVs participating in frequency response services, the underlying V2G control strategies are based on a forced charging process which allows EV

batteries to charge/discharge quickly with maximum charging/discharging power rates before the plug-out time (disconnection). However, this leads to other issues for both the grid and the EVs' owners. For the power grid, forced charging may create a new EV charging peak demand, therefore imposing additional stress on the grid. This will also reduce the time during which EVs can offer frequency response services, since EVs will reach their maximum SOC and then become unable to participate in frequency regulation. For EVs' users, the charging demands of EVs are not optimally satisfied, especially when ARR is dispatched for frequency regulation. In addition, EVs' owners cannot use their vehicles while they are participating in frequency regulation, even for their essential travel needs.

DRL combines the framework of RL with a multiple layer artificial neural network. DRL is most suitable for the optimal charging/discharging management of EVs connected to the electricity distribution grid. They have fast response and provide optimal and continuous control actions which is crucial for tracking the frequency of the power system in real-time. Multi-agent RL has been proposed for distributed EV charging coordination and fast V2G dispatch, considering the uncertainties and charging demands of EVs [103], However, multi-agent RL requires setting several agents, with each agent having different actions and rewards therefore making the learning process more complex. Other studies have focussed on using Markov Decision Process (MDP) algorithms for V2G control considering the mobility of EVs, SOC of EVs, and the estimated/actual [104]. However, these algorithms require historical data, such as driving patterns and battery SOC as inputs to compute the charging/discharging schedules in real-time.

In this chapter, an optimal real-time V2G control strategy is designed for EVs to perform SFR. The main feature that distinguishes the proposed approach from previous related works is that the scheduled charging power of an individual EV is optimally tracked and adjusted in real-time to fulfil the charging demand of EV's battery at the plug-out time without using the forced charging technique to maximise the frequency regulation capacity. Deep Deterministic Policy Gradient (DDPG), an improved class of DRL based on Deep Neural Networks (DNN) is used. DDPG is a model-free, off-policy actor-critic algorithm with reduced computational time. Furthermore, it can be used in continuous space using policy-function (actor) and Q-function (critic) framework, which is essential for tracking the frequency of the power system and taking continuous actions in response to varying load and generation. DDPG can be easily adapted to handle the randomness of the load disturbances and RESs.

6.2 Electrical Vehicles Participation in Supplementary Frequency Regulation (SFR)

6.2.1 Overview of frequency response in power systems

The grid frequency is an indicator of the balance between electricity supply and demand. If the total demand exceeds the total supply, then the frequency falls, while the frequency rises when the total supply is greater than the total demand. Thus, maintaining the frequency around the nominal value across the power network is of critical importance and requires a good control of the power output of the generator units in real time to ensure a reliable, secure and economic operation of the power grid. Therefore, the SFR seeks to keep the system frequency deviations within the normal limits.

Figure 6-1 presents the concept of SFR in the traditional power system, where ΔP_{tie} is the deviation occurring in tie-line power, the frequency bias constants are B, the speed regulation constants is R, and Δf is the frequency deviation in the system. Where the Area Control Error (ACE) signal is generated as a weighted summation of the frequency deviation and the tie-line power changes and in general has a Gaussian type distribution with zero mean and fast switching between positive and negative values. Therefore, the SFR aims mainly to mitigate the ACE fluctuations as much as possible and maintain the frequency within an allowable limit by regulating the outputs of the generating units. While Area Regulation Requirement (ARR) refers to the supply-demand mismatch that needs to be restored by the generator units and generally remains positive or negative for a long period of time.

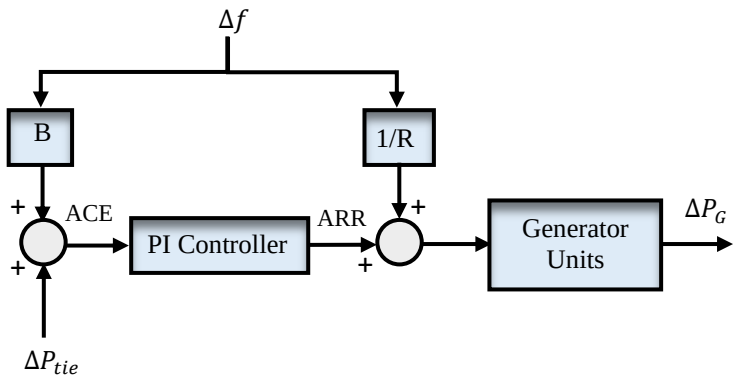

Figure 6-1 SFR in the traditional power system.

6.2.2 Participation of EVs in SFR

EVs with V2G technology can respond much faster to frequency response services than conventional generation units. Furthermore, EVs are usually utilised for about only 4 % of the day and are idle (parked at home or at the workplace) for the rest of time.

When EVs participate in SFR, the signals ACE and ARR become readily available to be dispatched for V2G control as illustrated in Figure 6-2 (a) and Figure 6-2 (b) respectively. However, there are some differences between ACE and ARR which must be considered when they are dispatched to EVs.

Since ACE has almost a zero-mean distribution, thus the average value of ACE is around zero and hence the charging demand of EVs may not be satisfied. Therefore, using ACE for frequency regulation will not affect EVs' batteries SOC levels. Conversely, when ARR is dispatched for frequency regulation, the EVs' batteries SOC levels will deviate from the initial values since ARR signal may have positive/negative mean. Consequently, EVs may lose their capacity for regulation which impacts the frequency stabilisation. Therefore, each of the ACE and ARR signals has its advantages and disadvantages when used for frequency regulation.

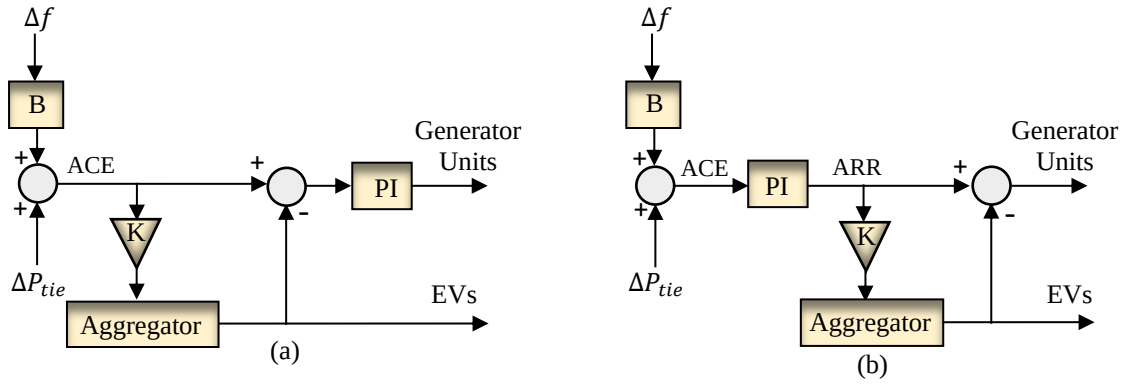

Figure 6-2 ACE and ARR signals for regulation (a) ACE, (b) ARR.

6.2.3 Dispatch Strategies of EVs Participating in SFR

Recently, with the emerging V2G technology, EV dispatching strategies for SFR have been the subject of extensive research. Figure 6-3 illustrates the hierarchical dispatch strategy which has three levels: Control Centre, EV Aggregator and EVs fleet. Since the V2G power of a single EV battery is not large enough, mostly around 3 kW to 10 kW, EVs must be aggregated to participate in SFR.

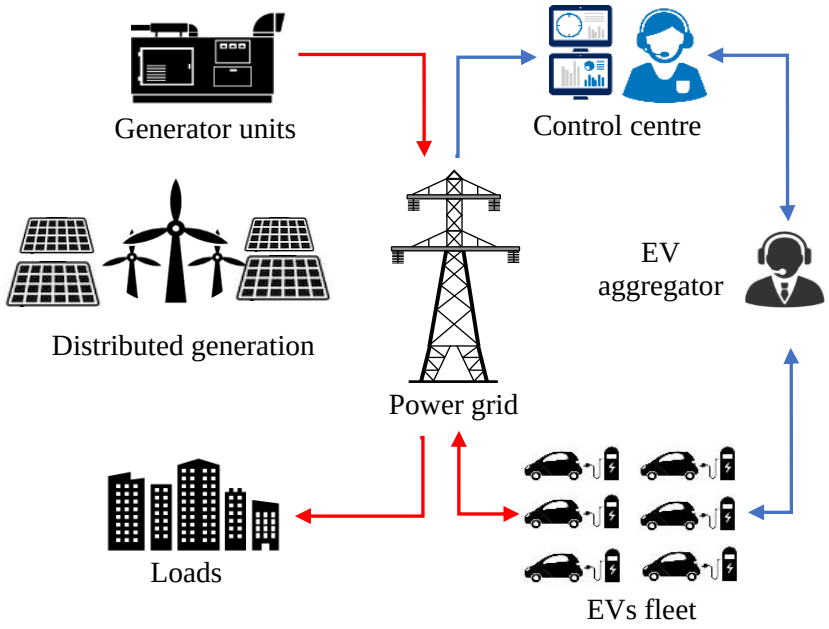

Figure 6-3 Hierarchical control of EVs in the power system.

- **Dispatch strategy in the control centre**

To minimise the energy mismatch between demand and supply as much as possible, the regulation signals (ACE or ARR) are dispatched to the generating units and EVs performing frequency regulation. While the regulation dispatch to EVs depends on many factors, such as the RES generation, the capacity of the generator units and the frequency regulation capacity (FRC) of EVs. Therefore, the dispatch regulation task to an EV aggregator from the control centre is formulated as:

$$P_t^{AG} = K \times \begin{cases} \max(S_t, -C_t^{up}, \Delta f \leq 0) \\ \min(S_t, C_t^{down}, \Delta f > 0\ ) \end{cases} \tag{6.1}$$

Where S_t is either the ACE or ARR signal at time t, P_t^{AG} indicates the dispatch regulation task undertaken via an individual EV aggregator, K is a ratio that determines the proportion dispatch based on which the EVs aggregator undertakes frequency regulation and takes a value between 0 and 1. C_t^{up} and C_t^{down} represent the total capacity of regulation-up and -down uploaded by the EV aggregator to the control centre respectively, which can be calculated by adding up the FRC of all EV charging stations ($C_{j,t}^{up}, C_{j,t}^{down}$) as follows:

$$\begin{cases} C_t^{up} = \sum_{j=1}^{J} C_{j,t}^{up} \\ C_t^{down} = \sum_{j=1}^{J} C_{j,t}^{down} \end{cases} \tag{6.2}$$

- **Dispatch strategy in the EV aggregator**

The role of the aggregator is to facilitate the integration of EVs in the electricity market. The aggregator agent acts as a commercial middleman or intermediary between EVs and the power grid. The aggregator receives the frequency control signal from the control centre and sends the power capacity collected from EVs back to the control centre. The aggregator then dispatches the charging or discharging commands to each EV considering the frequency control signals. Therefore, the grid operator (i.e. control centre) communicates with the aggregator agents only, and it does not need to manage each individual EV, as shown in Figure 6.2.

Once the regulation power signal reaches the EV aggregator from the control centre, the regulation power must be distributed proportionally among the charging stations based on their corresponding FRCs uploaded by the aggregator, the regulation power of each charging station is presented as follow:

$$P_{j,t}^{st} = \begin{cases} P_t^{AG} \times \dfrac{C_{j,t}^{up}}{C_t^{up}} & P_t^{AG} \leq 0 \\ P_t^{AG} \times \dfrac{C_{j,t}^{down}}{C_t^{down}} & P_t^{AG} > 0 \end{cases} \tag{6.3}$$

Where $P_{j,t}^{st}$ denotes the power regulation that needs to be provided by the j^{th} EV charging station at time t.

- **Dispatch strategy in EV charging stations**

In the charging station, the regulation power will be distributed to each EV based on the amount of FRC achieved in the previous time step:

$$\Delta P_{i,t}^{reg} = \begin{cases} P_{j,t}^{st} \times \dfrac{C_{i,t}^{up}}{C_{j,t}^{up}} & P_{j,t}^{st} \leq 0 \\ P_{j,t}^{st} \times \dfrac{C_{i,t}^{down}}{C_{j,t}^{down}} & P_{j,t}^{st} > 0 \end{cases} \tag{6.4}$$

Where $\Delta P_{i,t}^{reg}$ denotes the power deviation for the regulation of the i^{th} EV at time t and $C_{j,t}^{up}/C_{j,t}^{down}$ is the total capacity regulation-up/regulation-down of the charging station, and can be calculated as follows:

$$\begin{cases} C_{j,t}^{up} = \sum_{i=1}^{I} C_{i,t}^{up} \\ C_{j,t}^{down} = \sum_{i=1}^{I} C_{i,t}^{down} \end{cases} \tag{6.5}$$

Where

$$\begin{cases} C_{i,t}^{up} = P_{max} + P_{i,t} \\ C_{i,t}^{down} = P_{max} - P_{i,t} \end{cases} \tag{6.6}$$

With reference to as shown in Figure 6-4, when the V2G power is positive (negative), the FRC of regulation-up is higher (lower) than the FRC of regulation-down. Therefore, the regulation task, whether regulation-up or regulation-down, depends mainly on the corresponding FRC. This can lead to a deviation in the SOC of the EV battery from the expected level. To this end, the V2G power must be continuously regulated to ensure that the expected charging demands of EVs owners are satisfied while simultaneously providing frequency regulation services.

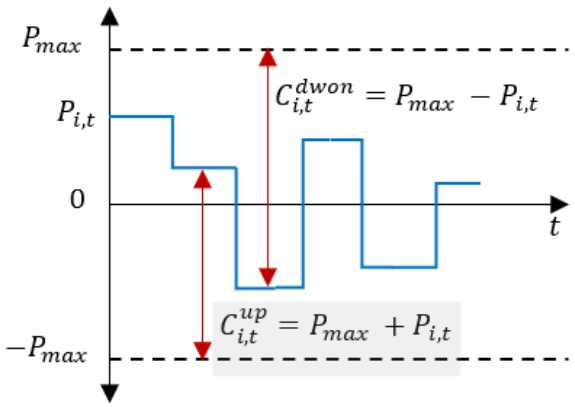

Figure 6-4 Available frequency regulation capacity of an individual EV.

6.3 Deep Reinforcement Learning for V2G Control

6.3.1 V2G Control Based on DDPG

The uncertain dispatches (ACE or ARR) from the control centre can be different since EVs have different FRCs. Consequently, this results in a change of the battery SOC from the expected level. Therefore, the Scheduled Charging/discharging Power (SCP) should be continuously regulated in real-time to satisfy the EV's charging demand.

However, when regulation-up is dispatched, the SCP needs to be increased for the next step, leading to an increase of the real-time V2G power. Consequently, the FRC of the EV will increase for regulation-up and will decrease for regulation-down. Conversely, when the SCP

decreases due to performing regulation-down, the FRC of the EV will decrease/increase for regulation-up/regulation-down. When the SCP reaches the maximum V2G power, EVs cannot perform SFR since, in this case, they have no capacity for regulation-down and performing regulation-up leads to a further loss in the battery SOC. Thus, in such a scenario, the only option is to charge the EV battery. Similarly, if the SCP reaches the negative maximum of V2G power, the EV battery is unable to perform SFR either.

Normally, when an EV is not participating in SFC, the expected battery charging level can be achieved by charging the battery under the Expected Charging Power (ECP). Thus, the expected SOC of the EV battery is defined as:

$$SOC_{i,k}^{exp}\big|_{P_i^{ecp}} = SOC_i^{init} + \frac{\Delta k.P_i^{ecp}}{E_i^{rat}} \tag{6.8}$$

Where the ECP can be calculated as:

$$P_i^{ecp} = \frac{(SOC_i^{exp} - SOC_i^{init})E_i^{rat}}{t^{out} - t^{in}} \tag{6.9}$$

$SOC_{i,k}^{exp}\big|_{P_i^{ecp}}$ denotes the real-time expected battery SOC undertaking only ECP, E_i^{rat} is the capacity of the i^{th} EV battery. SOC_i^{exp} and SOC_i^{init} are the predefined expected SOC and initial SOC of i^{th} EV, respectively, Δk represents the time step for adjusting SCP, t^{out} and t^{in} are the plug-out and plug-in times, respectively.

However, when the EV is performing SFC, its battery's SOC of its battery will change based on the regulation undertaken and the scheduled charging power and can be calculated in real time as:

$$SOC_{i,k}\big|_{P_i^{schd},P_i^{reg}} = SOC_i^{init} + \frac{\Delta t.\Delta P_{i,t}^{reg} + \Delta k.P_{i,k}^{schd}}{E_i^{rat}} \tag{6.10}$$

Where $SOC_{i,k}\big|_{P_i^{schd},P_i^{reg}}$ is the actual battery SOC undertaking regulation and SCP, $P_{i,k}^{schd}$ represents the SCP at time k and Δt is the time step for regulation.

In order to achieve the charging demand of EV participating frequency regulation at the plug-out time without the need for forced charging process, the expected battery SOC ($SOC_{i,k}^{exp}\big|_{P_i^{ecp}}$) and the actual battery level ($SOC_{i,k}\big|_{P_i^{schd},P_i^{reg}}$) should be tracked in real-time. The SCP is then

continuously adjusted to minimise the difference between the actual SOC and expected SOC of the EV battery.

Therefore, the objective function of the optimal V2G closed-loop control is a function of the change in SCP ($\Delta P_{i,k}^{schd}$) and can be expressed as:

$$\min f\left(\Delta P_{i,k}^{schd}\right) = \left| \frac{\Delta t \times \Delta P_{i,t}^{reg} + \Delta k(P_{i,k-1}^{schd} + \Delta P_{i,k}^{schd}) - \Delta k \times P_i^{ecp}}{E_i^{rat}} \right| \quad (6.11)$$

Where $\Delta P_{i,k}^{schd}$ is the change in SCP of the ith EV at time k and $P_{i,k-1}^{schd}$ is the SCP at time $k-1$.

Therefore, the objective of the DRL-based V2G control agent is to provide optimal actions, which is the scheduled charging power of the EV battery to minimise the objective function given by Equation (6.11). The DDPG algorithm employing the actor-critic approach is used to solve the Q-function of Equation (6.7), The actor network generates a V2G control action, where the quality of the taken action will be evaluated by the critic network. The actor network takes the vector state s_k of $SOC_{i,k}\big|_{P_i^{schd}, P_i^{reg}}$, difference between the actual and expected SOCs of the EV battery as an error e_k, and its integral $\int e_k \,.\, dk$ as input, and directly generates a continuous action a_k as the deviation of SCP ($\Delta P_{i,k}^{schd}$). The critic network, on the other hand, receives the state s_k and the action $\mu(s_k|\theta^{\mu})$ as input and produces a scalar Q-value ($Q(s_k, a_k|\theta^{Q})$) as shown in Figure 6-5.

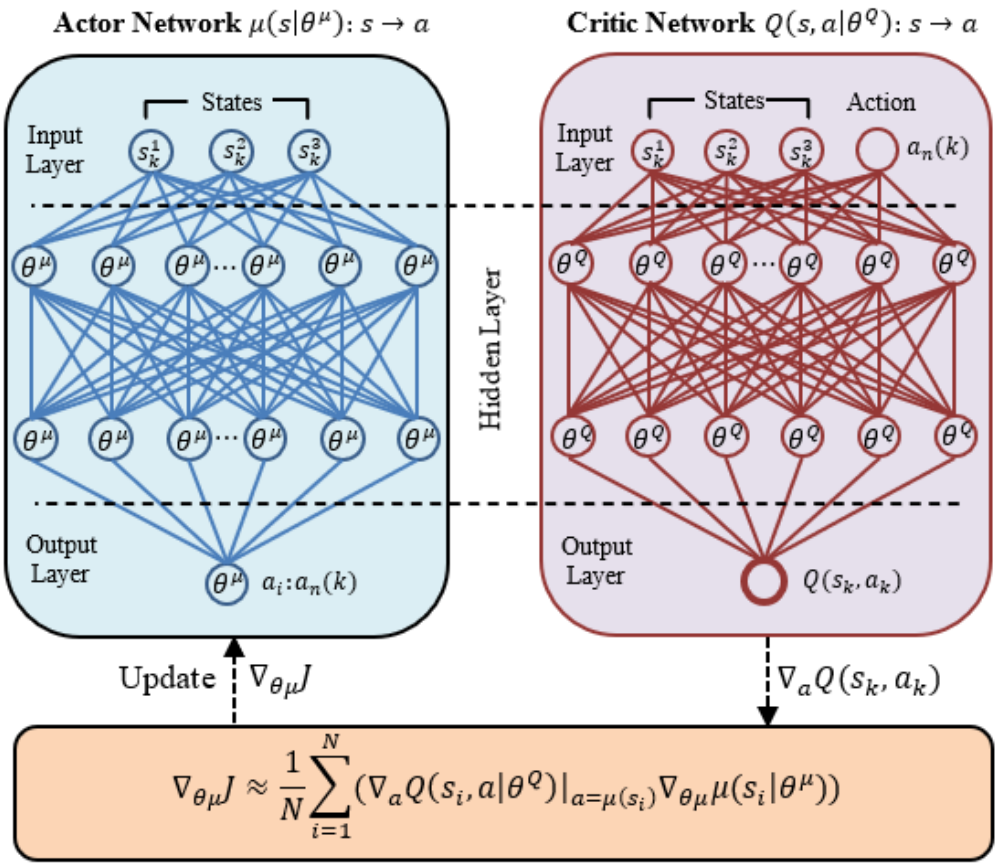

Figure 6-5 Architecture of the actor and critic networks.

To evaluate the performance of the V2G control with the accumulated reward, the reward function r_k in the DDPG algorithm is considered as:

$$r_k = \begin{cases} \text{Positive reward } (+R_p) & \forall\ |e_k| \in [0, 0.05] \\ \text{Negative reward } (-R_n) & \forall\ |e_k| \notin [0, 0.05] \\ \text{Large penalty } (-R_e) & \forall\ SOC_{i,k}\big|_{P_i^{schd}, P_i^{reg}} \in [20, 80] \end{cases} \tag{6.12}$$

Where $SOC_{i,k}\big|_{P_i^{schd}, P_i^{reg}}$ is the actual battery level of the EV, and e_k represents the error, which is the difference between the actual and expected SOCs of the EV battery. When training the DDPG agent, M episodes will be repeated, while each episode consists k steps corresponding to the instants at which the agent-environment interactions take place. The training episodes or scenarios are created by selecting random variables to initialise the environment. The training procedure of the DDPG agent is described by the pseudo-code presented in Table 6-1.

Table 6-1 Pseudo-code of the DDPG algorithm.

1: Initialise critic $Q(s_k, a_k|\theta^Q)$ and actor $\mu(s_k|\theta^\mu)$ networks.
2: Initialise target networks $Q'(s, a|\theta^{Q'})$ and $\mu'(s|\theta^{\mu'})$ with traditional networks' parameters θ^Q and θ^μ
3: Set up empty reply buffer $\mathcal{D}$.
4: **for** episode = $1, 2, \cdots, M$, **do**
5: Generate random values for the environment's variables.
6: Initialise the environment by simulating generated variables.
7: observe the initial state variables.
8: **for** $k = 1, 2, \cdots, K$, **do**
9: Select the action using $a_k = \mu(s_k|\theta^\mu) + \mathcal{N}(\sigma)$
10: Take action and receive the immediate reward r_k and the next state s_{k+1}.
11: Store tuples (s_k, a_k, r_k, s_{k+1}) in $\mathcal{D}$.
12: Sample a random minibatch of tuples from $\mathcal{D}$.
13: set $y_i = r_i + \gamma Q'\left(s_{i+1}, \mu'\left(s_{i+1}|\theta^{\mu'}\right)|\theta^{Q'}\right)$
14: Update critic network with the loss function: $L(\theta^Q) = \frac{1}{N}\sum_{i=1}^{N}\left(y_i - Q(s_i, a_i|\theta^Q)\right)^2$
15: Update actor networks using sampled policy gradient: $\nabla_{\theta^\mu} J \approx \frac{1}{N}\sum_{i=1}^{N}\left(\nabla_a Q(s_i, a|\theta^Q)|_{a=\mu(s_i)} \nabla_{\theta^\mu}\mu(s_i|\theta^\mu)\right)$
16: Update target networks using: $\begin{cases}\theta^{Q'} \leftarrow \tau\theta^Q + (1-\tau)\theta^{Q'} \\ \theta^{\mu'} \leftarrow \tau\theta^\mu + (1-\tau)\theta^{\mu'}\end{cases}$
17: **end for**
18: **end for**

6.4 Results and Discussion

Two-area interconnected power system is used for simulation, which has been extensively used to simulate the participation of EVs in frequency regulation in the literature. This is due to its simplicity and effectiveness in capturing the dynamic behaviour of the system, where the power system is modelled using transfer functions that are particularly well-suited for frequency regulation analysis. The two-area interconnected power system and the thermal power plant model, from [90] [100] , are shown in Figure 6-6 and Figure 6-7 respectively. The parameter values are listed in Table 6-2 [90]. The EVs are assumed to be connected to Area A. The random load and wind turbine power deviations follow a normal distribution with the zero mean as presented in Figure 6-8 and Figure 6-9, respectively.

Table 6-2 Parameters of two areas power system.

Parameters	**Area A**	**Area B**
Maximum load capacity (MW)	20,000	10,000
Proportional and integral gains	10,0.01	1,0.01
Frequency regulation sample time (s)	4	--
Scheduled charging power sample time(s)	60	--
Frequency bias factor (pu/Hz)	0.15	0.075
Inertia constant (pu. s)	0.32	0.16
Load damping coefficient (pu/Hz)	0.04	0.02
Dead band of primary frequency detection (s)	0.033	0.033
Communication delay (s)	1	1
Dead band of ACE (MW)	10	10

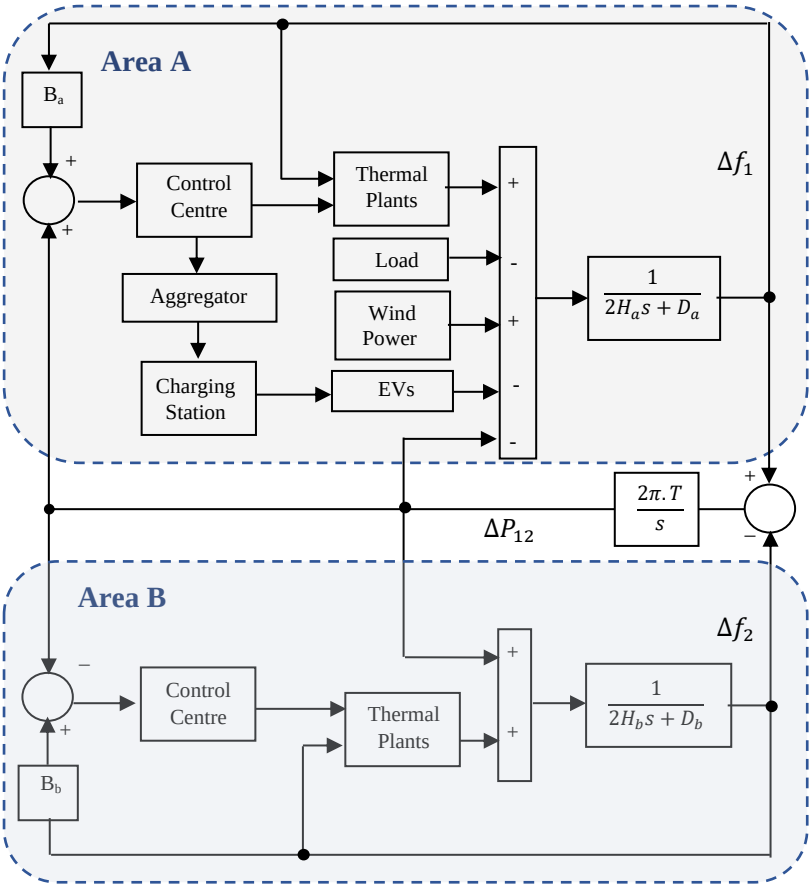

Figure 6-6 Two-area power system model [100].

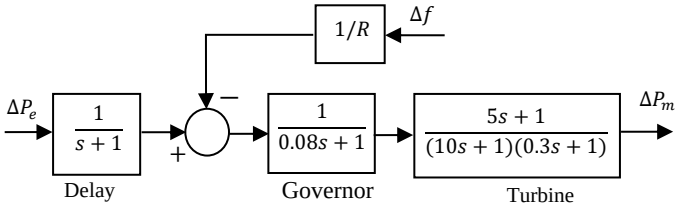

Figure 6-7 Thermal power generator for frequency control [100].

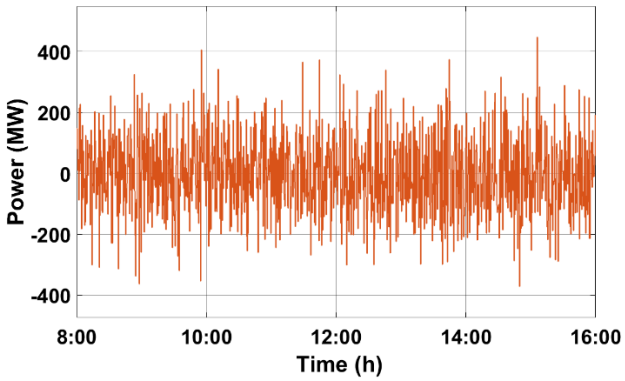

Figure 6-8 Load profile in Area A, adapted form [100].

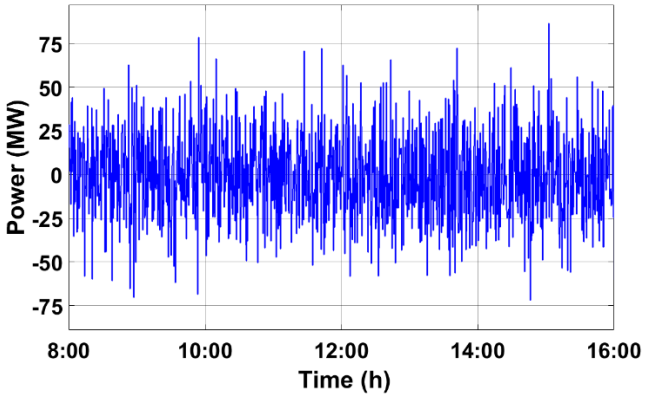

Figure 6-9 Random wind turbine power fluctuations, adapted form [100].

In this simulation study, the EV aggregator is assumed to manage 100 EV charging stations and each station accommodates 500 EVs, as illustrated in Table 6-3. The EVs initial SOCs, the expected SOCs, arrival times, and departure times are generated randomly using Monte Carlo simulation. Since the expected SOC levels depend on the driving behaviour of the EV owners, thus in this chapter, EVs are categorised into three types;

- **Type I** refers to those EVs that need to be charged.
- **Type II** are EVs that need to be discharged (selling energy).
- **Type III** refers to EVs whose owners are not interested in charging from the utility grid or selling energy to the grid.

The other parameters associated to EVs' batteries, such as rated capacity, higher/lower limit of SOC, and maximum charging/discharging power are also given in Table 6-3.

Table 6-3 EVs Parameters used in the simulations.

Parameters	
Total number of charging stations	100
Total number of EVs in charging station	500
Number of EVs of Type I	350
Number of EVs of Type II	100
Number of EVs of Type III	50
Arriving time (h)	Time ~ N (9,0.1)
Departure time (h)	Time ~ N (16,0.1)
Initial SOC for Type I	SOC ~ N (0.4,0.01), SOC ∈ [0.3,0.5]
Initial SOC for Type II	SOC ~ N (0.7,0.01), SOC ∈ [0.6,0.8]
Initial SOC for Type III	SOC ~ N (0.6,0.01), SOC ∈ [0.5,0.8]
Expected SOC for Type I	SOC ~ N (0.7,0.01), SOC ∈ [0.6,0.8]
Expected SOC for Type II	SOC ~ N (0.4,0.01), SOC ∈ [0.3,0.5]
Rated capacity of EV battery (kWh)	[24, 28, 32, 36, 40]
Rated charging and discharging power (kW)	7
Charging/discharging efficiency	0.9
SOC of EV battery limits (p.u)	0.8/0.2

To evaluate the effectiveness of the proposed dispatch strategy denoted as CS3, the results have been compared to two dispatching strategies from the literature. The first dispatch strategy is proposed in [99] and is termed CS1, which adjusts the SCP of the EV hourly to achieve the expected SOC level while participating in frequency regulation. The second dispatch strategy is proposed in [100] (referred to as CS2), which aims to satisfy the driving demand of EVs' owners while performing frequency regulation using the forced-charging method.

6.4.1 Impacts of the proposed V2G strategy on the EV battery

To evaluate the robustness of the proposed V2G control strategy, the dispatch signals ACE and AAR received from the control centre and implemented on the chosen EVs are simulated with large fluctuations and large mean values respectively and the results are compared to other strategies.

For EVs of Type I, the owners chose to charge their EVs' batteries to the upper SOC level. Therefore, the proposed V2G strategy has been tested on this type of EVs by dispatching regulation using ACE with zero-mean and higher amplitude, and large negative-mean of ARR as shown in Figure 6-10(a) and Figure 6-10(b), respectively.

Figure 6-10(c) and Figure 6-10(d) show the real-time SCP adjustments for the EV to satisfy the charging demand. Under CS0 (basic strategy), the SCP of the EV remains constant all the time while the EV is participating in frequency regulation. This leads to a poor performance while trying to fulfil the expected charging demand of the EV before the plug-out time as shown in Figure 6-10(e) and Figure 6-10(f). While using CS1, the EV is losing its capacity for regulation-down, and this is because of the increase in SCP at each hour to compensate for the accumulated decrement of the EV's battery storage due to a large negative mean of ARR, even though it is not able to achieve the desired SOC. The forced charging method is used in CS2, where the EV can participate in the frequency regulation as needed and then charging at the maximum rate (7 kWh) to reach the expected SOC. Although the use of this technique can satisfy the driving demand of the EV, but it has some disadvantages. During the period of charging at the maximum rate, the EV will lose its capacity for the regulation-down leading to a poor performance in the quality of EVs' participation in frequency regulation. On the other hand, the forced charging may cause a new EV charging peak demand, therefore imposing additional stress on the grid. In contrast to CS2, CS3 can keep the EV's capacity for regulation up and down throughout the plug-in period by continuously adjusting the SCP while considering the expected charging demand of the EV at plug-out time.

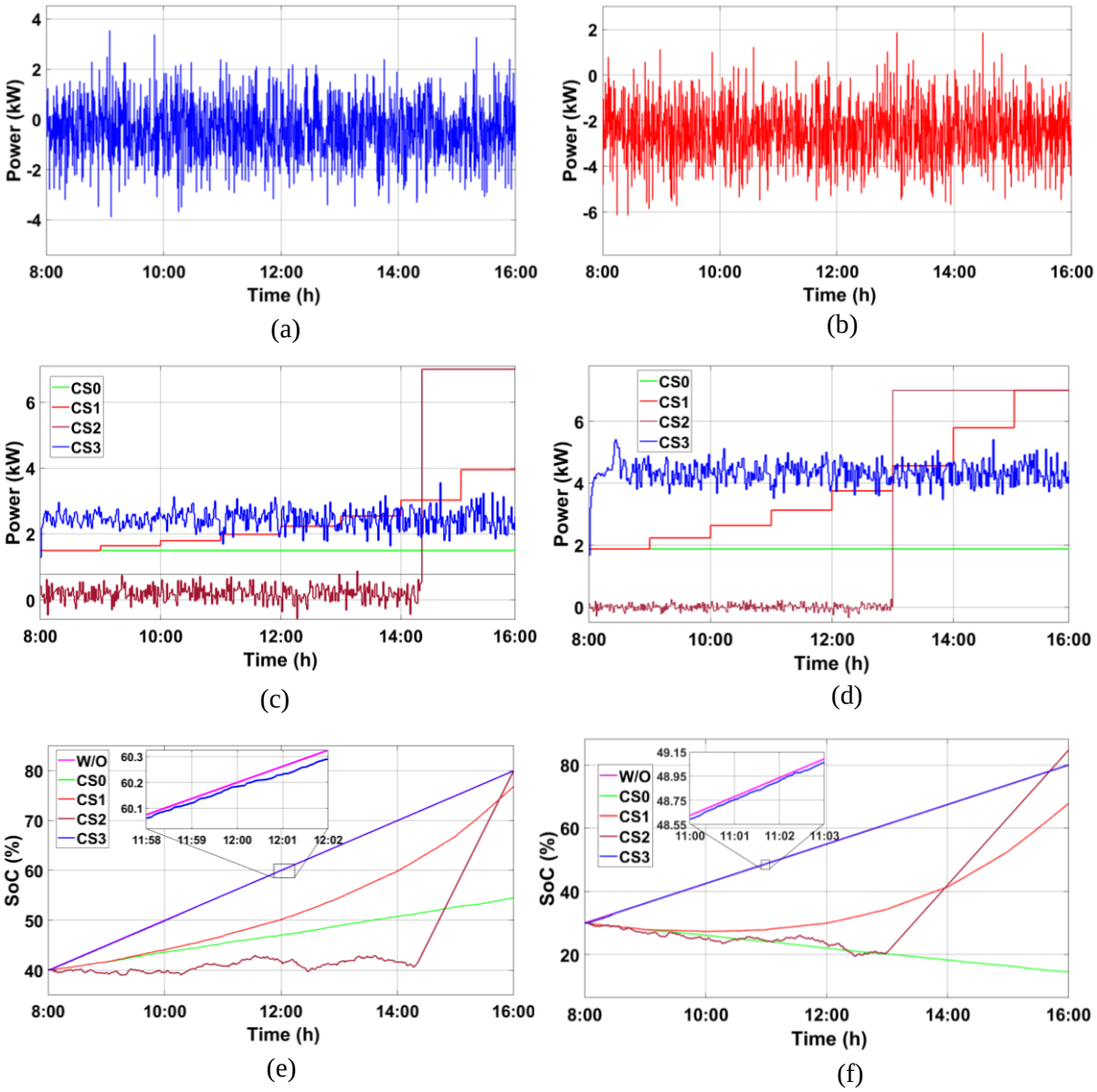

Figure 6-10 Implementation of ACE and ARR signals on EVs of Type I; (a) ACE dispatch (b) ARR dispatch (c) SCP of Type I under ACE (d) SCP of type I under ARR (e) SOC battery of Type I under ACE (f) SOC battery of Type I under ARR.

For Type II, EV owners may prefer to trade the extra energy stored in the EV battery with the utility grid, especially when the SOC is more than enough for travel needs. Therefore, this type of EVs may choose to discharge the battery's stored energy to the predefined SOC level. The dispatched regulation tasks using ACE and ARR are presented in Figure 6-11(a) and Figure 6-11(b), respectively. It can be observed that CS3 has advantages over CS0 and CS1 as it can participate in the regulation until the departure time due to its ability to keep the capacity for regulation-up as shown in Figure 6-11(c) and Figure 6-11(d). In addition, as shown in Figure 6-11(e) and Figure 6-11(f), CS3 can guarantee the satisfaction of the charging demand, while CS0 and CS1 cannot fulfil the expected SOC levels when a large negative mean of ARR is

dispatched to the EV. Although CS2 can optimally achieve the expected SOC of the EV at the plug-out time as shown in Figure 6-11(e) and Figure 6-11(f), however by using this strategy, the EV cannot participate in regulation-up for some time due to the maximum discharging rate as shown in Figure 6-11(c) and Figure 6-11(d).

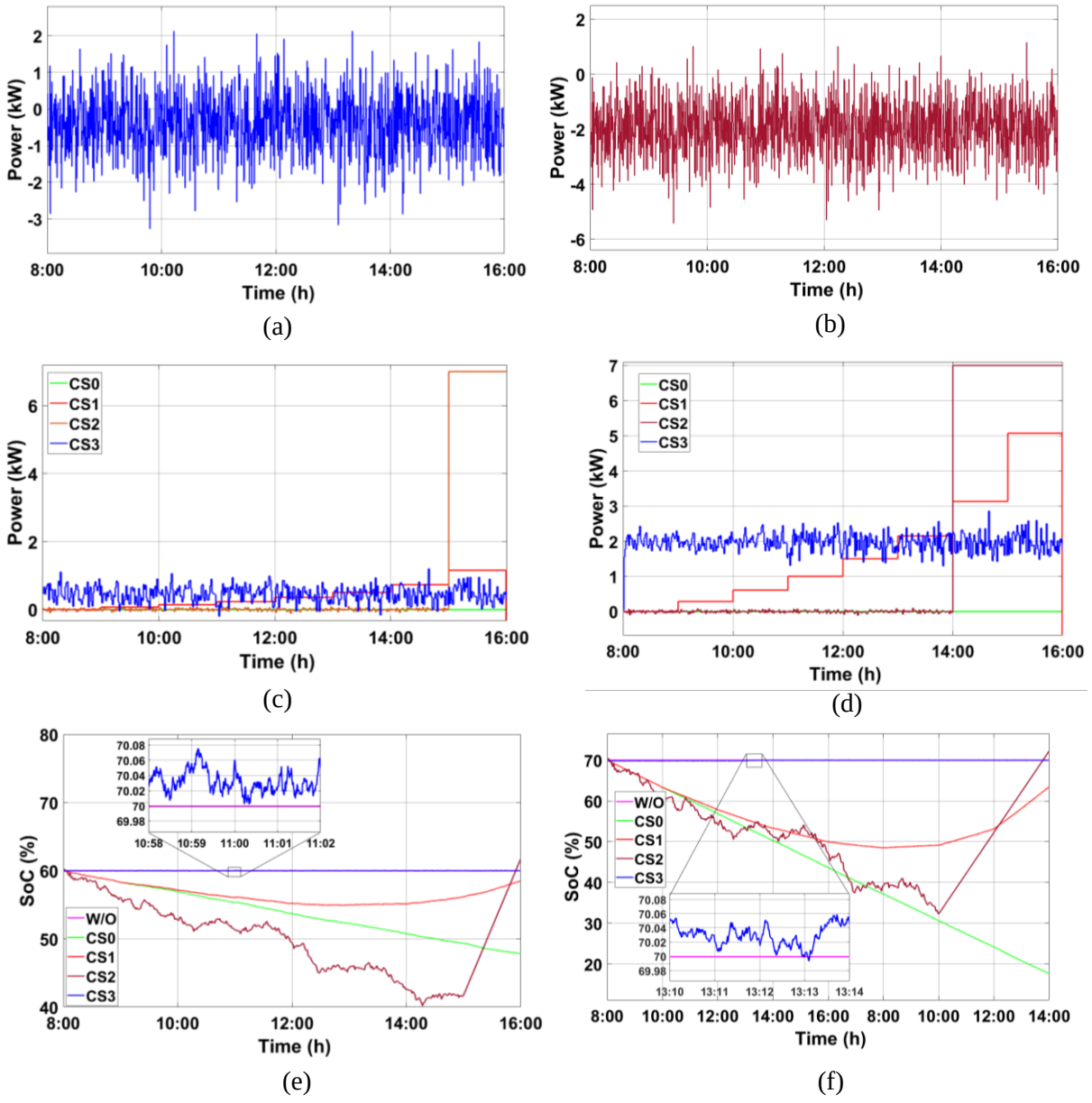

Figure 6-11 Implementation of ACE and ARR signals on EVs of Type II; (a) ACE dispatch (b) ARR dispatch (c) SCP of Type II under ACE (d) SCP of type II under ARR (e) SOC battery of Type II under ACE (f) SOC battery of Type II under ARR.

When EV owners have enough SOC in their EVs' battery for a next trip, they may prefer to keep their battery at the same SOC level. However, EVs can participate in SFC during plug-in time provided that the same initial SOC is returned at plug-out time. The ACE and ARR

dispatched to this type of EV are shown in Figure 6-12(a) and Figure 6-12(b). It can be noted that the optimal strategy (CS3) leads to a better performance as compared to all CS0, CS1 and CS2 strategies considering the large fluctuations in ACE and large mean of ARR as illustrated in Figure 6-12(c) and Figure 6-12(d). Besides achieving the regulation task, CS2 has good ability to minimise the difference between the real-time and the expected SOC as shown in Figure 6-12(e) and Figure 6-12(f).

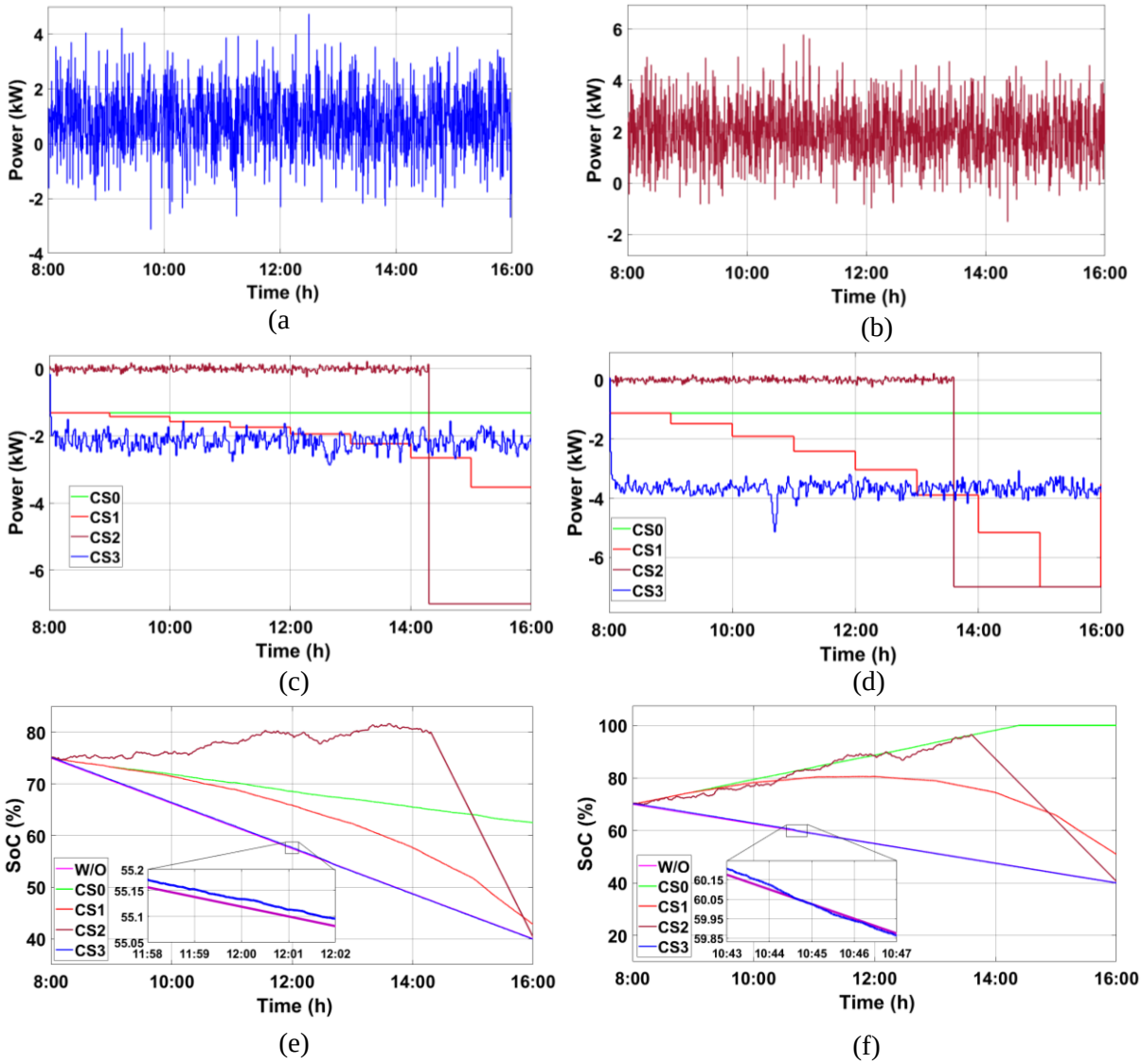

Figure 6-12 Implementation of ACE and ARR signals on EVs of Type III; (a) ACE dispatch (b) ARR dispatch (c) SCP of Type III under ACE (d) SCP of type III under ARR (e) SOC battery of Type III under ACE (f) SOC battery of Type III under ARR.

6.4.2 Impacts of EVs on grid frequency regulation

The frequency response capacity from EVs is influenced by the travelling time. The driving behaviour of EV owners working from 9:00 am to 16:00 pm is likely to follow the same pattern

every day. Therefore, a normal distribution is considered for the arrival and departure times of EVs as shown in Table 6-3.

Due to this distribution of times, the total FRC of EVs, including regulation up/down capacities is affected by the number of the EV arrivals to the charging stations. As expected, the FRC will start increasing from zero and reach the maximum capacity at the arriving time according to the number of EV arrivals and decreasing from the maximum capacity to zero at the departure time according to the number of EV departures from the charging stations as shown in Figure 6-13. The FCR of regulation-up and regulation-down will be uploaded in real-time to the control centre to dispatch the regulation tasks to EVs accordingly.

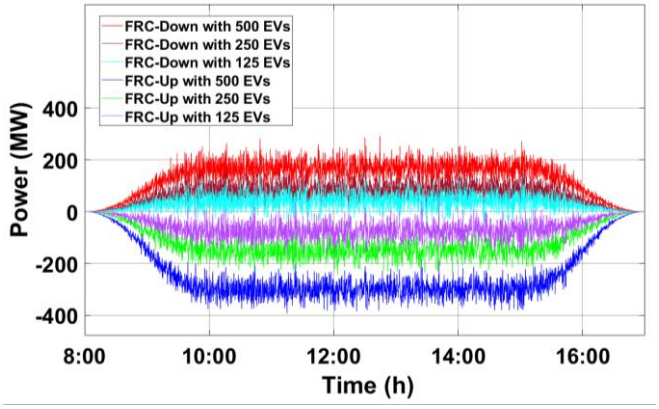

Figure 6-13 FRC of regulation-up and regulation-down under different number of EVs in the charging station.

The total number of EVs parked at the charging stations and able to participate in frequency regulation significantly influences the frequency response capacity. To assess the impact of EVs' number to be used for frequency regulation, we have tested the model under different sizes of EV fleets. Figure 6-13 shows the frequency capacity for regulation-up and regulation-down with different number of EVs participating in the frequency regulation. It can be observed that when the number of EVs is reduced to the half (250 EVs), the FRC also decreases accordingly, leading to a reduction in the capability of EVs for participating in frequency regulation. Therefore, the larger the number of EVs participating in frequency regulation leads to more FRC for regulation-up and regulation-down, and therefore a better frequency regulation service.

The dispatch strategy used for EVs to achieve the expected SOC can also influence the FRC. While considering CS1, CS2 and CS3, the regulation capacity of EVs under these strategies is

analysed and presented in Figure 6-14. It can be observed that EVs are gradually losing their FRC of regulation up and regulation down under CS1, and this reduction in FRC occurred because of the continuous adjusting SCP every hour to reach the EV's charging demand at the departure time. It is also noted that the FRC under CS2 starts decreasing at 13:00 pm, this is due to the forced charging used to satisfy the expected SOC of the EVs after participating in frequency regulation, leading to the inability of the EVs to perform regulation-up and down during that time.

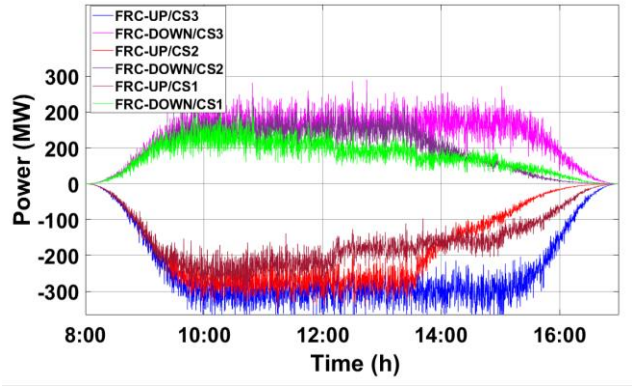

Figure 6-14 EVs' FRC of regulation-up and regulation-down under CS1, CS2 and CS3.

In addition, to achieving the charging demand of EVs using CS3, it is also able to keep the capacity of EVs to participate in frequency regulation and that is because the fast adjustments in the SCP of EVs resulted in the best suppression of ACE, frequency deviations and generators units' power as shown in Figure 6-15, Figure 6-16and Figure 6-17 respectively.

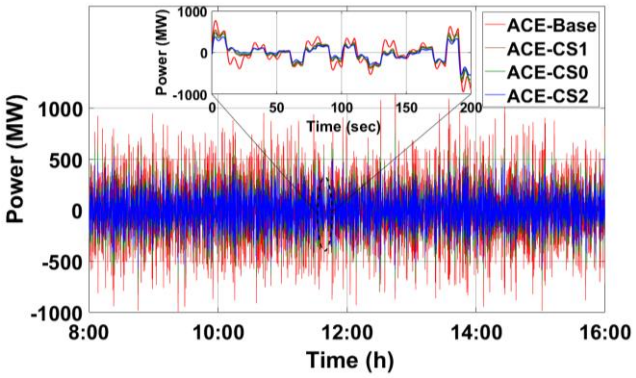

Figure 6-15 ACE signal after implementing CS0, CS1 and CS2.

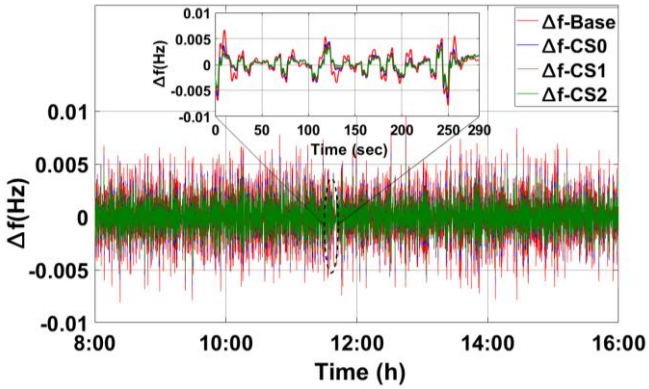

Figure 6-16 System frequency deviation after implementing CS0, CS1 and CS2.

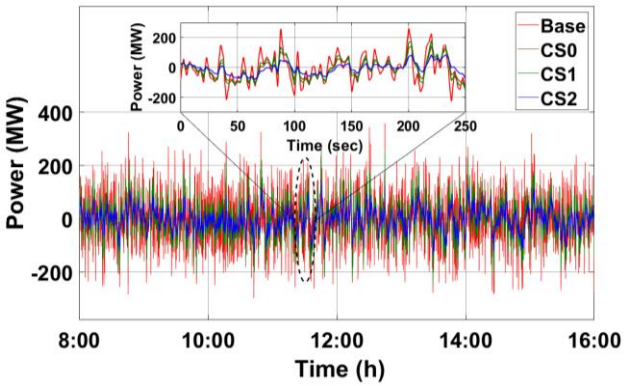

Figure 6-17 Dispatch power allocated to generators units for frequency regulation.

While considering CS1, CS2, and CS3 using ACE and ARR, the grid frequency deviation and ACE quality in Area A are given in Table 6-4 and Table 6-5, respectively. The Root Mean Square (RMS) values of the frequency deviations and ACE are calculated and presented in Table 6-4 and Table 6-5 respectively, to demonstrate the improvement achieved in the frequency regulation of Area A using the proposed V2G control strategy.

Table 6-4 Frequency Deviations in Area A.

Strategy	**RMS of frequency deviation (Hz)**	**Percentage of decrease (%)**
Basic Case	0.02784	--
CS1-ACE	0.02333	16.20
CS1-ARR	0.02284	17.96
CS2-ACE	0.02273	18.35
CS2-ARR	0.02165	22.23
CS3-ACE	0.02170	22.07
CS3-ARR	0.01961	29.57

Table 6-5 ACE in Area A.

Strategy	RMS of ACE (MW)	Percentage of decrease (%)
Basic Case	129.52	--
CS1-ACE	107.81	16.76
CS1-ARR	106.18	18.02
CS2-ACE	101.09	21.95
CS2-ARR	96.85	25.22
CS3-ACE	99.54	23.15
CS3-ARR	88.57	31.62

Although all strategies (CS1, CS2 and CS3) were able to reduce the frequency deviation and ACE of the grid, there are some differences between them. Firstly, CS1-ACE and CS1-ARR strategies have the lowest RMS of frequency deviation (16.20 % and 17.96 %, respectively) and lowest RMS of ACE (16.76 % and 18.02 %, respectively). This is because when CS1 strategy is used, the gradual adjusting in SCP causes a reduction in the regulation capacity of regulation-up or regulation-down throughout the plug-in period. In addition, this strategy exhibits poor performance in achieving the expected charging demand as discussed in Section 6.4.1.

CS2 has higher value of the reduction in the RMS of the frequency deviation (18.35 % and 22.23 %) and RMS of ACE (21.95 % and 25.22 %) using CS2-ACE and CS2-ARR. It is also able to satisfy the driving demand of EVs' owners. However, when compared to CS3, it can be noted that CS3-ACE and CS3-ARR have the highest reduction in the RMS of the frequency deviation (22.07 % and 29.57 %) and RMS of ACE (23.15 % and 31.62 %), besides their ability to optimally achieve the expected SOC levels of EVs. This is because using the proposed strategy, the SCP is tracking and regulating in real time according to the frequency regulation task and the expected SOC of the EV battery. It is worth noting that the use of ARR signal in all strategies can ensure better frequency and ACE quality as compared to ACE dispatch.

6.4.3 Impacts of different SOC distribution on regulation

As presented in Table 6-3, a normal distribution with a variance of 0.01 is used to simulate the initial SOC of the EV battery. However, initial SOCs may also have a higher variance. Therefore, to demonstrate the impacts of different initial SOC of EV batteries on the frequency regulation, both normal and uniform distributions with the same mean value are considered as shown in Figure 6-18. Although different initial SOC distributions are applied, it can be observed that the regulation is maintained at the same level and the expected charging demands are always satisfied for all three types of EVs.

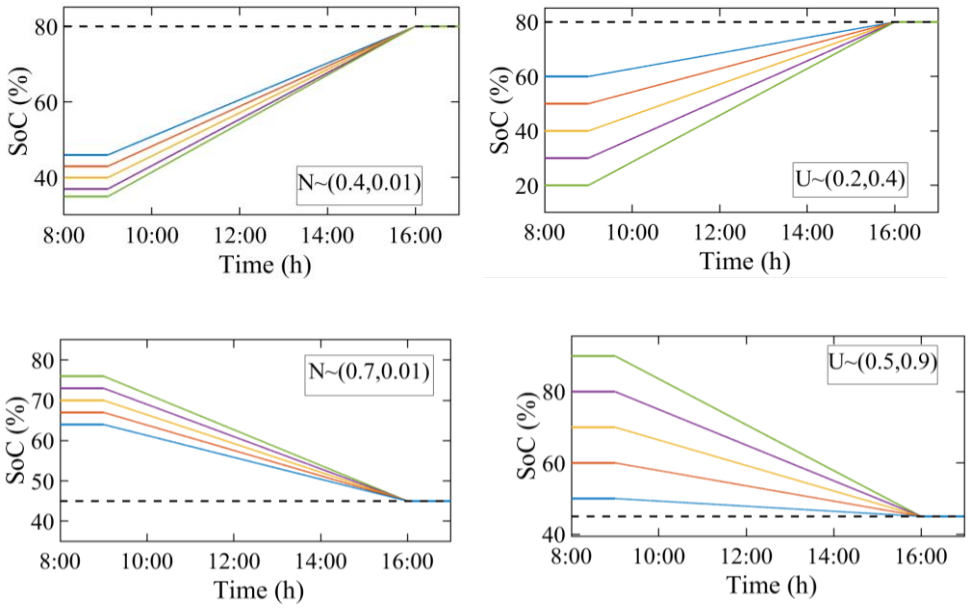

Figure 6-18 SOC curves for (a) Type I and (b) Type II with normal and uniform distributions.

6.5 Conclusion

This chapter proposed an optimal Vehicle-to-Grid (V2G) control strategy for Supplementary Frequency Regulation (SFR) considering the regulation tasks received from the control centre and the expected charging demands of Electric Vehicles (EVs). Deep Reinforcement Learning (DRL) is used for adjusting, in real-time, the scheduled charging power of the EV to satisfy the charging demand of the battery at plug-out time while performing frequency regulation. A Deep Deterministic Policy Gradient (DDPG) agent with a use of Neural Networks was utilised to automatically provide very fast decisions. Once the DDPG agent is trained, it can make decisions without a need for extensive calculations which leads to reduce the computational cost compared to other algorithms such as Q-learning or policy gradient methods. The advantages of using DDPG agent result in significantly improving the SFR of EVs and satisfying the preferences of EVs' owners.

It is worthy noted that the accuracy of this method is not evaluated. That is because the accuracy of DRL is not typically measured in the same way as traditional supervised learning tasks. In supervised learning, accuracy refers to the percentage of correctly predicted labels on a labelled dataset. However, in DRL, the goal is not to produce a specific output for a given input but to learn a policy that maximises cumulative rewards over time.

The proposed dispatch strategy is validated on a two-area interconnected power system. In this study, the EV aggregator was assumed to manage 100 EV charging stations each

accommodating 500 EVs. The EV parameters such as arriving time, departure time, and the initial and the expected SOC of EV batteries are generated randomly using Monte Carlo method. The simulation results show an improvement in the quality of the frequency regulation while satisfying the charging demands of EVs.

To evaluate the effectiveness of the proposed dispatch strategy, the results have been compared with two dispatching strategies from the literature. The first dispatch strategy adjusts the SCP of the EV hourly to achieve the expected SOC level while participating in frequency regulation. The second dispatch strategy aims to satisfy the driving demand of EVs' owners while performing frequency regulation using the forced-charging method. The proposed V2G strategy gives a better performance in achieving the expected charging demand for the EVs participating in SFR as compared to other strategies even under large fluctuations in the Area Control Error (ACE) and large negative means values in the Area Regulation Requirement (ARR) signals. The proposed strategy achieved highest reduction in frequency deviation (29.57%) and highest reduction in ACE (31.62%).

Chapter 7 P2P Electricity Market Model for a Community Microgrid with Price-Based Demand Response

7.1 Introduction

Electricity grids across the globe are undergoing a profound transformation from a rigid, fossil-fuel based generation and distribution to a new decentralized low-carbon infrastructure. In this gradual shift towards the adoption of alternative, cleaner and renewable energy sources and smart technology, small-scale consumers have now the control over their energy consumption and are becoming what is known as prosumers (i.e. producers and consumers) [105]. Prosumers can purchase electricity from the grid and sell their energy surplus back to the grid. However, sell back rates or feed-in-tariffs (FiT) remunerations that prosumers receive when selling electricity to the utility are generally much lower than consumer tariffs for the purchase of electricity from the utility [106].

Peer-to-Peer (P2P) energy sharing, where prosumers directly trade their local energy resources with each other without going through an intermediate retailer, has recently emerged as a flexible and cost-effective energy management mechanism which is about to transform the traditional centralized energy market. The P2P electricity model allows prosumers and consumers to initially trade with one another in a local market at a domestic price and then trade with a retailer. The domestic price is generally bounded between the retail price and the export price. As a result, peers can generate revenue from P2P energy exchange regardless of whether they are sellers or buyers of electricity.

The main advantage of the P2P energy exchange is that the locally generated electricity from renewable sources will not to be transported which will ultimately reduce transmission losses and the overall operation costs of the power system. Besides the monetary benefits it offers to consumers and prosumers, P2P electricity trading contributes substantially to increasing the deployment of RESs. Moreover, the adoption of P2P makes the community more resilient to power outages and improves electricity access to members of the community.

Creating a localized P2P energy market may also be beneficial to the power grid. P2P trading platforms enable an optimal management of decentralized generations through balancing local electricity demand and supply. Furthermore, an effective P2P energy trading scheme incentivizes end-users to consume electricity from the grid at appropriate times of the day which contributes to peak-load reduction. A number of P2P energy sharing pilot projects have been developed around the world mainly in Europe such as Piclo in the UK, Vandebron in the Netherland, Sonnen Community in Germany and Yeloha and Mosaic in the US. Some of these projects, such as Peer Energy Cloud and Smart Watts in Germany, worked on the information and communication technologies (ICT) to support the energy sharing. Some other projects, such as TransActive Grid in the US, have developed a P2P platform based on blockchain technology that enables members to trade energy secularly and automatically between each other [107].

Several studies focused on pricing mechanisms for P2P energy sharing. They can be classified in two categories: double auction model [108]–[112] and analytical model [113]–[116]. Using Double Auction (DA) model, the peers (sellers and buyers) can interact between each other to trade their energy in a step-by-step fashion as follows [117]; buyer/seller peers submit their bids/offers to an auctioneer, these bids/offers are then arranged in a decreasing/increasing order. Once bids and offers are ordered, the aggregated supply and demand curves are generated and intersected at an auction price. Therefore, the only peers who can engage in the trading process are buyers/sellers with bids greater than/offers lower than the auction price. While consumers with bids lower than the auction price cannot buy from prosumers with offers higher than the auction price, this means that the total surplus of PV generation after self-consumption will not be completely traded within the community microgrid as discussed in [108]–[110]. To address this issue, continuous double auctions (CDAs) which consists of repeating the DA for a certain number of rounds or within a specified time are proposed in [111], [112]. Although CDA has a great scalability and high efficiency for distributed energy transactions, the pricing rule and trading strategies of the CDA have some limitations. Due to different trading prices for a series of P2P trading contracts, the CDA does not ensure fairness among peers, in the sense that buyers/sellers may pay more than/earn less than other peers when buying/selling the same amount of energy [118]. In addition, trading prices decided by the auctioneer exhibit higher variation. Therefore, the CDA model cannot offer a fairer trading price that will stimulate the participation of prosumers in the P2P energy trading, which is the main goal of an ideal trading mechanism [119].

An analytical model refers to pricing the energy generated from Distributed Energy Resources (DERs) in a local market based on certain rules, calculation methods or game theoretic approaches. For example, in [113], [114], a Supply Demand Ratio (SDR) is proposed as the ratio of the total renewable energy supply to the total net energy demand in a microgrid, where P2P energy prices are a function of SDR. In [115], the mid-market rate (MMR) mechanism provides the trading price among prosumers at the average of the selling and buying prices set by the retailer, with some adjustment based on the difference between the total energy generation and consumption within the community. The Bill Sharing (BS) mechanism distributes the total energy costs and income among prosumers within a community based on the amount of each prosumer's energy production and consumption. However, these pricing mechanisms (SDR, MMR and BS) cannot guarantee that every participant in the P2P energy sharing market will generate economic benefits [120]. In addition, none of these pricing mechanisms has considered the impact of dynamic retail electricity prices on the P2P market as more retailers may adopt dynamic prices or implement DR programs [121]. Therefore, pricing mechanisms must be designed with considering dynamic retailer prices, so that prosumers can participate in demand response programs by scheduling and controlling their household appliances and energy storage via a HEMS.

Despite the large body of literature on P2P sharing, a limited number of studies have focused on the participation of EVs [122]. Indeed, EVs could serve as a temporary energy storage and supply power to home appliances via V2H technology, and/or feed power to the utility grid using V2G technology when needed. Therefore, the P2P energy market may not only depend on the excess of power from PV generation, but also involves EVs in energy trading during their charging and discharging operations. To enable the participation of EVs in P2P energy markets, an efficient pricing strategy must be adopted to balance the interests of all the players.

This chapter focuses on energy sharing problem within a residential community. A P2P pricing mechanism is proposed for a community consisting of 100 households to incentivise individual customers to participate in energy trading and to ensure that not a single household would be worse off with considering the physical network constrains. This will simultaneously generate revenue for the Energy Sharing Coordinator (ESC) to cover the maintenance and service operations costs.

7.2 Modelling of the Residential Microgrid Components

7.2.1 Household categories

As shown in Figure 7-1, electricity flow refers to the flow of electric power between buyers and sellers and cash flow refers to the cost involved, and income generated during the electricity trade.

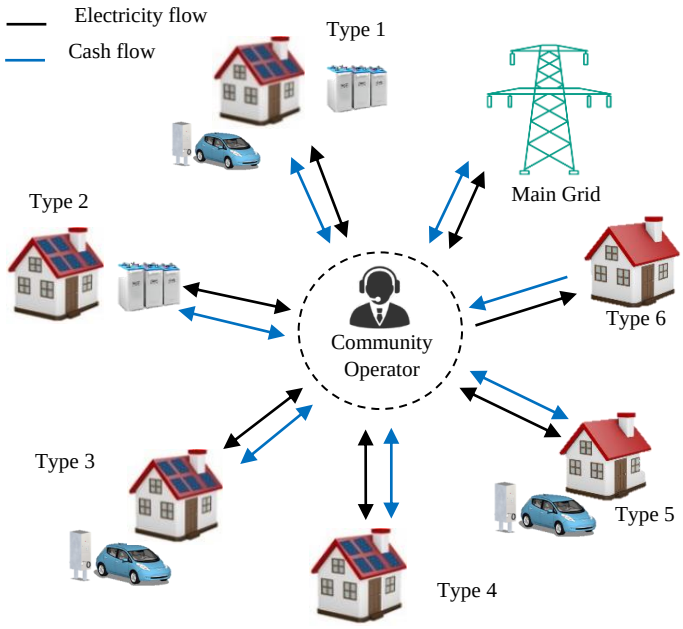

Figure 7-1 Different types of households participating in P2P energy sharing.

Generally, a residential network consists of different types of dwellings, depending on what their premises are equipped with, such as solar PV panels, BESSs and EVs. The type of household i in the residential microgrid can be categorised as $H_j^i, j \in \{1,2,3,4,5,6\}$:

$$H_j^i = \begin{bmatrix} 1 & 1 & 1 \\ 1 & 1 & 0 \\ 1 & 0 & 1 \\ 1 & 0 & 0 \\ 0 & 0 & 1 \\ 0 & 0 & 0 \end{bmatrix} [PV \quad BES \quad EV] \tag{7.1}$$

Where, matrix entry 1 means household i is equipped with the corresponding device and 0 means the household is not equipped with the corresponding device. Note that households $H_1^i, H_2^i, H_3^i, H_4^i$ and H_5^i could be prosumer (seller or buyer) in the residential microgrid whereas household H_6^i is considered as a consumer (buyer only) all the time.

7.2.2 Modelling of household components

A. *Modelling of the load and PV systems*

The energy consumption $E_L^i(\mathrm{t})$ of household i at every time slot over the operation time is defined as:

$$E_L^i(\mathrm{t}) \triangleq [E_L^i(1) \quad E_L^i(2) \quad \cdots \quad E_L^i(T)] \quad i \in \{1, 2, \dots, N\} \tag{7.2}$$

Where $\{1, 2, \cdots, T\}$ is the set of all time slots which are assumed to have equal interval $\Delta t = 5$ min, T denotes the number of time slots over the operation period, and N represents the number of households in the microgrid.

The local PV energy generation of each household during the time interval $[T_s, T_e]$ is defined as:

$$E_{PV}^i(\mathrm{t}) \triangleq H_j^i(PV) \,.\, \left[E_{PV}^i(T_s + 1), E_{PV}^i(T_s + 2), \dots, E_{PV}^i(T_e)\right], \; 0 < T_s < T_d < T \tag{7.3}$$

$E_{PV}^i(t)$ represents the PV generation of household i at each time step, $H_j^i(PV)$ indicates whether household i is equipped with PV or not as shown in Equation (7.1) and returns 1 if the household is equipped with PV and 0 otherwise.

B. Modelling of BES

BES enables the excess of power generated from PV to be stored and used later in the day when the solar PV is no longer available. The energy stored in the BES is described by following equation:

$$E_{BES}^i(t) = H_j^i(BES)\left[E_{BES}^i(t-1)\left(1 - \delta_{SD,BES}^i\right) + U_{BES}^i P_{BES,ch}^i(t)\mu_{BES,ch}^i - \frac{(1 - U_{BES}^i)P_{BES,dis}^i(t)}{\mu_{BES,dis}^i}\right] \tag{7.4}$$

$E_{BES}^i(t)$ and $E_{BES}^i(t-1)$ represent the stored energy at time slot t and $(t-1)$ respectively, δ_{SD}^i is the self-discharging rate, $P_{BES,ch}^i(t)$ and $P_{BES,dis}^i(t)$ denote the battery charging and discharging rates at a given time slot t, respectively, $\mu_{BES,ch}^i$ and $\mu_{BES,dis}^i$ are the charging and discharging efficiencies respectively. $H_j^i(BES)$ indicates whether a BES is available at household i as shown in Equation (7.1) and returns 1 if the household is equipped with BES

and 0 otherwise. U_{BES}^{i} is 1 when the battery is charging and 0 when the battery is discharging. The SoC of the battery is defined as:

$$\begin{cases} SoC_{BES}^{i} = \dfrac{E_{BES}^{i}(t)}{E_{BES,cap}^{i}} \times 100\% \\ SoC_{BES,min}^{i} < SoC_{BES}^{i} < SoC_{BES,max}^{i} \end{cases} \quad (7.5)$$

Where $E_{BES,cap}^{i}$ is the maximum battery capacity, $SoC_{BES,min}^{i}$ and $SoC_{BES,max}^{i}$ are the minimum and maximum SOC of the battery and are set to 20 % and 80 % respectively to avoid deep discharging and overcharging of the battery.

C. Electric vehicle modelling

The EV acts as a domestic battery storage and provides back-up power to supply the home appliances during short-term outages or during peak demand when electricity prices are higher. EV owners can participate in the P2P market by selling energy to other customers. With V2H technology, the EV becomes part of the smart home, and its charging-discharging operations are supervised by the HEMS. The energy stored in the EV battery $E_{EV}^{i}(t)$ during the availability time of the EV at home is given by:

$$E_{EV}^{i}(t) = H_{j}^{i}(EV)\left[E_{EV}^{i}(t-1)\left(1-\delta_{SD,EV}^{i}\right) + U_{EV}^{i}P_{EV,ch}^{i}(t)\,\mu_{EV,ch}^{i} - \frac{(1-U_{EV}^{i})P_{EV,dis}^{i}(t)}{\mu_{EV,dis}^{i}}\right] \quad (7.6)$$

$$P_{EV,ch}^{i}(t) = E_{EV,chfPV}^{i}(t) + E_{EV,bfG}^{i}(t) + E_{EV,bfP2P}^{i}(t), \forall t \in [T_a, T_d] \quad (7.7)$$

$$P_{EV,dis}^{i}(t) = E_{EV,tH}^{i}(t) + E_{EV,stG}^{i}(t) + E_{EV,stP2P}^{i}(t), \forall t \in [T_a, T_d] \quad (7.8)$$

$H_{j}^{i}(EV)$ returns 1 if the household is equipped with EV and 0 otherwise. To avoid charging and discharging to occur at the same time, the availability of the EV for charging and discharging, denoted U_{EV}^{i}, is introduced and takes the value 1 when the EV is charging and 0 when it is discharging. Equation (7.7) represents the charging power of the EV battery which can come from the PV ($E_{EV,chfPV}^{i}(t)$), from the grid ($E_{EV,bfG}^{i}(t)$) or purchased from the P2P market ($E_{EV,bfP2P}^{i}(t)$). Equation (7.8) represents the discharging power of the battery to supply the home appliances ($E_{EV,tH}^{i}(t)$), to be exported to the grid ($E_{EV,stG}^{i}(t)$) or to be exported to the P2P market ($E_{EV,stP2P}^{i}(t)$). The availability time of the EV is limited between the EV's arrival time (T_a) to the house and the departure time (T_d). The SOC of the EV battery, with its charging and discharging limits is given by:

$$\begin{cases} SOC_{EV}^{i} = \dfrac{E_{EV}^{i}(t)}{E_{EV,cap}^{i}} \times 100\% \\ SOC_{EV,min}^{i} < SOC_{EV}^{i} < SOC_{EV,max}^{i} \end{cases} \tag{7.9}$$

The energy consumed during each trip is calculated as:

$$E_{EV,trip}^{i} = \frac{D_{trip}}{D_{max}} \times E_{EV,cap}^{i} \tag{7.10}$$

Where D_{trip} and D_{max} represent the trip distance and the maximum distance the EV can travel when the battery is fully charged, respectively, $E_{EV,cap}^{i}$ denotes the maximum energy capacity of the EV battery.

D. Modelling of the net energy

Solar PV generation can be used to power the household appliances, charge the home BES and the EV battery. The extra power, if any, can be either sold to the P2P market and/or the main grid. Note that the home BES can only supply the household load and charge only from the PV when possible. The EV battery, on the other hand, can be charged from the PV, from the P2P market or the main grid and it can supply the household appliances and sell energy to the P2P market or the main grid. The net energy $E_{net}^{i}(t)$ of household i is the difference between the energy supply $E_{supply}^{i}(t)$ and demand $E_{demand}^{i}(t)$ at each time slot.

$$E_{net}^{i}(t) = E_{demand}^{i}(t) - E_{supply}^{i}(t), \forall t \in [0, T] \tag{7.11}$$

$$E_{demand}^{i}(t) = E_{L}^{i}(t) + U_{BES}^{i} P_{BES,ch}^{i}(t) + U_{EV}^{i} P_{EV,ch}^{i}(t), \forall t \in [0, T] \tag{7.12}$$

$$E_{supply}^{i}(t) = E_{PV}^{i}(t) + \left(1 - U_{BES}^{i}\right) P_{BES,dis}^{i}(t) + \ (1 - U_{EV}^{i}) P_{EV,dis}^{i}(t), \forall t [0, T] \tag{7.13}$$

Where $E_{L}^{i}(t)$is the household demand, $P_{BES,ch}^{i}(t)$ and $P_{BES,dis}^{i}(t)$ denote the battery charging and discharging rates at a given time slot t, respectively. $P_{EV,ch}^{i}(t)$ and $P_{EV,dis}^{i}$ denote the EV battery charging and discharging rates, respectively.

If $E_{net}^{i}(t) < 0$, the surplus power $E_{surplus}^{i}(t)$ the customer can sell is:

$$E_{surplus}^{i}(t) = -\left|E_{net}^{i}(t)\right|, \forall t \in [0, T] \tag{7.14}$$

If $E_{net}^{i}(t) > 0$, the deficiency power $E_{deficiency}^{i}(t)$ the customer needs to buy is:

$$E_{deficiency}^{i}(t) = \left|E_{net}^{i}(t)\right|, \forall t \in [0, T] \tag{7.15}$$

7.2.3 Home Energy Management System

With HEMS, the user can monitor, control, and optimize the amount of energy generated and consumed in real-time, based on the customer's preferences via a dedicated user interface. This enables users to actively participate in the P2P market. Thus, the HEMS should be designed to accommodate different types of household resources such as local generation from renewable RESs, BES and EV. The flowchart of Figure 7-2 describes the proposed HEMS. Generally, PV generation, when available, is first used to supply the household appliances. When the PV generation is higher than the household demand, the surplus of energy will be first stored in the batteries (BES or EV batteries), and the remaining will be sold to other peers in the microgrid. If the PV generation is lower than the household demand, the difference will be purchased from the P2P market if the energy price is low or provided from the batteries otherwise. However, when there is no PV generation, the required power for the household will be purchased from the P2P market if the price is low or taken from the batteries if the price in the P2P market is higher.

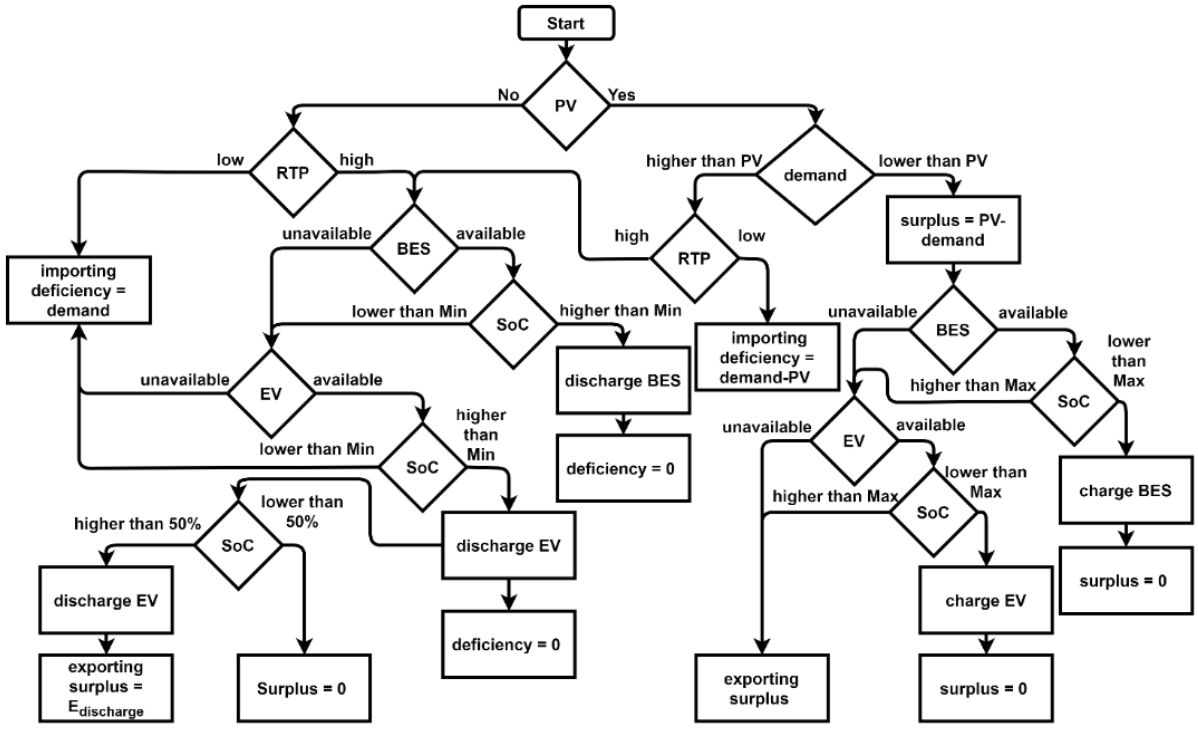

Figure 7-2 Flowchart of the proposed HEMS.

7.2.4 Consideration of physical network constraints

Although the P2P energy sharing benefits both peers and the main grid, technical challenges such as voltage stability and overflow in the physical layer arise with the implementation of a P2P market with the absent of control and management process in the P2P trading. Therefore,

the physical network constrains must be considered to avoid the violation of voltage and capacity issues. In this chapter, the proposed P2P trading mechanism is also proposed with taking in the account of the physical network constraints.

Consider a radial distribution network that consists of a set $\mathcal{N}$ of buses and a set $\mathcal{E}$ of distribution lines connecting these buses. The buses in $\mathcal{N}$ are indexed by $i = 0,1,2, \dots n$, and denote a line in $\mathcal{E}$ by the pair $(i,j)$of buses it connects and the index i denotes the bus that is closer to the feeder. Bus 0 denotes the feeder, which has fixed voltage but flexible power injection to balance the loads. For each link $(i,j) \in \mathcal{E}$, let $\mathrm{z}_{ij} = \mathrm{r}_{ij} + j\mathrm{x}_{ij}$ be the impedance of the line (i,j), where r_{ij} and x_{ij} refer to the resistance and reactance of the line. $S_{i,j} = P_{i,j} + jQ_{i,j}$ is the complex power, where $P_{i,j}$ and $Q_{i,j}$ are the real and reactive power, respectively. At each bus $i \in \mathcal{N}$, let $s_i = p_i + jq_i$ be the complex load, V_i the complex voltage and $I_{i,j}$ current flowing from bus i to bus j. As customary, we assume that the complex voltage V_0 on the feeder is given and fixed. The branch flow model, proposed in [123], models power flows in a steady state in a radial distribution network: for each $(i,j) \in \mathcal{E}$,

$$\frac{P_{i,j}^2 + Q_{i,j}^2}{v_i} = \mathrm{i}_{i,j} \tag{7.16}$$

$$P_{i,j} = \mathrm{r}_{i,j}\mathrm{i}_{i,j} + p_j + \sum_{k:(j,k)\in\mathcal{E}} P_{j,k} \tag{7.17}$$

$$Q_{i,j} = \mathrm{x}_{i,j}\mathrm{i}_{i,j} + q_j + \sum_{k:(j,k)\in\mathcal{E}} Q_{j,k} \tag{7.18}$$

$$v_i - v_j = 2\left(\mathrm{r}_{i,j}P_{i,j} + \mathrm{x}_{i,j}Q_{i,j}\right) - \left(\mathrm{r}_{i,j}^2 + \mathrm{r}_{i,j}^2\right)\mathrm{i}_{i,j} \tag{7.19}$$

Subject to:

$$v_i^{min} \le v_i \le v_i^{max}, i = 1, \dots, n \tag{7.20}$$

$$p_i^{min} \le p_i \le p_i^{max}, i = 1, \dots, n \tag{7.21}$$

$$q_i^{min} \le q_i \le q_i^{max}, i = 1, \dots, n \tag{7.22}$$

Where $\mathrm{i}_{i,j} = \left|I_{i,j}\right|^2$, $v_i = |V_i|^2$. It is worth noting that the net reactive power for each bus must thus be calculated for each time step t. For simplicity, it was decided to find an average power factor for each of the buses and keep it constant for all time steps. From the given network data,

it was obtained that all buses maintained a constant power factor of 0.98. The reactive power for each house i for each time step t was thus calculated with:

$$q_i = \sqrt{\frac{p_i^2}{cos\theta^2} - p_i^2} = \sqrt{\frac{p_i^2}{0.98^2} - p_i^2}\ , \forall i \in \mathcal{E} \tag{6.23}$$

Figure 7.3 presents the flowchart of the proposed bus voltage and line capacity control. To ensure that the P2P mechanism does not violate the physical constraints (Equations (7.20)-(7.22)), every time the Energy Sharing Coordinator (ECS) receives the selling/buying request from prosumers/consumers, voltage variation and line congestion are evaluated and then all participants receive a signal which informs them if they can still participate in the market without causing problems in the network. For example, one prosumer could reduce the injected power into the grid at a certain time due to the high risk of causing voltage problems in the network.

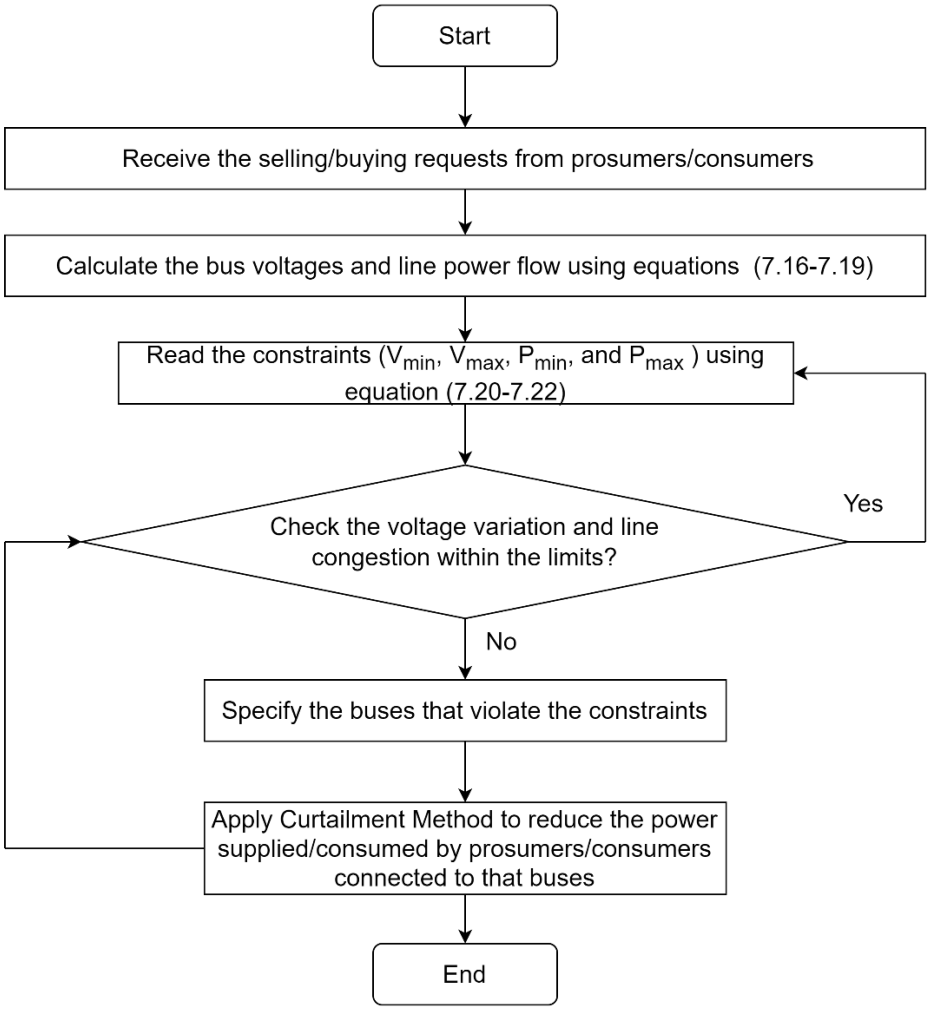

Figure 7-3 Flowchart of the proposed bus voltage control strategy.

7.3 P2P Energy Sharing Model

7.3.1 P2P Energy Sharing Structure

For the P2P energy trading structure of the community microgrid, it is assumed that all participants are connected to one another through the bidirectional energy and information flows, and the whole community is linked to the utility grid via a network connection point. Based on this structure, the peers can trade their excess energy among themselves, instead of directly trading with the utility grid. As shown in Figure 7-4, the P2P sharing system is assumed to have two layers: a physical layer and a virtual layer. The physical layer is responsible for the physical connection and transfer of energy between prosumers within the community through a local distribution network. In addition, it is assumed that all houses are equipped with smart meters to collect data such as PV generation, energy consumption, SOC of the ESS and EV, and energy transactions with P2P market or with the utility grid. Moreover, the communication network is used to enable the smart meters to exchange the data.

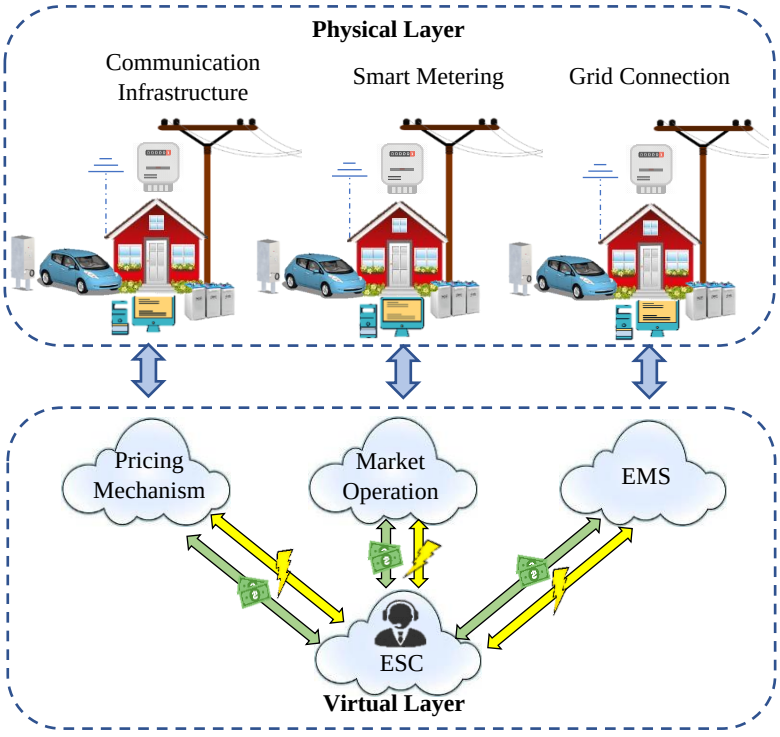

Figure 7-4 P2P energy sharing structure.

The virtual layer provides a secure network environment for all the peers to have equal access to the P2P market. In the virtual layer, it is assumed that each participant is equipped with an Energy management System (EMS), which is responsible for managing the energy flow within the household and energy import/export on behalf of the consumer/prosumer. As shown in

Figure 7.3, both the trading process and the communication of information are done in a centralized fashion via an ESC who can communicate with each peer within the community. The ESC manages energy transactions, price mechanism, purchase, and sale expenses settlement, and interacts with the utility grid considering the physical network constrains to avoid the violation of voltage and capacity issues. Peers, on the other hand, will pay/gain their energy cost/revenue based on the amount of energy imported/exported using the predefined pricing mechanism. It is worth noting that this study focuses only on the application of energy trading in the virtual layer of the P2P energy sharing model.

7.3.2 P2P Energy Sharing Mechanism

The P2P energy trading mechanism is designed to motivate residents to participate in the energy market. The basic principle of economics states that the goods price increases when the demand increases and the production decreases, and vice versa. In this chapter, a new P2P pricing mechanism is proposed to ensure all customers in a community make economic benefits, in other words they will be better off compared to the traditional utility grid market. The proposed pricing mechanism can be applied to any P2P energy sharing model. The proposed mechanism does not consider only the relationship of the surplus and deficiency of power, but also considers the RTP of the power grid and FiT which reflect the demand of the power system, where the price is high during peak demand and lower during off-demand. Then demand response (DR) program is implemented to encourage consumers to manage their energy consumption, to reduce the stress on the power grid and ensure that energy exchange among the peers does not violate network constraints. The proposed P2P model assumes that (i) the internal selling and buying prices are bounded between the FiT and RTP prices and (ii) the buying price is higher than selling price except in the case where the energy deficiency equals the energy surplus, in which case the buying and selling prices are equal.

For each time slot, the total energy surplus exported to the P2P market by n prosumers is defined as:

$$E_S(t) = \sum_{i=1}^{n} E_{surplus}^{i}(t), \forall t \in [0, T] \tag{7.24}$$

The total energy deficiency purchased by m consumers is defined as:

$$E_D(t) = \sum_{i=1}^{m} E_{deficiency}^{i}(t), \forall t \in [0, T] \tag{7.25}$$

Since the P2P prices depend on the relationship between the energy deficiency and energy surplus that need to be traded at the P2P market, this measure is defined by the α-ratio given by:

$$\alpha = \frac{E_D - E_S}{E_D + E_S} \qquad \alpha \in [-1, 1] \tag{7.26}$$

When $\alpha = 0$, the surplus equals the deficiency ($E_S(\mathrm{t}) = E_D(t)$) as shown in Figure 7-5, when $\alpha \approx -1$, there is no deficiency ($E_D(\mathrm{t}) = 0$) or the surplus is much larger than the deficiency ($E_S(\mathrm{t}) \gg E_D(\mathrm{t})$) and when $\alpha \approx 1$, there is no surplus exported or the surplus is much smaller than the deficiency ($E_S(\mathrm{t}) \ll E_D(\mathrm{t})$).

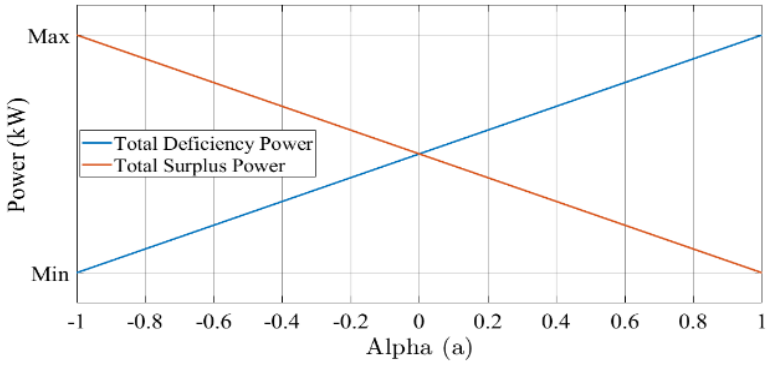

Figure 7-5 Different values of alpha α and among different values of surplus power $E_S(t)$ and deficiency power $E_D(t)$.

The energy price of the main grid fluctuates during the day; it is higher during peak demand periods and lower during off-peak periods which affects the internal P2P prices.

Therefore, the relationship between the import and FiT prices can be expressed as:

$$\beta = \frac{r_{ex}}{r_{ex} + r_g} \;, r_{ex} < r_g \tag{7.27}$$

Where r_g is the RTP of the main grid and r_{ex} is the FiT.

Therefore, the P2P market price is calculated based on (α) and (β) parameters as:

$$r_b = \begin{cases} \left(\frac{r_g - r_{ex}}{2}\right)\frac{(2-\beta)e^{2\alpha} + \beta e^{-2\alpha}}{e^{2\alpha} + e^{-2\alpha}} + r_{ex} & \alpha \geq 0 \\ \left(\frac{r_g - r_{ex}}{2}\right)\frac{(1+\beta)e^{2\alpha} + (1-\beta)e^{-2\alpha}}{e^{2\alpha} + e^{-2\alpha}} + r_{ex} & \alpha < 0 \\ r_g & E_S(\mathrm{t}) = 0 \end{cases} \tag{7.28}$$

$$r_s = \begin{cases} \left(\frac{r_g - r_{ex}}{2}\right)\frac{(1+\beta)e^{2\alpha}+(1-\beta)e^{-2\alpha}}{e^{2\alpha}+e^{-2\alpha}} + r_{ex} & \alpha \geq 0 \\ \left(\frac{r_g - r_{ex}}{2}\right)\frac{(2-\beta)e^{2\alpha}+\beta e^{-2\alpha}}{e^{2\alpha}+e^{-2\alpha}} + r_{ex} & \alpha < 0 \\ r_{ex} & E_D(\mathrm{t}) = 0 \end{cases} \quad (7.29)$$

The formulation of Equations (7.28) and (7.29) is shown in Appendix A. Figure 7-6 P2P market prices under the proposed price mechanism with different values of α and β.shows the P2P market prices under the proposed price mechanism with three different values of RTP as FiT is constant throughout the day.

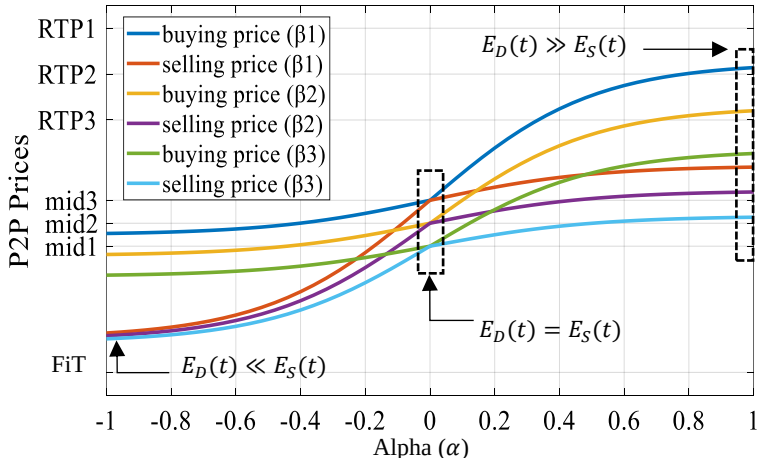

Figure 7-6 P2P market prices under the proposed price mechanism with different values of α and β.

The main features of this price mechanism are: (i) The P2P market prices are bounded between the RTP and FiT. (ii) When $E_D(\mathrm{t}) = E_S(t)$, the P2P prices are set to the Mid-Rate Ratio (MMR), which refers to the mean value of the RTP and FiT prices. (iii) P2P buying price is always higher than P2P selling price. (iv) P2P market prices are higher than MMR when $E_D(\mathrm{t}) > E_S(t)$, $\alpha > 0$. (v) P2P market prices are lower than MMR when $E_D(\mathrm{t}) < E_S(t)$, $\alpha < 0$. (vi) With increasing RTP, the P2P market prices increase based on β value, and vice versa.

7.3.3 Cost Function

The role of the ESC is to supervise the transactions in the P2P market. His main responsibilities are to set the trading rules and manage the trading activities, as well as supervise the metering, billing, and information sharing. After receiving a bid from a prosumer, the ESC runs the pricing model to obtain P2P prices based on the deficiency-surplus ratio, and RTP-FiT prices. At each time slot, the individual energy cost for each participant is calculated using Algorithm 1 given in Table 7-1. During the operation, the following possible cases could occur at each time step:

1. $E_D(t) > 0$ and $E_S(t) = 0$: When the ESC receives only the energy deficiency requests from consumers, he will buy energy from the main grid to meet the demand and the individual energy cost for each consumer i is defined as in line (8) of Algorithm 1.
2. $E_S(t) > 0$ and $E_D(t) = 0$: In this case, there is no energy deficiency request from consumers, thus the amount of energy surplus will be exported to the main grid under FiT price and the individual cost is calculated using line (11) of Algorithm 1.
3. $E_D(t) > E_S(t), E_S(t) \neq 0$: When the amount of deficiency is higher than the surplus, then the ESC needs to buy energy from the main grid to meet the energy deficiency. In this case, lines (12-21) are implemented. Firstly, the amount of energy purchased from the grid is defined using line (13). Consequently, calculating the individual energy cost depends on whether the participant is buying or selling energy. Lines (16) and (17) calculate respectively the cost of the energy purchased from P2P market and main grid, and then the total individual cost is determined using line (18). For users who are selling energy, the profit is calculated using line (20).
4. $E_S(t) > E_D(t), E_D(t) \neq 0$: In this case, the total energy surplus is greater than the total deficiency. Therefore, the extra energy will be sold to the main grid. The individual energy cost is calculated with lines (22-31).
5. Firstly, the amount of energy sold to the main grid is determined using line (23), then the energy cost is calculated using line (28) which is the sum of the cost from selling energy to consumers (line 26) and the main grid (line 27). The individual energy cost for users who are buying energy from the P2P market is calculated with line (30).
6. $E_S(t) = E_D(t)$: When the total surplus meets the deficiency, the P2P selling and buying prices are equal. The energy cost for prosumers and consumers are calculated using lines (35) and (37) respectively.

Table 7-1 Proposed cost function.

Algorithm 1

For t = 1 to 24
  Read RTP (r_g) and FiT (r_{ex}), number of households (N)
  Receive E_D and E_S requests
  Implement pricing model to specify r_b and r_s
  For i =1 to N
    if $E_D(t) > 0$ and $E_S(t) = 0$
      Calculate individual energy cost as:
      $C^i(t) = E^i_{deficiency}(t) * r_g$
    elseif $E_S(t) > 0$ *and* $E_D(t) = 0$
      Calculate individual energy cost as:
      $C^i(t) = E^i_{surplus}(t) * r_{ex}$
    elseif $E_D(t) > E_S(t)$ and $E_S(t) \neq 0$
      $E_{bfg}(t) = E_D(t) - E_S(t)$
      Calculate individual energy cost as:
      if $E^i_{deficiency}(t) > 0$
        $c^i_{bfP2P}(t) = \frac{E^i_{deficiency}(t) * E_S(t) * r_b}{E_D(t)}$
        $c^i_{bfg}(t) = \frac{E^i_{deficiency}(t) * E_{bfg}(t) * r_g}{E_D(t)}$
        $C^i(t) = c^i_{bfP2P}(t) + c^i_{bfg}$
      elseif $E^i_{surplus}(t) > 0$
        $C^i(t) = E^i_{surplus}(t) * r_s$
      endif
    elseif $E_S(t) > E_D(t)$ and $E_D(t) \neq 0$
      $E_{stg}(t) = E_S(t) - E_D(t)$
      Calculate individual cost as:
      if $E^i_{surplus}(t) > 0$
        $c^i_{stP2P}(t) = \frac{E^i_{surplus}(t) * E_D(t) * r_s}{E_S(t)}$
        $c^i_{stg}(t) = \frac{E^i_{surplus}(t) * E_{stg}(t) * r_{ex}}{E_D(t)}$
        $C^i(t) = c^i_{stP2P}(t) + c^i_{stg}(t)$
      elseif $E^i_{deficiency}(t) > 0$
        $C^i(t) = E^i_{deficiency}(t) * r_b$
      endif
    elseif $E_S(t) = E_D(t)$
      Calculate individual cost as:
      if $E^i_{surplus}(t) > 0$
        $C^i(t) = E^i_{surplus}(t) * r_s$
      elseif $E^i_{deficiency}(t) > 0$
        $C^i(t) = E^i_{deficiency}(t) * r_b$
      endif
    endif
  end
end

7.4 Results and Discussion

7.4.1 Simulation Setup

In this chapter, the uncertainties in the load demand of the houses, the PV generation, and the flexibility of EVs are simulated using the MCS which produces 1000 scenarios of possible probabilities. A suitable distribution function has been assigned to each parameter of the load demand, PV generation and EVs. Then the input data for the MCS is extracted from the Probability Density Function (PDF) generated by these distribution functions.

A. household demands

To address the uncertainty of the household demand, the residential area with 100 households is firstly classified into six types $[H_1, H_2, H_3, H_4, H_5, H_6]$ based on the type of household they own. The number of each type of these houses is extracted from the weighted uniform distribution as shown in Table 7-2.

Table 7-2 Types of households

Household Type	PV	BES	EV	Probability Density
1	Yes	Yes	Yes	0.07
2	Yes	Yes	No	0.1
3	Yes	No	Yes	0.1
4	Yes	No	No	0.18
5	No	No	Yes	0.15
6	No	No	No	0.4

The daily household load depends on the house's size and profile class as presented in Ofgem (UK's energy regulator) report [124]. According to this report, a typical household loads divided into two profiles. Profile 1 is domestic unrestricted, which most homes fall under (60%). While Profile 2 (40%) covers Domestic Economy 7, where users have a lower off-peak rate at night, when they pay less for their electricity as shown in Table 7-3. The probability density of the household size is based on the real data extracted from [125] which presents the number of household size by number of bedrooms in England/London, 2011.

Table 7-3 Typical household's energy usage in UK

Household Size	Electricity Consumption (kWh)			
	Profile Class 1		Profile Class 2	
	Annual	Daily	Annual	Daily
1–2-bedroom household/flat	1,800	5	2,400	6.7
3–4-bedroom house	2,900	8	4,200	11.7
5+ bedroom house	4,300	12	7,100	19.7

Figure 7-7 shows the weights of the uniform distribution function of each household size based on the number of bedrooms. Generally, peak electricity consumption occurs during morning hours [7:00 am-12:00 pm] when the household occupants wake up and during the evening [16:00 pm -21:00 pm] when the occupants start cooking, watching TV and doing other activities. Off-peak hours usually correspond to the period from mid-night till the morning.

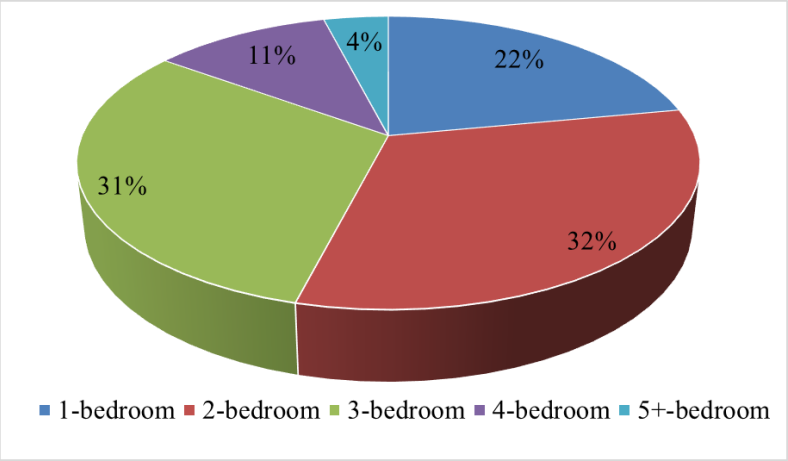

Figure 7-7 Distribution of household size by number of bedrooms.

B. Probability distribution for stochastic parameters of EVs

The availability of EVs depends on several factors, such as the EV owners' travelling patterns and usage, EVs' type, the capacities of their batteries, and the arrival and departure times. Therefore, it is essential to develop a comprehensive model to determine the availability of EVs. In this chapter, the distribution functions are used to create the PDF of all the parameters and variables for each EV to be used as an input to the MCS to produce different scenarios.

➢ *EVs classification*

In the UK, individual EVs based on their size and use are classified into the following four basic categories [81]:

- L7e: Quadricycle-four wheels, with a maximum unladen mass of 400 kg or 550 kg for goods carrying vehicles.
- M1: Passenger vehicle, four wheels up to 8 seats in addition to the driver's seat.
- N1: Goods-carrying vehicle, four wheels, with a maximum laden mass of 3500 kg.
- N2: Goods-carrying vehicle, four wheels, with a maximum laden mass between 3500 kg and 12,000 kg.

The real data presented in [81] regarding the number of the above four types of EVs in the UK in 2020 is used to create a weighted uniform distribution function. Figure 7-8 shows the PDF used to determine the category of each EV.

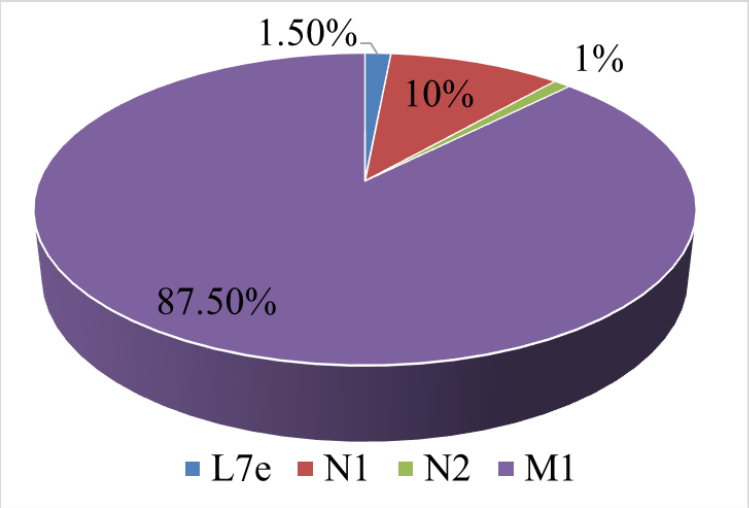

Figure 7-8 Distribution of EVs categories.

- *Departure and arrival times*

It is assumed that the peak-hour of departure time of EVs is 8:00 am as people start leaving their premises, while the peak -hour of arrival time is 18:00 pm as users return home. To address the uncertainties, Departure and arrival times are assumed to have a Weilbull distribution with scale and shape parameters as shown Figure 7-9 (a) and Figure 7-9 (b), respectively.

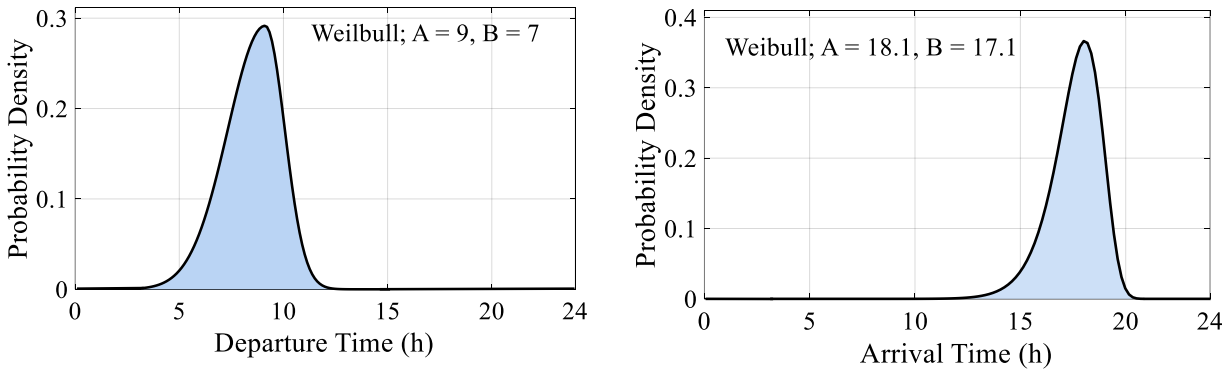

Figure 7-9 Probability density of departure and arrival times.

- *Battery characteristics and daily travelling distance*

The random values for the rated battery capacity for each type of EV are generated based on the Gamma and Normal distributions to create the most suitable probability density functions [81]. Figure 7-10 shows the PDFs of the battery capacities for each EV's category. For example, the Gamma distribution with shape set to 10.8 and scale set to 0.8 is used for L7e category and the battery capacity is bounded between 5 and 15 kWh.

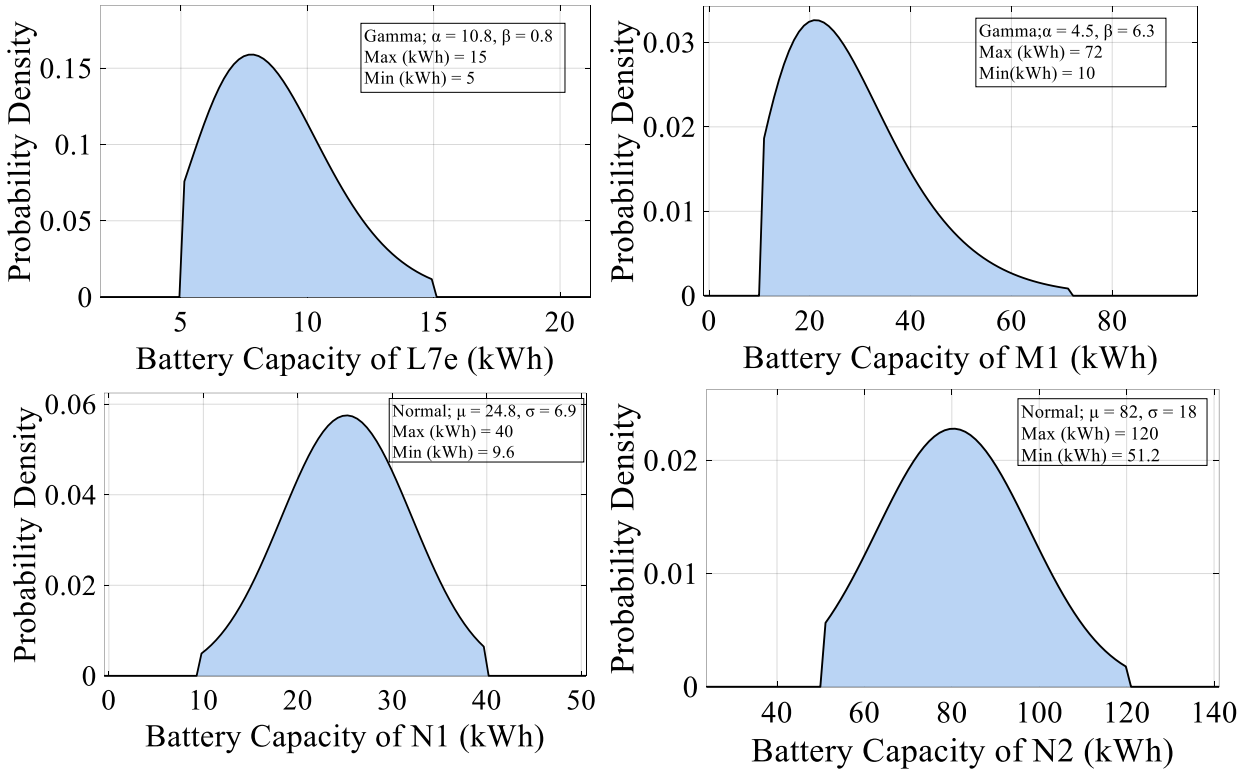

Figure 7-10 Probability of battery capacity of EVs' categories.

According to the statistical data set published by the Department of Transport in England 2020 [126], the distribution of daily distance is fitted as a normal distribution with the average value set to 39.9 km and the deviation set to 10 km to create the PDF of EV travelling distance as shown in Figure 7-11.

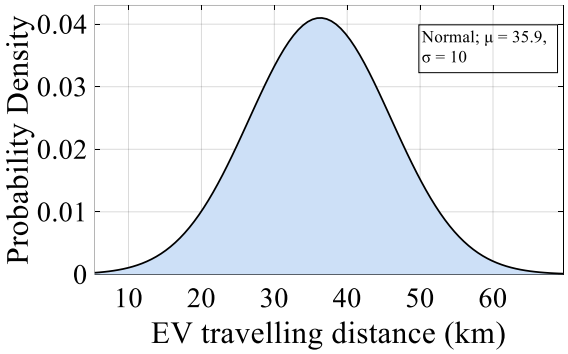

Figure 7-11 Probability of EV travelling distance.

To specify the initial amount of EV's SoC, it is essential to determine the energy consumption per kilometer. To this end, the weighted uniform distribution is used, where the distributions of EV energy consumption per kilometer for all types of EVs are shown in Figure 7-12 [81].

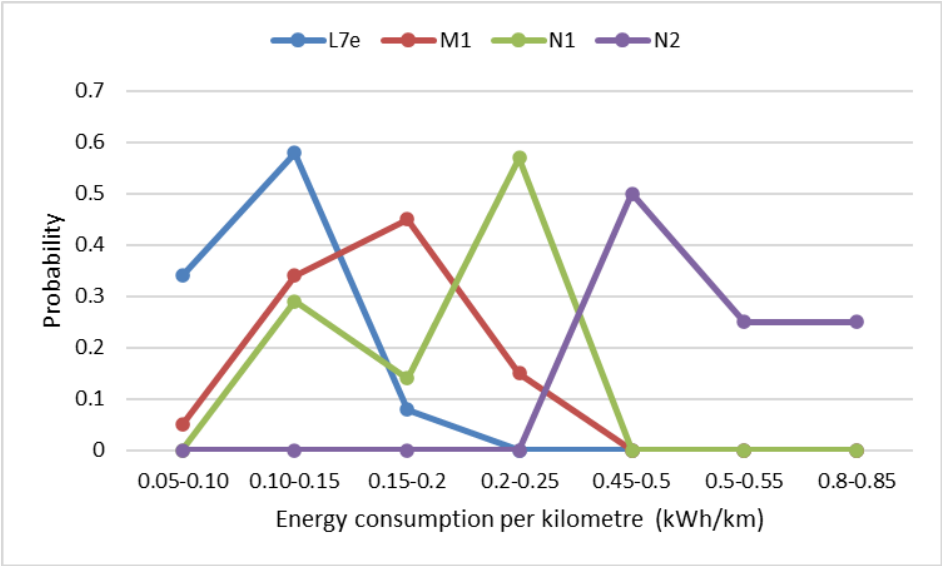

Figure 7-12 Probability of energy consumption of each EV category.

- *Initial SoC and target SoC of EVs*

To satisfy the charging demand for each EV, the target SoC of each EV is selected randomly using the uniform distribution [65%, 80%]. Based on the target SoC, the travelling distance and energy consumption per kilometer values, the initial SoC for each EV can then be calculated as:

$$SoC^i_{initial} = \varphi^i \cdot \left(SoC^i_{target} - \frac{C^i_{kWh/km} \times D^i_{trip}}{E^i_{EV,cap}} \right) \quad (7.30)$$

$C^i_{kWh/km}$ is the energy consumption per kilometer. φ^i is an energy efficiency coefficient which is used to consider the energy loss brought by the speed change process, and it varies uniformly in the range of [0.9,1.0].

C. Probability distribution for stochastic parameters of PV

As the PV power generation is highly uncertain due to variations in the solar irradiance level throughout different hours of the day. Hence, the modelling of PV uncertainty can be addressed either directly as a PDF of the PV power yield or indirectly as a PDF related to the solar irradiance which is subsequently fed into a PV system model. In this chapter, A stochastic model of PV production is built based on the adopted historical solar irradiance data extracted from [127] with zero mean and standard deviation of 15%. Figure 7-13 shows one of the random scenarios of power generation of the PV.

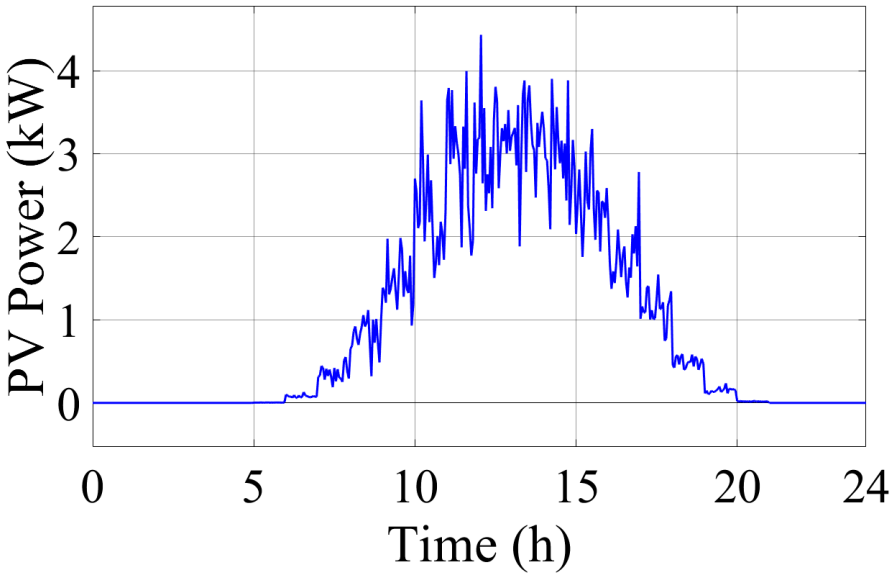

Figure 7-13 Stochastic PV generation.

7.4.2 Evaluation of the proposed HEMS

A. Impact HEMS on individual household demand

In this study, it is assumed that all participants in the P2P energy sharing are equipped with a HEMS in their households. The key function of the HEMS is to provide energy management services to minimise the power consumption in the smart home. This functionality includes monitoring, control and management of renewable energy generation, energy storage, and energy consumption. HEMS also receives price signals from the utility grid and the P2P market and performs demand response analysis. To investigate the performance of the proposed

HEMS to satisfy the household demand, one scenario that has the highest probabilities of MCS is selected to illustrate the power profiles of the six households' types. In Table 7-4, the details for this scenario are listed of each household.

Table 7-4 Details of the six test houses.

House type	House load (kWh)	PV (kWh)	BES		EV Battery	
			Cap. (kWh)	Initial SoC (%)	Cap. (kWh)	Initial SoC (%)
H_1	19.7	4	5	40	50	39
H_2	8	3	6	35	-	-
H_3	12	3	-	-	40	37
H_4	8	3	-	-	-	-
H_5	12	-	-	-	60	42
H_6	5	-	-	-	-	-

"-" = not applicable, "cap." = Capacity.

By using the proposed HEMS algorithm of Figure 7-2, the energy consumption profiles of the selected six households throughout the day are shown in Figure 7-14 . Household Type 1 (H_1) is equipped with PV, BES and EV as shown in Table 6.2. It can be noted that, during the time interval [12:00 am – 6:00 am], the HEMS sends a request of energy deficiency to the ESC as there is no PV generation, the energy demand and the electricity price are lower as shown in Figure 7-14(a). At 6:00 am, the price is high, then the BES starts discharging to supply the household demand, until there is no deficiency energy. During [7:00 am – 9:00 am], the solar PV starts generating. Therefore, the household load is supplied from the PV and the surplus is used to charge the BES. Once the BES reaches the maximum SoC, the remaining power is exported to the P2P market. This occurs during the time [9:00 am- 13:00 pm]. Once the EV returns home, and there is still PV generation, the surplus of power is used to charge the EV battery till the SoC reaches 80 %. Then the surplus of power is fed back to the P2P market again. During the time [16:00 pm-18:00 pm], the household load reaches the peak value, thus the BES is used to supply the household appliances. The EV battery is discharging to sell energy to the P2P market during [17:00 pm- 18:00 pm], as the SoC of the EV is at its full capacity, and the electricity price is also high. From 18:00 pm to 22:00 pm, the EV is selling energy to the P2P market and supplying energy to the household load.

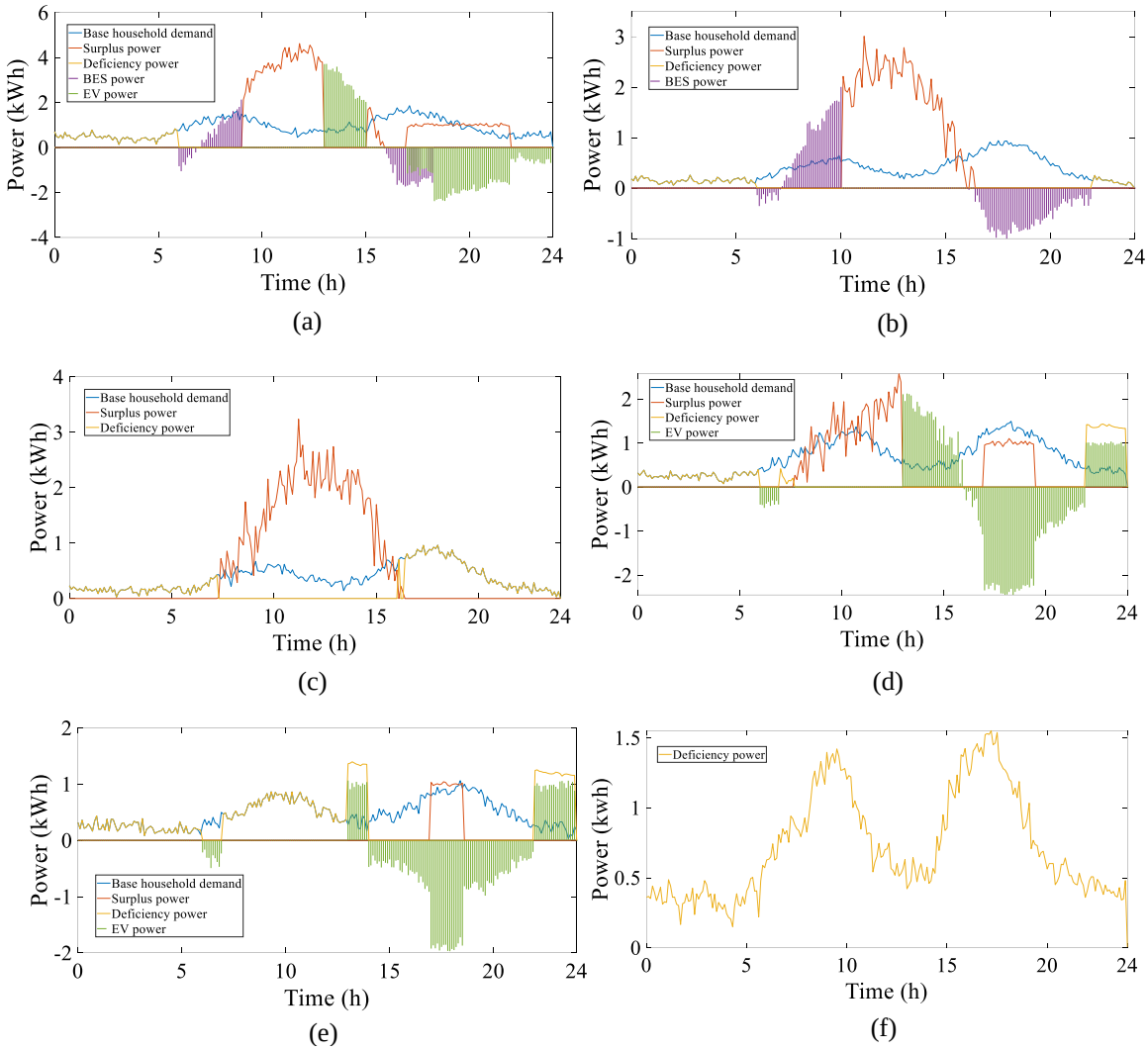

Figure 7-14 Random scenario of the power profiles for the six household types throughout the day under the proposed HEMS.

Household Type 2 (H_2) sends energy deficiency request to the P2P market during [12:00 am-6:00 am] and [22:00 pm – 12:00 am] and exports the surplus energy during [10:00 am – 16:00 pm] as shown in Figure 7-14 (b). Since this household type is equipped with PV and BES, the BES charges from the surplus of PV and then is used later to supply the household load during the evening peak demand.

For household Type 3 (H_3), the energy deficiency request is sent to the P2P market during early morning time [12:00 am-6:00 am] to supply the household appliances as there is no PV generation and the electricity price is lower. At 6:00 am, the electricity price becomes higher, hence it is better to use the EV battery to supply the household appliances. Since this household is not equipped with BES, the surplus energy request is sent to the P2P market during the PV generation [7:00 am-13:00 pm]. Once the EV returns home at 13:00 pm, the surplus power is

used to charge EV battery. During [16:00 pm-22:00 am], the household load is powered by discharging the EV battery. From 16:30 pm to 19:30 pm, the EV is utilized to sell energy to P2P market as there is enough SoC and the electricity price is high shown in Figure 7-14(c).

The load curve of household Type 4 (H_4) is presented in Figure 7-14(d), This household is equipped with solar PV only. Therefore, the surplus of energy can be sold only to the P2P market. When there is no PV generation, the user buys the required energy from the P2P market.

As Household Type 5 (H_5) owns only an EV, the household load is supplied by importing energy from the P2P market most of the time as shown in Figure 7-14(e). The EV battery is charged only during off-peak periods because energy prices are lower. While the surplus of energy is exported to the P2P market during [16:30 pm-18:00 pm] by discharging the EV battery. The evening peak demand is covered with the energy stored in the EV battery due to the higher electricity price.

Household Type 6 (H_6) is considered as consumer all the time; hence his load is supplied by purchasing the required power from the P2P market as shown in Figure 7-14(f).

To evaluate the overall performance of the proposed HEMS within the community, the average amount of deficit/surplus for each group of households that belongs to same type has been calculated over 1000 scenarios of MCS with and without implementing HEMS and presented in Figure 7-15. Clearly, the proposed HEMS can effectively manage the energy flow within each type of household and simultaneously enable the EVs to participate in P2P market. For example, for households of Type 1, the average energy deficit has decreased using HEMS from 4.6 kWh to 3.2 kWh, while the surplus energy exported to the P2P market has increased using HEMS from 10.9 kWh to 12.1 kWh as shown in Figure 7-15 (a) and Figure 7-15 (b), respectively.

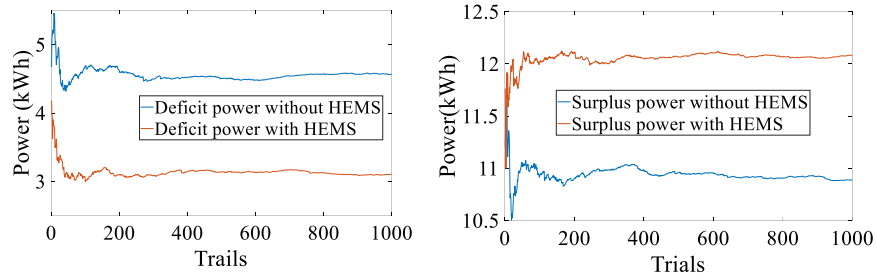

(a) Deficit and surplus power of Household Type 1.

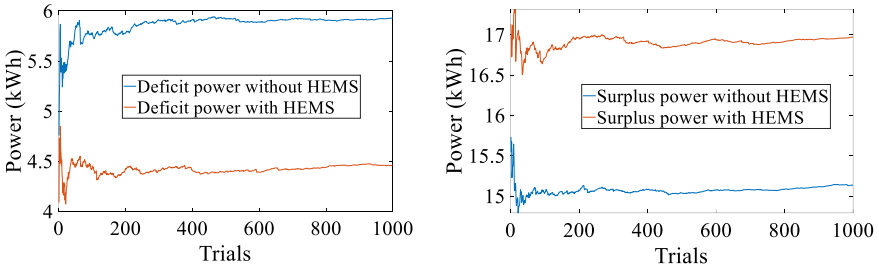

(b) Deficit and surplus power of Household Type 2.

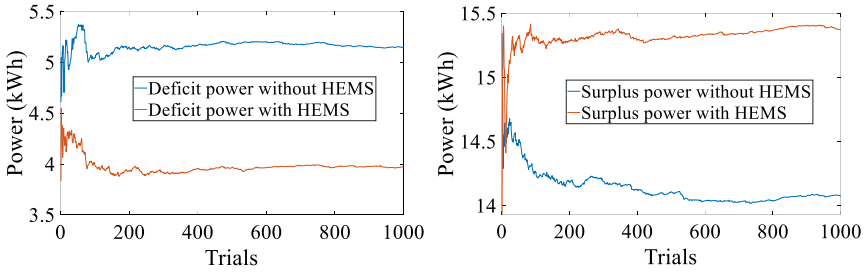

(c) Deficit and surplus power of Household Type 3.

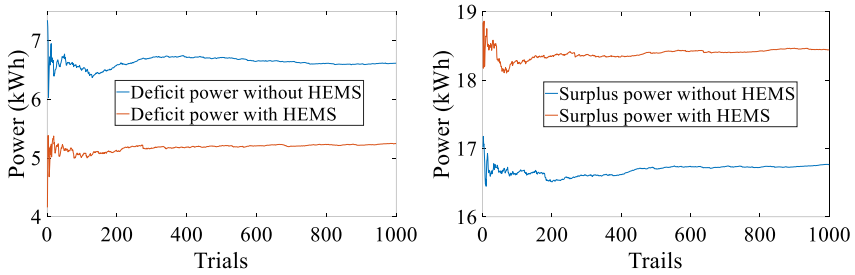

(d) Deficit and surplus power of Household Type 4.

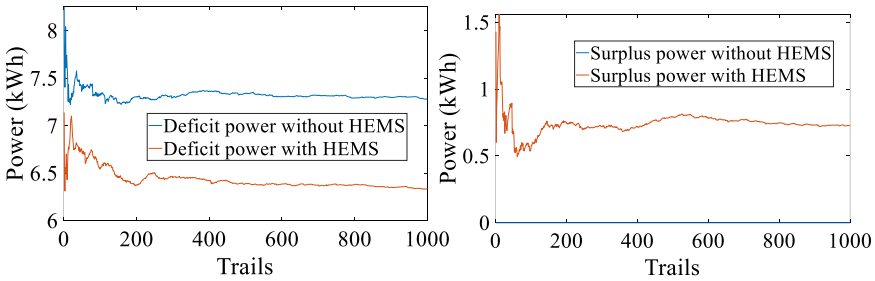

(e) Deficit and surplus power of Household Type 5.

Figure 7-15 Average amount of deficit/surplus for each group of households under 1000 scenarios of MCS.

B. Impacts HEMS on microgrid

In microgrids, self-consumption of energy from renewable sources, such as photovoltaic panels, results in immediate positive impacts such as reduction in energy losses and mitigation of congestion problems in the distribution network. The self-consumption rate (SCR) (the amount of energy locally generated and consumed with respect to the total local generation) is considered as a performance measure to assess a microgrid's ability to consume its own locally generated energy. Consequently, maximizing the self-consumption rate is an implicit goal in most microgrid settings. To this end, the self-consumption of each type of households is evaluated to validate the proposed HEMS.

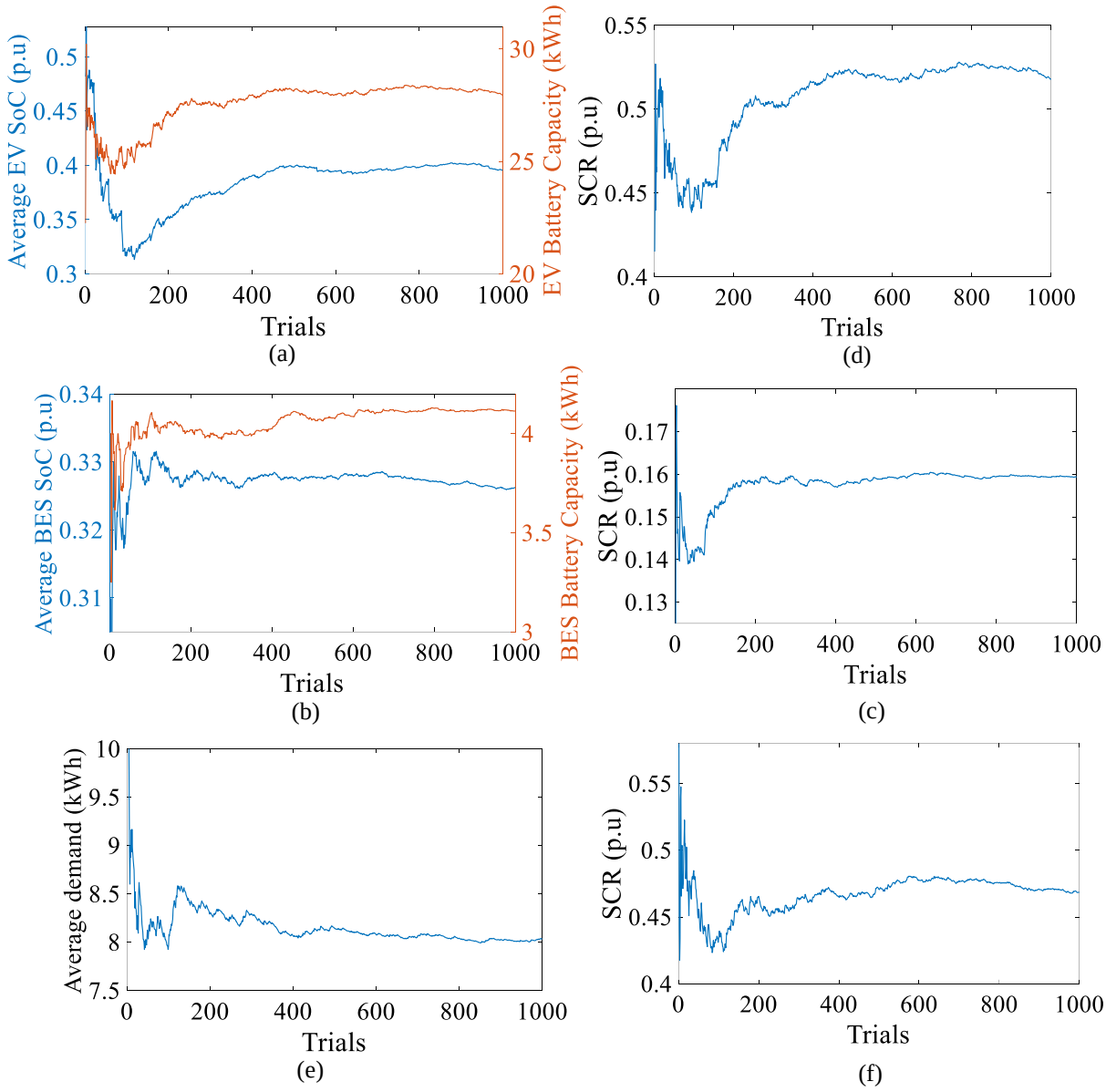

Figure 7-16 Average values of 1000 scenarios of (a) EVs' capacities and SoCs, (b) BESs' capacities and SoCs, (c) household demand, (d) SCR of Type 1, (e) SCR of Type 2, and (f) SCR of Type 3.

As the battery energy storage plays a key role in increasing the self-consumption rate by storing the excess of energy generated by PVs to be used later when needed. For this reason, the impact of different SoCs and capacities of BES and/or EVs on the SCR is analysed for the households of Types 1, Type 2 and Type 3, which have BES and/or EV as shown in Figure 7-16. Figure 7-16 (a) and Figure 7-16 (b) show the average initial SoCs and capacities of the EVs' and BESs' batteries respectively throughout the 1000 scenarios of the MCS. Figure 7-16 (c) shows the average daily load demand of the households in the community (8.01 kWh). As the households that belong to Type 1 have both EV and BES, these households have the highest SCR (52.5 %) as shown in Figure 7-16 (d).

It is noted that how the lower battery capacity of the EVs influenced the SCR in the first 200 iterations. Figure 7-16 (e) shows the SCR of the households belong to Type 2, as this type of households has only BESs with the small average battery capacity (4.2 kWh), the SCR is 15.9%, while the households Type 3 has 47.3% of SCR as shown in Figure 7-16 (f), since these households have only EVs. Therefore, the SCR depends mainly on the capacity of EV and BES batteries and their SoCs. The batteries with higher capacity and lower SoCs consume more energy when they are charged. Therefore, the higher capacity of batteries, the lower are the SoCs, and the higher self-consumption rate is.

7.4.3 Evaluation of the Proposed P2P Price Mechanism

One scenario with the highest possibilities is selected to evaluate dynamic performance of the proposed P2P price mechanism. To decide on the P2P market prices for each time slot, the ESC receives the total deficiency and surplus of energy in real-time from the 100 users as shown in Figure 7-17, and the dynamic electricity prices from the main power grid (RTP and FiT) as shown in Figure 7-18. Based on the total surplus and deficiency power, and the power grid prices, Equations (7.26) and (7.27) are used to determine the values of α and β. Figure 7-19 shows the variation of these parameters over one day period. Consequently, using equations (6.28) and (6.29), the P2P market buying and selling prices are decided as shown in Figure 7-20.

It is obvious that when $\alpha = 1$ (means there is no surplus of energy exported to the P2P market), the ESC purchases energy from the main power grid under the RTP. During [6:00 am-8:00 am], the energy deficiency is higher than the surplus of energy, hence the P2P trading prices are higher than the Mid-Market Rate (MMR) price. However, when the surplus of energy is

higher than energy deficiency during [8:00 am- 16:00 pm], the P2P buying and selling prices are less than the MMR price.

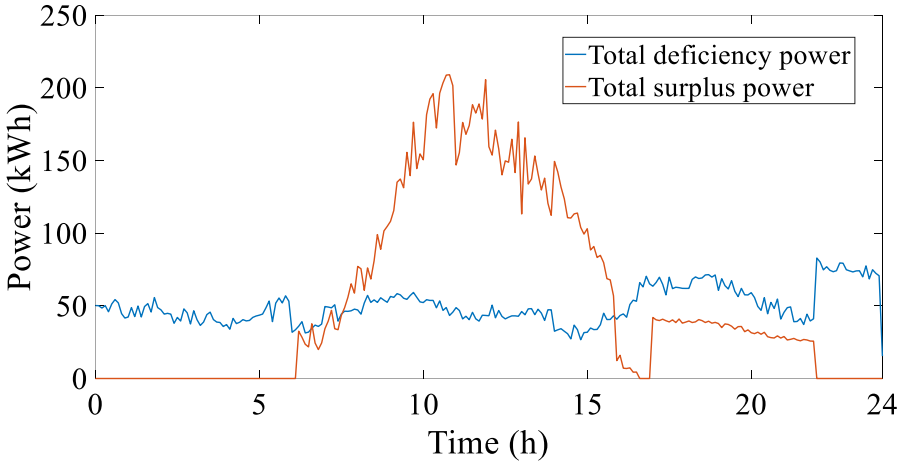

Figure 7-17 Surplus and deficiency power throughout a day.

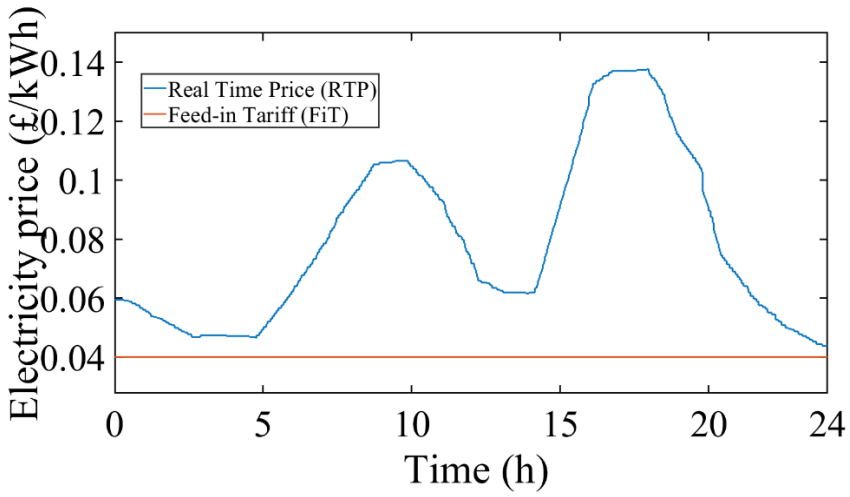

Figure 7-18 Real time price (RTP) and feed-in tariff (FiT).

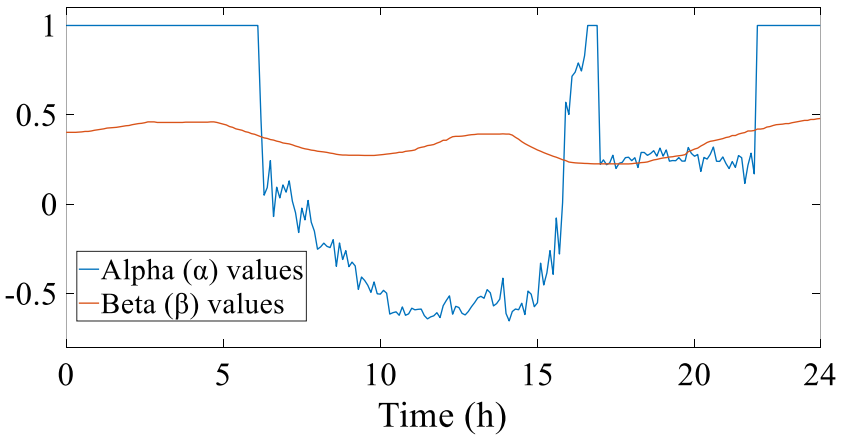

Figure 7-19 Alpha (α) and Beta (β) values.

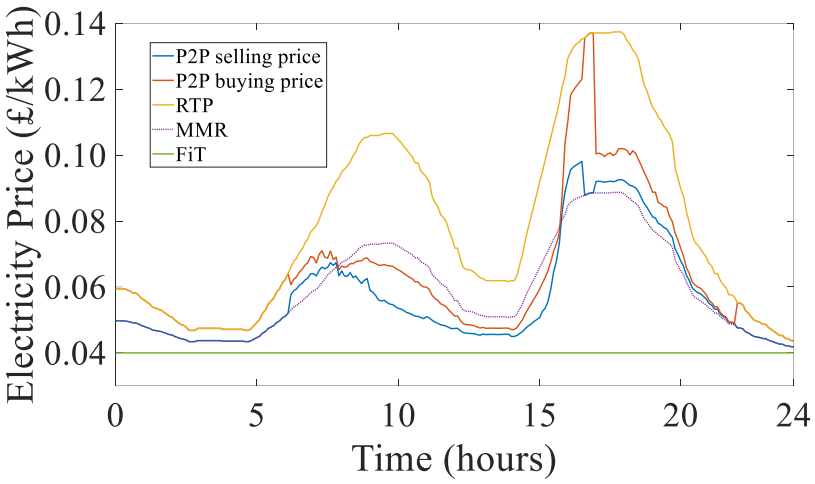

Figure 7-20 Internal P2P prices (buying and selling prices) under the proposed mechanism.

A. Comparison with other P2P models

The performance of the proposed pricing mechanism has been compared with three existing P2P energy sharing mechanisms, namely, the Bill Sharing (BS), Mid-Market Rate and Supply-Demand Ratio (SDR). A detailed description and definition of these three mechanisms is provided in Appendix B. The three pricing mechanisms were simulated and evaluated under 1000 scenarios, and results of the MCS are presented in Figure 6.20 that contains the profits/cost of the six types of households within the community.

From Figure 7-21, it can be observed that the proposed pricing mechanism can fairly guarantee the highest profit/cost for all prosumers/consumers within the community compared to other mechanisms as shown in Figure 7-16 (a)-(f). In terms of the overall performance, the proposed mechanism preformed the best with 42.1% of improvement in the economy index of all participants in the community.

Although the SDR mechanism has a better overall performance (with 37.3% of the overall performance) for all participants than both the BS and MMR mechanisms, it does not address the unfairness issue among participants. The reason behind this is that, using SDR mechanism as discussed in Appendix B.3, the P2P selling and buying prices are set to the FiT price when the total amount of energy surplus exported to the P2P market is higher than the total amount of energy deficiency (SDR>1). This confirms why the energy profits rate for Type 1 and Type 3 households (prosumers) is lower compared to MMR mechanism.

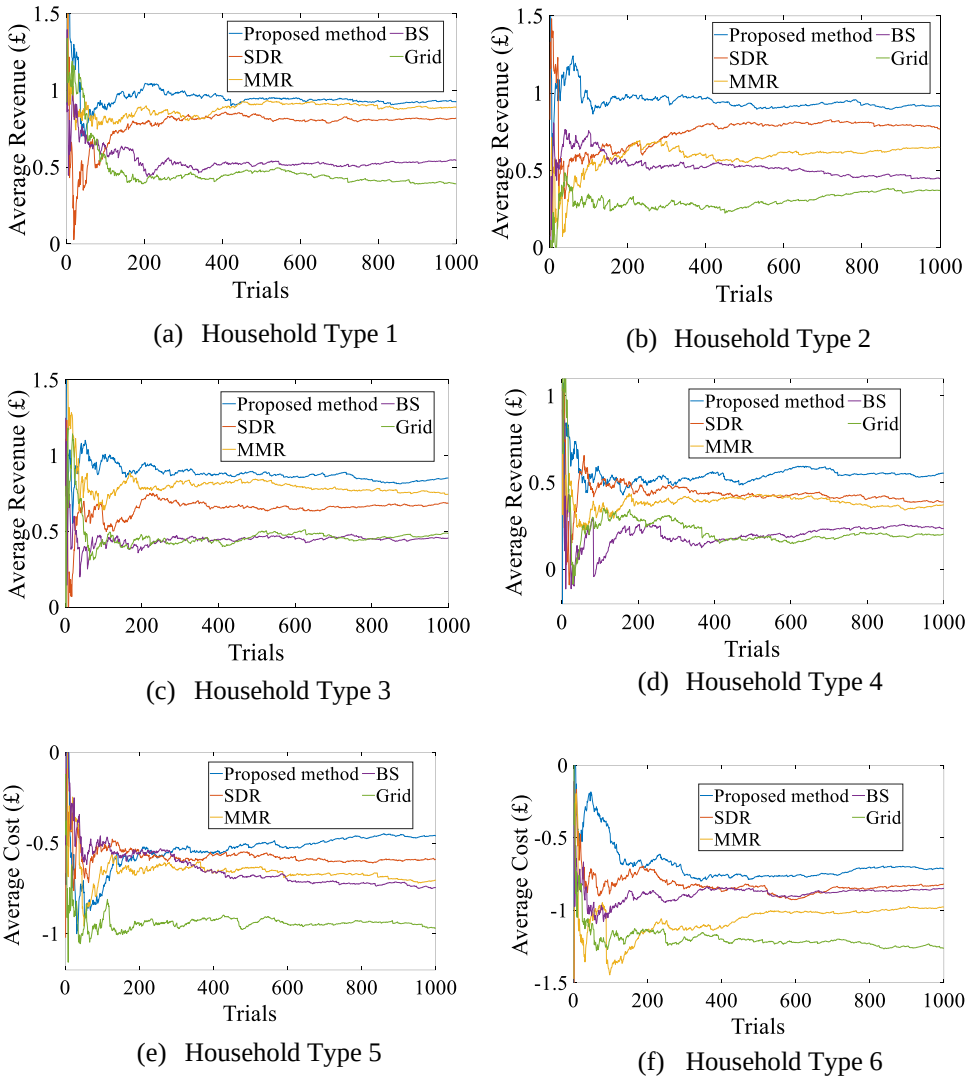

Figure 7-21 Evaluation results of three existing P2P energy sharing models (SDR, MMR and BS) under 1000 scenarios of MCS.

As for the MMR mechanism, the P2P prices are set to the average value of RTP and FiT without considering the amount of energy exported or imported by the participants as discussed in Appendix B.2. When the energy surplus exported to the P2P market is higher than the energy deficiency, the P2P prices under the MMR method are higher than the P2P buying and selling prices under the proposed mechanism and SDR. This conflicts with the basic principle of economics states that the goods price decreases when the production increases and the demand decreases, and vice versa. That is why the cost-saving rate for Type 5 and Type 6 (consumers) is lower under the MMR method compared to both proposed mechanism and SDR as shown in Figure 7-21 (e) and Figure 7-21 (f), respectively. As these households (Type 5 and Type 6) bought a large amount of energy with higher price compared to the buying price of the proposed

mechanism during [8:00 am- 16:00 pm]. However, the overall performance of MMR mechanism is 29.6%.

For the BS mechanism, although its overall performance was more than the conventional paradigm (trading with main grid) with an overall performance of 21.7% for all participants, some of the participants under the BS mechanism received lower income than that under the trading with the grid. The reason was that in the BS mechanism, the cost of electricity for a community is shared among the customers based on individual customer's total energy consumption and export, so that the ones with larger contribution (with high surplus energy) were not remunerated fairly because their energy was sold to the P2P market at a price lower than FiT.

B. Impacts P2P market on microgrid

To investigate how the proposed HEMS and P2P market can smooth the electricity demand of the community, the same scenario (with higher probabilities) as that selected in Section B and C is used.

In this scenario, the amounts of power that need to be purchased by the residential area from the main grid under different cases are shown in Figure 7-22, where CS0 refers to the base case of the total demand of all households within the community, CS1 refers to the total households' demand after implementing HEMS and CS2 refers to the total demand of all households' demand when participating in P2P market.

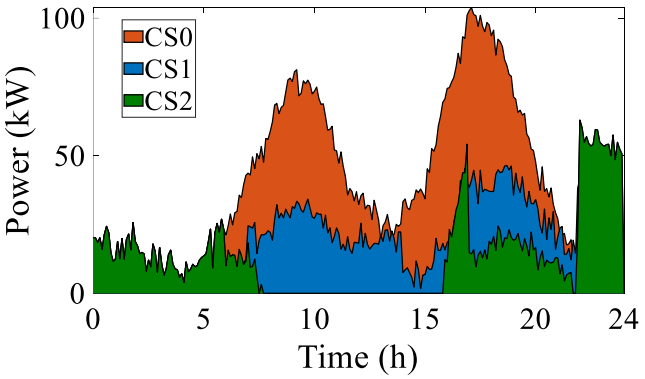

Figure 7-22 Community demand that needs to be purchased from the main grid under different scenarios.

According to Figure 7-22, the whole amount of deficit that needs to be purchased from the main grid under the three cases are the same during the time period [12:00 am-6:30 am]. That is because there is no surplus power traded in the P2P market. During the period [6:30 am – 7:30 am], the deficit of energy that was purchased from the grid under CS1 and CS2 are the same. However, this amount of power is lower than that under CS0. This is because the

households that own batteries started to use them to supply their appliances due to higher electricity prices. Around 7:30 am under CS2, the households that have PVs started to export their surplus of energy to the P2P market. It is noted that the whole community can satisfy its energy demand and there is no need to purchase energy from the main grid during [7:30 am-15:30 pm] as the P2P market covers the whole community demand. In addition, by motivating EV owners to participate in the P2P market during evening peak demand [16:00 pm-22:00 pm], they sell energy by discharging their EVs batteries and generate more revenue.

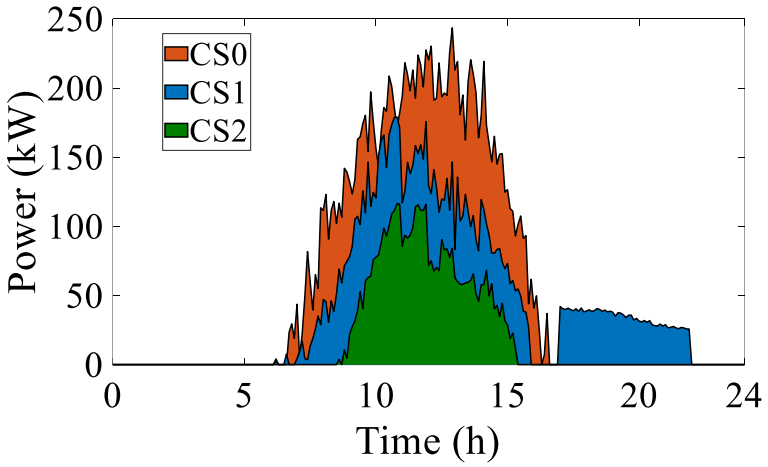

Figure 7-23 Energy exported to the main grid under different scenarios.

On the other hand, the amount of energy surplus exported to the main grid by all households is decreased by 31% as a result of using the proposed HEMS (CS1) in every household as shown in Figure 7-23. The P2P trading (CS2) can contribute to a further reduction of the exported energy (up to 43%) by sharing energy within the community.

Overall, P2P trading enable better energy management by matching local demand and supply. Along with the higher local consumption of renewable energy, P2P electricity trading can help reduce investments related to the generation capacity and transmission infrastructure needed to meet peak demand.

C. Evaluation of P2P mechanism with considering physical network constrains

For the simulation, the 11-bus radial distribution network that proposed in [128] has been analysed and modified. The network consists of the six types of households with the same probabilities as discussed in Section II.A. The distribution of the households within the network is shown in a Figure 7-24. It is assumed that the bus 1 is the slack bus where the ESC is located, who is responsible for preventing any network constraint violation.

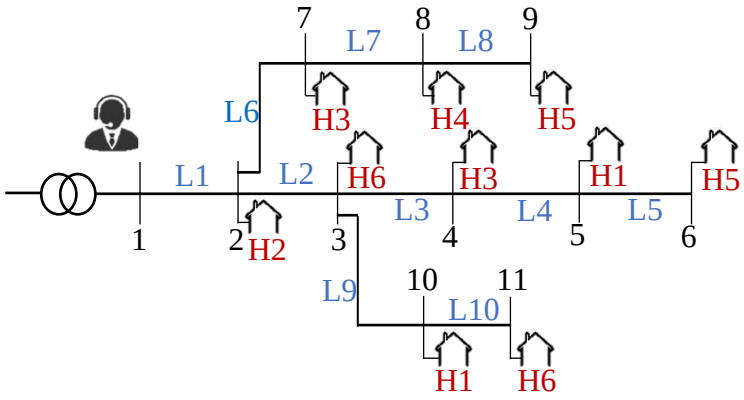

Figure 7-24 11-bus distribution system diagram.

Therefore, to ensure the safe and reliable operation of the distribution network, the proposed P2P energy model considered the bus voltages and line capacity constraints. While the bus voltages do not violate the standard, which is ±5% of 1 per unit (p.u) as specified by the American National Standards Institute [129]. The maximum/minimum power flow of each line in a distribution network refers to the highest/lowest amount of electricity that can be delivered to/consumed at specific bus to maintain network stability and meet the electricity demand of the connected consumers. In this work, we assumed the maximum and minimum line power flows are 10 kW and −10 kW, respectively. The imported power profiles of the consumers are shown in Figure 7-25, while the exported power profiles of the prosumers are shown in Figure 7-26 after implementing HEMS.

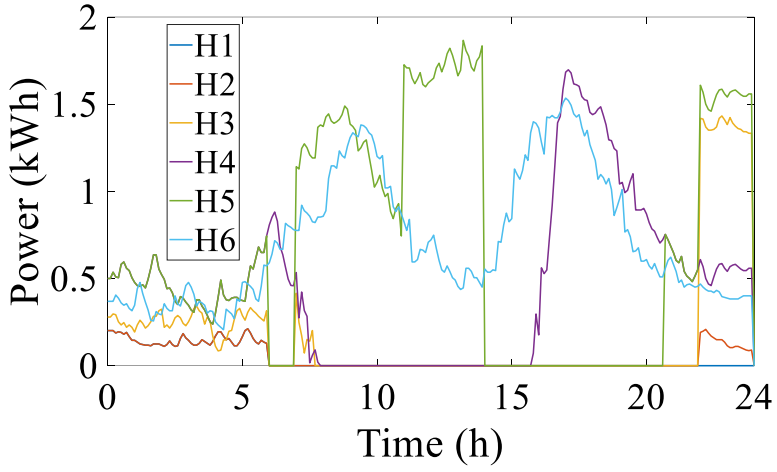

Figure 7-25 Consumers' energy deficiency throughout a day.

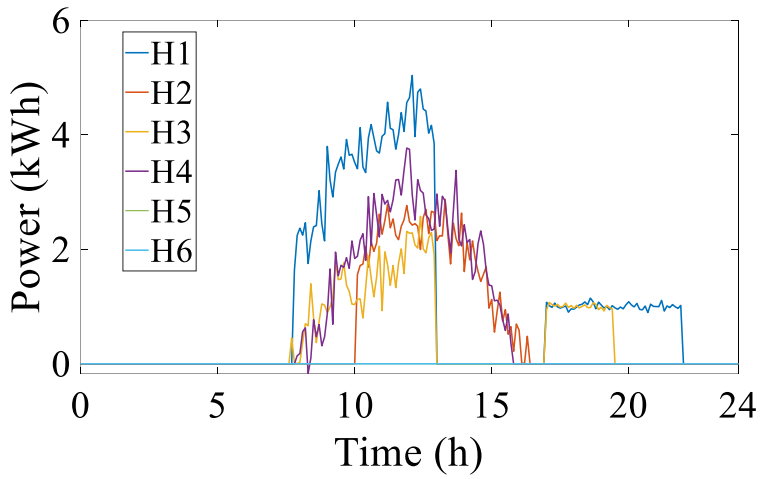

Figure 7-26 Prosumers' energy surplus throughout a day.

It is noted from Figure 7-27 that the voltage in the buses 2,4,5 and 10 violate the maximum voltage limit of 1.05 p.u. while the network constraints were not considered. According to the network constrains in equations 38-40 that applied on the distribution network shown in Figure 7-24, the voltages stay inside the limits of 0.95 p.u. to 1.05 p.u. by decreasing the amount of power injection energy by associated prosumers in different buses as shown in Figure 7-26. It is observed from Figure 7-27 that the line power flow constraints are also satisfied in the proposed P2P energy trading approach, where the power flow between the buses does not exceed the upper limit of the capacity of each line. This may protect the power line from being over-congested in a given system. It should be noted that the violation of these constraints may adversely affect the reliability and stability of a distribution system. In that context, the proposed trading approach will enhance the power system performance in P2P energy sharing.

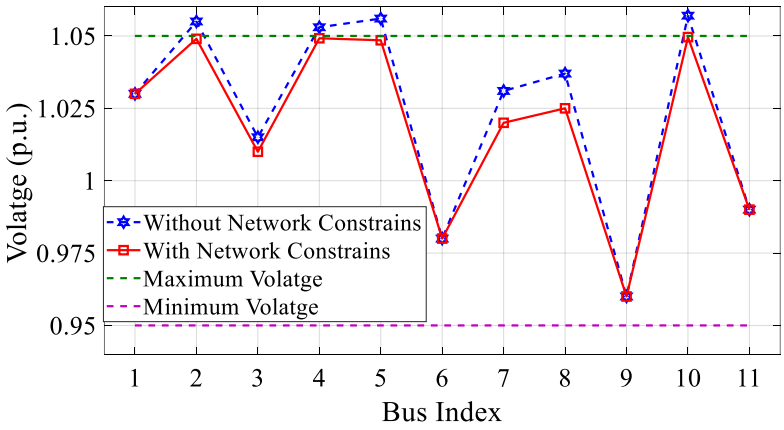

Figure 7-27 Bus voltages with and without considering the distribution network constraints.

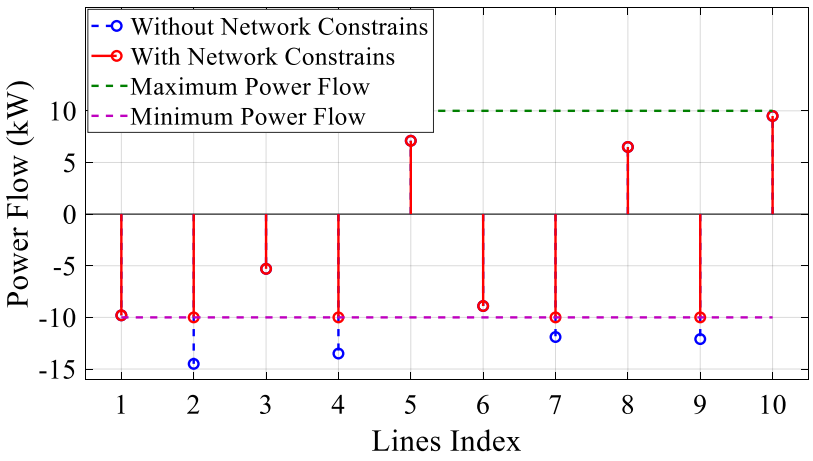

Figure 7-28 Power flow in different lines with and without considering network constraints.

7.5 Conclusion

This chapter proposed a P2P energy sharing model for residential microgrids with stochastic models of different types of households equipped with PV distributed generation, EVs, and BESs to address the uncertainties using 1000 scenarios of the Monte-Carlo simulation. The P2P energy sharing mechanism is designed based on the relationships between energy demand and supply, and Feed-in Tariff (FiT) and Real-Time Price (RTP). Furthermore, HEMS is also designed to manage the energy produced and consumed within a household. The proposed model is simulated and evaluated on a local community of 100 households subject to constraints associated with household load profile, PV, EVs, BESs and market signals including FiT and retail prices. The simulation results show that the proposed HEMS can effectively manage the energy flow within each type of household and simultaneously enable EVs to participate in P2P market. The proposed HEMS can also increase the self-consumption rate within the community which depends mainly on the batteries capacity and their SoCs. The results show that the effective performance of the proposed P2P pricing mechanism in achieving cost saving/income for consumers/prosumers with considering that not a single household would be worse off. This leads to motivates peers to participate in P2P energy trading. To validate the performance of the proposed pricing mechanism, it is evaluated by comparing to three popular P2P sharing mechanisms; the supply and demand ratio (SDR), mid-market rate (MMR) and bill sharing (BS). The simulation results verify the effectiveness the proposed mechanism in terms the economic revenue and ensure the fairness among all peers considering the physical network constrains.

Chapter 8 Conclusions and Future Work

This dissertation contributes to the development of new Demand Response (DR) management strategies based on machine learning techniques such as Reinforcement Learning (RL) and Deep Reinforcement Learning (DRL) combined with Fuzzy Logic (FL) and Neural Network (NN) in the smart grid.

8.1 Main findings and contributions

In this thesis, DR management and control strategies for smart grids have been investigated from the three following aspects:

Firstly, to motivate consumers to participate in DR programs, the two conflicting objectives of HEMS (minimising the electricity bills and maximising the user's satisfaction) for consumers are addressed in Chapter 4. Firstly, we proposed an effective DR algorithm to be utilised in smart homes to schedule household appliances in response to electricity prices. The design was of the DR approach was based on Q-learning method due to its ability to deal with dynamic electricity prices and different household power consumption patterns. More specifically, Q-learning was employed to make optimal decisions to schedule the operation of household appliances by shifting controllable appliances from peak periods, when the electricity prices are high to off-peak hours when the electricity prices are lower. A human comfort-oriented control approach for HEMS has also been designed to increase the user's satisfaction as much as possible while responding to DR schemes. Four comfort factors were used namely, the priority of the appliance to be shifted, the power rate of the appliances, the operating time interval, and the waiting time. The simulation results presented in Chapter 4 showed that the proposed algorithm leads to minimising energy consumption, reducing household electricity bills, and maximising the user's satisfaction.

Secondly, Chapters 5 and 6 focused on investigating the benefits of EVs for promoting the implementation of DR programs in the residential sector and performing ancillary services for the power system such as frequency regulation. As a new type of household appliance, EVs can provide opportunities as an energy storage unit, where the consumers can charge their EVs during low-price periods and sell back the energy to the power grid during high-price periods using Vehicle-to-Grid (V2G) technology or supply the household loads using Vehicle-to-Home

(V2H) technology. In Chapter 4, an effective DR approach for V2G and V2H energy management using Reinforcement Learning (RL) is presented. The RL strategy based on a reward mechanism is used to make optimal decisions to charge or delay the charging of the EV battery pack and/or dispatch the stored electricity back to the grid without compromising the driving needs. The results presented demonstrate how the proposed DR strategy can effectively manage the charging/discharging schedule of the EV battery and how V2H and V2G can contribute to smooth the household load profile, minimise electricity bills and maximise revenue. In Chapter 6, we focused on the participation of EVs in the grid frequency response due to the ability of their batteries to provide bidirectional power flow and faster response. An optimal V2G control strategy is designed to allow EVs to be utilised in Supplementary Frequency Regulation (SFR). DRL is used for adjusting in real-time the scheduled charging power of the EV to satisfy the charging demand of the battery at plug-out time while performing frequency regulation. A Deep Deterministic Policy Gradient (DDPG) agent was used to automatically provide very fast decisions without a need for extensive calculations which has significantly reduced the computational cost. The advantages of using the DDPG agent has significantly improved the SFR of EVs without compromising the preferences of EVs' owners. The proposed strategy has been tested on a two-area interconnected power system. The results showed that the proposed V2G strategy provides an improvement in the quality of the frequency regulation while satisfying the charging demands of EVs compared to other strategies existing in the literature.

Thirdly, for further minimisation in the electricity cost of the residents, P2P energy sharing enables prosumers within a community to directly trade their available excess energy among each other. A P2P energy-sharing mechanism has been developed in Chapter 7 for a residential microgrid with price-based DR. The proposed P2P model was tested on a residential neighbourhood of 100 households subject to constraints associated with household load profile, PV, EVs, BESs and market signals including FiT and retail prices. The proposed P2P pricing mechanism achieved a cost saving/income for consumers/prosumers considering that not a single household would be worse off. The P2P model was compared against three popular P2P sharing mechanisms including the Supply and Demand Ratio (SDR), Mid-Market Rate (MMR) and Bill Sharing (BS) and has demonstrated superior performance.

8.2 Limitations of the work

The implementation of DR programs with their application such as HEMS and P2P energy trading, in the residential areas faces a set of complex challenges that need to be addressed.

The key consideration is the initial cost associated with installing HEMS and establishing P2P trading platforms. The financial burden of purchasing and installing smart devices, meters, and the required software can act as a constraint for homeowners and small-scale energy producers.

Consumer awareness and understanding also play a significant role in the successful implementation of these technologies. Without a clear understanding of the benefits and functioning of DR programs, consumers may be unwilling to participate in these programs. Overcoming this knowledge gap is crucial to encourage wider adoption.

Finally, data privacy and security are critical considerations when implementing P2P energy trading. The collection and sharing of sensitive energy consumption data raise concerns about privacy and cybersecurity. Establishing robust measures to protect data and ensure secure transactions is crucial for building trust among consumers and prosumers.

8.3 Future works

Although our research fulfils the aims of developing efficient strategies to DR management for the smart grid using machine learning techniques, there is still scope for further research and developments.

- In Chapter 4, the Q-learning algorithm was used to provide discrete actions for scheduling the typical household appliances. However, this method is not applicable to other appliances that need to be controlled in real-time such as heaters and ACs. As the Q-learning algorithm deals with discrete actions, and the DDPG algorithm handles continuous actions. As a future work, this study can be extended to proposing a Mixed Deep Reinforcement Learning, which integrates the Q-learning algorithm and deep deterministic policy gradient (DDPG) algorithm to provide discrete-continuous hybrid action space.
- In Chapter 5, we have presented a DR strategy for charging/discharging energy management of Electrical Vehicles (EVs) equipped with bidirectional V2G and V2H technologies. The proposed method is implemented under the assumption that the EVs are connected only to the owners' houses. However, the EV could be connected to the grid at any other location such as the destination of the trip or others' houses. As future

work, the proposed approach can be expanded and assessed while considering the mobility of the EV. Investigation of the impacts of our proposed framework considering the movement of the EV in the expanded large-scale model is remained on a future work. Regarding the EV driving schedule, it was assumed that the EV owner added the driving schedule to the HEMS. However, it is more convenient if the HEMS automatically forecasts the driving schedule to be readily used by the EV owner. The HEMS should conduct this operation considering the impact on the forecast error which can be investigated as the future work.

- Chapter 7 presents a dynamic P2P energy market model for a community microgrid. In this work, we considered the physical network constraints such as power capacity and overvoltage by evaluating our model on a small microgrid (11-bus network). As a future work, the proposed energy trading model can be tested on a larger distribution network to investigate the impact of the power flows on the physical constraints of the network.

References

[1] H. T. Haider, O. H. See, and W. Elmenreich, "A review of residential demand response of smart grid," *Renewable and Sustainable Energy Reviews*, vol. 59, pp. 166–178, 2016.

[2] "Annual electricity demand in the United Kingdom (UK) from 2000 to 2021," *Statista Research Department, Dec 7, 2020*, 2022. https://www.statista.com/statistics/323381/total-demand-for-electricity-in-the-united-kingdom-uk/ (accessed May 12, 2023).

[3] Bruna Alves, "Electricity Demand,2020 ," *Statista Research Department*. https://www.statista.com/statistics/280704/world-power-consumption/ (accessed Jan. 11, 2023).

[4] "Global electricity demand," *Our World in Data*, 2022. https://ourworldindata.org/grapher/primary-energy-cons (accessed Jan. 14, 2023).

[5] "Electricity generation from fossil fuels," *Our World in Data*, 2022. https://ourworldindata.org/grapher/electricity-fossil-fuels?tab=chart (accessed Jan. 14, 2023).

[6] "Annual CO2 emissions," *Our World in Data*, 2022. https://ourworldindata.org/co2-emissions#annual-co2-emissions (accessed Feb. 14, 2023).

[7] "Electricity Market Report," *iea*. https://www.iea.org/news/surging-electricity-demand-is-putting-power-systems-under-strain-around-the-world (accessed Jan. 15, 2023).

[8] S. Panda *et al.*, "Residential Demand Side Management model, optimization and future perspective: A review," *Energy Reports*, vol. 8, pp. 3727–3766, 2022.

[9] M. A. Judge, A. Khan, A. Manzoor, and H. A. Khattak, "Overview of smart grid implementation: Frameworks, impact, performance and challenges," *J Energy Storage*, vol. 49, p. 104056, 2022.

[10] O. F. Darteh, Q. Liu, X. Liu, I. Bah, F. M. Nakoty, and A. Acakpovi, "Emerging Simulation Frameworks for Analyzing Smart Grid Cyberattack: A Literature Review," in *2022 IEEE Intl Conf on Dependable, Autonomic and Secure Computing, Intl Conf on Pervasive Intelligence and Computing, Intl Conf on Cloud and Big Data Computing, Intl Conf on Cyber Science and Technology Congress (DASC/PiCom/CBDCom/CyberSciTech)*, IEEE, 2022, pp. 1–7.

[11] Department of Energy & Climate Change, "Smart Grid Vision and Routemap," London, Feb. 2014. Accessed: Jan. 20, 2023. [Online]. Available: https://assets.publishing.service.gov.uk/government/uploads/system/uploads/attachment_data/file/285417/Smart_Grid_Vision_and_RoutemapFINAL.pdf

[12] "Statista Research Department," *Energy & Environment*, 2022. https://www.statista.com/statistics/246154/global-smart-grid-market-size-by-region/?locale=en (accessed Jan. 27, 2023).

[13] F. Sissine, "Energy Independence and Security Act of 2007: a summary of major provisions," Library of Congress Washington DC Congressional Research Service, 2007. Accessed: Jan. 28, 2023. [Online]. Available: https://www1.eere.energy.gov/manufacturing/tech_assistance/pdfs/crs_report_energy_act_2007.pdf

[14] J. Alabid, A. Bennadji, and M. Seddiki, "A review on the energy retrofit policies and improvements of the UK existing buildings, challenges and benefits," *Renewable and sustainable energy reviews*, vol. 159, p. 112161, 2022.

[15] "Smart grids and meters," *European Comission*, 2022. https://energy.ec.europa.eu/topics/markets-and-consumers/smart-grids-and-meters_en (accessed Feb. 02, 2023).

[16] N. H. Riedel and M. Špaček, "Challenges of renewable energy sourcing in the process industries: the example of the German chemical industry," *Sustainability*, vol. 14, no. 20, p. 13520, 2022.

[17] N. Khan *et al.*, "Energy Management Systems Using Smart Grids: An Exhaustive Parametric Comprehensive Analysis of Existing Trends, Significance, Opportunities, and Challenges," *International Transactions on Electrical Energy Systems*, vol. 2022, 2022.

[18] M. Shakeri *et al.*, "An intelligent system architecture in home energy management systems (HEMS) for efficient demand response in smart grid," *Energy Build*, vol. 138, pp. 154–164, 2017.

[19] P. Stoll, N. Brandt, and L. Nordström, "Including dynamic CO2 intensity with demand response," *Energy Policy*, vol. 65, pp. 490–500, 2014.

[20] M. Beaudin and H. Zareipour, "Home energy management systems: A review of modelling and complexity," *Renewable and sustainable energy reviews*, vol. 45, pp. 318–335, 2015.

[21] C. Silva, P. Faria, Z. Vale, and J. M. Corchado, "Demand response performance and uncertainty: A systematic literature review," *Energy Strategy Reviews*, vol. 41, p. 100857, 2022.

[22] H. T. Haider, O. H. See, and W. Elmenreich, "A review of residential demand response of smart grid," *Renewable and Sustainable Energy Reviews*, vol. 59, pp. 166–178, 2016.

[23] K. Tamashiro *et al.*, "Investigation of Home Energy Management with Advanced Direct Load Control and Optimal Scheduling of Controllable Loads," *Energies (Basel)*, vol. 14, no. 21, p. 7314, 2021.

[24] M. T. Ahmed, P. Faria, O. Abrishambaf, and Z. Vale, "Electric water heater modelling for direct load control demand response," in *2018 IEEE 16th International Conference on Industrial Informatics (INDIN)*, IEEE, 2018, pp. 490–495.

[25] K. Phetsuwan and W. Pora, "A Direct Load Control Algorithm for Air Conditioners Concerning Customers' Comfort," in *2018 IEEE International Conference on Consumer Electronics-Asia (ICCE-Asia)*, IEEE, 2018, pp. 206–212.

[26] M. H. Imani, K. Yousefpour, M. T. Andani, and M. J. Ghadi, "Effect of changes in incentives and penalties on interruptible/curtailable demand response program in microgrid operation," in *2019 IEEE Texas power and energy conference (TPEC)*, IEEE, 2019, pp. 1–6.

[27] J. Aghaei, M.-I. Alizadeh, P. Siano, and A. Heidari, "Contribution of emergency demand response programs in power system reliability," *Energy*, vol. 103, pp. 688–696, 2016.

[28] N. G. Paterakis, O. Erdinç, and J. P. S. Catalão, "An overview of Demand Response: Key-elements and international experience," *Renewable and Sustainable Energy Reviews*, vol. 69, pp. 871–891, 2017.

[29] L. Zhao, Z. Yang, and W.-J. Lee, "The impact of time-of-use (TOU) rate structure on consumption patterns of the residential customers," *IEEE Trans Ind Appl*, vol. 53, no. 6, pp. 5130–5138, 2017.

[30] N. A. M. Azman, M. P. Abdullah, M. Y. Hassan, D. M. Said, and F. Hussin, "Enhanced time of use electricity pricing for industrial customers in Malaysia," *Indonesian Journal of Electrical Engineering and Computer Science*, vol. 6, no. 1, pp. 155–160, 2017.

[31] X. Yan, Y. Ozturk, Z. Hu, and Y. Song, "A review on price-driven residential demand response," *Renewable and Sustainable Energy Reviews*, vol. 96, pp. 411–419, 2018.

[32] M. Kerai, "Smart Meter Statistics in Great Britain: Quarterly Report to end December 2019. Official Statistics, Department for Business, Energy & Industrial Strategy (2020)." 2022.

[33] M. Shokry, A. I. Awad, M. K. Abd-Ellah, and A. A. M. Khalaf, "Systematic survey of advanced metering infrastructure security: Vulnerabilities, attacks, countermeasures, and future vision," *Future Generation Computer Systems*, vol. 136, pp. 358–377, 2022.

[34] D. Sloot, N. Lehmann, and A. Ardone, "Explaining and promoting participation in demand response programs: The role of rational and moral motivations among German energy consumers," *Energy Res Soc Sci*, vol. 84, p. 102431, 2022.

[35] L. Rubinger, A. Gazendam, S. Ekhtiari, and M. Bhandari, "Machine learning and artificial intelligence in research and healthcare☆,☆☆," *Injury*, 2022.

[36] H. Ghoddusi, G. G. Creamer, and N. Rafizadeh, "Machine learning in energy economics and finance: A review," *Energy Econ*, vol. 81, pp. 709–727, 2019.

[37] L. S. Iyer, "AI enabled applications towards intelligent transportation," *Transportation Engineering*, vol. 5, p. 100083, 2021.

[38] R. Rai, M. K. Tiwari, D. Ivanov, and A. Dolgui, "Machine learning in manufacturing and industry 4.0 applications," *International Journal of Production Research*, vol. 59, no. 16. Taylor & Francis, pp. 4773–4778, 2021.

[39] K. Arulkumaran, M. P. Deisenroth, M. Brundage, and A. A. Bharath, "Deep reinforcement learning: A brief survey," *IEEE Signal Process Mag*, vol. 34, no. 6, pp. 26–38, 2017.

[40] H. Shareef, M. S. Ahmed, A. Mohamed, and E. Al Hassan, "Review on home energy management system considering demand responses, smart technologies, and intelligent controllers," *Ieee Access*, vol. 6, pp. 24498–24509, 2018.

[41] B. Zhou *et al.*, "Smart home energy management systems: Concept, configurations, and scheduling strategies," *Renewable and Sustainable Energy Reviews*, vol. 61, pp. 30–40, 2016.

[42] G. Huang, J. Yang, and C. Wei, "Cost-Effective and comfort-aware electricity scheduling for home energy management system," in *2016 IEEE International Conferences on Big Data and Cloud Computing (BDCloud), Social Computing and Networking (SocialCom), Sustainable Computing and Communications (SustainCom)(BDCloud-SocialCom-SustainCom)*, IEEE, 2016, pp. 453–460.

[43] S. Rajalingam and V. Malathi, "HEM algorithm based smart controller for home power management system," *Energy Build*, vol. 131, pp. 184–192, 2016.

[44] M. S. Ahmed, A. Mohamed, R. Z. Homod, and H. Shareef, "A home energy management algorithm in demand response events for household peak load reduction," *PrzeglAd Elektrotechniczny*, vol. 93, no. 3, p. 2017, 2017.

[45] A. Ahmad *et al.*, "An optimized home energy management system with integrated renewable energy and storage resources," *Energies (Basel)*, vol. 10, no. 4, p. 549, 2017.

[46] K. Ma, T. Yao, J. Yang, and X. Guan, "Residential power scheduling for demand response in smart grid," *International Journal of Electrical Power & Energy Systems*, vol. 78, pp. 320–325, 2016.

[47] P. Samadi, V. W. S. Wong, and R. Schober, "Load scheduling and power trading in systems with high penetration of renewable energy resources," *IEEE Trans Smart Grid*, vol. 7, no. 4, pp. 1802–1812, 2015.

[48] R. Lu, S. H. Hong, and M. Yu, "Demand response for home energy management using reinforcement learning and artificial neural network," *IEEE Trans Smart Grid*, vol. 10, no. 6, pp. 6629–6639, 2019.

[49] C. Zhang, S. R. Kuppannagari, C. Xiong, R. Kannan, and V. K. Prasanna, "A cooperative multi-agent deep reinforcement learning framework for real-time residential load scheduling," in *Proceedings of the International Conference on Internet of Things Design and Implementation*, 2019, pp. 59–69.

[50] S. Lee and D.-H. Choi, "Reinforcement learning-based energy management of smart home with rooftop solar photovoltaic system, energy storage system, and home appliances," *Sensors*, vol. 19, no. 18, p. 3937, 2019.

[51] J. R. Vázquez-Canteli and Z. Nagy, "Reinforcement learning for demand response: A review of algorithms and modeling techniques," *Appl Energy*, vol. 235, pp. 1072–1089, 2019.

[52] N. Chauhan, N. Choudhary, and K. George, "A comparison of reinforcement learning based approaches to appliance scheduling," in *2016 2nd International Conference on Contemporary Computing and Informatics (IC3I)*, IEEE, 2016, pp. 253–258.

[53] S. Kim and H. Lim, "Reinforcement learning based energy management algorithm for smart energy buildings," *Energies (Basel)*, vol. 11, no. 8, p. 2010, 2018.

[54] A. Faustine, N. H. Mvungi, S. Kaijage, and K. Michael, "A survey on non-intrusive load monitoring methodies and techniques for energy disaggregation problem," *arXiv preprint arXiv:1703.00785*, 2017.

[55] R. Lu, S. H. Hong, and X. Zhang, "A dynamic pricing demand response algorithm for smart grid: Reinforcement learning approach," *Appl Energy*, vol. 220, pp. 220–230, 2018.

[56] U. Datta, N. Saiprasad, A. Kalam, J. Shi, and A. Zayegh, "A price-regulated electric vehicle charge-discharge strategy for G2V, V2H, and V2G," *Int J Energy Res*, vol. 43, no. 2, pp. 1032–1042, 2019.

[57] A. Dik, S. Omer, and R. Boukhanouf, "Electric Vehicles: V2G for Rapid, Safe, and Green EV Penetration," *Energies (Basel)*, vol. 15, no. 3, p. 803, 2022.

[58] E. Vega-Fuentes and M. Denai, "Enhanced electric vehicle integration in the UK low-voltage networks with distributed phase shifting control," *IEEE Access*, vol. 7, pp. 46796–46807, 2019.

[59] U. Datta, A. Kalam, and J. Shi, "Electric vehicle (EV) in home energy management to reduce daily electricity costs of residential customer," 2018.

[60] Y.-W. Chen and J. M. Chang, "Fair demand response with electric vehicles for the cloud based energy management service," *IEEE Trans Smart Grid*, vol. 9, no. 1, pp. 458–468, 2016.

[61] Y. Li and K. Li, “Incorporating demand response of electric vehicles in scheduling of isolated microgrids with renewables using a bi-level programming approach,” *IEEE Access*, vol. 7, pp. 116256–116266, 2019.

[62] T. U. Solanke, V. K. Ramachandaramurthy, J. Y. Yong, J. Pasupuleti, P. Kasinathan, and A. Rajagopalan, “A review of strategic charging–discharging control of grid-connected electric vehicles,” *J Energy Storage*, vol. 28, p. 101193, 2020.

[63] P. Akhade, M. Moghaddami, A. Moghadasi, and A. Sarwat, “A Review on control strategies for integration of electric vehicles with power systems,” in *2018 IEEE/PES Transmission and Distribution Conference and Exposition (T&D)*, IEEE, 2018, pp. 1–5.

[64] K. Wang *et al.*, “Distributed energy management for vehicle-to-grid networks,” *IEEE Netw*, vol. 31, no. 2, pp. 22–28, 2017.

[65] P. Lazzeroni, S. Olivero, M. Repetto, F. Stirano, and M. Vallet, “Optimal battery management for vehicle-to-home and vehicle-to-grid operations in a residential case study,” *Energy*, vol. 175, pp. 704–721, 2019.

[66] S. Umetani, Y. Fukushima, and H. Morita, “A linear programming based heuristic algorithm for charge and discharge scheduling of electric vehicles in a building energy management system,” *Omega (Westport)*, vol. 67, pp. 115–122, 2017.

[67] A. Chiş, J. Lundén, and V. Koivunen, “Reinforcement learning-based plug-in electric vehicle charging with forecasted price,” *IEEE Trans Veh Technol*, vol. 66, no. 5, pp. 3674–3684, 2016.

[68] S. Najafi, M. Shafie-khah, P. Siano, W. Wei, and J. P. S. Catalão, “Reinforcement learning method for plug-in electric vehicle bidding,” *IET Smart Grid*, vol. 2, no. 4, pp. 529–536, 2019.

[69] Z. Wan, H. Li, H. He, and D. Prokhorov, “Model-free real-time EV charging scheduling based on deep reinforcement learning,” *IEEE Trans Smart Grid*, vol. 10, no. 5, pp. 5246–5257, 2018.

[70] K. Sayed and H. A. Gabbar, “Electric vehicle to power grid integration using three-phase three-level AC/DC converter and PI-fuzzy controller,” *Energies (Basel)*, vol. 9, no. 7, p. 532, 2016.

[71] S. Habib, M. Kamran, and U. Rashid, “Impact analysis of vehicle-to-grid technology and charging strategies of electric vehicles on distribution networks–a review,” *J Power Sources*, vol. 277, pp. 205–214, 2015.

[72] J. Waldron, L. Rodrigues, M. Gillott, S. Naylor, and R. Shipman, “The Role of Electric Vehicle Charging Technologies in the Decarbonisation of the Energy Grid,” *Energies (Basel)*, vol. 15, no. 7, p. 2447, 2022.

[73] S. Deb, E. A. Al Ammar, H. AlRajhi, I. Alsaidan, and S. M. Shariff, “V2G Pilot Projects: Review and Lessons Learnt,” *Developing Charging Infrastructure and Technologies for Electric Vehicles*, pp. 252–267, 2022.

[74] H. Li, X. Dai, R. Kotter, N. Aslam, and Y. Cao, “A simulation environment of solar-wind powered electric vehicle car park for reinforcement learning and optimization,” in *International Symposium on New Energy and Electrical Technology*, Springer, 2022, pp. 979–991.

[75] Jeremy Barnes, “Mitsubishi Motors Makes World Premiere of the ENGELBERG TOURER,” *Bussinesswire*, 2019. https://www.mitsubishi-motors.com/en/innovation/motorshow/2019/gms2019/dendo/ (accessed Aug. 12, 2023).

[76] Schmidt, “Nissan sees Leaf as home energy source, says Tesla big battery ‘waste of resources,’” *The Driven*, 2019. https://thedriven.io/2019/07/11/nissan-sees-leaf-as-home-energy-source-says-tesla-big-battery-waste-of-resources/ (accessed Aug. 15, 2023).

[77] J. Shair, H. Li, J. Hu, and X. Xie, “Power system stability issues, classifications and research prospects in the context of high-penetration of renewables and power electronics,” *Renewable and Sustainable Energy Reviews*, vol. 145, p. 111111, 2021.

[78] A. Fernández-Guillamón, E. Gómez-Lázaro, E. Muljadi, and Á. Molina-García, “Power systems with high renewable energy sources: A review of inertia and frequency control strategies over time,” *Renewable and Sustainable Energy Reviews*, vol. 115, p. 109369, 2019.

[79] J. Tan and Y. Zhang, “Coordinated control strategy of a battery energy storage system to support a wind power plant providing multi-timescale frequency ancillary services,” *IEEE Trans Sustain Energy*, vol. 8, no. 3, pp. 1140–1153, 2017.

[80] J. Li, R. Xiong, Q. Yang, F. Liang, M. Zhang, and W. Yuan, “Design/test of a hybrid energy storage system for primary frequency control using a dynamic droop method in an isolated microgrid power system,” *Appl Energy*, vol. 201, pp. 257–269, 2017.

[81] J. Meng, Y. Mu, H. Jia, J. Wu, X. Yu, and B. Qu, “Dynamic frequency response from electric vehicles considering travelling behavior in the Great Britain power system,” *Appl Energy*, vol. 162, pp. 966–979, 2016.

[82] K. M. Tan, V. K. Ramachandaramurthy, and J. Y. Yong, “Integration of electric vehicles in smart grid: A review on vehicle to grid technologies and optimization techniques,” *Renewable and Sustainable Energy Reviews*, vol. 53, pp. 720–732, 2016.

[83] S. Habib, M. Kamran, and U. Rashid, “Impact analysis of vehicle-to-grid technology and charging strategies of electric vehicles on distribution networks–a review,” *J Power Sources*, vol. 277, pp. 205–214, 2015.

[84] K. Davies, I. S. Bayram, and S. Galloway, “Challenges and Opportunities for Car Retail Business in Electric Vehicle Charging Ecosystem,” in *2022 3rd International Conference on Smart Grid and Renewable Energy (SGRE)*, IEEE, 2022, pp. 1–6.

[85] S. S. Rangarajan *et al.*, “Lithium-ion batteries—The crux of electric vehicles with opportunities and challenges,” *Clean Technologies*, vol. 4, no. 4, pp. 908–930, 2022.

[86] P. M. R. Almeida, F. J. Soares, and J. A. P. Lopes, “Electric vehicles contribution for frequency control with inertial emulation,” *Electric Power Systems Research*, vol. 127, pp. 141–150, 2015.

[87] M.-H. Khooban, “Secondary load frequency control of time-delay stand-alone microgrids with electric vehicles,” *IEEE Transactions on Industrial Electronics*, vol. 65, no. 9, pp. 7416–7422, 2017.

[88] A. Khalil, Z. Rajab, A. Alfergani, and O. Mohamed, “The impact of the time delay on the load frequency control system in microgrid with plug-in-electric vehicles,” *Sustain Cities Soc*, vol. 35, pp. 365–377, 2017.

[89] V. Vita and P. Koumides, “Electric vehicles and distribution networks: Analysis on vehicle to grid and renewable energy sources integration,” in *2019 11th Electrical Engineering Faculty Conference (BulEF)*, IEEE, 2019, pp. 1–4.

[90] H. Liu, K. Huang, Y. Yang, H. Wei, and S. Ma, “Real-time vehicle-to-grid control for frequency regulation with high frequency regulating signal,” *Protection and Control of Modern Power Systems*, vol. 3, no. 1, pp. 1–8, 2018.

[91] M. Wang, Y. Mu, H. Jia, J. Wu, X. Yu, and Y. Qi, “Active power regulation for large-scale wind farms through an efficient power plant model of electric vehicles,” *Appl Energy*, vol. 185, pp. 1673–1683, 2017.

[92] S.-A. Amamra and J. Marco, “Vehicle-to-grid aggregator to support power grid and reduce electric vehicle charging cost,” *IEEE Access*, vol. 7, pp. 178528–178538, 2019.

[93] N. B. Arias, S. Hashemi, P. B. Andersen, C. Træholt, and R. Romero, “Assessment of economic benefits for EV owners participating in the primary frequency regulation markets,” *International Journal of Electrical Power & Energy Systems*, vol. 120, p. 105985, 2020.

[94] S. Robson, A. M. Alharbi, W. Gao, A. Khodaei, and I. Alsaidan, “Economic viability assessment of repurposed EV batteries participating in frequency regulation and energy markets,” in *2021 IEEE Green Technologies Conference (GreenTech)*, IEEE, 2021, pp. 424–429.

[95] A. Y. S. Lam, K.-C. Leung, and V. O. K. Li, “Capacity estimation for vehicle-to-grid frequency regulation services with smart charging mechanism,” *IEEE Trans Smart Grid*, vol. 7, no. 1, pp. 156–166, 2015.

[96] S. Han and S. Han, “Economic feasibility of V2G frequency regulation in consideration of battery wear,” *Energies (Basel)*, vol. 6, no. 2, pp. 748–765, 2013.

[97] N. Kumar, T. Kumar, S. Nema, and T. Thakur, “A comprehensive planning framework for electric vehicles fast charging station assisted by solar and battery based on Queueing theory and non-dominated sorting genetic algorithm-II in a co-ordinated transportation and power network,” *J Energy Storage*, vol. 49, p. 104180, 2022.

[98] C. Peng, J. Zou, L. Lian, and L. Li, “An optimal dispatching strategy for V2G aggregator participating in supplementary frequency regulation considering EV driving demand and aggregator’s benefits,” *Appl Energy*, vol. 190, pp. 591–599, 2017.

[99] H. Liu, J. Qi, J. Wang, P. Li, C. Li, and H. Wei, “EV dispatch control for supplementary frequency regulation considering the expectation of EV owners,” *IEEE Trans Smart Grid*, vol. 9, no. 4, pp. 3763–3772, 2016.

[100] H. Liu *et al.*, “Optimal dispatch for participation of electric vehicles in frequency regulation based on area control error and area regulation requirement,” *Appl Energy*, vol. 240, pp. 46–55, 2019.

[101] M. Wang, Y. Mu, Q. Shi, H. Jia, and F. Li, “Electric vehicle aggregator modeling and control for frequency regulation considering progressive state recovery,” *IEEE Trans Smart Grid*, vol. 11, no. 5, pp. 4176–4189, 2020.

[102] C.-N. Wang, V. T. Nguyen, J.-T. Chyou, T.-F. Lin, and T. N. Nguyen, “Fuzzy multicriteria decision-making model (MCDM) for raw materials supplier selection in plastics industry,” *Mathematics*, vol. 7, no. 10, p. 981, 2019.

[103] W. Zhang, O. Gandhi, H. Quan, C. D. Rodríguez-Gallegos, and D. Srinivasan, "A multi-agent based integrated volt-var optimization engine for fast vehicle-to-grid reactive power dispatch and electric vehicle coordination," *Appl Energy*, vol. 229, pp. 96–110, 2018.

[104] H. Ko, S. Pack, and V. C. M. Leung, "Mobility-aware vehicle-to-grid control algorithm in microgrids," *IEEE Transactions on Intelligent Transportation Systems*, vol. 19, no. 7, pp. 2165–2174, 2018.

[105] C. Zhang, J. Wu, C. Long, and M. Cheng, "Review of existing peer-to-peer energy trading projects," *Energy Procedia*, vol. 105, pp. 2563–2568, 2017.

[106] E. McKenna, J. Pless, and S. J. Darby, "Solar photovoltaic self-consumption in the UK residential sector: New estimates from a smart grid demonstration project," *Energy Policy*, vol. 118, pp. 482–491, 2018.

[107] C. Zhang, J. Wu, C. Long, and M. Cheng, "Review of existing peer-to-peer energy trading projects," *Energy Procedia*, vol. 105, pp. 2563–2568, 2017.

[108] H. T. Doan, J. Cho, and D. Kim, "Peer-to-peer energy trading in smart grid through blockchain: A double auction-based game theoretic approach," *Ieee Access*, vol. 9, pp. 49206–49218, 2021.

[109] S. Thakur, B. P. Hayes, and J. G. Breslin, "Distributed double auction for peer to peer energy trade using blockchains," in *2018 5th International Symposium on Environment-Friendly Energies and Applications (EFEA)*, IEEE, 2018, pp. 1–8.

[110] C. Zhang, T. Yang, and Y. Wang, "Peer-to-Peer energy trading in a microgrid based on iterative double auction and blockchain," *Sustainable Energy, Grids and Networks*, vol. 27, p. 100524, 2021.

[111] K. Chen, J. Lin, and Y. Song, "Trading strategy optimization for a prosumer in continuous double auction-based peer-to-peer market: A prediction-integration model," *Appl Energy*, vol. 242, pp. 1121–1133, 2019.

[112] P. Angaphiwatchawal, P. Phisuthsaingam, and S. Chaitusaney, "A k-Factor Continuous Double Auction-Based Pricing Mechanism for the P2P Energy Trading in a LV Distribution System," in *2020 17th International Conference on Electrical Engineering/Electronics, Computer, Telecommunications and Information Technology (ECTI-CON)*, IEEE, 2020, pp. 37–40.

[113] N. Liu, X. Yu, C. Wang, C. Li, L. Ma, and J. Lei, "Energy-sharing model with price-based demand response for microgrids of peer-to-peer prosumers," *IEEE Transactions on Power Systems*, vol. 32, no. 5, pp. 3569–3583, 2017.

[114] C. Long, J. Wu, Y. Zhou, and N. Jenkins, "Peer-to-peer energy sharing through a two-stage aggregated battery control in a community Microgrid," *Appl Energy*, vol. 226, pp. 261–276, 2018.

[115] C. Long, J. Wu, C. Zhang, L. Thomas, M. Cheng, and N. Jenkins, "Peer-to-peer energy trading in a community microgrid," in *2017 IEEE power & energy society general meeting*, IEEE, 2017, pp. 1–5.

[116] W. Tushar, C. Yuen, D. B. Smith, and H. V. Poor, "Price discrimination for energy trading in smart grid: A game theoretic approach," *IEEE Trans Smart Grid*, vol. 8, no. 4, pp. 1790–1801, 2016.

[117] W. Tushar, T. K. Saha, C. Yuen, D. Smith, and H. V. Poor, "Peer-to-peer trading in electricity networks: An overview," *IEEE Trans Smart Grid*, vol. 11, no. 4, pp. 3185–3200, 2020.

[118] K. Kotani, K. Tanaka, and S. Managi, "Which performs better under trader settings, double auction or uniform price auction?," *Exp Econ*, vol. 22, no. 1, pp. 247–267, 2019.

[119] S. Xu, Y. Zhao, Y. Li, and Y. Zhou, "An iterative uniform-price auction mechanism for peer-to-peer energy trading in a community microgrid," *Appl Energy*, vol. 298, p. 117088, 2021.

[120] Y. Zhou, J. Wu, and C. Long, "Evaluation of peer-to-peer energy sharing mechanisms based on a multiagent simulation framework," *Appl Energy*, vol. 222, pp. 993–1022, 2018.

[121] B. Zhang, Y. Du, E. G. Lim, L. Jiang, and K. Yan, "Design and simulation of Peer-to-Peer energy trading framework with dynamic electricity price," in *2019 29th Australasian Universities Power Engineering Conference (AUPEC)*, IEEE, 2019, pp. 1–6.

[122] S. Aznavi, P. Fajri, M. B. Shadmand, and A. Khoshkbar-Sadigh, "Peer-to-peer operation strategy of PV equipped office buildings and charging stations considering electric vehicle energy pricing," *IEEE Trans Ind Appl*, vol. 56, no. 5, pp. 5848–5857, 2020.

[123] N. Li, "A market mechanism for electric distribution networks," in *2015 54th IEEE Conference on Decision and Control (CDC)*, IEEE, 2015, pp. 2276–2282.

[124] C. Topping, "Average electricity usage in the UK," *ovoenergy*, Mar. 2021. https://www.ovoenergy.com/guides/energy-guides/how-much-electricity-does-a-home-use (accessed Mar. 29, 2023).

[125] "Tenure by household size by number of bedroom," *Office for national statistics*, Mar. 2011. https://www.nomisweb.co.uk/census/2011/dc4405ew (accessed Mar. 29, 2023).

[126] Department for Transport, "Transport Statistics Great Britain 2020," Dec. 2020. Accessed: Mar. 29, 2023. [Online]. Available: https://www.gov.uk/government/statistics/transport-statistics-great-britain-2020

[127] "Power Data Access Viewer," Jan. 2021. https://power.larc.nasa.gov/data-access-viewer/ (accessed Mar. 29, 2023).

[128] W. Zhou, Y. Wang, F. Peng, Y. Liu, H. Sun, and Y. Cong, "Distribution network congestion management considering time sequence of peer-to-peer energy trading," *International Journal of Electrical Power & Energy Systems*, vol. 136, p. 107646, 2022.

[129] A. M. M. Nour, A. Y. Hatata, A. A. Helal, and M. M. El-Saadawi, "Review on voltage-violation mitigation techniques of distribution networks with distributed rooftop PV systems," *IET Generation, Transmission & Distribution*, vol. 14, no. 3, pp. 349–361, 2020.

Appendixes

Appendix A: MATLAB/Simulink model of HEMS

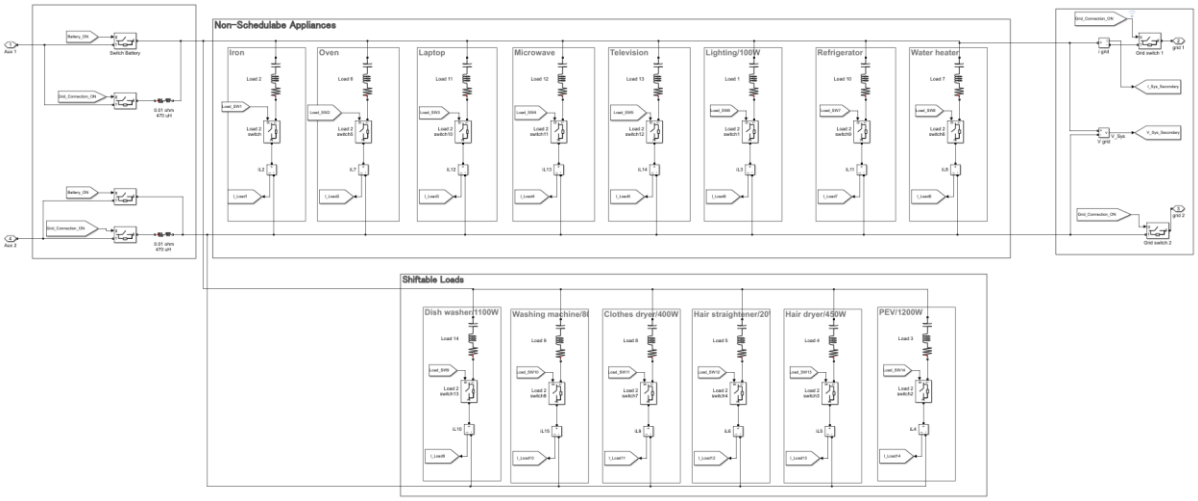

Figure A.1: Household Appliances model

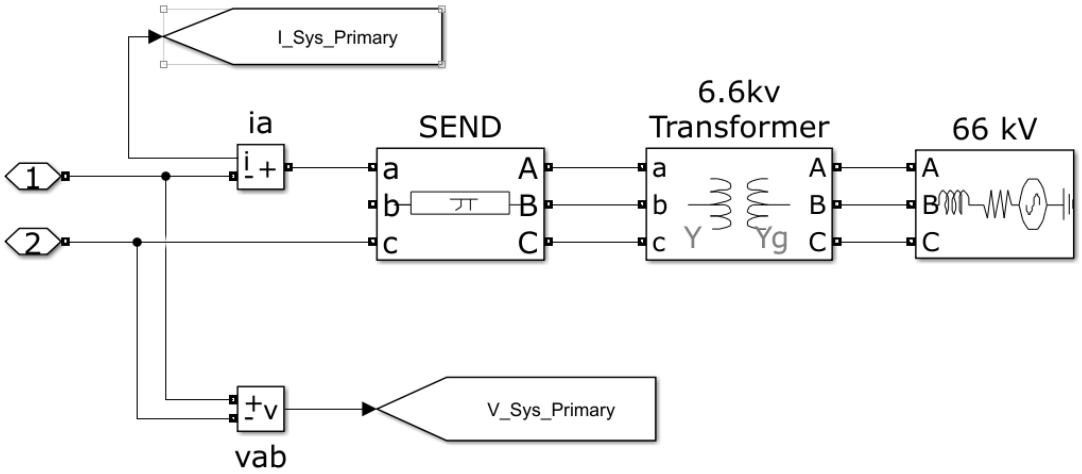

Figure A.2: Power grid model

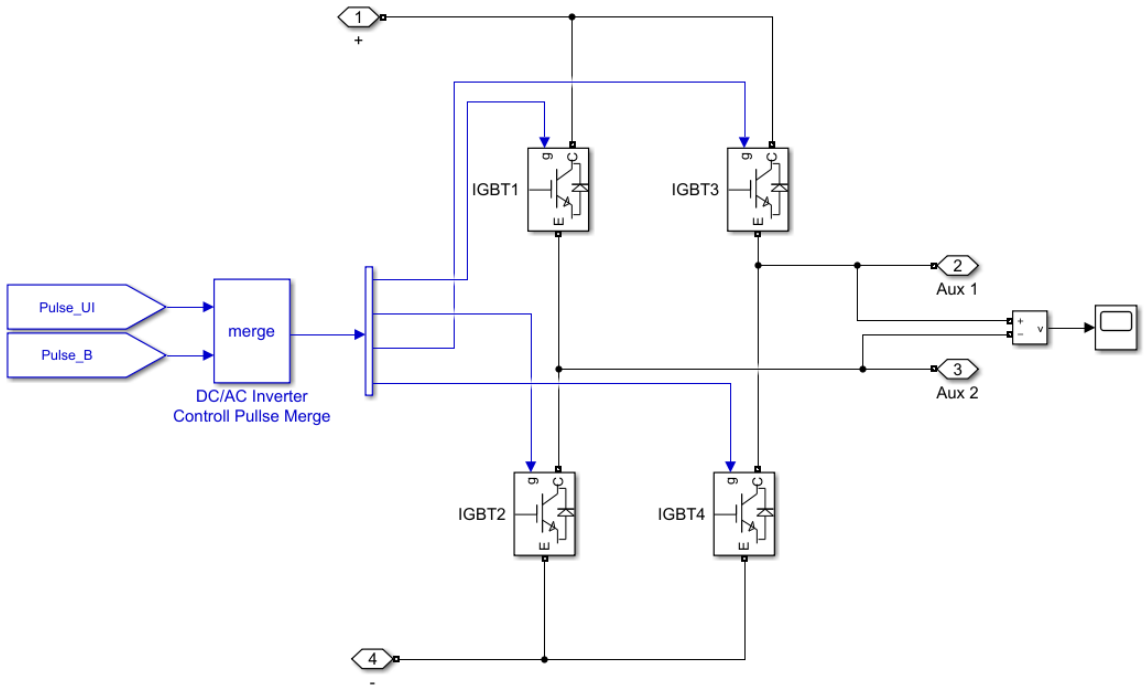

Figure A.3: Bidirectional DC/AC inverter model

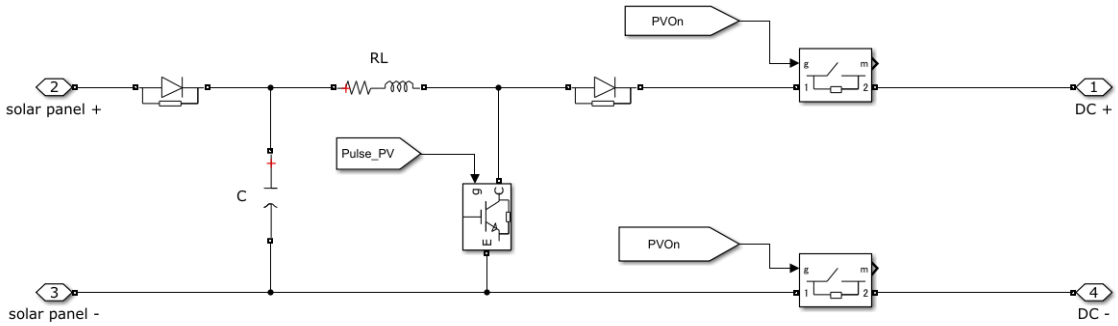

Figure A.4: DC/DC converter model

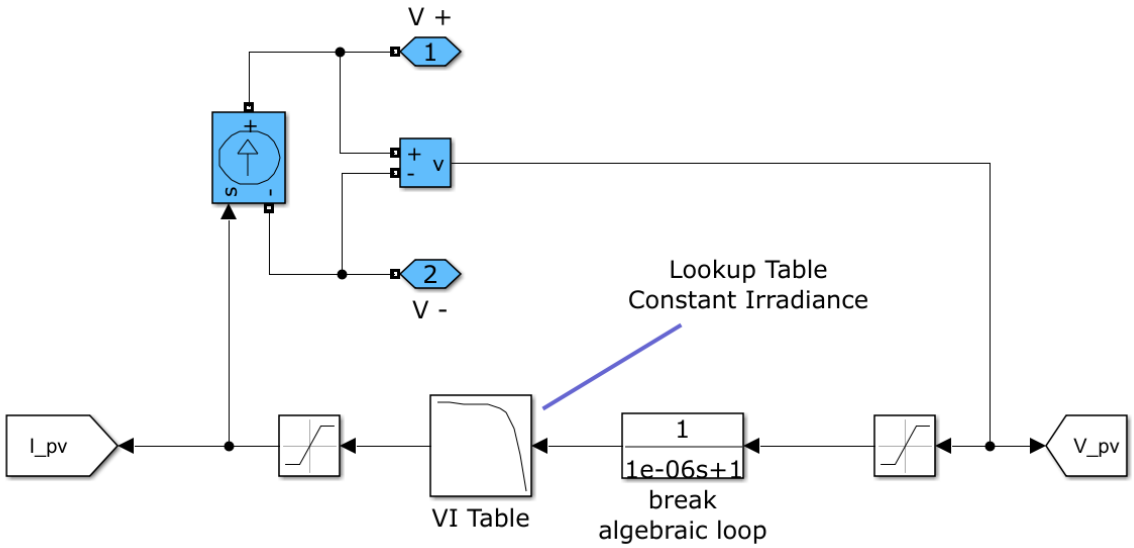

Figure A.5: Solar Panel model

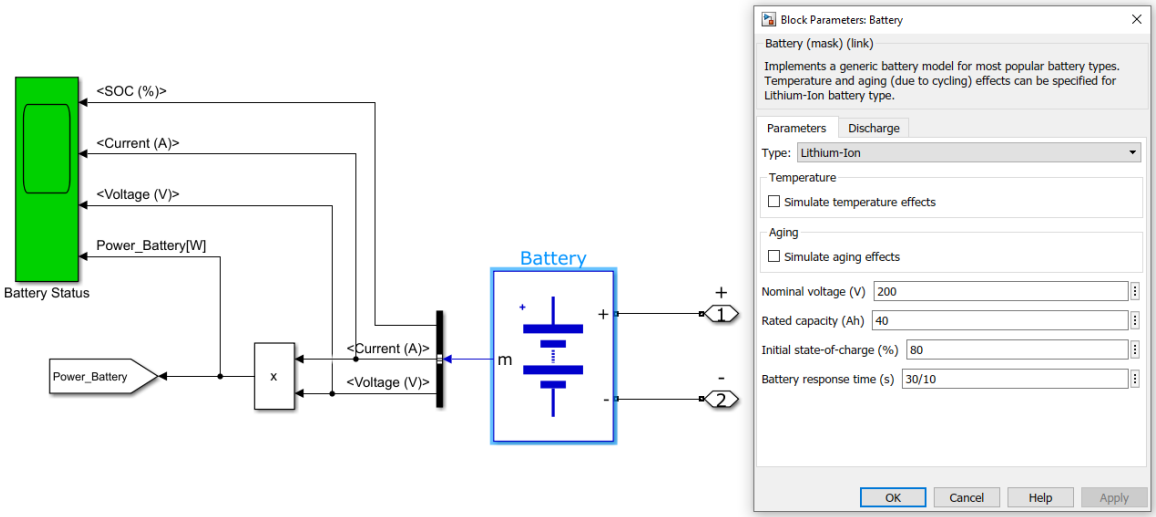

Figure A.6: Home Energy storage model

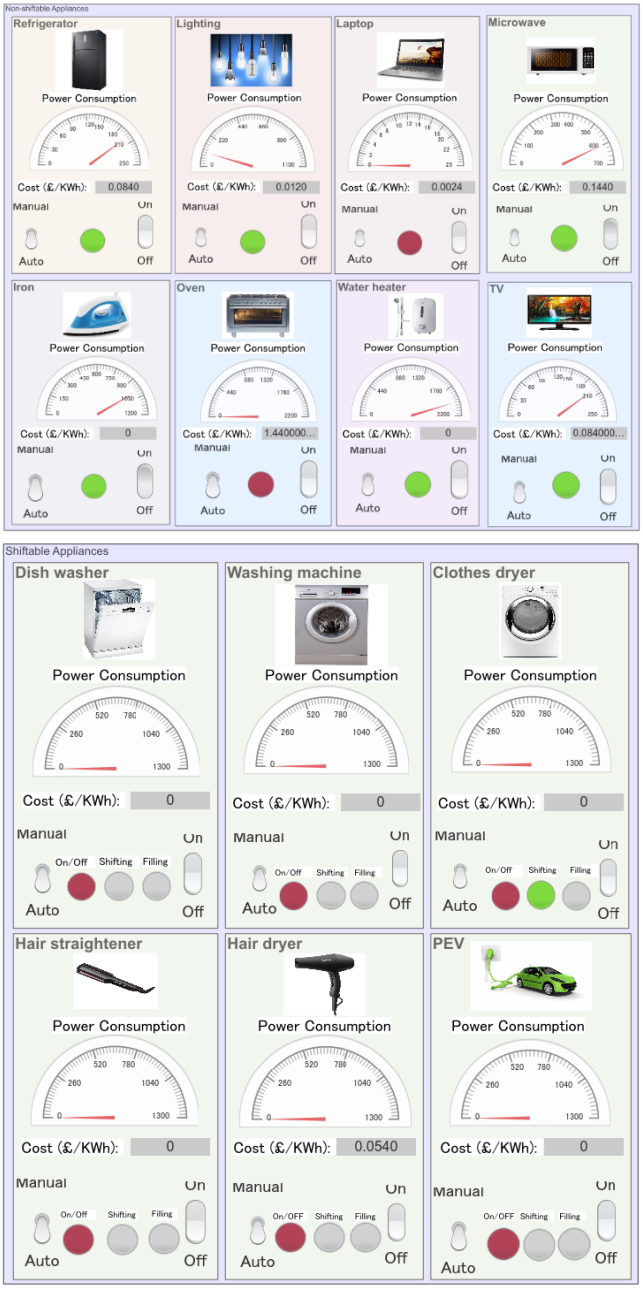

Figure A.7: User interface model.

Appendix B: MATALB/Simulink of Low-voltage (LV) distribution network

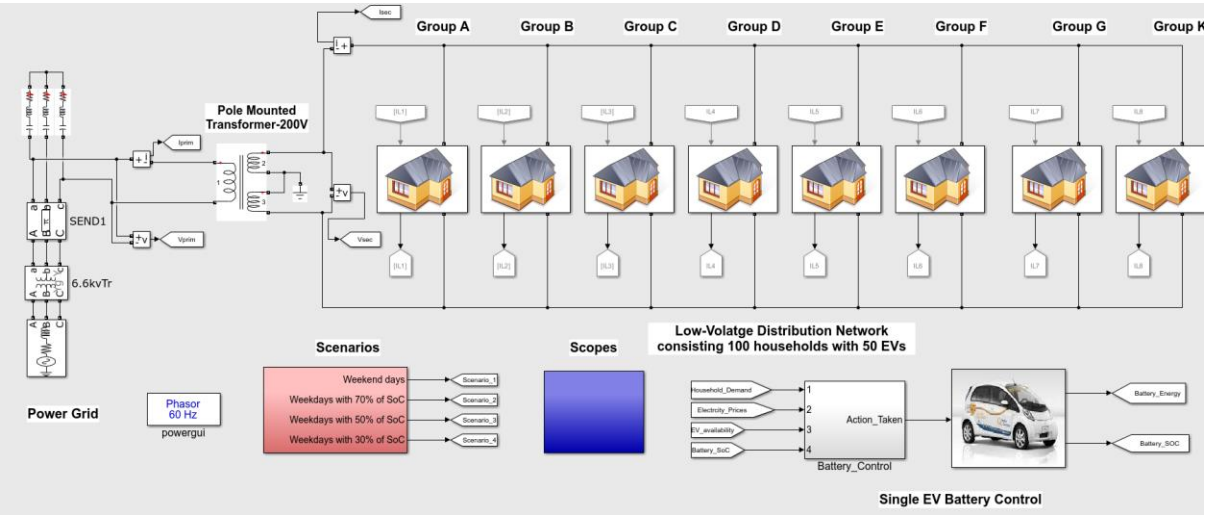

Figure B.1: Low-voltage distribution network in MATLAB/Simulink

Appendix C: DDPG agent Model and two-area power system model in MATLAB/Simulink

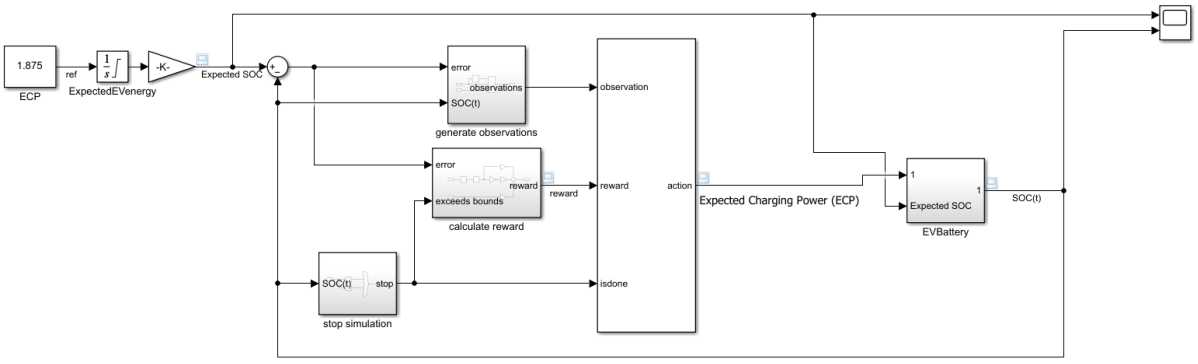

Figure C.1: EV energy management Using DRL

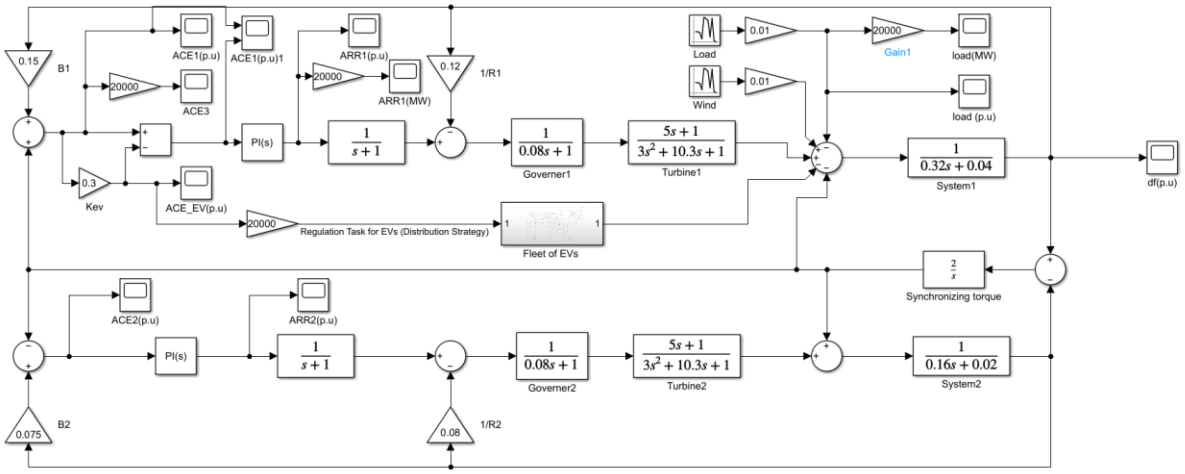

Figure C.2: Two-area power system model in Simulink.

MATLAB code of DDPG agent model of EV battery:

```
open_system('Mymodel')


%%%%% specification obsInfo and action specification actInfo
obsInfo = rlNumericSpec([3 1],...
    'LowerLimit',[-inf -inf 0  ]',...
    'UpperLimit',[ inf  inf inf]');
obsInfo.Name = 'observations';
obsInfo.Description = 'integrated error, error, and measured height';
numObservations = obsInfo.Dimension(1);

actInfo = rlNumericSpec([1 1]);
actInfo.Name = 'flow';
numActions = actInfo.Dimension(1);


%%%%% environment interface object

env = rlSimulinkEnv('Mymodel','Mymodel/RL Agent',...
    obsInfo,actInfo);


%%%% Resetting function that randomises the reference values for the model

env.ResetFcn = @(in)localResetFcn(in);

%%%%%  simulation time Tf and the agent sample time Ts in seconds

Ts = 5/3;
Tf = 800;


%%% random generator seed for reproducibility

rng(0)
```

```
%%%% DDPG Agent


statePath = [
    featureInputLayer(numObservations,'Normalization','none','Name','State')
    fullyConnectedLayer(50,'Name','CriticStateFC1')
    reluLayer('Name','CriticRelu1')
    fullyConnectedLayer(25,'Name','CriticStateFC2')];
actionPath = [
    featureInputLayer(numActions,'Normalization','none','Name','Action')
    fullyConnectedLayer(25,'Name','CriticActionFC1')];
commonPath = [
    additionLayer(2,'Name','add')
    reluLayer('Name','CriticCommonRelu')
    fullyConnectedLayer(1,'Name','CriticOutput')];

criticNetwork = layerGraph();
criticNetwork = addLayers(criticNetwork,statePath);
criticNetwork = addLayers(criticNetwork,actionPath);
criticNetwork = addLayers(criticNetwork,commonPath);
criticNetwork = connectLayers(criticNetwork,'CriticStateFC2','add/in1');
criticNetwork = connectLayers(criticNetwork,'CriticActionFC1','add/in2');


%%% critic network configuration

figure
plot(criticNetwork)

criticOpts = rlRepresentationOptions('LearnRate',1e-03,'GradientThreshold',1);
critic =
rlQValueRepresentation(criticNetwork,obsInfo,actInfo,'Observation',{'State'},'Acti
on',{'Action'},criticOpts);

%%% actor network configuration


actorNetwork = [
    featureInputLayer(numObservations,'Normalization','none','Name','State')
    fullyConnectedLayer(3, 'Name','actorFC')
    tanhLayer('Name','actorTanh')
    fullyConnectedLayer(numActions,'Name','Action')
    ];

actorOptions = rlRepresentationOptions('LearnRate',1e-04,'GradientThreshold',1);

actor =
rlDeterministicActorRepresentation(actorNetwork,obsInfo,actInfo,'Observation',{'St
ate'},'Action',{'Action'},actorOptions);

%%% My agent

agentOpts = rlDDPGAgentOptions(...
    'SampleTime',Ts,...
    'TargetSmoothFactor',1e-3,...
    'DiscountFactor',1.0, ...
    'MiniBatchSize',96, ...
    'ExperienceBufferLength',1e6);
agentOpts.NoiseOptions.StandardDeviation = 0.3;
```

```
agentOpts.NoiseOptions.StandardDeviationDecayRate = 1e-9;


%%%%% Train My Agent


maxepisodes = 5000;
maxsteps = ceil(Tf/Ts);
trainOpts = rlTrainingOptions(...
    'MaxEpisodes',maxepisodes, ...
    'MaxStepsPerEpisode',maxsteps, ...
    'ScoreAveragingWindowLength',20, ...
    'Verbose',false, ...
    'Plots','training-progress',...
    'StopTrainingCriteria','AverageReward',...
    'StopTrainingValue',5000);


doTraining = false;

if doTraining
    % Train the agent.
    trainingStats = train(agent,env,trainOpts);
else

    load('initialAgent1.mat','agent')
end
%save("initialAgent1.mat","agent")


%%%% Validate Trained Agent


simOpts = rlSimulationOptions('MaxSteps',maxsteps);
experiences = sim(env,agent,simOpts);


%%%%%%% Local Function

function in = localResetFcn(in)
% randomize the Type of EV
EVType = 3; %randi([1 3],1,1); % 1 means Charging, 2 means Discharging and 3 means
do-nothing

if EVType == 1
    % randomize reference signal
    blk = sprintf('Mymodel/ECP');
    SOCexp=80; %70 + (80-70)*rand(1);
    SOCint=30; %30 + (40-30)*rand(1); %randi([30 40],1,1);
    EVcap= 30; %randi([24 30],1,1);

    ECP = ((SOCexp-SOCint)*0.01*EVcap)/8;
    in = setBlockParameter(in,blk,'Value',num2str(ECP));

    Eint = SOCint*EVcap;
    blk = 'Mymodel/EVBattery/EVenergy';
    in = setBlockParameter(in,blk,'InitialCondition',num2str(Eint));

    Eint = SOCint*EVcap;
```

```
    blk = 'Mymodel/ExpectedEVenergy';
    in = setBlockParameter(in,blk,'InitialCondition',num2str(Eint));

    blk = 'Mymodel/EVBattery/Gain';
    in = setBlockParameter(in,blk,'Gain',num2str(1/EVcap));
    blk = 'Mymodel/Gain';
    in = setBlockParameter(in,blk,'Gain',num2str(1/EVcap));

elseif EVType == 2
    % randomize reference signal
    blk = sprintf('Mymodel/ECP');
    SOCexp= 40; %40 + (60-40)*rand(1);%randi([40 60],1,1);
    SOCint= 70; %60 + (80-60)*rand(1);%randi([70 80],1,1);
    EVcap= 30; %randi([24 30],1,1);

    ECP = ((SOCexp-SOCint)*0.01*EVcap)/8;
    in = setBlockParameter(in,blk,'Value',num2str(ECP));

    Eint = SOCint*EVcap;
    blk = 'Mymodel/EVBattery/EVenergy';
    in = setBlockParameter(in,blk,'InitialCondition',num2str(Eint));

    Eint = SOCint*EVcap;
    blk = 'Mymodel/ExpectedEVenergy';
    in = setBlockParameter(in,blk,'InitialCondition',num2str(Eint));

    blk = 'Mymodel/EVBattery/Gain';
    in = setBlockParameter(in,blk,'Gain',num2str(1/EVcap));
    blk = 'Mymodel/Gain';
    in = setBlockParameter(in,blk,'Gain',num2str(1/EVcap));

elseif EVType == 3
    % randomize reference signal
    blk = sprintf('Mymodel/ECP');
    SOCexp= 70; %50 + (70-50)*rand(1);%randi([50 70],1,1);
    SOCint= SOCexp;
    EVcap= 30; %randi([24 30],1,1);

    ECP = ((SOCexp-SOCint)*0.01*EVcap)/8;
    in = setBlockParameter(in,blk,'Value',num2str(ECP));

    Eint = SOCint*EVcap;
    blk = 'Mymodel/EVBattery/EVenergy';
    in = setBlockParameter(in,blk,'InitialCondition',num2str(Eint));

    Eint = SOCint*EVcap;
    blk = 'Mymodel/ExpectedEVenergy';
    in = setBlockParameter(in,blk,'InitialCondition',num2str(Eint));

    blk = 'Mymodel/EVBattery/Gain';
    in = setBlockParameter(in,blk,'Gain',num2str(1/EVcap));
    blk = 'Mymodel/Gain';
    in = setBlockParameter(in,blk,'Gain',num2str(1/EVcap));
end


% randomize Regulation Task signal (Mean and Variance)
RegulationMean = 0.5; %-3 + (3--3)*rand(1);
blk = 'Mymodel/EVBattery/RegulationTask';
```

```
in = setBlockParameter(in,blk,'Mean',num2str(RegulationMean));

RegulationVariance = 1; %0.5 + (1.5-0.5)*rand(1);
blk = 'Mymodel/EVBattery/RegulationTask';
in = setBlockParameter(in,blk,'Variance',num2str(RegulationVariance));
end
```

Appendix D: P2P energy model and formulation

Appendix D.1: Formulation of proposed P2P pricing mechanism

According to the basic principle of economics, prices decrease with higher supply/lower demand and increase with the higher demand/ lower supply. In the P2P energy market, when there is no energy surplus exported from a prosumer ($E_S(t) = 0$) to the P2P market, the P2P buying price is set to the grid price (RTP). In contrast, when there is no energy deficiency requests ($E_D(t) = 0$) from the P2P market, the P2P selling price is set to FiT. When the ESC receives both energy surplus and deficiency requests ($-1 < \alpha < 1$), the P2P prices trend tends to follow the function $\tanh(2\alpha)$. Thus, $\tanh(2\alpha)$ can be used to model the relationship between P2P prices and α/β:

$$r_b = f(\alpha,\beta) = \begin{cases} (1-\beta)\tanh(2\alpha) & ,\alpha \geq 0 \\ \beta\tanh(2\alpha) & ,\alpha < 0 \\ r_g & ,E_S = 0 \end{cases} \quad (D.1)$$

$$r_s = f(\alpha,\beta) = \begin{cases} \beta\tanh(2\alpha) \\ (1-\beta)\tanh(2\alpha) & ,\alpha < 0 \\ r_{ex} & ,E_D = 0 \end{cases} \quad (D.2)$$

Substituting $\tanh(x) = \frac{e^x - e^{-x}}{e^x + e^{-x}}$, in (D.1) and (D.2):

$$r_b = f(\alpha,\beta) = \begin{cases} (1-\beta)\dfrac{e^{2\alpha} - e^{-2\alpha}}{e^{2\alpha} + e^{-2\alpha}} & ,\alpha \geq 0 \\ \beta\dfrac{e^{2\alpha} - e^{-2\alpha}}{e^{2\alpha} + e^{-2\alpha}} & ,\alpha < 0 \\ r_g & ,E_S = 0 \end{cases} \quad (D.3)$$

$$r_s = f(\alpha,\beta) = \begin{cases} \beta\dfrac{e^{2\alpha}-e^{-2\alpha}}{e^{2\alpha}+e^{-2\alpha}} & ,\alpha \geq 0 \\ (1-\beta)\dfrac{e^{2\alpha}-e^{-2\alpha}}{e^{2\alpha}+e^{-2\alpha}} & ,\alpha < 0 \\ r_{ex} & ,E_D = 0 \end{cases} \quad (C.4)$$

Where α is in the range [-1, 1] as shown in Equation (6.26), and to convert this range to [0,1], the formula ($X_{new} = \frac{X_{old}-min}{max-min}$) is used:

$$r_b = f(\alpha,\beta) = \begin{cases} \dfrac{(2-\beta)e^{2\alpha}+\beta e^{-2\alpha}}{2(e^{2\alpha}+e^{-2\alpha})} & ,\alpha \geq 0 \\ \dfrac{\beta e^{2\alpha}+(1-\beta)e^{-2\alpha}}{2(e^{2\alpha}+e^{-2\alpha})} & ,\alpha < 0 \\ r_g & ,E_S = 0 \end{cases} \quad (D.5)$$

$$r_s = f(\alpha,\beta) = \begin{cases} \dfrac{(2-\beta)e^{2\alpha}+\beta e^{-2\alpha}}{2(e^{2\alpha}+e^{-2\alpha})} & ,\alpha \geq 0 \\ \dfrac{\beta e^{2\alpha}+(1-\beta)e^{-2\alpha}}{2(e^{2\alpha}+e^{-2\alpha})} & ,\alpha < 0 \\ r_{ex} & ,E_D = 0 \end{cases} \quad (D.6)$$

Finally, to map the P2P prices into $[r_{ex}, r_g]$, the formula ($X \times (max - min) + min$) is used. The function of P2P prices can be formulated as:

$$r_b = \begin{cases} \left(\dfrac{r_g - r_{ex}}{2}\right)\dfrac{(2-\beta)e^{2\alpha}+\beta e^{-2\alpha}}{e^{2\alpha}+e^{-2\alpha}} + r_{ex} & ,\alpha \geq 0 \\ \left(\dfrac{r_g - r_{ex}}{2}\right)\dfrac{(1+\beta)e^{2\alpha}+(1-\beta)e^{-2\alpha}}{e^{2\alpha}+e^{-2\alpha}} + r_{ex} & ,\alpha < 0 \\ r_g & ,E_S = 0 \end{cases}$$

$$r_s = \begin{cases} \left(\dfrac{r_g - r_{ex}}{2}\right)\dfrac{(1+\beta)e^{2\alpha}+(1-\beta)e^{-2\alpha}}{e^{2\alpha}+e^{-2\alpha}} + r_{ex} & ,\alpha \geq 0 \\ \left(\dfrac{r_g - r_{ex}}{2}\right)\dfrac{(2-\beta)e^{2\alpha}+\beta e^{-2\alpha}}{e^{2\alpha}+e^{-2\alpha}} + r_{ex} & ,\alpha < 0 \\ r_{ex} & ,E_D = 0 \end{cases}$$

Appendix D.2: formulation of BS, MMR and SDR mechanisms

Bill sharing mechanism (BS)

In this method, the cost of electricity for a community is shared among customers based on individual customer's total energy consumption and export. The buy and sell prices for the P2P mechanism as determined by this method are given by equations (D.7) and (D.8) respectively.

$$r_b = r_g \left(\frac{E_D^{BFG}}{E_D} \right) \tag{D.7}$$

$$r_s = r_{ex} \left(\frac{E_S^{STG}}{E_S} \right) \tag{D.8}$$

E_D^{BFG} and E_S^{STG} are respectively the total energy import and export of the community from/to the grid after P2P trading. Therefore, the electricity bill of individual households is calculated as follows:

$$C^i = (E_{D_i}^{BFG}.r_g - E_{S_i}^{STG}.r_{ex}) + (E_{D_i}^{P2P}.r_b - E_{S_i}^{P2P}.r_s) \tag{D.9}$$

$E_{D_i}^{BFG}$ and $E_{D_i}^{P2P}$ denote the energy purchased from the main grid and P2P market by individual users respectively. $E_{S_i}^{STG}$ and $E_{S_i}^{P2P}$ are the energy sold to the main grid and P2P market respectively.

Mid-Market Rate Mechanism (MMR)

In this pricing mechanism, the P2P prices are bounded between the RTP and FiT. Therefore, the MMR method assumes that the P2P prices are set to the average value of RTP and FiT when the total energy surplus equals the energy deficiency, thus:

$$r_b, r_s = \frac{r_g + r_{ex}}{2} \tag{D.10}$$

However, the peers will buy/sell their energy under RTP/FiT in case the total energy surplus does not meet the energy deficiency in the P2P market.

Supply-Demand Ratio (SDR)

In this mechanism, P2P prices can be adjusted with the change of Supply-Demand Ratio (SDR) based on the basic principle of economics, as the relation between price and SDR is inverse-proportional. the relationship of supply and demand in the energy sharing zone can be represented by:

$$SDR = \frac{E_S}{E_D} \tag{D.11}$$

The P2P buying and selling prices are identified by equations (C.12) and (C.13) according to SDR values:

$$r_s = \begin{cases} \dfrac{r_g . r_{ex}}{(r_g - r_{ex}).SDR + r_{ex}} & ,0 \le SDR \le 1 \\ r_{ex} & ,SDR > 1 \end{cases} \tag{D.12}$$

$$r_b = \begin{cases} r_s.SDR + r_g(1 - SDR), & 0 \le SDR \le 0 \\ r_{ex} & SDR > 1 \end{cases} \tag{D.13}$$

The relationship between the internal price and SDR is shown in Figure A.1 which shows that r_s and r_b decline with the increase of SDR in the interval [0, 1], and they are set to r_{ex} when SDR is greater than 1.

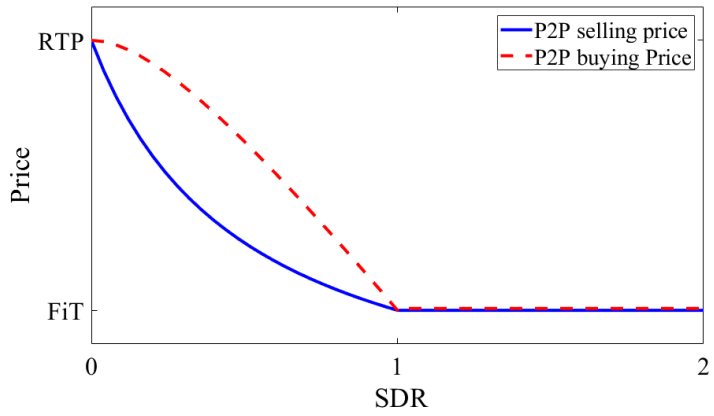

Figure D.1: Relationship between the P2P prices and SDR.

Appendix D.3: MATALB code of P2P energy model

```
clc
clear

hours = 24;
% peak mornoing form 7-10     (4 hrs)
% peak evening form 17-21     (5 hrs)
% off-peak form 0-6 & 22-23   (9 hrs)
% mid-peak form 11-16         (6 hrs)
%%%%%%%%%%%%%%%%%%%%%%%%%%%%%%%%%%%%%%%%%%%%%%%%%%%%%%%%%%%%%%%%%%%%%%%%%%%%
Max_household_Demand = 20;   %maximum household power demand
Min_household_Demand = 8.5;  %minimum household power demand
%%%%%%%%%%%%%%%%%%%%%%%%%%%%%%%%%%%%%%%%%%%%%%%%%%%%%%%%%%%%%%%%%%%%%%%%%%%%
%Household Types = [PV, BESS, EV]
HouseholdTypesIndex = [1,1,1;1,1,0;1,0,1;1,0,0;0,0,1;0,0,0];
%%%%%%%%%%%%%%%%%%%%%%%%%%%%%%%%%%%%%%%%%%%%%%%%%%%%%%%%%%%%%%%%%%%%%%%%%%%%
```

```
Number_households = 100;

Household_Types = TypeOfHouse(Number_households);
[Individual_Household_demand,Household_Demand_Distribution,
Total_households_Demand] = Household_Demand(Number_households);
[PV_Individual, Total_PV_Gen,PV_Curve,PV_Type] = PV(Number_households,
Household_Types,HouseholdTypesIndex);
[Capacity_of_BESs, initial_SOCs_BES] = BESS(Number_households,
Household_Types,HouseholdTypesIndex);
[Capacity_of_EVs,initial_SOCs_EV,Trip_Duration] = EV(Number_households,
Household_Types,HouseholdTypesIndex);
[Capacity_of_Pool, initial_SOC_Pool] = Pool_Battery();
%%%%%%%%%%%%%%%%%%%%%%%%%%%%%%%%%%%%%%%%%%%%%%%%%%%%%%%%%%%%%%%%%%%%%%%%%%%%
Total_Current_Demand = zeros(1, 240);
Total_surplus_power = zeros(1, 240);
Total_deficiency_power = zeros(1, 240);
Total_Net_Household_Demand = zeros(1, 240);

Z = 0;
T = [];
%%%%%%%%%%%%%%Test of Household 2%%%%%%%%%%%%%%%%%%%%%%%%%
Net_Household2_Demand = zeros(1, 240);
Daily_current_demand2 = zeros(1, 240);
Individual_surplus2 = zeros(1, 240);

Individual_deficiency = zeros(Number_households, 240);
Individual_surplus = zeros(Number_households, 240);

%%%%%%%%%%%%%%%%%%%%%%%%%%%%%%%%BESS Parameters%%%%%%%%%%%%%%%%%%%%%%%%%%%
Initial_BES_power = (Capacity_of_BESs.*initial_SOCs_BES)./100;
BES_Inividual_power = Initial_BES_power;
BES_Power = zeros(1, 240);
SOCs_BES = initial_SOCs_BES;
Min_SOC_BES = 20;
Max_SOC_BES = 80;
%%%%%%%%%%%%%%%%%%%%%%%%%%%%%%%%EV Parameters%%%%%%%%%%%%%%%%%%%%%%%%%%%%
Initial_EV_power = (Capacity_of_EVs.*initial_SOCs_EV)./100;
EV_Inividual_power = Initial_EV_power;
EV_Power = zeros(1, 240);
SOCs_EV = initial_SOCs_EV;
Min_SOC_EV = 20;
Max_SOC_EV = 80;
Trip_power = 4;
Availability_EV = zeros(1, Number_households);
%%%%%%%%%%%%%%%%%%%%%%%%%%%%%%Pool Battery of Micro Grid%%%%%%%%%%%%%
Initial_Pool_power = (Capacity_of_Pool*initial_SOC_Pool)/100;
Pool_power = Initial_Pool_power;
Pool_SOC = initial_SOC_Pool;
Min_SOC_Pool = 20;
Max_SOC_Pool = 80;
Pool_Power = zeros(1, 240);
Pool_deficiency = 0;
Pool_surplus = 0;
Pool_Deficiency = zeros(1, 241);
Pool_Surplus = zeros(1, 241);

%%%%%%%%%%%%%%%%%%%%%%%%%%%%%%%%Pricing%%%%%%%%%%%%%%%%%%%%%%%%%%%%%%%%%
Total_Surplus = 0;
Total_Deficiency = 0;
```

```
Price_Selling = zeros(1,240);
Price_Buying = zeros(1,240);
grid_price = zeros(1,240);
MMR = zeros(1,240);
Individual_Cost_Households = zeros(240,Number_households);

for h = 0:0.1:hours
Current_household_demand = zeros(1,Number_households);
Surplus_power = zeros(1, Number_households);
Deficiency_power = zeros(1, Number_households);
Net_Household_Demand = zeros(1, Number_households);


    if h >= 0 && h < 6
        %%%%%%%%%%%%%%%%%%%%%%%%%%%%%%%%PV Management%%%%%%%%%%%%%%%%%%%%
        %%%%To calculate PV Generation, Surplus Power and Deficiency Power
        for i = 1: Number_households
            Current_household_demand(i) = Household_Demand_Distribution (i, 1);
            Deficiency_power (i) =  - Current_household_demand(i);
            Net_Household_Demand(i) = Current_household_demand(i);

            SOCs_BES(i) = (BES_Inividual_power(i)*100)/ Capacity_of_BESs(i);
            if SOCs_BES(i) >= Min_SOC_BES && Deficiency_power (i) < 0
                BES_Inividual_power(i) = (BES_Inividual_power(i) +
(Deficiency_power (i)*0.1))* HouseholdTypesIndex(Household_Types(i),2);
                Net_Household_Demand(i) = Net_Household_Demand(i) +
Deficiency_power (i);
                Deficiency_power (i) = 0;
            else
                BES_Inividual_power(i) = BES_Inividual_power(i);
            end

            SOCs_EV(i) = (EV_Inividual_power(i)*100)/ Capacity_of_EVs(i);
            if SOCs_EV(i) >= Min_SOC_EV && Deficiency_power (i) < 0
                EV_Inividual_power(i) = (EV_Inividual_power(i) + (Deficiency_power
(i)*0.1))* HouseholdTypesIndex(Household_Types(i),3);
                Net_Household_Demand(i) = Net_Household_Demand(i) +
Deficiency_power (i);
                Deficiency_power (i) = 0;
            else
                BES_Inividual_power(i) = BES_Inividual_power(i);
            end
        end

    elseif   h >= 6 && h < 7

        %%%%%%%%%%%%%%%%%%%%%%%%%%%%%%%%PV Management%%%%%%%%%%%%%%%%%%%%
        %%%%To calculate PV Generation, Surplus Power and Deficiency Power
        for i = 1: Number_households
            Current_household_demand(i) = Household_Demand_Distribution (i, 1);
            if PV_Curve(i, 1) >= Current_household_demand(i)
                Surplus_power(i) =  PV_Curve(i, 1) - Current_household_demand(i);
                Net_Household_Demand(i) = 0;

            else
                Deficiency_power (i) = PV_Curve(i, 1) -
Current_household_demand(i);
```

```
                Net_Household_Demand(i) = Current_household_demand(i) -
PV_Curve(i, 1) ;

            end

            SOCs_BES(i) = (BES_Inividual_power(i)*100)/ Capacity_of_BESs(i);
            if SOCs_BES(i) <= Max_SOC_BES && Surplus_power(i) > 0
                BES_Inividual_power(i) = (BES_Inividual_power(i) +
(Surplus_power(i)*0.1)) * HouseholdTypesIndex(Household_Types(i),2);
                Net_Household_Demand(i) = Net_Household_Demand(i);
                Surplus_power(i) = 0;
            elseif SOCs_BES(i) >= Min_SOC_BES && Deficiency_power (i) < 0
                BES_Inividual_power(i) = (BES_Inividual_power(i) +
(Deficiency_power (i)*0.1)) * HouseholdTypesIndex(Household_Types(i),2);
                Net_Household_Demand(i) = Net_Household_Demand(i) +
Deficiency_power (i);
                Deficiency_power (i) = 0;
            elseif SOCs_BES(i) >= Max_SOC_BES
                BES_Inividual_power(i) = BES_Inividual_power(i);
            end

            SOCs_EV(i) = (EV_Inividual_power(i)*100)/ Capacity_of_EVs(i);
            if SOCs_EV(i) <= Max_SOC_EV && Surplus_power(i) > 0
                EV_Inividual_power(i) = (EV_Inividual_power(i) +
(Surplus_power(i)*0.1)) * HouseholdTypesIndex(Household_Types(i),3);
                Net_Household_Demand(i) = Net_Household_Demand(i);
                Surplus_power(i) = 0;
            elseif SOCs_EV(i) >= Min_SOC_EV && Deficiency_power (i) < 0
                EV_Inividual_power(i) = (EV_Inividual_power(i) + (Deficiency_power
(i)*0.1)) * HouseholdTypesIndex(Household_Types(i),3);
                Net_Household_Demand(i) = Net_Household_Demand(i) +
Deficiency_power (i);
                Deficiency_power (i) = 0;
            elseif SOCs_EV(i) >= Max_SOC_EV
                EV_Inividual_power(i) = EV_Inividual_power(i);
            end


        end

    elseif h >= 7 && h < 11
        for i = 1: Number_households
            Current_household_demand(i) = Household_Demand_Distribution (i, 2);
            if PV_Curve(i, floor(h-5)) >= Current_household_demand(i)
                Surplus_power(i) =  PV_Curve(i, floor(h-5)) -
Current_household_demand(i);
                Net_Household_Demand(i) = 0 ;
            else
                Deficiency_power (i) = PV_Curve(i, floor(h-5)) -
Current_household_demand(i);
                Net_Household_Demand(i) = Current_household_demand(i) -
PV_Curve(i, floor(h-5)) ;
            end

            SOCs_BES(i) = (BES_Inividual_power(i)*100)/ Capacity_of_BESs(i);
            if SOCs_BES(i) <= Max_SOC_BES && Surplus_power(i) > 0
                BES_Inividual_power(i) = (BES_Inividual_power(i) +
(Surplus_power(i)*0.1)) * HouseholdTypesIndex(Household_Types(i),2);
                Net_Household_Demand(i) = Net_Household_Demand(i);
```

```
                Surplus_power(i) = 0;
            elseif SOCs_BES(i) >= Min_SOC_BES && Deficiency_power (i) < 0
                BES_Inividual_power(i) = (BES_Inividual_power(i) +
(Deficiency_power (i)*0.1)) * HouseholdTypesIndex(Household_Types(i),2);
                Net_Household_Demand(i) = Net_Household_Demand(i) +
Deficiency_power (i);
                Deficiency_power (i) = 0;
            elseif SOCs_BES(i) >= Max_SOC_BES
                BES_Inividual_power(i) = BES_Inividual_power(i);
            end

        end

    elseif h >= 11 && h < 17
         for i = 1: Number_households
            Current_household_demand(i) = Household_Demand_Distribution (i, 3);
            if PV_Curve(i, floor(h-5)) >= Current_household_demand(i)
                Surplus_power(i) =  PV_Curve(i, floor(h-5)) -
Current_household_demand(i);
                Net_Household_Demand(i) = 0;
            else
                Deficiency_power (i) = PV_Curve(i, floor(h-5)) -
Current_household_demand(i);
                Net_Household_Demand(i) = Current_household_demand(i) -
PV_Curve(i, floor(h-5));
            end

            SOCs_BES(i) = (BES_Inividual_power(i)*100)/ Capacity_of_BESs(i);
            if SOCs_BES(i) <= Max_SOC_BES && Surplus_power(i) > 0
                BES_Inividual_power(i) = (BES_Inividual_power(i) +
(Surplus_power(i)*0.1)) * HouseholdTypesIndex(Household_Types(i),2);
                Net_Household_Demand(i) = Net_Household_Demand(i);
                Surplus_power(i) = 0;
            elseif SOCs_BES(i) >= Min_SOC_BES && Deficiency_power (i) < 0
                BES_Inividual_power(i) = (BES_Inividual_power(i) +
(Deficiency_power (i)*0.1)) * HouseholdTypesIndex(Household_Types(i),2);
                Net_Household_Demand(i) = Net_Household_Demand(i) +
Deficiency_power (i);
                Deficiency_power (i) = 0;
            elseif SOCs_BES(i) >= Max_SOC_BES
                BES_Inividual_power(i) = BES_Inividual_power(i);
            end

            if (Trip_Duration(i) + 7) == 11 && h == 11
                EV_Inividual_power(i) = EV_Inividual_power(i) - Trip_power;
                Availability_EV(i) = 1;
            elseif (Trip_Duration(i) + 7) == 12 && h == 12
                EV_Inividual_power(i) = EV_Inividual_power(i) - (Trip_power+1);
                Availability_EV(i) = 1;
            elseif (Trip_Duration(i) + 7) == 13 && h == 13
                EV_Inividual_power(i) = EV_Inividual_power(i) - (Trip_power+2);
                Availability_EV(i) = 1;
            end

            SOCs_EV(i) = (EV_Inividual_power(i)*100)/ Capacity_of_EVs(i);

            if SOCs_EV(i) <= Max_SOC_EV && Surplus_power(i) > 0 &&
Availability_EV(i) == 1
```

```
                EV_Inividual_power(i) = (EV_Inividual_power(i) +
(Surplus_power(i)*0.1)) * HouseholdTypesIndex(Household_Types(i),3);
                Net_Household_Demand(i) = Net_Household_Demand(i);
                Surplus_power(i) = 0;
            elseif SOCs_EV(i) < Max_SOC_EV && Surplus_power(i) == 0 &&
Availability_EV(i) == 1 && Household_Types(i) ~= 1 && Household_Types(i) ~= 3 && h
< 16
                EV_Inividual_power(i) = (EV_Inividual_power(i) + (2*0.1)) *
HouseholdTypesIndex(Household_Types(i),3);
                Net_Household_Demand(i) = Net_Household_Demand(i) + (2);
                Deficiency_power (i) = -1*Net_Household_Demand(i);
            elseif SOCs_EV(i) <= Max_SOC_EV && Deficiency_power (i) < 0 &&
Availability_EV(i) == 1
                EV_Inividual_power(i) = (EV_Inividual_power(i) + (Deficiency_power
(i)*0.1)) * HouseholdTypesIndex(Household_Types(i),3);
                Net_Household_Demand(i) = Net_Household_Demand(i) +
Deficiency_power (i);
                Deficiency_power (i) = 0;
            elseif SOCs_EV(i) >= Max_SOC_EV
                EV_Inividual_power(i) = EV_Inividual_power(i);
            end
         end

    elseif h >= 17 && h < 22
        for i = 1: Number_households
            Current_household_demand(i) = Household_Demand_Distribution (i, 4);
            Deficiency_power (i) = - Current_household_demand(i);
            Net_Household_Demand(i) = Current_household_demand(i);

            SOCs_BES(i) = (BES_Inividual_power(i)*100)/ Capacity_of_BESs(i);
            if SOCs_BES(i) <= Max_SOC_BES && Surplus_power(i) > 0
                BES_Inividual_power(i) = (BES_Inividual_power(i) +
(Surplus_power(i)*0.1)) * HouseholdTypesIndex(Household_Types(i),2);
                Net_Household_Demand(i) = Net_Household_Demand(i);
                Surplus_power(i) = 0;
            elseif SOCs_BES(i) >= Min_SOC_BES && Deficiency_power (i) < 0
                BES_Inividual_power(i) = (BES_Inividual_power(i) +
(Deficiency_power (i)*0.1)) * HouseholdTypesIndex(Household_Types(i),2);
                Net_Household_Demand(i) = Net_Household_Demand(i) +
Deficiency_power (i);
                Deficiency_power (i) = 0;
            elseif SOCs_BES(i) >= Max_SOC_BES
                BES_Inividual_power(i) = BES_Inividual_power(i);
            end

            SOCs_EV(i) = (EV_Inividual_power(i)*100)/ Capacity_of_EVs(i);
            if SOCs_EV(i) >= Min_SOC_EV && Deficiency_power (i) < 0
                EV_Inividual_power(i) = (EV_Inividual_power(i) + (Deficiency_power
(i)*0.1)) * HouseholdTypesIndex(Household_Types(i),3);
                Net_Household_Demand(i) = Net_Household_Demand(i) +
Deficiency_power (i);
                Deficiency_power (i) = 0;
            elseif SOCs_EV(i) >= Max_SOC_EV
                EV_Inividual_power(i) = EV_Inividual_power(i);
            end
            SOCs_EV(i) = (EV_Inividual_power(i)*100)/ Capacity_of_EVs(i);
            if SOCs_EV(i) >= 40 && Deficiency_power (i) == 0
                EV_Inividual_power(i) = (EV_Inividual_power(i) - (1*0.1)) *
HouseholdTypesIndex(Household_Types(i),3);
```

```
                Net_Household_Demand(i) = Net_Household_Demand(i);
                Surplus_power(i) = 1;
            end
        end

    elseif h >= 22 && h < 24
        for i = 1: Number_households
            Current_household_demand(i) = Household_Demand_Distribution (i, 5);
            Deficiency_power (i) = - Current_household_demand(i);
            Net_Household_Demand(i) = Current_household_demand(i);

            SOCs_BES(i) = (BES_Inividual_power(i)*100)/ Capacity_of_BESs(i);
            if SOCs_BES(i) <= Max_SOC_BES && Surplus_power(i) > 0
                BES_Inividual_power(i) = (BES_Inividual_power(i) +
(Surplus_power(i)*0.1)) * HouseholdTypesIndex(Household_Types(i),2);
                Net_Household_Demand(i) = Net_Household_Demand(i);
                Surplus_power(i) = 0;
            elseif SOCs_BES(i) >= Min_SOC_BES && Deficiency_power (i) < 0
                BES_Inividual_power(i) = (BES_Inividual_power(i) +
(Deficiency_power (i)*0.1)) * HouseholdTypesIndex(Household_Types(i),2);
                Net_Household_Demand(i) = Net_Household_Demand(i) +
Deficiency_power (i);
                Deficiency_power (i) = 0;
            elseif SOCs_BES(i) >= Max_SOC_BES
                BES_Inividual_power(i) = BES_Inividual_power(i);
            end

            SOCs_EV(i) = (EV_Inividual_power(i)*100)/ Capacity_of_EVs(i);
            if SOCs_EV(i) >= Min_SOC_EV && Deficiency_power (i) < 0
                EV_Inividual_power(i) = (EV_Inividual_power(i) + (Deficiency_power
(i)*0.1)) * HouseholdTypesIndex(Household_Types(i),3);
                Net_Household_Demand(i) = Net_Household_Demand(i) +
Deficiency_power (i);
                Deficiency_power (i) = 0;
            elseif SOCs_EV(i) < Max_SOC_EV && SOCs_EV(i)> 50
                EV_Inividual_power(i) = (EV_Inividual_power(i) - (1*0.1)) *
HouseholdTypesIndex(Household_Types(i),3);
                Net_Household_Demand(i) = Net_Household_Demand(i);
                Surplus_power(i) = 1;
            end
            SOCs_EV(i) = (EV_Inividual_power(i)*100)/ Capacity_of_EVs(i);
            if SOCs_EV(i) < 50 && Deficiency_power (i) == 0
                EV_Inividual_power(i) = (EV_Inividual_power(i) + (1*0.1)) *
HouseholdTypesIndex(Household_Types(i),3);
                Net_Household_Demand(i) = Net_Household_Demand(i) + (1);
                Deficiency_power (i) = -1*Net_Household_Demand(i);
            end

        end

    end

    Z = Z+1;
    T(Z) = h;
    Total_Current_Demand(Z) = sum(Current_household_demand);
    Total_surplus_power(Z) = sum(Surplus_power);
    Total_deficiency_power(Z) = -sum(Deficiency_power);
    Total_Net_Household_Demand(Z) = sum(Net_Household_Demand);
```

```
    Total_Surplus = sum(Surplus_power);
    Total_Deficiency = -sum(Deficiency_power);
    Grid_price = GridPrice(h);
    [Price_B, Price_S,mmr] = Pricing(Total_Surplus, Total_Deficiency, Grid_price);
    Price_Buying(Z) = Price_B;
    Price_Selling (Z) = Price_S;
    grid_price(Z) = Grid_price;
    MMR(Z) = mmr;
    Individual_cost = Cost_Function (Number_households, Total_Surplus,
Total_Deficiency, Surplus_power, Deficiency_power, Grid_price, Price_B, Price_S);
    Individual_Cost_Households (Z,:) = Individual_cost;

    %%%%%%%%%%%%%%%%%%%%%%%%%Pool Battery%%%%%%%%%%%%%%%%%%%%%%%
    Pool_SOC = (Pool_power*100)/ Capacity_of_Pool;
    if Pool_SOC < Max_SOC_Pool && Pool_SOC > Min_SOC_Pool
        Pool_power = Pool_power + (sum(Surplus_power)*0.1 +
sum(Deficiency_power)*0.1);
        Pool_Power(Z) =  Pool_power;
        Pool_Surplus(Z) = Pool_surplus;
        Pool_Deficiency(Z) = Pool_deficiency;
    elseif Pool_SOC >= Max_SOC_Pool
        Pool_power = Pool_power + (sum(Deficiency_power)*0.1);
        Pool_Power(Z) =  Pool_power;
        Pool_surplus = Pool_surplus + (sum(Surplus_power)*0.1);
        Pool_Surplus(Z) = Pool_surplus;
    elseif Pool_SOC < Min_SOC_Pool
        Pool_power = Pool_power + (sum(Surplus_power)*0.1);
        Pool_Power(Z) =  Pool_power;
        Pool_deficiency = Pool_deficiency - (sum(Deficiency_power)*0.1);
        Pool_Deficiency(Z) = Pool_deficiency;
    end


    Net_Household2_Demand(Z) = Net_Household_Demand(5);
    Daily_current_demand2(Z) = Current_household_demand(5);
    Individual_surplus2(Z) = Surplus_power(5);
    BES_Power(Z)=BES_Inividual_power(5);
    EV_Power(Z) = EV_Inividual_power(5);
    for i = 1:Number_households
        Individual_deficiency(i,Z) = Surplus_power(i);
        Individual_surplus(i,Z) = -Deficiency_power(i);
    end


end
Indiv_cost = zeros(1,Number_households);
for i = 1 : Number_households
    Indiv_cost(i) = sum (Individual_Cost_Households(:,i))/1000;
end
sum(Indiv_cost)
for i = 1: Number_households
    figure
    plot (T,Individual_deficiency(i,:),T,Individual_surplus(i,:))
    hold on
end
figure
plot(T, Price_Selling , T,  Price_Buying, T, grid_price, T, MMR,':')
```

```
plot(T, Net_Household2_Demand, T, Individual_surplus2, T,BES_Power,'--', T,
Daily_current_demand2,':', T, EV_Power)
hold on
figure
plot(T, Total_surplus_power, T, Total_Net_Household_Demand)
hold on
figure
plot( T, Pool_Power, T, Pool_Deficiency, T, Pool_Surplus)


Total_Current_Demand = sum(Total_Current_Demand)*0.1
Total_surplus_power = sum(Total_surplus_power)*0.1;
Total_deficiency_power = -sum(Total_deficiency_power)*0.1;
Total_Net_Household_Demand = sum(Total_Net_Household_Demand)*0.1
Total_surplus2 = sum(Individual_surplus2)*0.1;


%%%%%%%%%%Initialisation of the household type Function%%%%%%%%%%%%%%%%%%%%%%
function HouseholdTypes = TypeOfHouse (Number_households)
HouseholdTypes = zeros(1,Number_households);
    for i = 1: Number_households
        HouseholdTypes(i) = randi([1 6],1,1);
    end
end

function [Demand_indiv,Demand_dis, Demand_total] = Household_Demand
(Number_households)
Demand_dis = zeros(Number_households,5);
Demand_indiv = zeros(1,Number_households);
Demand_total = 0;
Higher_Demand = 17;
Lower_Demand = 8;
    for i = 1:Number_households

        n = sum(~mod(Lower_Demand:Higher_Demand,0.5));
        Rand_Demand = ((randi(n)-1)*0.5 + Lower_Demand);
        Demand_indiv (i) = Rand_Demand;
        Demand_total = Demand_total + Demand_indiv(i);
        Demand_dis(i,1) = Rand_Demand * 0.07/7;
        Demand_dis(i,2) = Rand_Demand * 0.30/4;
        Demand_dis(i,3) = Rand_Demand * 0.20/6;
        Demand_dis(i,4) = Rand_Demand * 0.40/5;
        Demand_dis(i,5) = Rand_Demand * 0.03/2;
    end

end

function [individ_PV, PV_total,PV_Curve,PV_Type] =
PV(Number_households,Household_Types,HouseholdTypesIndex)
individ_PV = zeros(1, Number_households);
PV_total = 0;
PV_Curve = zeros(Number_households, 11);
PV_Type = zeros(1, Number_households);

    for i = 1: Number_households
        PV_Type(i) = (randi([3 5],1,1)) *
HouseholdTypesIndex(Household_Types(i),1);
        individ_PV(i) = (PV_Type(i) * 4) *
HouseholdTypesIndex(Household_Types(i),1);
```

```
        PV_total = PV_total + individ_PV(i);
            PV_Curve = [];
            for i = 1:100

                R = [1:0.1:24];
                Irr = [];
                Temp = [];
                    for i = 1:0.1:24
                        h = floor (i);
                        irr = London_irr(h);
                        temp = London_Tem(h);
                        delta_irr = normrnd(0,0.1);
                        delat_temp = normrnd(0,0.1);
                        irr = London_irr(h) + London_irr(h) * delta_irr;
                        temp = London_Tem(h) + London_Tem(h) * delat_temp;
                        Irr = [Irr irr];
                        Temp = [Temp temp];
                    end
                Irr = transpose(Irr);
                Temp = transpose(Temp);
                R = transpose(R);
                Irr = [R, Irr];
                Temp = [R, Temp];

                sim("PV_irr.slx");

                PV_curve = ans.PV_generation.signals.values;

                PV_Curve = [PV_Curve PV_curve];
                i

            end
    end
end

function [BES_Capacity, initial_SOCs] = BESS(Number_households, Household_Types,
HouseholdTypesIndex)
initial_SOCs = zeros(1,Number_households);
BES_Capacity = zeros(1, Number_households);
Min_Capacity = 3;
Max_Capacity = 7;
Min_SOC = 20;
Max_SOC = 80;
    for i = 1: Number_households
        BES_Capacity(i) = randi ([Min_Capacity Max_Capacity], 1,
1)*HouseholdTypesIndex(Household_Types(i),2);
        n = sum(~mod(Min_SOC:Max_SOC,5));
        initial_SOCs(i) = ((randi(n)-1)*5 +
Min_SOC)*HouseholdTypesIndex(Household_Types(i),2);
    end
end

function [EV_Capacity,initial_SOCs,Trip_Duration] = EV(Number_households,
Household_Types, HouseholdTypesIndex)
initial_SOCs = zeros(1,Number_households);
EV_Capacity = zeros(1, Number_households);
Trip_Duration = zeros(1, Number_households);
Min_capacity = 15;
Max_capacity = 25;
```

```
Min_SOC = 40;
Max_SOC = 80;

    for i =1:Number_households
        n = sum(~mod(Min_capacity:Max_capacity,5));
        EV_Capacity(i) = ((randi(n)-1)*5 +
Min_capacity)*HouseholdTypesIndex(Household_Types(i),3);
        m = sum(~mod(Min_SOC:Max_SOC,5));
        initial_SOCs(i) = ((randi(m)-1)*5 +
Min_SOC)*HouseholdTypesIndex(Household_Types(i),3);

        Trip_Duration(i) = randi([4
6],1,1)*HouseholdTypesIndex(Household_Types(i),3);

    end
end

function [Pool_Capacity, initial_SOC] = Pool_Battery( )

Pool_Capacity = 200;
Min_SOC = 30;
Max_SOC = 40;

n = sum(~mod(Min_SOC:Max_SOC,5));
initial_SOC = ((randi(n)-1)*5 + Min_SOC);
end

function Grid_Price = GridPrice (h)
persistent p;
persistent t;
t = h;

function [Buying, Selling,MMR] = Pricing (Total_Surplus, Total_Deficiency,
Grid_Price)
persistent Buying_Price
persistent Selling_Price
FiT = 5;
Alpha = (Total_Deficiency - Total_Surplus) / (Total_Deficiency + Total_Surplus);
gamma1 = FiT/(FiT + Grid_Price);%Total_Surplus/Total_Deficiency;
gamma2 = FiT/(FiT + Grid_Price);

MMR = (Grid_Price+FiT)/2;

if Alpha >= 0 && Total_Surplus ~= 0
    Beta = tanh(2*Alpha);
    Buying_Price = ((((1-gamma1) * Beta + 1)/2) * (Grid_Price - FiT)) + FiT;
   Selling_Price = (((gamma1 * Beta + 1)/2) * (Grid_Price - FiT)) + FiT;
elseif Alpha < 0 && Total_Deficiency ~= 0
   Beta1 = tanh(2*Alpha);
   Beta2 = tanh(2*Alpha);
    Buying_Price = (((gamma2 * Beta1 + 1)/2) * (Grid_Price - FiT)) + FiT;
    Selling_Price = ((((1-gamma2) * Beta2 + 1)/2) * (Grid_Price - FiT)) + FiT;
elseif Alpha > 0 && Total_Surplus == 0
    Buying_Price = Grid_Price;
    Selling_Price = Grid_Price;
elseif Alpha < 0 && Total_Deficiency == 0
    Buying_Price = FiT;
    Selling_Price = FiT;
end
```

```
Buying = Buying_Price;
Selling = Selling_Price;
end
function [Total_individual_Cost] = Cost_Function(Number_households, Total_Surplus,
Total_Deficiency, Surplus_power, deficiency_power, Grid_Price, Price_B, Price_S)

persistent total_individual_cost
total_individual_cost = zeros(1, Number_households);
Deficiency_power = -1 * deficiency_power;
FiT = 5;

for i = 1 : Number_households
    if Total_Surplus > 0 && Total_Deficiency == 0
        total_individual_cost(i) = -1 * Surplus_power(i) * FiT;

    elseif Total_Deficiency > 0 && Total_Surplus == 0
        total_individual_cost(i) = Deficiency_power(i) * Grid_Price;

    elseif Total_Deficiency > Total_Surplus && Total_Surplus ~= 0
        if Deficiency_power(i) > 0
            PowerFromGrid = Total_Deficiency - Total_Surplus;
            Individual_Cost_Peer = (Deficiency_power(i) * Total_Surplus * Price_B)
/ Total_Deficiency;
            Individual_Cost_Grid =  (Deficiency_power(i) * PowerFromGrid *
Grid_Price) / Total_Deficiency;

            total_individual_cost(i) = Individual_Cost_Peer +
Individual_Cost_Grid;
        elseif Surplus_power(i) > 0
            total_individual_cost(i) = -1 * Surplus_power(i) * Price_S;
        end

    elseif Total_Surplus > Total_Deficiency && Total_Deficiency ~= 0
        if Surplus_power(i) > 0

            PowerToGrid =  Total_Surplus - Total_Deficiency;

            Individual_Cost_Peer = (Surplus_power(i) * Total_Deficiency * Price_S)
/ Total_Surplus;
            Individual_Cost_Grid = (Surplus_power(i) * PowerToGrid * FiT) /
Total_Surplus;

            total_individual_cost(i) = -1 * (Individual_Cost_Peer +
Individual_Cost_Grid);
        elseif Deficiency_power(i) > 0
            total_individual_cost(i) = Deficiency_power(i) * Price_B;
        end
    elseif Total_Surplus == Total_Deficiency
        if Deficiency_power(i) > 0
            total_individual_cost(i) = Deficiency_power(i) * Price_B;
        elseif Surplus_power(i) > 0
            total_individual_cost(i) = -1 * Surplus_power(i) * Price_S;
        end

    end
    Total_individual_Cost = total_individual_cost;
end
end
```